Theory and Applications of Mathematics & Computer Science

(ISSN 2067-2764)
http://www.uav.ro/applications/se/journal/index.php/tamcs

Theory and Applications of Mathematics & Computer Science 3 (1) (2013) 1–12

Approach Merotopies and Associated Near Sets

James Peters[a,b,*], Surabhi Tiwari[c], Rashmi Singh[d]

[a]*Computational Intelligence Laboratory, University of Manitoba, Winnipeg, Manitoba R3T 5V6, Canada.*
[b]*School of Mathematics & Computer / Information Sciences, University of Hyderabad, Central Univ. P.O., Hyderabad 500046, India.*
[c]*Department of Mathematics, Motilal Nehru National Institute of Technology, Allahabad- 211 004, U.P., India.*
[d]*Department of Mathematics, Amity Institute of Applied Sciences, Noida, U.P., India.*

Abstract

This article introduces associated near sets of a collection of sets. The proposed approach introduces a means of defining as well as describing an ε-approach merotopy in terms of the members of associated sets of collections that are sufficiently near. A characterization for continuous functions is established using associated near sets. This article also introduces p-containment considered in the context of near sets. An application of the proposed approach is given in terms of digital image classification.

Keywords: Approach space, associated set, p-containment, merotopy, near sets.
2010 MSC: Primary 26A21, Secondary 26A24, 54D35, 54A20, 54E99, 18B30.

1. Introduction

For any real-valued function f of a real variable, the associated sets of f (Agronsky, 1982) are the sets

$$E^{\alpha}(f) = \{x : f(x) < \alpha\} \text{ and } E_{\alpha}(f) = \{x : f(x) > \alpha\},$$

where $\alpha \in \mathbb{R}$ (the set of all real numbers). Many classes of functions can be characterized in terms of their associated sets. The study of associated sets of a function started in 1922 (Coble, 1922) and elaborated in (Zahorski, 1950; Bruckner, 1967; Agronsky, 1982; Petrakiev, 2009). For example, a function is continuous, if and only if, all of its associated sets are open, a function is approximately continuous if, and only if, all of its associated sets F sets with the property that every point of an associated set is a point of Lebesgue density of that set. More generally, A. Bruckner (Bruckner, 1967, p. 228) has shown that if κ is a class of functions characterized in terms of an associated set P and h is a homeomorphism, then the associated sets of the function $h \circ f$ are all members

*Corresponding author
Email addresses: jfpeters@ee.umanitoba.ca (James Peters), au.surabhi@gmail.com (Surabhi Tiwari)

of P and $h \circ f \in \kappa$. S. Agronsky (Agronsky, 1982, p. 767) has observed that an associated set for a function in $\mathcal{M}_i$ must be 'more dense' near each of its members than an associated set for a function in $\mathcal{M}_{i-1}$.

In this paper, associated sets defined in terms of ε-approach merotopies are considered. In particular, we consider associated sets containing members that are sufficiently near each other relative to ε-approach merotopies. Carrying forward the idea of defining and characterizing a function in terms of an associated set, it is possible to define and characterize an approach merotopy in terms of an associated set of collections. Using the concept of associated sets, an equivalent condition for continuous functions is obtained.

2. Preliminaries

Let X be a nonempty ordinary set. The power set of X is denoted by $\mathcal{P}(X)$, the family of all collections of subsets of $\mathcal{P}(X)$ is denoted by $\mathcal{P}^2(X)$. We denote by $\aleph_0$ the first infinite cardinal number, by J an arbitrary index set, and $|A|$ is the cardinality of A, where $A \subseteq X$. For $\mathcal{A}, \mathcal{B} \in \mathcal{P}^2(X)$, we say $\mathcal{A} \vee \mathcal{B} \equiv \{A \cup B : A \in \mathcal{A}, B \in \mathcal{B}\}$; $\mathcal{A}$ *corefines* $\mathcal{B}$ (written as $\mathcal{A} \prec \mathcal{B}$), if and only if, for all $A \in \mathcal{A}$, there exists $B \in \mathcal{B}$ such that $B \subseteq A$. For $\mathcal{A} \subseteq \mathcal{P}(X)$, $stack(\mathcal{A}) = \{A \subseteq X : B \subseteq A$, for some $B \in \mathcal{A}\}$ and $sec(\mathcal{A}) = \{B \subseteq X : A \cap B \neq \emptyset$, for all $A \in \mathcal{A}\} = \{B \subseteq X : X - B \notin$ stack$(\mathcal{A})\}$. Observe that $\text{sec}^2(\mathcal{A}) = \text{stack}(\mathcal{A})$, for all $\mathcal{A} \in \mathcal{P}^2(X)$. A *filter* on X is a nonempty subset $\mathcal{F}$ of $\mathcal{P}(X)$ satisfying: $\emptyset \notin \mathcal{F}$; if $A \in \mathcal{F}$ and $A \subseteq B$, then $B \in \mathcal{F}$; and if $A \in \mathcal{F}$ and $B \in \mathcal{F}$, then $A \cap B \in \mathcal{F}$. A maximal filter on X is called an *ultrafilter* on X. A *grill* on X is a subset $\mathcal{G}$ of $\mathcal{P}(X)$ satisfying: $\emptyset \notin \mathcal{G}$; if $A \in \mathcal{G}$ and $A \subseteq B$, then $B \in \mathcal{G}$; and if $A \cup B \in \mathcal{G}$, then $A \in \mathcal{G}$ or $B \in \mathcal{G}$. Note that for any $x \in X, \dot{x} = \{A \subseteq X : x \in A\}$ is an ultrafilter on X, which is also a grill on X. There is one-to-one correspondence between the set of all filters and the set of all grills on X by the relation: $\mathcal{F}$ is a filter on X if and only if $\text{sec}(\mathcal{F})$ is a grill on X; and $\mathcal{G}$ is a grill on X if and only if, $\text{sec}(\mathcal{G})$ is a filter on X.

In its most basic form, an approach merotopy is a measure of the nearness of members of a collection. For collections $\mathcal{A}, \mathcal{B} \in \mathcal{P}^2(X)$, a function $\nu : \mathcal{P}^2(X) \times \mathcal{P}^2(X) :\longrightarrow [0, \infty]$ satisfying a number of properties is a called an ε-approach merotopy. A pair of collections are near, provided $\nu(\mathcal{A}, \mathcal{B}) = 0$. For $\varepsilon \in (0, \infty]$, the pair $\mathcal{A}, \mathcal{B}$ are *sufficiently near*, provided $\nu(\mathcal{A}, \mathcal{B}) < \varepsilon$.

Let cl be a Kuratowski closure operator on X. Then the topological space (X, cl) is called a *symmetric topological space* if and only if $x \in cl(\{y\}) \Longrightarrow y \in cl(\{x\})$, for all $x, y \in X$.

Definition 2.1. A function $\delta : X \times \mathcal{P}(X) \longrightarrow [0, \infty]$ is called a distance on X (Lowen, 1997; Lowen *et al.*, 2003) if for any $A, B \subseteq X$ and $x \in X$, the following conditions are satisfied:
(**D**.1) $\delta(x, \{x\}) = 0$,
(**D**.2) $\delta(x, \emptyset) = \infty$,
(**D**.3) $\delta(x, A \cup B) = \min\{\delta(x, A), \delta(x, B)\}$,
(**D**.4) $\delta(x, A) \leq \delta(x, A^{(\alpha)}) + \alpha$, for all $\alpha \in [0, \infty]$, where $A^{(\alpha)} \doteqdot \{x \in X : \delta(x, A) \leq \alpha\}$.
The pair (X, δ) is called an approach space.

Definition 2.2. A generalized approach space (X, ρ) (Peters & Tiwari, 2011, 2012) is a nonempty set X equipped with a generalized distance function $\rho : \mathcal{P}(X) \times \mathcal{P}(X) \longrightarrow [0, \infty]$, if and only if, for all nonempty subsets $A, B, C \in \mathcal{P}(X)$, ρ satisfies properties (A.1)-(A.5), *i.e.*,

(**A**.1) $\rho(A, A) = 0$,
(**A**.2) $\rho(A, \emptyset) = \infty$,
(**A**.3) $\rho(A, B \cup C) = \min\{\rho(A, B), \rho(A, C)\}$,
(**A**.4) $\rho(A, B) = \rho(B, A)$,
(**A**.5) $\rho(A, B) \leq \rho(A, B^{(\alpha)}) + \alpha$, for every $\alpha \in [0, \infty]$, where $B^{(\alpha)} = \{x \in X : \rho(\{x\}, B) \leq \alpha\}$.

It has been observed that the notion of distance in an approach space is closely related to the notion of nearness (Khare & Tiwari, 2012, 2010; Tiwari, Jan. 2010). In particular, consider the Čech distance between sets.

Definition 2.3. Čech Distance (Čech, 1966). For nonempty subsets $A, B \in \mathcal{P}(X)$, $\rho(a, b)$ is the standard distance between $a \in A, b \in B$ and the Čech distance $D_\rho : \mathcal{P}(X) \times \mathcal{P}(X) \longrightarrow [0, \infty]$ is defined by

$$D_\rho(A, B) \doteqdot \begin{cases} \inf\{\rho(a, b) : a \in A, b \in B\}, & \text{if } A \text{ and } B \text{ are not empty,} \\ \infty, & \text{if } A \text{ or } B \text{ is empty.} \end{cases}$$

Remark. Observe that (X, D_ρ) is a generalized approach space. The distance $D_\rho(A, B)$ is a variation of the distance function introduced by E. Čech in his 1936–1939 seminar on topology (Čech, 1966) (see, also, (Beer *et al.*, 1992; Hausdorff, 1914*a*; Leader, 1959)).

3. Approach merotopic spaces

Definition 3.1. Let $\varepsilon \in (0, \infty]$. Then a function $\nu : \mathcal{P}^2(X) \times \mathcal{P}^2(X) \longrightarrow [0, \infty]$ is an ε-approach merotopy on X, if and only if, for any collections $\mathcal{A}, \mathcal{B}, C \in \mathcal{P}^2(X)$, the properties (AN.1)-(AN.5) are satisfied.

(AN.1) $\mathcal{A} \prec \mathcal{B} \Longrightarrow \nu(C, \mathcal{A}) \leq \nu(C, \mathcal{B})$,

(AN.2) $\mathcal{A} \neq \emptyset, \mathcal{B} \neq \emptyset$ and $(\bigcap \mathcal{A}) \cap (\bigcap \mathcal{B}) \neq \emptyset \Longrightarrow \nu(\mathcal{A}, \mathcal{B}) < \varepsilon$,

(AN.3) $\nu(\mathcal{A}, \mathcal{B}) = \nu(\mathcal{B}, \mathcal{A})$ and $\nu(\mathcal{A}, \mathcal{A}) = 0$,

(AN.4) $\mathcal{A} \neq \emptyset \Longrightarrow \nu(\emptyset, \mathcal{A}) = \infty$,

(AN.5) $\nu(C, \mathcal{A} \vee \mathcal{B}) \geq \nu(C, \mathcal{A}) \wedge \nu(C, \mathcal{B})$.

The pair (X, ν) is termed as an *ε-approach merotopic space*.

For an ε-approach merotopic space (X, ν), we define: $cl_\nu(A) \doteqdot \{x \in X : \nu(\{\{x\}\}, \{A\}) < \varepsilon\}$, for all $A \subseteq X$. Then cl_ν is a Čech closure operator on X.

Let $cl_\nu(\mathcal{A}) \doteqdot \{cl_\nu(A) : A \in \mathcal{A}\}$. Then an ε-approach merotopy ν on X is called an *ε-approach nearness* on X, if the following condition is satisfied:

(AN.6) $\nu(cl_\nu(\mathcal{A}), cl_\nu(\mathcal{B})) \geq \nu(\mathcal{A}, \mathcal{B})$.

In this case, cl_ν is a Kuratowski closure operator on X.

Lemma 3.1. *Let $\varepsilon \in (0,\infty]$, and let (X,ν) and (Y,ν') be ε-approach nearness spaces. Then $f : (X,\nu) \longrightarrow (Y,\nu')$ is a contraction if and only if*
$\nu(f^{-1}(\mathcal{A}), f^{-1}(\mathcal{B})) \geq \nu'(\mathcal{A},\mathcal{B})$, *for all* $\mathcal{A},\mathcal{B} \in \mathcal{P}^2(Y)$.

Example 3.1. Let D_ρ be a gap functional. Then the function $\nu_{D_\rho} : \mathcal{P}^2(X) \times \mathcal{P}^2(X) \longrightarrow [0,\infty]$ defined as

$$\nu_{D_\rho}(\mathcal{A},\mathcal{B}) \doteqdot \sup_{A\in\mathcal{A},B\in\mathcal{B}} D_\rho(A,B); \quad \nu_{D_\rho}(\mathcal{A},\mathcal{A}) \doteqdot \sup_{A\in\mathcal{A}} D_\rho(A,A) = 0,$$

is an ε-approach merotopy on X. Define $cl_\rho(A) = \{x \in X : \rho(\{x\},A) < \varepsilon\}$, $A \subseteq X$. Then cl_ρ is a Čech closure operator on X. Further, if $\rho(cl_\rho(A), cl_\rho(B)) \geq \rho(A,B)$, for all $A,B \subseteq X$, then cl_ρ is a Kuratowski closure operator on X, and we call ρ as an *ε-approach function* on X; and (X,ρ) is an *ε-approach space*. In this case, ν_{D_ρ} is an ε-approach nearness on X.

So, there are many instances of ε-approach nearness on X just as there are many instances of ε-approach spaces (Lowen, 1997) and metric spaces on X.

Definition 3.2. Near and Almost Near Collections
For collections $\mathcal{A},\mathcal{B} \in \mathcal{P}^2(X)$, assume that the function $\nu : \mathcal{P}^2(X) \times \mathcal{P}^2(X) :\longrightarrow [0,\infty]$ is an ε-approach merotopy. A pair of collections are *near*, provided $\nu(\mathcal{A},\mathcal{B}) = 0$. For $\varepsilon \in (0,\infty]$, the pair $\mathcal{A},\mathcal{B}$ are *ε-near* (*almost near*), provided $\nu(\mathcal{A},\mathcal{B}) < \varepsilon$ (Peters & Tiwari, 2011). Otherwise, collections $\mathcal{A},\mathcal{B}$ are far, *i.e.*, *sufficiently apart*, provided $\nu(\mathcal{A},\mathcal{B}) \geq \varepsilon$.

4. Associated collections

It is possible to characterise ε-approach merotopies in terms of associated collections.

Definition 4.1. Associated Collections of an ε-Approach Merotopy
Let X denote an ordinary nonempty set and let $\mathcal{A} \in \mathcal{P}^2(X)$ denote collections of subsets of X. Suppose that $\varepsilon \in (0,\infty]$ and ν be an ε-approach merotopic space. The upper associated set of $\mathcal{A}$ with respect to ν is defined by

$$E^\varepsilon(\mathcal{A}) \doteqdot \{\mathcal{B} \in \mathcal{P}^2(X) : \ \nu(\mathcal{A},\mathcal{B}) > \varepsilon\}.$$

and the lower associated set of $\mathcal{A}$ with respect to ν is defined by

$$E_\varepsilon(\mathcal{A}) \doteqdot \{\mathcal{B} \in \mathcal{P}^2(X) : \ \nu(\mathcal{A},\mathcal{B}) < \varepsilon\}.$$

Example 4.1. Let D_ρ be a gap functional. For $\mathcal{A},\mathcal{B} \in \mathcal{P}^2(X)$, the function $\nu_{D_\rho} : \mathcal{P}^2(X) \times \mathcal{P}^2(X) \longrightarrow [0,\infty]$ is defined by

$$\nu_{D_\rho}(\mathcal{A},\mathcal{B}) \doteqdot \sup_{A\in\mathcal{A},B\in\mathcal{B}} D_\rho(A,B); \quad \nu_{D_\rho}(\mathcal{A},\mathcal{A}) \doteqdot \sup_{A\in\mathcal{A}} D_\rho(A,A) = 0.$$

From Def. 4.1, $E_\varepsilon(\mathcal{A})$ is the lower associated set of $\mathcal{A}$ for a given $\varepsilon \in \mathbb{R}$. Similarly, obtain the upper associated set $E^\varepsilon(\mathcal{A})$ of $\mathcal{A}$ as a collection $\mathcal{B} \in \mathcal{P}^2(X)$, provided $\nu_{D_\rho}(\mathcal{A},\mathcal{B}) > \varepsilon$.

Additional examples of lower and upper associated collections are given next.

Example 4.2. Let (X, ν) be an ε-approach nearness on X, $r < \varepsilon < \infty$ and $\varepsilon' < \varepsilon$. Then

(**ASet**.1) Associated sets $E^{\varepsilon}(\mathcal{A}), E_{\varepsilon}(\mathcal{A})$ of $\mathcal{A}$ with respect to $\nu_1 : \mathcal{P}^2(X) \times \mathcal{P}^2(X) \longrightarrow [0, \infty]$ such that

$$\nu_1(\mathcal{A}, \mathcal{B}) = \begin{cases} \infty, & \text{if } \emptyset \in \mathcal{A} \text{ or } \emptyset \in \mathcal{B}, \\ r, & \text{otherwise,} \end{cases}$$

is defined by:
if $\emptyset \in \mathcal{A}$, $E^{\varepsilon}(\mathcal{A}) = \mathcal{P}^2(X)$ and $E_{\varepsilon}(\mathcal{A}) = \emptyset$,
if $\emptyset \notin \mathcal{A}$, $E^{\varepsilon}(\mathcal{A}) = \{\mathcal{A} \in \mathcal{P}^2(X) : \emptyset \in \mathcal{B}\}$ and $E_{\varepsilon}(\mathcal{A}) = \{\mathcal{A} \in \mathcal{P}^2(X) : \emptyset \notin \mathcal{B}\}$.

(**ASet**.2) Associated sets $E^{\varepsilon}(\mathcal{A}), E_{\varepsilon}(\mathcal{A})$ of $\mathcal{A}$ with respect to $\nu_2 : \mathcal{P}^2(X) \times \mathcal{P}^2(X) \longrightarrow [0, \infty]$ such that

$$\nu_2(\mathcal{A}, \mathcal{B}) = \begin{cases} \infty, & \text{if } \emptyset \in \mathcal{A} \text{ or } \emptyset \in \mathcal{B}, \\ \inf\{\nu(\mathcal{A}, \mathcal{B}), \varepsilon'\}, & \text{otherwise,} \end{cases}$$

is defined by:
if $\emptyset \in \mathcal{A}$, $E^{\varepsilon}(\mathcal{A}) = \mathcal{P}^2(X)$ and $E_{\varepsilon}(\mathcal{A}) = \emptyset$,
if $\emptyset \notin \mathcal{A}$, $E^{\varepsilon}(\mathcal{A}) = \{\mathcal{A} \in \mathcal{P}^2(X) : \emptyset \in \mathcal{B}\}$ and $E_{\varepsilon}(\mathcal{A}) = \{\mathcal{A} \in \mathcal{P}^2(X) : \emptyset \notin \mathcal{B}\}$.

Proposition 1. *A collection in the lower associated set of $\mathcal{A}$ with respect to the ε-approach merotopy ν is sufficiently near $\mathcal{A}$.*

Proof. Assume $\mathcal{B} \in E_{\varepsilon}(\mathcal{A})$, the lower associated set of $\mathcal{A}$ with respect to ν. From Def. 3.2, $\mathcal{A}, \mathcal{B}$ are sufficiently near. □

Proposition 2. *A collection in upper associated set of $\mathcal{A}$ with respect to the ε-approach merotopy ν are sufficiently apart.*

Proof. Immediate from from Def. 4.1 and Def. 3.2. □

We now present a characterization for continouous functions.

Theorem 4.1. *Let ν_X and ν_Y be ε-approach merotopies on X and Y, respectively. A mapping $f : X \longrightarrow Y$ is continuous, if and only if, $\mathcal{A} \in E_{\varepsilon}(x) \implies f(\mathcal{A}) \in E_{\varepsilon}(f(x))$, for all $\mathcal{A} \in \mathcal{P}^2(X)$ and for all $x \in X$.*

Proof. Let $f : X \longrightarrow Y$ be continuous, $x \in X$ and $\mathcal{A} \in \mathcal{P}^2(X)$. Suppose that $\mathcal{A} \in E_{\varepsilon}(x)$. Then $\nu(\mathcal{A}, \{\{x\}\}) < \varepsilon$, which gives $\nu(\{A\}, \{\{x\}\}) < \varepsilon$, for all $A \in \mathcal{A}$. That is, $x \in cl_{\nu_X}(A)$, for all $A \in \mathcal{A}$. Consequently, $f(x) \in f(cl_{\nu_X}(A)) \subseteq cl_{\nu_Y}(f(A))$, for all $A \in \mathcal{A}$. Hence, $f(\mathcal{A}) \in E_{\varepsilon}(f(x))$. The converse is obvious. □

Definition 4.2. Finite Strong Containment Property (Agronsky, 1982).
Let p be a property defined for sets of real numbers with respect to sets containing them. If $A \subset B$, then A is p-contained in B (written $A \underset{p}{\subset} B$), provided A has the property p with respect to B. Put $k \in [0, \infty)$. Then p is a finite strong containment property, provided

(**p**.1) If $A \underset{p}{\subset} B \subset F$ and p is defined for $A \subset F$, then $A \underset{p}{\subset} F$,

(**p**.2) If $A \subset B \underset{p}{\subset} F$, then $A \underset{p}{\subset} F$,

(**p**.3) If, for each $n \in \mathbb{N}, E_n \underset{p}{\subset} F_n$, then $\bigcup_{n=1}^{k} E_n \underset{p}{\subset} \bigcup_{n=1}^{k} F_n$.

Example 4.3. Strong Containment of Sufficiently Near Collections
Put $\varepsilon \in (0, \infty]$. Let (X, ν) be an ε-approach nearness on X and $p \div$ 'sufficiently near' defined for $\mathcal{A}, \mathcal{B} \in \mathcal{P}(X)$ such that $\nu(\mathcal{A}, \mathcal{B}) < \varepsilon$. From Example 4.2, assume $\mathcal{A}, \mathcal{B} \in E_\varepsilon(\nu_2)$ and $\mathcal{A} \subset \mathcal{B}$, then $\mathcal{A} \underset{p}{\subset} \mathcal{B}$.

Proof.

(**p**.1) Assume $\mathcal{A}, \mathcal{B}, \mathcal{C} \in E_\varepsilon(\nu_2)$. By definition, $\mathcal{A} \underset{p}{\subset} \mathcal{B}$. Assume $\mathcal{B} \subset \mathcal{C}$, then $\mathcal{A} \underset{p}{\subset} \mathcal{B} \subset \mathcal{C}$. Since $\mathcal{B}, \mathcal{C} \in E_\varepsilon(\nu_2)$, then $\mathcal{A} \underset{p}{\subset} \mathcal{C}$.

(**p**.2) Assume $\mathcal{A}, \mathcal{B}, \mathcal{C} \in E_\varepsilon(\nu_2)$ and that $\mathcal{A} \subset \mathcal{B} \subset \mathcal{C}$. By definition, $\mathcal{A} \subset \mathcal{B} \underset{p}{\subset} \mathcal{C}$ and by assumption $\mathcal{A} \subset \mathcal{C}$. Since $\mathcal{A}, \mathcal{C} \in E_\varepsilon(\nu_2)$, then $\mathcal{A} \underset{p}{\subset} \mathcal{C}$.

(**p**.3) The proof of this strong containment property follows by mathematical induction.

□

5. Description-based neighbourhoods

For N. Bourbaki, a set is a neighbourhood of each of its points if, and only if, the set is open (Bourbaki, 1971, §1.2) (Bourbaki, 1966, §1.2, p. 18). A set A is *open*, if and only if, for each $x \in A$, all points *sufficiently near*[1] x belong to A.

For a Hausdorff neighbourhood (denoted by N_r), *sufficiently near* is explained in terms of the distance between points y and x being less than some radius r (Hausdorff, 1914*b*, §22). In other words, a Hausdorff neighbourhood of a point is an open set such that each of its points is sufficiently close to its centre.

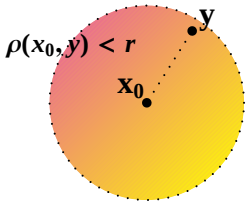

Figure 1: Nbd $N_r(x_0)$

Traditionally, nearness of points is measured in terms of the location of the points. Let $\rho : X \times X :\to [0, \infty]$ denote the standard distance[2] between points in X. For $r \in (0, \infty]$, a neighbourhood of $x_0 \in X$ is the set of all $y \in X$ such that $\rho(x_0, y) < r$ (see, *e.g.*, Fig. 1, where the distance $\rho(x, y)$ between each pair x_0, y is less than r in the neighbourhood). In that case, a neighbourhood is called an open ball (Engelking, 1989, §4.1) or spherical neighbourhood (Hocking & Young, 1988, §1-4). In the plane, the points in a spherical neighhourhood (nbd) are contained in the interior of a circle.

Next, an alternative to a spherical neighbourhood is called a visual neighbourhood (denoted nbd_v), which stems from recent work on descriptively near sets (Naimpally & Peters, 2013; Peters, 2013; Peters & Naimpally, 2012).

[1] *...tous les points assez voisins d'un point x* (Bourbaki, 1971, p. TG I.3)
[2] *i.e.*, for $x, y \in X \subset, \rho(x, y) = |x - y|$.

Definition 5.1. Visual Neighbourhood
A visual nbd_v of a point x_0 (denoted N_{r_ϕ}) is an open set A such that the visual information values extracted from all of the points in A are sufficiently near the corresponding visual information values at x_0. Let ϕ denote a probe function used to extract visual information from a point in nbd_v. Sufficient nearness of points in a visual nbd_v is defined in terms of bound r_ϕ, a real number. That is, points $x_0, x \in A$ are sufficiently near, *i.e.*, provided

$$\rho_\phi(x_0, y) = |\phi(x_0) - \phi(y)| < r_\phi.$$

Example 5.1. Visual Neighbourhood in a Drawing
In its simplest form (see, *e.g.*, Fig. 2), a nbd_v (denoted by N_{r_ϕ}) is defined in terms of a real-valued probe function ϕ used to extract visual information from the pixels in a digital image, reference point x_0 (*not* necessarily the centre of the nbd_v) and 'radius' r_ϕ such that

$X =$ {drawing visual pixels}, $x, y \in X$,

$\phi : X \to [0, \infty]$, (probe function, *e.g.*, probe $\phi(x)$ = pixel x intensity),

$\rho_\phi(x_0, y) = |\phi(x_0) - \phi(y)|$, (visual distance),

$x_0 \in X$,(nbd_v reference point),

$r_\phi \in (0, \infty]$, (sufficient nearness bound),

$N_{r_\phi}(x_0) = \{y \in X : \rho_\phi(x_0, y) < r_\phi\}$, (visual nbd_v).

At this point, observe that the appearance of a visual neighbourhood can be quite different from the appearance of a spherical neighbourhood. For this reason, x_0 is called a *reference point* (not a centre) in a nbd_v. A visual neighbourhood results from a consideration of the features of a point in the neighbourhood and the measurement of the distance between neighbourhood points[3]. For example, $\phi(x_0)$ in Fig. 2 is a description of x_0 (probe ϕ is used to extract a feature value from x in the form of pixel intensity). Usually, a complete description of a point x in a nbd_v is in the form of a feature vector containing probe function values extracted from x (see, *e.g.*, (Henry, 2010, §4), for a detailed explanation of the near set approach to perceptual object description). Observe that the members $y \in N_{r_\phi}(x_0)$ in the visual neighbourhood in Fig. 2 have descriptions that are *sufficiently near* the description of the reference point x_0.

For example, each of the points in the green shaded regions in Fig. 2 have intensities that are very close to the intensity of the point x_0. By contrast, many points in the purple shaded region have higher intensities (*i.e.*, more light) than the pixel at x_0, For example, consider the intensities of the points in the visual nbd represented by the green wedge-shaped region and some outlying green circular regions and the point x_4 in the purple region in Fig. 2, where

$r_\phi = 5$ low intensity difference,

[3]It is easy to prove that *a visual neighbourhood is an open set*

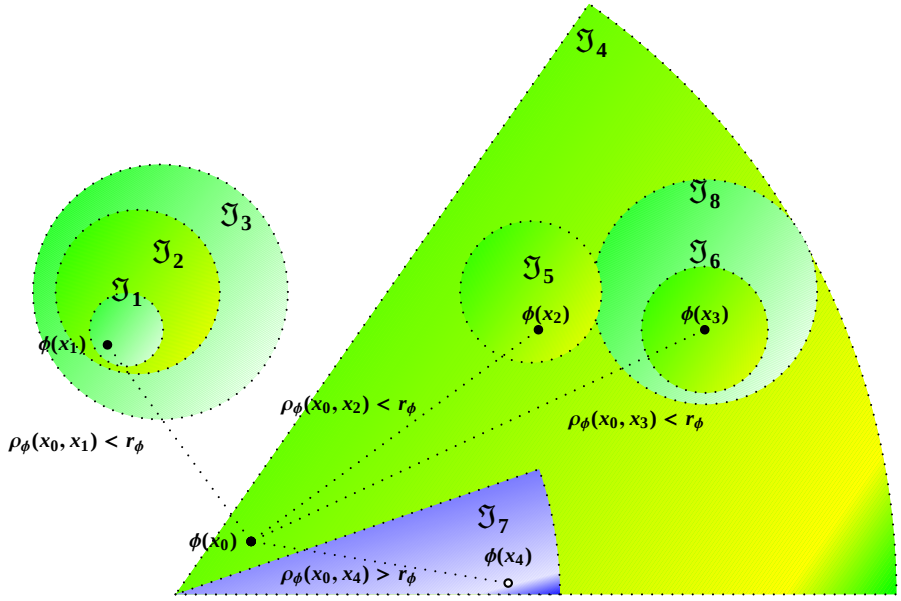

Figure 2: Sample Visual Nbd $N_{r_\phi}(x_0)$ in a Drawing

$\rho_\phi(x_0, x_1) = |\phi(x_0) - \phi(x_1)| < r_\phi$,

$\rho_\phi(x_0, x_2) = |\phi(x_0) - \phi(x_2)| < r_\phi$,

$\rho_\phi(x_0, x_3) = |\phi(x_0) - \phi(x_3)| < r_\phi$, but

$\rho_\phi(x_0, x_4) = |\phi(x_0) - \phi(x_4)| > r_\phi$, where $\phi(x_4)$ = high intensity (white).

In the case of the point x_4 in Fig. 2, the intensity is high (close to white), *i.e.*, $\phi(x_4) \sim 255$. By contrast the point x_0 has low intensity (less light), *e.g.*, $\phi(x_0) \sim 20$. Assume $r_\phi = 5$. Hence, $|\phi(x_0) - \phi(x_4)| > r_\phi$. As in the case of C. Monet's paintings[4], the distance between probe function values representing visual information extracted from image pixels can be sufficiently near a centre x_0 (perceptually) but the pixels themselves can be *far apart*, *i.e.*, not sufficiently near, if one considers the locations of the pixels.

Remark. **Filters and Grills**
In Fig. 2, observe that $\mathcal{F}_1 = \mathfrak{I}_1 \subset \mathfrak{I}_2 \subset \mathfrak{I}_3$ is a filter. Again, observe that $\mathcal{F}_2 = \{\mathfrak{I}_4, \mathfrak{I}_6, \mathfrak{I}_8\}$ is a filter. It can be shown that the set $\mathcal{G} = \{\mathfrak{I}_4, \mathfrak{I}_6, \mathfrak{I}_8\}$ is a grill.

Proof. Let $A = \mathfrak{I}_6, B = \mathfrak{I}_4$ in Fig. 2. From $\mathcal{F}_2$, we know that $\mathfrak{I}_6 \subset \mathfrak{I}_4$ and $\mathfrak{I}_4 \subset \mathcal{G}$. Then $B \in \mathcal{G}$. Observe that $\mathfrak{I}_5 \cup \mathfrak{I}_6 \in \mathcal{G}$, then $\mathfrak{I}_5 \in \mathcal{G}$ or $\mathfrak{I}_6 \in \mathcal{G}$.

[4] A comparison between Z. Pawlak's and C. Monet's waterscapes is given in Peters (2011).

In addition, let X denote the set of regions shown in Fig. 2. Obviously, $\mathcal{F} = \{\mathfrak{I}_4, \mathfrak{I}_6, \mathfrak{I}_8\}$ is a filter, if and only if, $sec(\mathcal{F})$ is a grill $\mathcal{G}_2$ on X. Further, $\mathcal{G}_3 = \{\mathfrak{I}_1, \mathfrak{I}_2, \mathfrak{I}_3\}$ is a grill, if and only if, $sec(\mathcal{G}_3)$ is a filter. □

Example 5.2. Sample Associated Sets
Let D_{ρ_ϕ} be a gap functional such that

$$D_{\rho_\phi}(A, B) \div \begin{cases} \inf\{\rho_\phi(a, b) : a \in A, b \in B\}, & \text{if } A \text{ and } B \text{ are not empty,} \\ \infty, & \text{if } A \text{ or } B \text{ is empty.} \end{cases}$$

Then the function $\nu_{D_{\rho_\phi}} : \mathcal{P}^2(X) \times \mathcal{P}^2(X) \longrightarrow [0, \infty]$ defined as

$$\nu_{D_{\rho_\phi}}(\mathcal{A}, \mathcal{B}) \div \sup_{A\in\mathcal{A}, B\in\mathcal{B}} D_{\rho_\phi}(A, B); \quad \nu_{D_{\rho_\phi}}(\mathcal{A}, \mathcal{A}) \div \sup_{A\in\mathcal{A}} D_{\rho_\phi}(A, A) = 0,$$

is an ε-approach merotopy on X. In terms of the labelled sets $\mathfrak{I}_1, \mathfrak{I}_2, \mathfrak{I}_3, \mathfrak{I}_4, \mathfrak{I}_5, \mathfrak{I}_6$ in Fig. 2, we can identify the following lower associated set E_ε in (Assoc.1) and upper associated E^ε in (Assoc.2) with respect to $\nu_{D_{\rho_\phi}}$.
(**Assoc**.1) $E_\varepsilon(\mathfrak{I}_1) = \{\mathfrak{I}_2, \mathfrak{I}_3, \mathfrak{I}_4, \mathfrak{I}_5, \mathfrak{I}_6\}$, where

$$\nu_{D_{\rho_\phi}}(\mathfrak{I}_1, \mathfrak{I}_i) < \varepsilon \text{ for } i \in \{2, 3, 5, 6\},$$

i.e., for $a \in \mathfrak{I}_1, b \in \mathfrak{I}_i, i \neq 1$, $\rho_\phi(a, b) < \varepsilon$, since the colours of all of the pixels are similar in each set $\mathfrak{I}_i \in E_\varepsilon(\mathfrak{I}_1)$ in Fig. 2. The sets in $E_\varepsilon(\mathfrak{I}_1)$ are sufficiently near $\mathfrak{I}_1$.
(**Assoc**.2) $E^\varepsilon(\mathfrak{I}_4) = \{\mathfrak{I}_7\}$, where

$$\nu_{D_{\rho_\phi}}(\mathfrak{I}_4, \mathfrak{I}_7) > \varepsilon,$$

i.e., for $a \in \mathfrak{I}_4, b \in \mathfrak{I}_7$, $\rho_\phi(a, b) > \varepsilon$, due to the fact that the green colour of each the pixels in $\mathfrak{I}_4$ is dissimilar to the purple or white colour of the pixels in $\mathfrak{I}_7$ in Fig. 2. In effect, the sets in $E^\varepsilon(\mathfrak{I}_4)$ are far apart from $\mathfrak{I}_4$ with respect to $\nu_{D_{\rho_\phi}}$.

Example 5.3. Sufficiently Near Strong p-Containment
After a manner similar to Example 4.3, let (X, ν_{ρ_ϕ}) be an ε-approach nearness on X and $p \div$ 'sufficiently near' defined for $\{A\}, \{B\} \in \mathcal{P}(X)$ such that $\nu_{\rho_\phi}(\{A\}, \{B\}) < \varepsilon$. Consider $\mathfrak{I}_1, \mathfrak{I}_2, \mathfrak{I}_3$ in Fig. 2. It is a straightforward task to verify that
(**p**.1) $\mathfrak{I}_1 \underset{p}{\subset} \mathfrak{I}_2 \subset \mathfrak{I}_3$ implies $\mathfrak{I}_1 \underset{p}{\subset} \mathfrak{I}_3$,
(**p**.2) $\mathfrak{I}_1 \subset \mathfrak{I}_2 \underset{p}{\subset} \mathfrak{I}_3$ implies $\mathfrak{I}_1 \underset{p}{\subset} \mathfrak{I}_3$,
(**p**.3) Considering only $\mathfrak{I}_1, \mathfrak{I}_2, \mathfrak{I}_3$,

$$\mathfrak{I}_1 \underset{p}{\subset} \mathfrak{I}_3 \text{ and} \mathfrak{I}_2 \underset{p}{\subset} \mathfrak{I}_3 \text{ implies } \bigcup_{i=1}^{2} \mathfrak{I}_i \underset{p}{\subset} \mathfrak{I}_3.$$

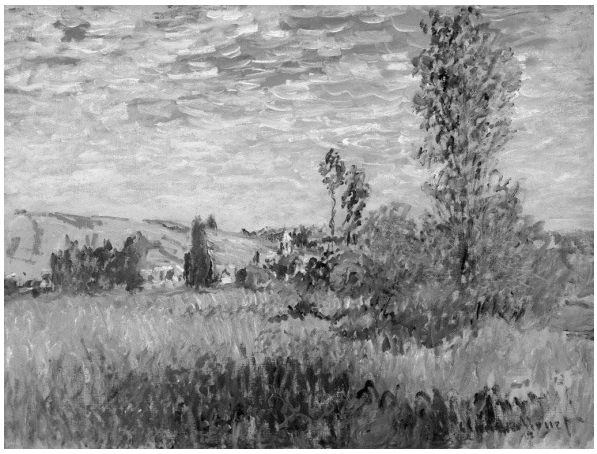

3.1: Monet meadow

3.2: Nbd $N_{r_{\phi_{grey}}}$

Figure 3: Sample Monet Meadow nbd $N_{r_{\phi_{grey}}}$, with $r_{\phi_{grey}}$=10

Example 5.4. Visual Neighbourhood in a Digital Image
Consider visual neighbourhoods in digital images, where each point is an image pixel (picture element). A pixel is described in terms of its feature values. Pixel features include grey level intensity and primary colours red, green, and blue with wavelengths 700 nm, 546.1 nm and 435.8 nm, respectively)[5], texture, and shape information. Visual information (feature values) is extracted from each pixel with a variety of probe functions.

For example, consider a xixth century, St. Martin, Vetheuil landscape by C. Monet rendered as a greyscale image in Fig. 3.1. Let $\phi_{grey}(x)$ denote a probe that extracts the greylevel intensity from a pixel x and let $r_{\phi_{grey}} = 10$. This will lead to the single visual neighbourhood represented by the green-shaded regions shown in Fig. 3.2. To obtain the visual nbd in Fig. 3.2, replace the greylevel intensity of each point sufficiently near the intensity $\phi_{grey}(x_0)$ with a green colour. The result is green-coloured visual nbd $N_{r_{\phi_{grey}}}$ in Fig. 3.2. This set of intensities in the visual nbd shown in $N_{r_{\phi_{grey}}}$ is an example of an open set contain numbers representing intensities that are sufficiently near x_0. To verify this, notice that the pixel intensities for large regions of the sky, hills and meadow in Fig. 3.1 are quite similar. This is the case with the sample pixels (points of light) x_0, x_1, x_2 in Fig. 3.2, where the in $\left|\phi_{grey}(x_0) - \phi_{grey}(x_1)\right| < r_{\phi_{grey}}$ and $\left|\phi_{grey}(x_0) - \phi_{grey}(x_2)\right| < r_{\phi_{grey}}$.

In summary, the lower associated set $E_\varepsilon(\{\{x_i\}\})$ is the set of all visual neighbourhoods of the pixel x_i in Fig. 3.2 that are descriptively ε-near each other. In addition, one can also observe

[5]The amounts of red, green and blue that form a particular colour are called *tristimulus* values. Let R, G, B denote red, green, blue tristimulus values, respectively, with green almost in the middle of the wavelengths of the visual spectrum, which is at 568 nm. Then define the following probe functions to extract the colour components of a pixel.

$$r = \frac{R}{R+G+B}, \quad g = \frac{G}{R+G+B}, \quad b = 1 - r - g.$$

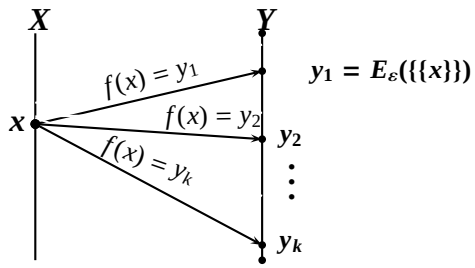

Figure 4: $f(x) = |E_\varepsilon(\{\{x\}\})| > 0$

that the upper associated set $E_\varepsilon(\{\{x_i\}\})$ contains all visual neighbourhoods that are descriptively dissimilar to x_i.

Example 5.5. Bipartite Graph for Associated Sets
Although this example continues the discussion of paintings, the proposed bipartite graph representation of associated sets is easily extended to members of any pair of nonempty sets. For example, consider classifying paintings by a particular artist by collecting together nonempty associated lower sets of sufficiently near neighbourhoods extracted from pairs of pictures. To see this, let X denote a set of query images and let Y denote a set of test images (*i.e.*, X contains pictures showing paintings, where each painting in X is compared with the paintings in the set of sample paintings Y).

The goal is to collect together those pictures in Y containing neighbourhoods of points in $y \in Y$ that are sufficiently similar to neighbourhoods of points in a picture $x \in X$. Let $N_a \in X, N_b \in Y$ denote neighbourhoods that are sufficiently near. Then construct the lower associated set $E_\varepsilon(N_a) = \{N_b, \dots\}$. A query image is similar to a test image if, and only if, $E_\varepsilon(N_a) > 0$.

Given approach spaces $(X, \nu_{D_{\rho_{\phi_{grey}}}}), (Y, \nu_{D_{\rho_{\phi_{grey}}}})$, consider a function $f : X \to Y$ defined by $f(x) = |E_\varepsilon(x)|$, where $x \in X$. Then the relation between a particular painting and one or more associated lower sets can be represented by a bipartite graph (see Fig. 4). The image set

$$O = \{f(x_i) : i \in \text{ and } |f(x_i)| > 0\}$$

can be extracted from Fig. 4. The set O has interest, since two of its members reveal the least similar and most similar paintings in relation to a particular query image. That is, $\inf\{O\}, \sup\{O\}$ function values correspond to the least similar and most similar of the paintings that are sufficiently near the query image $x \in X$.

Similarly, one can determine the collection of those paintings dissimilar to a given query picture with a nonempty associated upper set containing visual neighbourhoods taken from the query image and a test image.

References

Agronsky, S.J. (1982). A generalization of a theorem of maximoff and applications. *Trans. Amer. Math. Soc.* **273**(2), 767–779.

Beer, G., A. Lechnicki, S. Levi and S.A. Naimpally (1992). Distance functionals and suprema of hyperspace topologies. *Annali di Matematica pura ed applicata* **CLXII**(IV), 367–381.

Bourbaki, N. (1966). *Elements of Mathematics. General Topology, Part 1*. Hermann & Addison-Wesley. Paris & Reading, MA, U.S.A. i-vii, 437 pp.

Bourbaki, N. (1971). *Topologie générale, 1-4*. Hermann. Paris. Springer-Verlag published a new edition in 2007.

Bruckner, A.M. (1967). On characterizing classes of functions in terms of associated sets. *Canad. Math. Bull.* **10**(2), 227–231.

Čech, E. (1966). *Topological Spaces, revised Ed. by Z. Frolik and M. Katătov*. John Wiley & Sons. NY.

Coble, A.B. (1922). Associated sets of points. *Trans. Amer. Math. Soc.* **24**(1), 1–20.

Engelking, R. (1989). *General Topology, Revised & completed edition*. Heldermann Verlag. Berlin.

Hausdorff, F. (1914*a*). *Grundzüge der Mengenlehre*. Veit and Company. Leipzig. viii + 476 pp.

Hausdorff, F. (1914*b*). *Set Theory*. AMS Chelsea Publishing. Providence, RI. 352 pp.

Henry, C.J. (2010). Near Sets: Theory and Applications, Ph.D. dissertation, supervisor: J.F. Peters. PhD thesis. Department of Electrical & Computer Engineering.

Hocking, J.G. and G.S. Young (1988). *Topology*. Dover. NY.

Khare, M. and S. Tiwari (2010). Grill determined *L*-approach merotopological spaces. *Fund. Inform.* **48**, 1–12.

Khare, M. and S. Tiwari (2012). *L*-approach merotopies and their categorical perspective. *Demonstratio Math.* **45**(3), 699–716.

Leader, S. (1959). On clusters in proximity spaces. *Fundamenta Mathematicae* **47**, 205–213.

Lowen, R. (1997). *Approach Spaces: The Missing Link in the Topology-Uniformity-Metric Triad*. Oxford Mathematical Monographs, Oxford University Press. Oxford, UK. viii + 253pp.

Lowen, R., D. Vaughan and M. Sioen (2003). Completing quasi metric spaces: an alternative approach. *Houstan J. Math.* **29**(1), 113–136.

Naimpally, S.A. and J.F. Peters (2013). *Topology with Applications. Topological Spaces Via Near and Far*. World Scientific. Singapore.

Peters, J. F. and S. Tiwari (2012). Completing extended metric spaces: an alternative approach. *Appl. Math. Letters* **25**, 1544–1547.

Peters, J.F. (2011). How near are Zdzisław Pawlak's paintings? Merotopic distance between regions of interest. pp. 1–19. , *in* A. Skowron, S. Suraj, Eds., Intelligent Systems Reference Library volume dedicated to Prof. Zdzisław Pawlak, Springer, Berlin.

Peters, J.F. (2013). Local near sets: Pattern discovery in proximity spaces. *Math. Comp. Sci.* **7**(1), *to appear*.

Peters, J.F. and S. Tiwari (2011). Approach merotopies and near filters. *Gen. Math. Notes* **3**(1), 32–45.

Peters, J.F. and S.A. Naimpally (2012). Applications of near sets. *Amer. Math. Soc. Notices* **59**(4), 536–542.

Petrakiev, I. (2009). On self-associated sets of points in small projective spaces. *Comm. in Algebra* **37**(2), 397–405.

Tiwari, S. (Jan. 2010). Some Aspects of General Topology and Applications. Approach Merotopic Structures and Applications, supervisor: M. Khare. PhD thesis. Department of Mathematics, Allahabad (U.P.), India.

Zahorski, Z. (1950). Sur la première dérivée. *Trans. Amer. Math. Soc.* **69**, 1–54.

Theory and Applications of Mathematics & Computer Science

(ISSN 2067-2764)
http://www.uav.ro/applications/se/journal/index.php/tamcs

Theory and Applications of Mathematics & Computer Science 3 (1) (2013) 13–31

Unsupervised Detection of Outlier Images Using Multi-Order Image Transforms

Lior Shamir[a,*]

[a]*Lawrence Technological University, 21000 W Ten Mile Rd., Southfield, MI 48075, United States.*

Abstract

The task of unsupervised detection of peculiar images has immediate applications to numerous scientific disciplines such as astronomy and biology. Here we describe a simple non-parametric method that uses multi-order image transforms for the purpose of automatic unsupervised detection of peculiar images in image datasets. The method is based on computing a large set of image features from the raw pixels and the first and second order of several combinations of image transforms. Then, the features are assigned weights based on their variance, and the peculiarity of each image is determined by its weighted Euclidean distance from the centroid such that the weights are computed from the variance. Experimental results show that features extracted from multi-order image transforms can be used to automatically detect peculiar images in an unsupervised fashion in different image datasets, including faces, paintings, microscopy images, and more, and can be used to find uncommon or peculiar images in large datasets in cases where the target image of interest is not known. The performance of the method is superior to general methods such as one-class SVM. Source code and data used in this paper are publicly available, and can be used as a benchmark to develop and compare the performance of algorithms for unsupervised detection of peculiar images.

Keywords: Outlier detection, peculiar images, image analysis, image transform, multi-order transforms.
2010 MSC: 68T10, 62H35, 68T45, 62H30 .

1. Introduction

Unsupervised detection of peculiar images is the ability of a computer system to automatically detect images that are different from the other "regular" images in an image dataset. While in tasks such as image classification the system can be trained in a supervised fashion using "ground truth" samples, in unsupervised detection of peculiar images the algorithm cannot rely on data samples or models that reflect the "regular" images or the target images of interest.

The problem of detecting data points significantly different from the other data is often referred to as *outlier detection* (Hodge & Austin, 2004). Many established algorithms consider outlier

*Corresponding author
Email address: lshamir@mtu.edu (Lior Shamir)

detection as a by-product of clustering algorithms by searching for background noise samples that do not belong in a cluster (Aggarwal & Yu, 2000; Guha, Rastogi & Shim, 2001). Other methods are based on searching for samples that do not belong in a cluster and are also not background noise, but are substantially different from the other samples in the dataset (Breunig et al., 2000; Knorr & Ng, 1999; Fan et al., 2006). While many of the outlier detection algorithms were designed and tested using lower dimensionality, other methods aim at automatic outlier detection in higher dimensionality data (Aggarwal & Yu, 2001; Roth, 2005; Fan, Cehn & Lin, 2005; Lukashevich, Nowak & Dunker, 2009). Applications of outlier detection include credit card fraud, network intrusion detection, surveillance, financial applications, cell phone fraud, safety critical systems, loan application processing, defect detection in factory production lines, and sensor networks (Zhang et al., 2007).

While outlier detection has been studied in the context of a broad range of applications, less work has yet been done on unsupervised detection of peculiar images in image datasets. Here we describe a generic method that can be used for automatic detection of peculiar images in image datasets based on a large set of image content descriptors extracted from the raw pixels, image transforms, and compound image transforms. Applications include, for instance, the search for peculiar cells or tissues in large datasets of microscope images, which can be used to detect phenotypes of particular scientific interest (d'Onofrio & Mango, 1984; Carpenter, 2007; Jonesa et al., 2009).

When the target image is known, the task of detecting a peculiar image can be related to the problem of Content-Based Image Retrieval, and numerous effective methods of measuring similarities between images in the context of CBIR have been proposed (Bilenko, Basu, & Mooney, 2004; Kameyama et al., 2006). However, since in this study the detection of a peculiar image in an image dataset should be done automatically in an unsupervised manner, no assumptions can be made neither about the target image nor about the context of the images in the data base. That is, the computer system should automatically characterize the "typical" image in the dataset, and detect images that are different from it. Since no pre-defined model of the data can be used, effective systems for unsupervised automatic detection of peculiar images need to extract different image features that will cover different aspects of the image content, and thus be able to characterize and analyze a broad spectrum of image data.

Here we use a large set of image content descriptors extracted from the raw images, image transforms, and multi-order transforms, and apply a statistical analysis to weight the different image features by their ability to reflect the data and detect peculiar images. The primary advantage of the method is its generality, which makes it effective for the analysis of a broad variety of image datasets without the need for tuning or adjustments. In Section 2 we briefly describe the set of image features and multi-order transform model used in this study, in Section 3 we describe the unsupervised detection of the peculiar images, in Section 4 the performance evaluation method of the proposed algorithm is discussed, and in Section 5 the experimental results are presented.

2. Image features

The set of image content descriptors used in this study is based on the feature set used by the *wndchrm* algorithm, which is a large set of numerical image content descriptors that cover a broad

range of aspects of the visual content (Shamir et al., 2008a; Orlov et al., 2008; Shamir et al., 2010). Basically, the *wndchrm* feature set includes several generic image features such as high-contrast features (object statistics, edge statistics, Gabor filters), textures (Haralick, Tamura), statistical distribution of the pixel values (multi-scale histograms, first four moments), factors from polynomial decomposition of the image (Chebyshev statistics, Chebyshev-Fourier statistics, Zernike polynomials), Radon features, and fractal features. A detailed description of these image content descriptors and the way they are used in the context of the *wndchrm* feature set is available in (Shamir et al., 2008a; Orlov et al., 2008; Shamir et al., 2010; Shamir, 2008; Shamir et al., 2009). The reason for using a large set of features is that the search for peculiar images is unsupervised, and no assumptions can be made regarding the possible difference between the peculiar and non-peculiar images. Therefore, it is important that the set of image content descriptors is comprehensive enough so that at least some of the image features will be likely to sense differences between a regular and a peculiar image in a given image dataset.

As will be discussed in Section 5, a key contributor to the ability of the method proposed in this paper to detect peculiar images in an unsupervised fashion is the extraction of the image content descriptors not just from the raw pixels, but also from image transforms and compound image transforms. The extraction of image features from compound image transforms has been shown to contribute significantly to the performance of general-purpose image classifiers (Shamir et al., 2008a; Orlov et al., 2008; Shamir et al., 2010, 2009), and can therefore be effective for peculiar image detection in cases where the differences between the typical and the peculiar image should be determined automatically, without using "ground truth" samples or any other prior knowledge about the data. The image transforms include the Fourier, Chebyshev, Wavelet, and the edge-magnitude transform, as well as multi-order transform combinations. The combinations of transforms include the Fourier transform of the Chebyshev transform, the wavelet transform of the Chebyshev transform, the Fourier transform of the wavelet transform, the wavelet transform of the Fourier transform, the Chebyshev transform of the Fourier transform, and the Fourier and Chebyshev transforms of the edge magnitude transform. A detailed description of the tandem transform combinations can be found in (Shamir et al., 2010; Shamir, 2008), and the total number of images features extracted using these transforms is 2659 (Shamir et al., 2008a; Shamir, 2008). The length of the chain of transforms is limited to the first and second order of the image transforms, as experiments showed that using compound transforms with order higher than two typically does not contribute to the informativeness of the image analysis system (Shamir et al., 2009). The effect of using the multi-order image transforms on the ability of the algorithm to automatically detect peculiar images will be discussed in Section 5.

For color images we used a color transform, which is based on transforming the RGB pixels into the HSV space, followed by classification of the HSV triplets into one of 16 color classes using fuzzy logic modeling of the human perception of these colors (Shamir et al., 2006). Then, the Fourier, Chebyshev, and wavelet transforms of the color transform are computed, and the set of image features is extracted as described in (Shamir et al., 2010). When the color transform is also used, the total number of image features is 3658 (Shamir et al., 2010). Figure 1 illustrates the paths of the transforms and compound transforms used by the feature set.

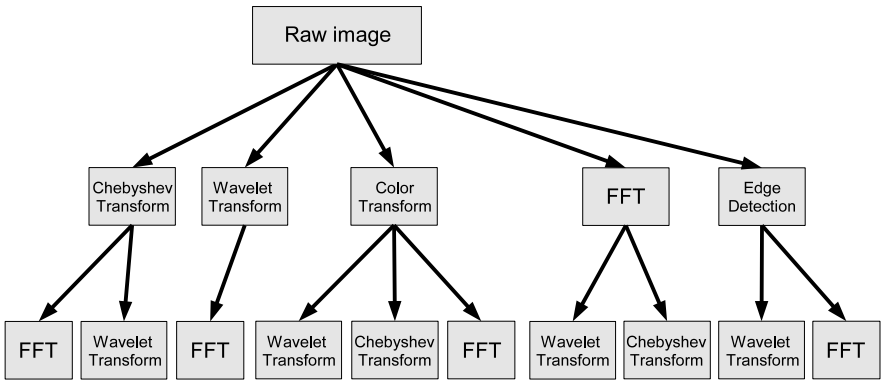

Figure 1. Paths of multi-order image transforms.

3. Automatic detection of peculiar images

In order to automatically detect peculiar images, it is first required to characterize the "typical" image in the dataset. Since many image features are used without prior knowledge about the dataset, it can be assumed that not all content descriptors are relevant to the image dataset at hand, and might represent noise. Therefore, it is required to select the image features that are the most informative, and can potentially discriminate between peculiar and non-peculiar images.

In the first stage of the algorithm, all image features are normalized to the interval [0, 1], so that the differences between the values of different image features can be compared without introducing a numerical bias. For instance, if the values of one image feature are in the range of [0, 1000] while the values of another are in the range of [0, 10], a numerical difference of 5 between the values of the first feature extracted from two different images can be considered small, while the same numerical difference can be much more substantial for the second feature, in which it is half of the entire range.

In the next step, the mean, median, and variance of each image feature are computed. To characterize the "typical" feature values of an image in the dataset, the highest 5% and the lowest 5% of the values of each image feature are ignored when computing the mean and standard deviation, so that extreme values that results from noise, artifacts, or peculiar images will not affect the mean and variance of the "typical" images.

After these values are computed, each image in the dataset is compared to the "typical" image using Equation 3.1

$$D_i = \sum_{f \in F} (1 - \sigma_f)^k \cdot \frac{|f_i - \overline{f}|}{\sigma_f}, \tag{3.1}$$

where D_i is the dissimilarity value of image i from the "typical" image in the dataset, f is a feature in the feature set F, $\overline{f}$ is the median of the values of feature f in the given image dataset, f_i is the value of the feature f computed from the image i, σ_f is the standard deviation of feature f, and k is a constant value set to 25. The value of k will be thoroughly discussed in Section 5. The D_i dissimilarity value can be conceptualized as the sum of Z scores computed for each feature separately, such that each score's contribution to the total distance is inversely dependent on

the standard deviation. That is, features that have lower standard deviation are considered more "representative" features, while feature that their values are more sparsely distributed are assumed to provide a weaker representation of the "typical" image and are therefore assigned with a lower score and have a weaker affect on the dissimilarity value.

Clearly, image features that their values are constant across the dataset (and therefore $\sigma = 0$) cannot provide any useful information in this model, and can therefore be safely ignored without affecting the performance. On the other hand, the values of some of the other features can be sparsely distributed across the image dataset, and therefore the median of these values cannot be considered as a value that reliably represents the typical image. For that reason, the effect of each image feature is weighted by its standard deviation, which is used as an assessment of the feature's informativeness and its ability to characterize the typical image.

While in Equation 3.1 the effect of features that their values are sparsely distributed is weakened by using the standard deviation as a measurement of their informativeness, it can be assumed that many of the features will not be informative for a given image dataset at hand, and therefore the high number of irrelevant features can add noise to the analysis and negatively affect the performance. In order to reduce the effect of non-informative features, 90% of the features with the highest σ are ignored, and the remaining 10% are used by Equation 3.1 to compute the distance between a given image and the "typical" image in the dataset. Since the image features are also weighted by their standard deviation, the performance of this method is not highly sensitive to small changes in the number of features that are used, as will be discussed in Section 5. This approach of combining feature selection and feature weighting is conceptually similar to the approach of the feature selection in the *wndchrm* image classifier (Shamir et al., 2008a; Orlov et al., 2008; Shamir et al., 2010).

In many cases, using σ to assess the informativeness of the features and their ability to differentiate between a peculiar and a typical image might not be optimal and can lead to the sacrifice of some of the information. For instance, if the values of a certain image feature range between 0 and 0.8 for most images in the dataset, but is always 1 for a certain peculiar image, this feature could have been effectively used to detect the peculiar image, but will be assigned with a low score due to the sparse distribution of the values. On the other hand, features can be assigned with high scores due to the consistency of their values, while these image features might have little ability to differentiate between a typical and a peculiar image. Since the goal of the method described in this paper is to detect peculiar images in an unsupervised fashion, no assumptions or prior knowledge about the data can be used, and therefore the image content descriptors cannot be selected or scored based on a target peculiar image. However, by using a large set of image features, it can be expected that some of the features that are assigned with high scores will be able to differentiate between a peculiar and a typical image. This will be demonstrated in Section 5.

In summary, the following pseudo code summarizes the outlier detection algorithm:

Step 1: Compute image features for all images.

Step 2: Reject the lowest and highest 5% values of each feature.

Step 3: Compute the mean M_f of the values of each feature f.

Step 4: Compute the σ_f of the values of each feature f.

Step 5: Reject 90% of the features with the lowest σ.

Step 6: Compute d for each image I such that $d = \sqrt{\sum_f (1-\sigma_f)^k \cdot \frac{(I_f - M_f)}{\sigma_f}}$.

Step 7: Sort the images in the dataset by d.

The computational complexity of the algorithm is $O(F \cdot I \log I)$, where I is the number of images and F is the number of features computed for each image. The computational complexity is determined by the complexity of sorting all values of each feature, which is the most computationally demanding task in the algorithm described above. The bottleneck of the process, however, is the computational complexity of the Wndchrm feature set, which is much more complex as described in (Shamir et al., 2008a, 2009).

4. Performance evaluation

In order to test the performance of the proposed method, several different image datasets were used. These datasets include the Brodatz texture album (Brodatz, 1966), the COIL-20 object image collection (Nene, Nayar & Murase, 1996), JAFFE and AT&T face datasets (Samaria & Harter, 1994; Lynos et al., 1998), the MNIST handwritten digit collection (LeCun et al., 1998; Liu et al., 2003), and a dataset of digitized paintings of Van Gogh, Monet, Dali, and Pollock Shamir et al. (2010). Since the MNIST dataset contains a large number of images, a subset of 100 images from the first two classes (0 and 1) were used in the experiment. For microscopy images we used the CHO (Chinese Hamster Ovary) dataset (Boland & Murphy, 2001), consisting of fluorescence 512×382 microscopy images of different sub-cellular compartments, and the Pollen dataset (Duller et al., 1999), which is a dataset of 25×25 images of geometric features of pollen grains. The CHO dataset might not be considered a perfect representation of biological content (Shamir et al., 2011), but it is used in this study for general-purpose outlier detection. These two datasets are available for download as part of the IICBU-2008 benchmark suite at `http://ome.grc.nia.nih.gov/iicbu2008` (Shamir et al., 2008b), and sample images of the different classes are shown by Figures 2 and 3. The image datasets used in this study are listed in Table 1.

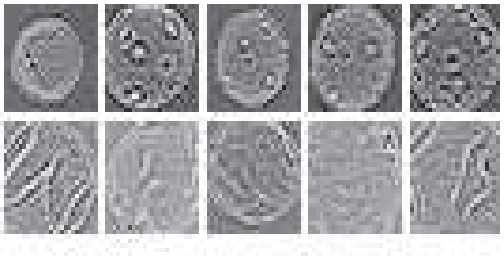

Figure 2. Sample images of class “obj_198” (top) and “obj_212” (bottom) taken from the pollen dataset.

Table 1. Image datasets used for the experiments.

dataset	typical class	peculiar class	images per class
Pollen	obj_198	obj_212	45
CHO	giantin	hoechst	69
JAFFE	KA	KL	22
AT&T	1	2	10
Painters 1	Pollock	Dali	30
Painters 2	Monet	Van Gogh	30
Brodatz 1	Bark	Brick	4
Brodatz 2	Wood	Wool	4
MNIST	0	1	100
COIL-20	obj1	obj2	71

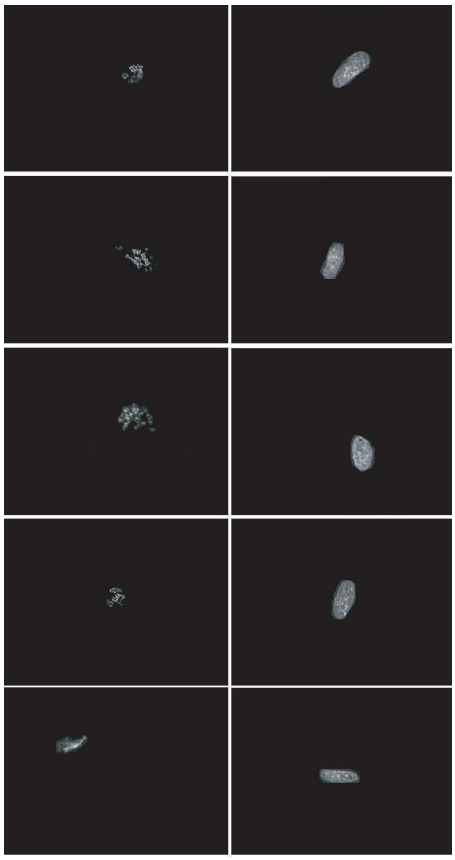

Figure 3. Sample images of giantin (left) and hoechst (right) taken from the CHO dataset.

As the table shows, these datasets were used such that two classes from each dataset were selected: one class was used as the "typical" class and the other as a pool of "peculiar" images.

In each run the tested dataset included all images from the typical class, and one image from the peculiar class. The experiment was repeated for each image in the peculiar class, such that in each run a different image from the peculiar class served as the peculiar image. For instance, the AT&T face dataset has 10 images in each class, and therefore it was tested 10 times such that in each run all 10 images of person *1* were used and one image of person *2* (a different image in each of the 10 runs). The goal of the algorithm was to automatically detect the single image of person *2* among the dataset of 11 images (10 images of person *1* and one image of person *2*).

The performance was evaluated by the number of times the algorithm correctly detected the peculiar image in the set (which included the "typical" images and the one "peculiar" image), divided by the total number of images in the peculiar class. Another performance metrics used in this study is the rank-10 detection accuracy, which was measured as the percentage of the cases in which the peculiar image was among the first 10 candidates with the highest dissimilarity value as determined by Equation 3.1.

5. Results

The performance of the automatic detection of peculiar images was evaluated as described in Section 4, and the rank-1 and rank-10 detection accuracies for each of the tested datasets are listed in Table 2.

Table 2. Rank-1 and rank-10 accuracy of the detection of the peculiar image.

Dataset	Rank-1 accuracy	Rank-10 accuracy
Pollen	29/45	34/45
CHO	57/69	69/69
Jaffe	16/22	22/22
AT&T	10/10	10/10
Painters 1	26/30	30/30
Painters 2	0/30	18/30
Brodatz 1	4/4	4/4
Brodatz 2	4/4	4/4
MNIST	29/100	92/100
COIL-20	38/71	71/71

As the table shows, in almost all cases the proposed algorithm was able to automatically detect the peculiar images in accuracy significantly better than random. For instance, with the Pollen dataset the algorithm was able to automatically find the peculiar image in 29 times out of 45 attempts (each attempt with a different image), and the rank-10 detection was accurate in 34 times. The noticeable exception is the second datasets of painters, which consists of paintings of Monet and Van Gogh. In that case, the proposed method was not able to automatically detect any of the tested Van Gogh paintings in a set of Monet paintings, and the rank-10 accuracy was 60%. Since Monet and Van Gogh were inspired from each other, their artistic styles are similar to each other, and it usually requires knowledge in art to differentiate between the works of the two painters.

The other painter dataset that was tested demonstrated a much higher detection accuracy since the two painters, Jackson Pollock and Salvador Dali, belong in different schools of art (Abstract Expressionism and Surrealism, respectively) and the differences between their styles are highly noticeable even without any previous knowledge or training in art.

The results specified in Table 2 demonstrate the generality of the method and its ability to handle very different image datasets in a fully automatic fashion, and without the need to select or tune parameters. The generality of the method can also be demonstrated by the different classes of the Pollen dataset. While the results in Table 2 are based on obj_198 as the "typical" class and "obj_212" as the peculiar class, the pollen dataset includes seven classes (Shamir et al., 2008b). Table 3 shows the rank-1 detection accuracy of all combinations of the seven classes in the pollen dataset, such that each cell is the detection accuracy when the row the "typical" class and the column is the "peculiar" class. As the table shows, the detection accuracy is significantly higher than random in all combinations of "typical" and "peculiar" classes, demonstrating the generality of the proposed method.

Table 3. Rank-1 detection accuracy (%) of all combinations of typical and peculiar classes using the pollen dataset.

Regular\Peculiar	198	212	216	360	361	405	406
198	-	64	51	67	53	69	67
212	55	-	55	65	58	67	67
216	63	67	-	63	58	64	64
360	61	64	67	-	64	72	69
361	57	67	65	67	-	72	69
405	66	71	73	69	67	-	71
406	63	59	65	69	69	61	-

As discussed in Section 3, 90% of the image features with the highest σ are ignored. Changing the number of features that are rejected and not used by the image dissimilarity evaluation of Equation 3.1 can change the dissimilarity value determined by the Equation for each image, and consequently affect the performance of the algorithm. Figures 4 and 5 show the rank-1 and rank-10 detection accuracy of the peculiar images when the number of used features is changed.

As the graphs show, while the peculiar image detection accuracy of some image datasets peaks when 10% of the features are used, in other datasets such as MNIST or COIL-20 the detection accuracy peaks when 40% of the features are used. In the case of MNIST, the rank-1 detection accuracy was elevated from 29% when 10% of the features were used to 94% with 40% of the image features. This shows that the detection of peculiar images can be optimized if the number of used image features is adjusted for the specific dataset. However, since the detection of the peculiar image is unsupervised, and in many cases the target peculiar image is unknown, adjusting the parameters for optimizing the performance based on sample target peculiar images might not be possible, and it is therefore required to use a general pre-defined parameter setting as was done for the performance figures reported in Table 2.

Another value that was determined experimentally is the K values in Equation 3.1. Figures 6

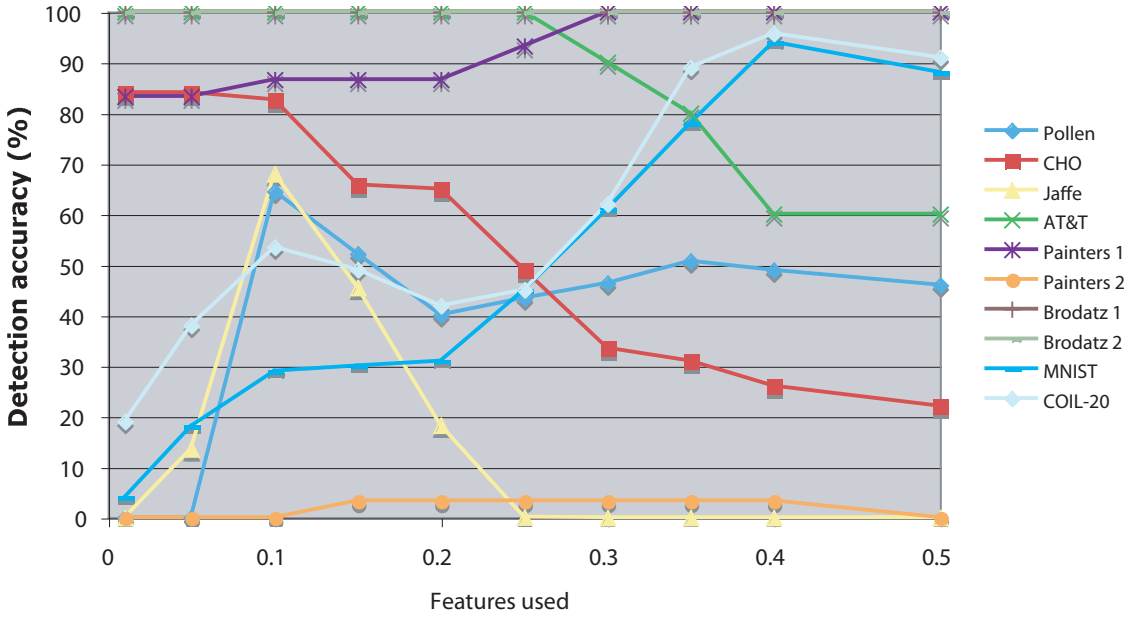

Figure 4. The rank-1 detection accuracy of the peculiar image as a function of the amount of features used.

and 7 show the rank-1 and rank-10 detection accuracy of the peculiar image as a function of the value of this parameter. In all cases, 10% of the image content descriptors were used as described in Section 3.

As the graphs show, the detection accuracy of the CHO dataset drops as the value of K increases, and the detection of a Dali painting in a set of Jackson Pollock paintings also peaks when the value of K is low. However, in most cases the detection accuracy of the peculiar image reaches its maximum when the value of K is around 25. In some of the tested image datasets, such as the Brodatz texture datasets and the rank-10 of the *Painters 1* and COIL-20 datasets, the detection accuracy of the peculiar image remained perfect regardless of the value of K.

A single peculiar image is expected to be detected more easily among a smaller dataset of regular images. That is, finding a peculiar image hidden in a dataset of millions of images is expected to be a more difficult task than finding a peculiar image in a dataset of just a dozen regular images. On the other hand, the presence of a large number of regular images allows the algorithm to find the image features that can discriminate between peculiar and regular images, and better estimate the weights of the features by their informativeness and ability to discriminate between a regular and a peculiar image as described in Section 3. To study the effect of the number of the regular images in the dataset we used the MNIST dataset, which provides a sufficient number of images of handwritten digits "0" and "1". Figure 8 shows the rank-1 and rank-10 detection accuracy of a peculiar image when changing the number of regular images in the dataset using 1000 images of the handwritten digit "0".

As the graph shows, the detection accuracy generally drops as more regular images are added

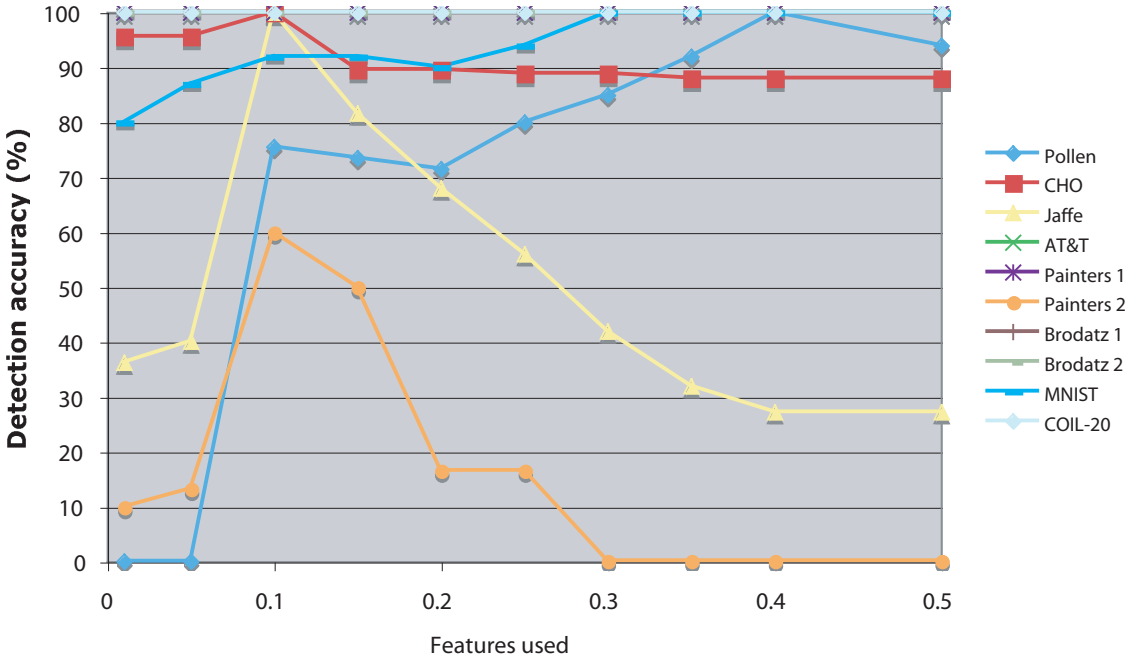

Figure 5. The rank-10 detection accuracy of the peculiar image as a function of the amount of features used.

to the dataset. Clearly, this is due to the lower difficulty of finding a peculiar image in a dataset of 50 images compared to correctly finding a single peculiar image among a dataset of 1000 regular images. However, while the rank-10 accuracy decreases as the number of regular images gets higher, the rank-1 detection accuracy drops to ~30% at around 80 regular images, but marginally changes when more regular images are added to the dataset. This can be due to the effect of the better weights assigned to the image features when the number of non-peculiar images in the dataset increases, which improve the ability of the algorithm to characterize the "typical" image in the dataset and differentiate it from peculiar images.

It should be noted, however, that while a higher number of regular images improves the feature weights, it also increases the probability that one the regular images in the dataset will be assigned with a high dissimilarity value computed by Equation 3.1. Since the algorithm aims to detect the irregular images in an unsupervised fashion, any difference between one of the images in the dataset and the "typical" image might lead to the detection of that image as "peculiar". For instance, in the MNIST dataset of the handwritten digit "0" the 10 most common images that were detected by the proposed algorithm as peculiar are shown in Figure 9.

As the figure shows, some of these handwritten digits are noticeably different from a standard handwritten digit "0". For instance, the top left digit has a black dot near it, while other images of handwritten "0" feature incomplete circles or thick lines. These images can confuse the algorithm since they are different from the typical image of the digit "0". Repeating the same experiment with a dataset of 100 manually selected "0" images that seemed relatively uniform led to perfect

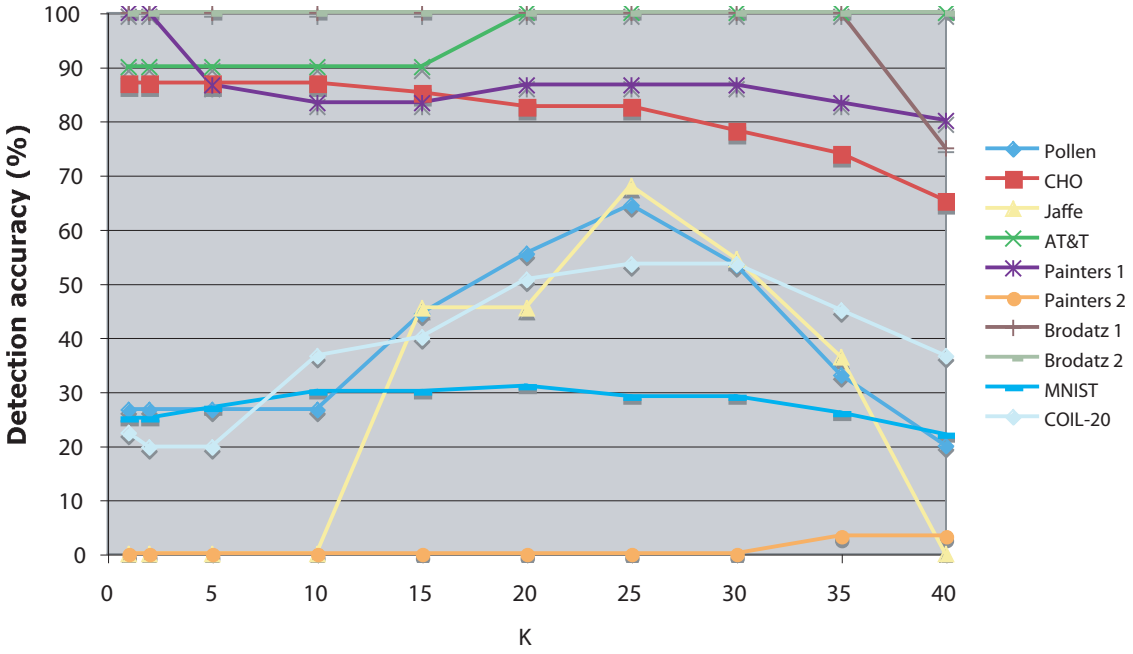

Figure 6. The rank-1 detection accuracy of the peculiar image as a function of K.

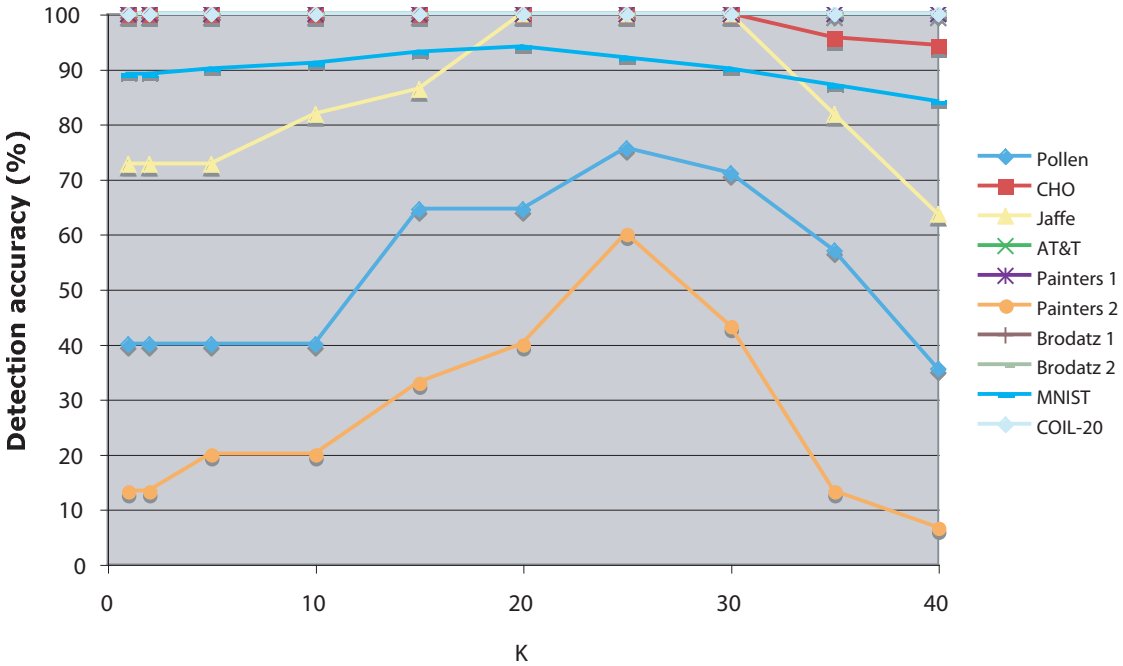

Figure 7. The rank-10 detection accuracy of the peculiar image as a function of K.

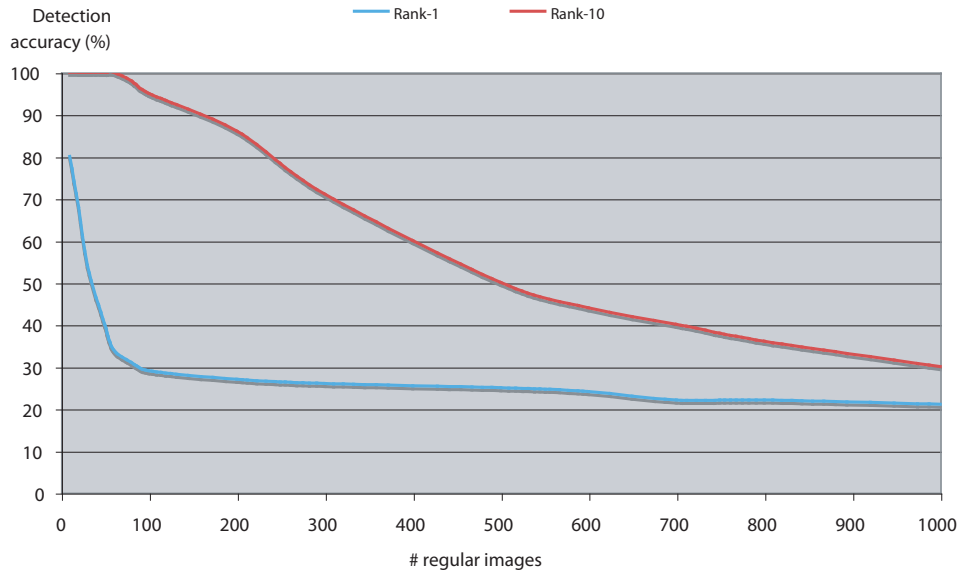

Figure 8. Rank-1 and rank-10 accuracy as a function of the number of regular images using the MNIST handwritten digits dataset using 10% of the image features.

Figure 9. The 10 most different images in the dataset of 1000 regular images of handwritten "0" digit.

detection accuracy of the "1" images.

Similarly, the most peculiar images of the CHO dataset and the AT&T dataset are shown in Figures 10 and 11, respectively. As the figures show, in the AT&T dataset the images are relatively similar to each other, and it is difficult to identify specific images that are significantly more different from the rest of the images. However, in the CHO dataset the peculiar images are noticeably different from the "typical" giantin images showed in Figure 3.

As showed by Figure 5, the detection of an image of the handwritten digit "1" in a large set of images of the handwritten digit "0" can be improved when using 40% of the image features. Figure 12 shows the detection accuracy when 40% of the image content descriptors are used.

As the figure shows, when using 40% of the features the detection accuracy also drops as the number of regular images gets larger, but the detection accuracy is significantly higher compared to the detection accuracy when using just 10% of the image content descriptors. The rank-10

Figure 10. The 10 most different images in the AT&T dataset. The leftmost image is the most peculiar.

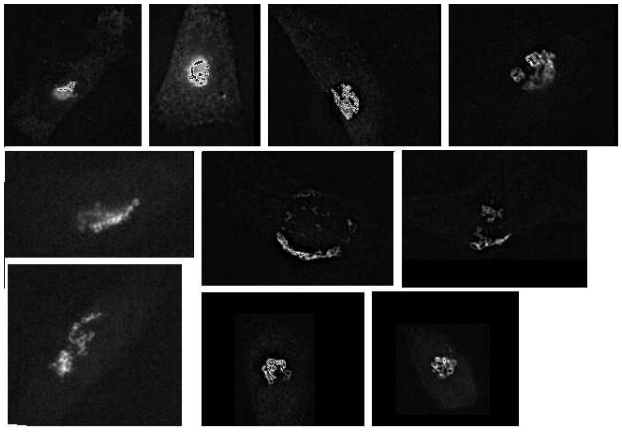

Figure 11. The 10 most different images in the CHO (giantin) dataset. The upper left image is the most peculiar and the lower right image is the least peculiar of the 10 samples.

accuracy, however, remains steady at 100% regardless of the number of regular images among which the peculiar image should be detected.

A key element in the proposed algorithm is the use of the large set of image features extracted from the raw pixels, but also from image transforms and compound transforms. To test the contribution of the features extracted from transforms and compound transforms, the performance of the proposed method was tested using features extracted from the raw pixels only, raw pixels and transforms, and raw pixel, transforms, and transforms of transforms. Table 4 shows the rank-1 and rank-10 detection accuracy when using image features computed using the raw pixels alone, and Table 5 shows the performance of the method when using also the image features extracted from the first-order image transforms. Table 2 shows the detection performance when using the raw pixels, image transforms, and transforms of transforms.

As the tables show, the use of image features extracted from transforms and multi-order image transforms has a significant effect on the performance of the method, and demonstrates the informativeness of standard image features extracted not just from the raw pixels, but also from image transforms and compound transforms (Rodenacker & Bengtsson, 2003; Gurevich & Koryabkina, 2006; Shamir et al., 2010, 2009).

5.1. Comparison the previous methods

The performance of the peculiar image detection method was also compared to the performance of one-class SVM (Scholkopf et al., 2001). The experiments were done with the LibSVM

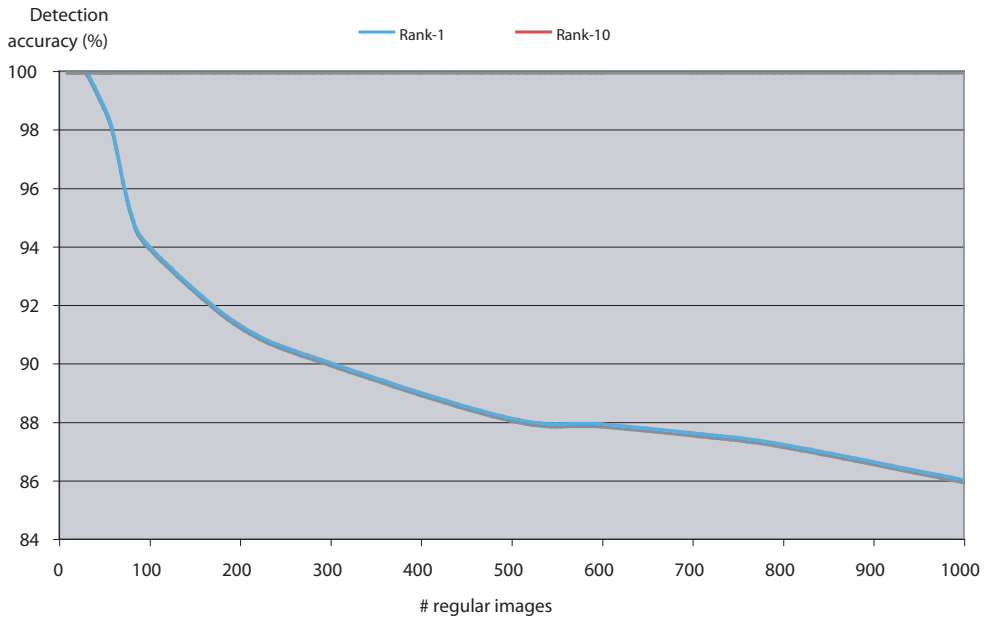

Figure 12. Rank-1 and rank-10 accuracy as a function of the number of regular images using the MNIST handwritten digits image dataset using 40% of the image features.

Table 4. Rank-1 and rank-10 accuracy of the peculiar image detection when using image features extracted from the raw pixels only.

Dataset	Rank-1 accuracy	Rank-10 accuracy
Pollen	11/45	19/45
CHO	21/69	36/69
Jaffe	9/22	14/22
AT&T	4/10	10/10
Painters 1	16/30	23/30
Painters 2	0/30	14/30
Brodatz 1	4/4	4/4
Brodatz 2	4/4	4/4
MNIST	9/100	56/100
COIL-20	11/71	44/71

support vector machine library using the "one-class" option with RBF (γ=5) and polynomial (d=5) kernels, where *nu* was set to 0.5 (Scholkopf et al., 2001; Fan, Cehn & Lin, 2005). The value K in Equation 3.1 was set to 25. Figure 13 shows the rank-1 detection accuracies using the method described in this paper and the one-class SVM with the two kernels.

As the graph shows, the detection using weighted distances from the means as described in this paper is substantially better compared to one-class SVM. The better performance when using the weighted distances from the means can be explained by the ability of the weighted feature space to

Table 5. Rank-1 and rank-10 accuracy of the peculiar image detection when using image features extracted from the raw pixels and image transforms.

Dataset	Rank-1 accuracy	Rank-10 accuracy
Pollen	18/45	25/45
CHO	39/69	53/69
Jaffe	13/22	22/22
AT&T	8/10	10/10
Painters 1	22/30	26/30
Painters 2	0/30	17/30
Brodatz 1	4/4	4/4
Brodatz 2	4/4	4/4
MNIST	29/100	92/100
COIL-20	38/71	68/71

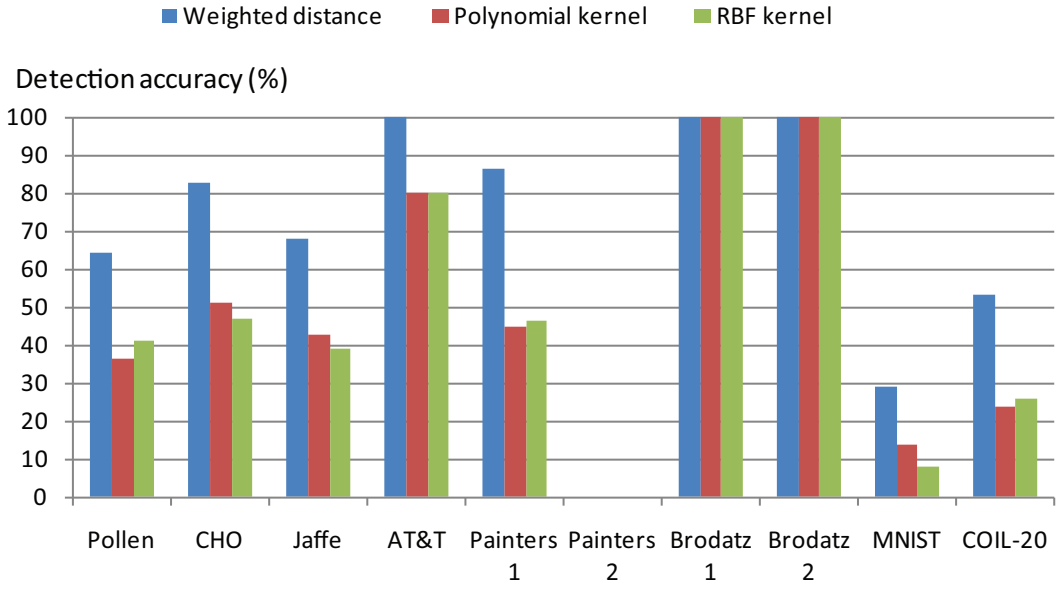

Figure 13. Detection accuracy using the proposed method and one-class SVM using the image feature set.

work efficiently when the variance in the informativeness of the different image features is large. These results are in agreement with previous experiments of automatic image classification using the large image feature set used in this study (Shamir et al., 2010), which also indicated that SVM classifiers have difficulty to effectively handle the strong variance in the informativeness of the image features included in the large feature set. The significant effect of assigning weights to the features compared to using a non-weighted feature space is also discussed in (Orlov et al., 2008;

Shamir et al., 2010).

6. Conclusions

This paper describes a method that applies multi-order image transforms to unsupervised detection of peculiar images in image datasets. The detection of the peculiar images is done in an unsupervised fashion, without prior knowledge that can be used to define the peculiarity of an image in the context of the given image analysis problem at hand. This approach can be useful in cases where it is required to detect unusual images, in the absence of a clear definition of what an unusual image is or how a "peculiar" image is different from a "typical" image in the dataset. For instance, screens in Cell Biology might result in microscopy images of very many cells, and the researcher might be interested in detecting the irregular and uncommon phenotypes (d'Onofrio & Mango, 1984). In many cases the phenotypes of the highest scientific interest can be "new" types of cells, which the researcher has never seen before, and therefore cannot characterize or use previous samples to train a machine vision system to detect. Other examples can include automatic search for peculiar astronomical objects in image datasets acquired by autonomous sky surveys driven by robotic telescopes, or uncommon ground features in datasets of satellites images of the Earth or other planets. Future work will include the application of the proposed system to practical tasks in biology, astronomy, and remote sensing.

The experiments described in this paper show that the detection accuracy of the peculiar image can in some cases be improved if the parameters are adjusted for a specific dataset. However, the pre-defined parameter settings used in this study demonstrated detection accuracy significantly better than random, and showed that in some cases the rank-10 detection accuracy can be as high as 100%. This shows that image features extracted from multi-order image transforms can be used to automatically detect peculiar images in image datasets without using any prior knowledge about the regular images, but more importantly, without any prior knowledge about the target peculiar images.

One limitation of this method is that since the detection of the peculiar image is done in an unsupervised fashion, the feature representation of the regular images should be similar to each other so that the algorithm can differentiate between them and the peculiar image. That is, the variation among the regular images should be smaller than the difference between the peculiar images and the regular images.

Another downside of the method described in this paper is its relatively high computational complexity. Since no prior knowledge about the images can be used, a large and comprehensive set of image features is computed for each image in order to cover many different aspects of the visual content, and then select the most informative features that can differentiate between a regular and a peculiar image. Computing the full set of image content descriptors and transforms can be a computationally expensive task. For instance, computing the feature set for a single 256×256 image takes ~100 seconds using a 2.6GHZ AMD Opteron with 2 GB of RAM. A more comprehensive analysis of the response-time as a function of the image size is available in (Shamir et al., 2008a).

7. Acknowledgments

This research was supported in part by the Intramural Research Program of the NIH, National Institute on Aging, and NSF grant number 1157162.

References

Aggarwal, C.C. and P. Yu (2000). Finding generalized projected clusters in high dimensional spaces. *Proc. ACM Intl. Conf. on Management of Data*, pp. 70–81.

Aggarwal, C.C. and P.S. Yu (2001). Outlier detection for high dimensional data. *ACM SIGMOD* **30** pp. 37–46.

Bilenko, M., S. Basu and R. Mooney (2004). Integrating constraints and metric learning in semi-supervised clustering. *Proceedings of the 21st International Conference on Machine Learning*, pp. 81–88.

Boland, M.V. and R. F. Murphy (2001). A Neural Network Classifier Capable of Recognizing the Patterns of all Major Subcellular Structures in Fluorescence Microscope Images of HeLa Cells. *Bioinformatics* **17**, 1213-1223.

Breunig, M.M., H. P. Kriegel, R. T. Ng and J. Sander (2000). LOF: Identifying density-based local outliers. *ACM SIGMOD* **29**, 93–104.

Brodatz, P. Textures, Dover Pub., New York, NY, 1966.

Carpenter, A.E. (2007) Image-based chemical screening. *Nature Chemical Biology* **3**, 461–465.

d'Onofrio, G. and G. Mango (1984). Automated cytochemistry in acute leukemias. *Acta Haematologica* **72**, 221–230.

Duller., A.W.G., G.A.T Duller, I. France and H.F. Lamb (1999). A pollen image database for evaluation of automated identification systems. *Quaternary Newsletter* **89**, 4–9.

Fan, H., O.R. Zaiane, A. Foss and J. Wu (2006). A nonparametric outlier detection for effectively discovering top-N outliers from engineering data. *Proc. Advances in Knowledge Discovery and Data Mining*, pp. 557–566.

Fan, R.E., P.H. Chen and C.J. Lin (2005). Working set selection using the second order information for training SVM. *Journal of Machine Learning Research* **6**, 1889–1918.

Guha, S. (2001). Cure: an efficient clustering algorithm for large databases. *Information Systems* **26**, 35–58.

Gurevich, I.B. and I.V. Koryabkina (2006). Comparative analysis and classification of features for image models. *Pattern Recognition and Image Analysis* **16**, 265–297.

Hodge, V. and J. Austin (2004). A survey of outlier detection methodologies. *Artificial Intelligence Review* **22**, 85–126.

Jones, T.R., A.E. Carpenter, M.R. Lamprecht, J. Moffat, S. J. Silver, J. K. Grenier, A.B. Castoreno, U.S. Eggert, D.E. Root, P. Golland, and D.M. Sabatini (2009). Scoring diverse cellular morphologies in image-based screens with iterative feedback and machine learning. *Publications of the National Academy of Science* **106**. 1826–1831.

Kameyama, K., S.N. Kim, M. Suzuki, K. Toraichi, and T. Yamamoto (2006). Content-based image retrieval of Kaou images by relaxation matching of region features. *International Journal of Uncertainty, Fuzziness and Knowledge-Based Systems* **14**, 509–523.

Knorr E. and R. Ng (1999). Finding intensional knowledge of distance-based outliers. *Proc. VLDB*, pp. 211–222.

LeCun, Y., L. Bottou, Y. Bengio and P. Haffner (1998). Gradient-based learning applied to document recognition. *Proceedings of the IEEE* **86**, 2278–2324.

Liu, C.L., K. Nakashima, H. Sako and H. Fujisawa (2003). Handwritten digit recognition: benchmarking of state-of-the-art techniques. *Pattern Recognition* 36, 2271–2285.

Lukashevich, H., S. Nowak and P. Dunker (2009). Using one-class SVM outliers detection for verification of collaboratively tagged image training sets. *Proc. IEEE ICME*, pp. 682–685.

Lynos, M., S. Akamatsu, M. Kamachi and J. Gyboa (1998). Coding facial expressions with Gabor wavelets. *Proceedings of the Third IEEE International Conference on Automatic Face and Facial Recognition*, 200–205.

Nene, S.A., S.K. Nayar and H. Murase, Columbia Object Image Library (COIL-20), Technical Report No. CUCS-006-96. Columbia University, 1996.

Orlov, N., L. Shamir, T. Macura, J. Johnston, D. M. Eckley and I. G. Goldberg (2008). WND-CHARM: Multi-purpose Image Classification Using Compound Image Transforms. *Pattern Recognition Letters* 29, 1684–1693.

Rodenacker, K. and E. Bengtsson (2003). A feature set for cytometry on digitized microscopic images. *Anal. Cell. Pathol.* **25**, 1–36.

Roth, V. (2005). Outlier detection with one-class kernel Fisher discriminants. *Proc. Advances in Neural Information Processing Systems*, pp. 1169–1176.

Samaria, F. and A. Harter, A. (1994). Parameterisation of a stochastic model for human face identification. *Proc. of the 2nd IEEE Workshop on Applications of Computer Vision*, pp. 138–142.

Scholkopf, B., J. Platt, J. Shawe-Taylor, A.J. Smola and R.C. Williamson. (2001). Estimating the support of a high-dimensional distribution. *Neural Computation* **13**, 1443–1471.

Shamir, L. (2006). Human perception-based color segmentation using fuzzy logic. *International Conference on Image Processing Computer Vision and Pattern Recognition* 2, 496–505.

Shamir, L., N. Orlov, D. M. Eckley, T. Macura, J. Johnston and I. G. Goldberg (2008a). Wndchrm - an open source utility for biological image analysis. *Source Code for Biology and Medicine* 3, 13.

Shamir, L., N. Orlov, D.M. Eckley, T. Macura and I. G. Goldberg (2008b). IICBU 2008 - A proposed benchmark suite for biological image analysis. *Medical & Biological Engineering & Computing* **46**, 943–947.

Shamir, L. (2008) Evaluation of Face Datasets as Tools for Assessing the Performance of Face Recognition Methods. *International Journal of Computer Vision* 79, 225–230.

Shamir, L., S. M. Ling, W. Scott, A. Boss, T., N. Orlov, Macura, D. M. Eckley, L. Ferrucci and I. Goldberg (2009) Knee X-ray image analysis method for automated detection of Osteoarthritis. *IEEE Transactions on Biomedical Engineering* 56, 407–415.

Shamir, L., N. Orlov and I. Goldberg, "Evaluation of the informativeness of multi-order image transforms," *International Conference on Image Processing Computer Vision and Pattern Recognition*, 2009, 37–42.

Shamir, L., T. Macura, N. Orlov, D. M. Eckley and I. G. Goldberg (2010). Impressionism, expressionism, surrealism: Automated recognition of painters and schools of art. *ACM Transactions on Applied Perception* **7**, 2:8.

Shamir, L. (2011) Assessing the efficacy of low-level image content descriptors for computer-based fluorescence microscopy image analysis. *J*ournal of Microscopy **243(3)**, 284–292.

Zhang, K., S. Shi, H. Gao and J. Li (2007). Unsupervised outlier detection in sensor networks using aggregation tree. *Lecture Notes in Artificial Intelligence* **4632**, 158–169.

Theory and Applications of Mathematics & Computer Science

(ISSN 2067-2764)
http://www.uav.ro/applications/se/journal/index.php/tamcs

Theory and Applications of Mathematics & Computer Science 3 (1) (2013) 32–37

On an Unified Class of Functions of Complex Order

T. M. Seoudy[a,*], M. K. Aouf[b]

[a]*Department of Mathematics, Faculty of Science, Fayoum University, Fayoum 63514, Egypt.*
[b]*Department of Mathematics, Faculty of Science, Mansoura University, Mansoura 35516, Egypt.*

Abstract

In this paper, we obtain a necessary and sufficient condition for functions in an unified class of functions of complex order. Some of our results generalize previously known results.

Keywords: Analytic function, univalent, starlike, convex, subordination.
2012 MSC: 30C45.

1. Introduction

Let $\mathcal{A}$ denote the class of functions of the form

$$f(z) = z + \sum_{n=2}^{\infty} a_n z^n, \tag{1.1}$$

which are analytic in the open unit disk $\mathbb{U} = \{z \in \mathbb{C} : |z| < 1\}$. Suppose that f and g are analytic in $\mathbb{U}$. We say that the function f is subordinate to g in $\mathbb{U}$, or g superordinate to f in $\mathbb{U}$, and we write $f \prec g$ or $f(z) \prec g(z)$ $(z \in \mathbb{U})$, if there exists an analytic function ω in $\mathbb{U}$ with $\omega(0) = 0$ and $|\omega(z)| < 1$, such that $f(z) = g(\omega(z))$ $(z \in \mathbb{U})$. If g is univalent in $\mathbb{U}$, then the following equivalence relationship holds true, see (Miller & Mocanu, 1981) and (Miller & Mocanu, 2000):

$$f(z) \prec g(z) \Longleftrightarrow f(0) = g(0) \quad \text{and} \quad f(\mathbb{U}) \subset g(\mathbb{U}).$$

Let $\mathcal{S}$ be the subclass of $\mathcal{A}$ consisting of univalent functions. Let $\phi(z)$ be an analytic function with positive real part on ϕ with $\phi(0) = 1$, $\phi'(0) > 0$ which maps the unit disk $\mathbb{U}$ onto a region starlike with respect to 1 which is symmetric with respect to the real axis. Let $\mathcal{S}^*(\phi)$ be the class of functions in $f \in \mathcal{S}$ for which

$$\frac{zf'(z)}{f(z)} \prec \phi(z), \tag{1.2}$$

*Corresponding author
Email addresses: tms00@fayoum.edu.eg (T. M. Seoudy), mkaouf127@yahoo.com (M. K. Aouf)

and $C(\phi)$ class of functions in $f \in \mathcal{S}$ for which

$$1 + \frac{zf''(z)}{f'(z)} \prec \phi(z). \tag{1.3}$$

These classes were introduced and studied by (Ma & Minda, 1992). (Ravichandran *et al.*, 2005) defined classes $\mathcal{S}_b^*(\phi)$ and $C_b(\phi)$ of complex order defined as follows :

$$\mathcal{S}^*(\phi; b) = \left\{ f \in \mathcal{A} : 1 + \frac{1}{b}\left(\frac{zf'(z)}{f(z)} - 1\right) \prec \phi(z) \quad (b \in \mathbb{C}^* = \mathbb{C}\setminus\{0\}) \right\} \tag{1.4}$$

and

$$C(\phi; b) = \left\{ f \in \mathcal{A} : 1 + \frac{1}{b}\frac{zf''(z)}{f'(z)} \prec \phi(z) \quad (b \in \mathbb{C}^*) \right\}. \tag{1.5}$$

From (1.4) and (1.5), we have

$$f \in C(\phi; b) \Longleftrightarrow zf' \in \mathcal{S}^*(\phi; b).$$

Now, we introduce a more general class of complex order $\mathcal{T}(\phi; \lambda, b)$ as follows:

Definition 1.1. Let $\phi(z)$ be an analytic function with positive real part on ϕ with $\phi(0) = 1$, $\phi'(0) > 0$ which maps the unit disk $\mathbb{U}$ onto a region starlike with respect to 1 which is symmetric with respect to the real axis. Then the class $\mathcal{T}(\phi; \lambda, b)$ consists of all analytic functions $f \in \mathcal{A}$ satisfying:

$$1 + \frac{1}{b}\left[(1-\lambda)\frac{zf'(z)}{f(z)} + \lambda\left(1 + \frac{zf''(z)}{f'(z)}\right) - 1\right] \prec \phi(z) \ (b \in \mathbb{C}^*; \lambda \geq 0). \tag{1.6}$$

We note that

(*i*) $\mathcal{T}(\phi; 0, b) = \mathcal{S}^*(\phi; b)$ and $\mathcal{T}(\phi; 1, b) = C(\phi; b)$ (Ravichandran *et al.*, 2005);

(*ii*) $\mathcal{T}(\phi; 0, 1) = \mathcal{S}^*(\phi)$ and $\mathcal{T}(\phi; 1, 1) = C(\phi)$ (Ma & Minda, 1992);

(*iii*) $\mathcal{T}\left(\frac{1+(1-2\alpha)z}{1-z}; 0, b\right) = \mathcal{S}_\alpha^*(b)$ and $\mathcal{T}\left(\frac{1+(1-2\alpha)z}{1-z}; 1, b\right) = C_\alpha(b)$ $(0 \leq \alpha < 1; b \in \mathbb{C}^*)$ (Frasin, 2006);

(*iv*) $\mathcal{T}\left(\frac{1+z}{1-z}; 0, b\right) = \mathcal{T}\left(\frac{1+(2b-1)z}{1-z}; 0, 1\right) = \mathcal{S}^*(b)$ $(b \in \mathbb{C}^*)$ (Nasr & Aouf, 1985) and (Wiatrowski, 1970);

(*v*) $\mathcal{T}\left(\frac{1+z}{1-z}; 1, b\right) = \mathcal{T}\left(\frac{1+(2b-1)z}{1-z}; 1, 1\right) = C(b)$ $(b \in \mathbb{C}^*)$ (Nasr & Aouf, 1982) and (Wiatrowski, 1970);

(*vi*) $\mathcal{T}\left(\frac{1+z}{1-z};0,1-\alpha\right)=\mathcal{T}\left(\frac{1+(1-2\alpha)z}{1-z};0,1\right)=\mathcal{S}^{*}(\alpha)$

and $\mathcal{T}\left(\frac{1+z}{1-z};1,1-\alpha\right)=\mathcal{T}\left(\frac{1+(1-2\alpha)z}{1-z};1,1\right)=C(\alpha)\,(0\leq\alpha<1)$ (Robertson, 1936);

(*vii*) $\mathcal{T}\left(\frac{1+z}{1-z};0,be^{-i\gamma}\cos\gamma\right)=\mathcal{S}^{\gamma}(b)$ and $\mathcal{T}\left(\frac{1+z}{1-z};1,be^{-i\gamma}\cos\gamma\right)=C^{\gamma}(b)\left(|\gamma|<\frac{\pi}{2},b\in\mathbb{C}^{*}\right)$ (Al-Oboudi & Haidan, 2000) and (Aouf *et al.*, 2005).

Motivated essentially by the aforementioned works, we obtain certain necessary and sufficient conditions for the unified class of functions $\mathcal{T}(\phi;\lambda,b)$ which we have defined. The motivation of this paper is to generalize the results obtained by (Ravichandran *et al.*, 2005), (Aouf *et al.*, 2005), (Srivastava & Lashin, 2005) and also (Obradovic *et al.*, 1989).

2. Main Results

Unless otherwise mentioned, we assume throughout the sequel that $b\in\mathbb{C}^{*}$, $\lambda\geq 0$ and all powers are understood as principle values. To prove our main result, we need the following lemmas.

Lemma 2.1. *(Ruscheweyh, 1982) Let ϕ be a convex function defined on $\mathbb{U}$, $\phi(0)=1$. Define $F(z)$ by*

$$F(z)=z\,\exp\left(\int_{0}^{z}\frac{\phi(t)-1}{t}dt\right). \tag{2.1}$$

Let $p(z)=1+p_1z+p_2z^2+\ldots$ be analytic in $\mathbb{U}$. Then

$$1+\frac{zq'(z)}{q(z)}\prec\phi(z) \tag{2.2}$$

if and only if for all $|s|\leq 1$ and $|t|\leq 1$, we have

$$\frac{p(tz)}{p(sz)}\prec\frac{sF(tz)}{tF(sz)}. \tag{2.3}$$

Lemma 2.2. *(Miller & Mocanu, 2000) Let $q(z)$ be univalent in $\mathbb{U}$ and let $\varphi(z)$ be analytic in a domain containing $q(\mathbb{U})$. If $\frac{zq'(z)}{q(z)}$ is starlike, then*

$$zp'(z)\varphi(p(z))\prec zq'(z)\varphi(q(z)),$$

then $p(z)\prec q(z)$ and $q(z)$ is the best dominant.

Theorem 2.1. *Let $\phi(z)$ and $F(z)$ be as in Lemma 2.1. The function $f\in\mathcal{T}(\phi;\lambda,b)$ if and only if for all $|s|\leq 1$ and $|t|\leq 1$, we have*

$$\left[\left(\frac{sf(tz)}{tf(sz)}\right)^{1-\lambda}\left(\frac{f'(tz)}{f'(sz)}\right)^{\lambda}\right]^{\frac{1}{b}}\prec\frac{sF(tz)}{tF(sz)}. \tag{2.4}$$

Proof. Define the function $p(z)$ by

$$p(z) = \left[\frac{f(z)}{z}\left(\frac{zf'(z)}{f(z)}\right)^{\lambda}\right]^{\frac{1}{b}} \quad (z \in \mathbb{U}). \tag{2.5}$$

Taking logarithmic derivative of (2.5), we get

$$1 + \frac{zp'(z)}{p(z)} = 1 + \frac{1}{b}\left[(1-\lambda)\frac{zf'(z)}{f(z)} + \lambda\left(1 + \frac{zf''(z)}{f'(z)}\right) - 1\right].$$

Since $f \in \mathcal{T}(\phi; \lambda, b)$, then we have

$$1 + \frac{zp'(z)}{p(z)} \prec \phi(z)$$

and the result now follows from Lemma 2.1. □

Putting $\lambda = 0$ in Theorem 2.1, we obtain the following result of (Shanmugam *et al.*, 2009).

Corollary 2.1. *Let $\phi(z)$ and $F(z)$ be as in Lemma 2.1. The function $f \in \mathcal{S}^*(\phi; b)$ if and only if for all $|s| \leq 1$ and $|t| \leq 1$, we have*

$$\left(\frac{sf(tz)}{tf(sz)}\right)^{\frac{1}{b}} \prec \frac{sF(tz)}{tF(sz)}. \tag{2.6}$$

For $\lambda = 1$ in Theorem 2.1, we obtain the following result of (Shanmugam *et al.*, 2009).

Corollary 2.2. *Let $\phi(z)$ and $F(z)$ be as in Lemma 2.1. The function $f \in C(\phi; b)$ if and only if for all $|s| \leq 1$ and $|t| \leq 1$, we have*

$$\left(\frac{f'(tz)}{f'(sz)}\right)^{\frac{1}{b}} \prec \frac{sF(tz)}{tF(sz)}. \tag{2.7}$$

Theorem 2.2. *Let $\phi(z)$ be starlike with respect to 1 and $F(z)$ given by (2.1) be starlike. If $f \in \mathcal{T}(\phi; \lambda, b)$, then we have*

$$\frac{f(z)}{z}\left(\frac{zf'(z)}{f(z)}\right)^{\lambda} \prec \left(\frac{F(z)}{z}\right)^{b}. \tag{2.8}$$

Proof. Let $p(z)$ be given by (2.5) and $q(z)$ be given by

$$q(z) = \frac{F(z)}{z} \quad (z \in \mathbb{U}). \tag{2.9}$$

After a simple computation we obtain

$$1 + \frac{zp'(z)}{p(z)} = 1 + \frac{1}{b}\left[(1-\lambda)\frac{zf'(z)}{f(z)} + \lambda\left(1 + \frac{zf''(z)}{zf'(z)}\right) - 1\right].$$

and

$$\frac{zq'(z)}{q(z)} = \frac{zF'(z)}{F(z)} - 1 = \phi(z) - 1.$$

Since $f \in \mathcal{T}(\phi; \lambda, b)$, we have

$$\frac{zp'(z)}{p(z)} \prec \frac{zq'(z)}{q(z)}.$$

The result now follows by an application of Lemma 2.2. □

Putting $\lambda = 0$ in Theorem 2.2, we obtain the following results of (Shanmugam *et al.*, 2009).

Corollary 2.3. *Let $\phi(z)$ be starlike with respect to 1 and $F(z)$ given by* (2.1) *be starlike. If $f \in \mathcal{S}^*(\phi; b)$, then we have*

$$\frac{f(z)}{z} \prec \left(\frac{F(z)}{z}\right)^b.$$

Taking $\phi(z) = \dfrac{1+Az}{1+Bz}$ $(-1 \le B < A \le 1)$ in Theorem 2.2, we get the following corollary.

Corollary 2.4. *If $f \in \mathcal{T}\left(\dfrac{1+Az}{1+Bz}; \lambda, b\right)(-1 \le B < A \le 1)$, then we have*

$$\frac{f(z)}{z}\left(\frac{zf'(z)}{f(z)}\right)^{\lambda} \prec (1+Bz)^{\frac{(A-B)b}{B}} \quad (B \neq 0).$$

For $\phi(z) = \dfrac{1+z}{1-z}$ and $\lambda = 0$ in Theorem 2.2, we get the following result of (Obradovic *et al.*, 1989), and (Srivastava & Lashin, 2005).

Corollary 2.5. *If $f \in \mathcal{S}^*(b)$, then we have*

$$\frac{f(z)}{z} \prec (1-z)^{-2b}.$$

Putting $\phi(z) = \dfrac{1+z}{1-z}$ and $\lambda = 1$ in Theorem 2.2, we get the following result of (Obradovic *et al.*, 1989), and (Srivastava & Lashin, 2005).

Corollary 2.6. *If $f \in C(b)$, then we have*

$$f'(z) \prec (1-z)^{-2b}.$$

For $\phi(z) = \dfrac{1+z}{1-z}, \lambda = 0$ and replacing b by $be^{-i\gamma}\cos\gamma$ $\left(|\gamma| < \dfrac{\pi}{2}, b \in \mathbb{C}^*\right)$ in Theorem 2.2, we get the following result of (Aouf *et al.*, 2005).

Corollary 2.7. *If $f \in \mathcal{S}^{\gamma}(b)$, then we have*

$$\frac{f(z)}{z} \prec (1-z)^{-2be^{-i\gamma}\cos\gamma} .$$

Taking $\phi(z) = \dfrac{1+z}{1-z}$, $\lambda = 1$ and replacing b by $be^{-i\gamma}\cos\gamma \left(|\gamma| < \dfrac{\pi}{2}, b \in \mathbb{C}^*\right)$ in Theorem 2.2, we get the following result of (Aouf *et al.*, 2005).

Corollary 2.8. *If $f \in C^{\gamma}(b)$, then we have*

$$f'(z) \prec (1-z)^{-2be^{-i\gamma}\cos\gamma} .$$

References

Al-Oboudi, F. M. and M. M. Haidan (2000). Spirallike functions of complex order. *J. Natural Geom.* **19**, 53–72.

Aouf, M. K., F. M. Al-Oboudi and M. M. Haidan (2005). On some results for λ−spirallike and λ−robertson functions of complex. *Publ. Instit. Math. Belgrade* **77**(91), 93–98.

Frasin, B. A. (2006). Family of analytic functions of complex order. *Acta Math. Acad. Paedagog. Nyházi. (N. S.)* **22**(2), 179–191.

Ma, W. C. and D. Minda (1992). A unified treatment of some special classes of univalent functions. In: *Proceedings of the Conference on Complex Analysis (Tianjin, 1992), Internat. Press, Cambridge, MA*. pp. 157–169.

Miller, S. S. and P. T. Mocanu (1981). Differential subordinations and univalent functions. *Michigan Math. J.* **28**, 157–171.

Miller, S. S. and P. T. Mocanu (2000). *Differential Subordinations: Theory and Applications, Serieson Monographs and Textbooks in Pure and Applied Mathematics*. Vol. 225, Marcel Dekker, New York and Basel.

Nasr, M.A. and M. K. Aouf (1982). On convex functions of complex order. *Mansoura Bull. Sci.* **8**, 565–582.

Nasr, M.A. and M. K. Aouf (1985). Starlike function of complex order. *J. Natur. Sci. Math.* **25**, 1–12.

Obradovic, M., M. K. Aouf and S. Owa (1989). On some results for starlike functions of complex order. *Publ. Inst. Math., Nouv. Ser.* **46**(60), 79–85.

Ravichandran, V., Y. Polatoglu, M. Bolcal and A. Sen (2005). certain subclasses of starlike and convex functions of complex order. *Hacettepe J. Math. Stat.* **34**, 9–15.

Robertson, M. S. (1936). On the theory of univalent functions. *Ann. Math.* **37**, 374–408.

Ruscheweyh, St. (1982). *Convolutions in geometric function theory*. Séminaire de mathématiques supérieures. Montréal, Québec, Canada : Presses de l'Université de Montréal.

Shanmugam, T. N., S. Sivasubramanian and S. Kavitha (2009). On certain subclasses of functions of complex order. *South. Asian Bull. Math.* **33**, 535–541.

Srivastava, H. M. and A.Y. Lashin (2005). Some applications of the briot-bouquet differential subordination. *J. Inequal. Pure Appl. Math.* **6**(2, Art. 41), 1–7.

Wiatrowski, P. (1970). On the coefficients of some family of holomorphic functions. *Zeszyty Nauk. Uniw. Łódz Nauk. Mat.-Przyrod.* **39**, 75–85.

Theory and Applications of Mathematics & Computer Science

(ISSN 2067-2764)
http://www.uav.ro/applications/se/journal/index.php/tamcs

Theory and Applications of Mathematics & Computer Science 3 (1) (2013) 38–55

The Scale-Curvature Connection and its Application to Texture Segmentation

Eli Appleboim[a], Yedidya Hyams[a], Shai Krakovski[a], Chen Sagiv[b], Emil Saucan[c,*]

[a]*Department of Electrical Engineering, Technion, Haifa 32000, Israel*
[b]*SagivTech Ltd., Eliezer Yaffe 37/18, Ra'anana 43451, Israel*
[c]*Department of Mathematics, Technion, Haifa 32000, and Department of Mathematics and Computer Science, The Open University of Israel, Ra'anana 43537, Israel*

Abstract

In this work we establish a theoretical relation between the notions of scale and a discrete Finsler-Haantjes curvature. Based on this connection we demonstrate the applicability of the interpretation of scale in terms of curvature, to signal processing in the context of analysis and segmentation of textures in images. The outcome of this procedure is a novel scheme for texture segmentation that is based on scaled metric curvature. The presented method proves itself to be efficient even when the multiscale analysis is done up to scales of 19 and more. Our main conclusions are that the discrete curvature calculated on sampled images can give us an indication on the local scale within the image, and therefore can be used for many additional tasks in image analysis.

Keywords: Wavelets, scale-space, Finsler-Haantjes curvature, texture segmentation.
2010 MSC: 42C40, 68U10, 51K10.

1. Introduction

Several tasks in image and signal processing require the calculation and usage of scale. Determining the typical scale at some image location can be useful for de-convolution, detection and recognition tasks. The popular image registration algorithms, SIFT (Lowe, 1999) and SURF (Bay *et al.*, 2006) account for the scale at image locations as a pre-processing step for calculating scale invariant key points, that are used in turn for matching.

Typical approaches to calculate scale in the signal processing community rely on analyzing a multi scale representation of the images, via the scale space approach or the wavelet transform.

*Corresponding author
Email addresses: eliap@ee.technion.ac.il (Eli Appleboim), gwavelet gwavelet@gmail.com (Yedidya Hyams), gwavelet gwavelet@gmail.com (Shai Krakovski), chen@sagivtech.com (Chen Sagiv), semil@tx.technion.ac.il (Emil Saucan)

The versatility and adaptability of scale space theory and wavelets for a variety of tasks in Image Processing and related fields is too well established in the scientific community, and the bibliography pertaining to it is far too extensive, to even begin to review it here.

On the other hand, the concept of curvature is well established in the field of computational geometry. Intuitively, scale and curvature are related. High curvature account for phenomenon that happen at smaller scales than those that are related to low curvature. This relation is further stressed analytically and formally in the smooth category, as the curvature of a smooth curve at some point is defined to be the inverse of the squared radius of the osculatory circle at that point so specifically making curvature a function of scale. Curvature decreases as the inverse of the square root of scale (Petersen, 1998).

The multiresolution property of wavelets has been already applied in determining the curvature of planar curves (Antoine & Jaques, 2003) and to the intelligence and reconstruction of meshed surfaces (see, e.g. (Lounsbery *et al.*, 1997), (Valette & Prost, 2004), amongst many others). Moreover, the intimate relation between scale and differentiability in natural images has also been stressed (Florack *et al.*, 1992).

An intriguing issue is whether one can replace the intuitive trade-off between scale and curvature, by a formal concept of *wavelet curvature*, in particular in cases such as the Strömberg wavelets (Strömberg, 1983) that are based on piecewise-linear functions, and if so then,to what extent this can be further extended to the more difficult case of Haar wavelets that are not even piecewise linear and to what extent this can be made general.

Apparently, this can be done by using *metric curvatures* (Blumenthal & Menger, 1970) (and (Saucan, 2006) for a short presentation). It turns out that the best candidate, for the desired metric curvature is the *Finsler-Haantjes curvature*, due to its adaptability to both continuous and discrete settings (see, e.g. (Saucan & Appleboim, 2005), (Saucan & Appleboim, 2009)).

We have first introduced a formal relation between discrete curvature and scale in (Saucan *et al.*, 2010). In the present paper, that represents a continuation of our previous, above mentioned article, we suggest that a simple curvature calculation can replace the tedious work of convolving images with a large number of multi scaled filters. We show how scale and curvature are related to each other, for a variety of families of wavelets. Afterwards we present the Finsler-Haantjes curvature measure for images and develop a novel scheme for texture separation. Our main goal is, however, more far-reaching, namely to try and bridge, at least partly, the the gap between the two basic, largely non-intersecting, approaches prevalent in Image Processing and related fields: The geometric one, that is closely related to the Graphics community philosophy; and the more classical, Fourier Analysis/Wavelets driven one.

The paper is organized as follows: First, we introduce the mathematical background needed and discuss the notion of scale in Section 2.1. We then elaborate on the Finsler-Haantjes curvature in Section 2.2 and introduce the Fisler-Haantjes curvature of wavelets and for images in Section 3. In section 4 we suggest a scheme for texture analysis in images that is based on our discrete scaled curvature measure. In addition to texture segmentation there is a huge variety of further possible applications to the ideas and methods presented herein, as well as open issues for further research. Some of those are mentioned in Section 5 in which we summarize the paper.

2. Mathematical Background

In this section we present both the notion of scale and that of the Finsler-Haantjes Curvature. While these two components are derived from completely different worlds, we show that they are strongly related to each other.

2.1. The Notion of Scale

The notion of scale is fundamental in many mathematical and applicative discussions. Scale is one of these terms that has a clear intuitive meaning, but is hard to be defined mathematically. The question of finding a measure for calculating the local scale in signals and images has been addressed in the past in the context of scale space analysis and wavelets transform. It plays a significant role in the framework of image matching and registration, where scale invariant descriptors are desired. Evaluating the dominant scale within image data is highly important for real life applications. For a computer vision system analyzing an unknown scene, there is no way to know a priori what scales are appropriate for describing the interesting structures in the image data. Hence, the only reasonable approach is to consider descriptions at multiple scales in order to be able to capture the unknown scale variations that may occur. Scale-space theory is a formal theory for handling image structures at different scales, by representing an image as a one-parameter family of smoothed images, the scale-space representation. This representation is parameterized by the size of the smoothing kernel used for suppressing fine-scale structures.

In the early eighties Witkin (Witkin, 1983a),(Witkin, 1983b) proposed to consider scale as a continuous parameter and formulated the principal rules of modern scale-space theory relating image structures represented at different scales. Since then, scale-space representation and its properties have been extensively studied and important contributions have been made by Koenderink (Koenderink, 1984), Lindeberg (Lindeberg, 1998) and Florack (Florack *et al.*, 1992). In many cases it is necessary to select locally appropriate scales for further analysis. This need for scale selection originates from the need to process real-world objects that may have different sizes and because the distance between the object and the camera can vary. The seminal work of Lindenberg (Lindeberg, 1998) dealt with the issue of automatic scale selection. The idea was to determine the characteristic scale for which a given function attains an extremum over scales. The name characteristic is somewhat arbitrary as a local structure can exist at a range of scales and within this range there is no preferred scale of perception. However, a scale can be named characteristic, if it conveys more information comparing to other scales. In his work, Lindenberg noted that a highly useful property of scale-space representation is that image representations can be made invariant to scales, by performing automatic local scale selection based on local maxima (or minima) over scales of normalized derivatives.

This work served as the basis for tasks such as blob detection, corner detection, ridge detection and edge detection. Scale space theory is fundamental for detecting invariant features within signals and images that can be used for various tasks such as registration, detection and recognition among others. Multi-scale representation of data is crucial for extracting local features used for determining regions of interest for subsequent detection of scale-invariant interest points for computing image descriptors, most notable are the SIFT (Lowe, 1999) and SURF (Bay *et al.*, 2006) frameworks.

Both the SIFT and the SURF algorithms rely on Scale-space extrema detection, where the first stage of computation searches over all scales and image locations. It is implemented by using a Laplacian-of-Gaussian or a difference-of-Gaussian function to identify potential interest points that are invariant to scale and orientation.

A common practice for scale determination relies on the convolution of the data with a bank of functions that have different scales. The characteristic scale usually corresponds to the local extremum of the convolution results, taken over scales. The characteristic scale is related to structure. The common methodology for finding this exterma values in scale space involves analysis of the behavior of the Laplacian of Gaussian (Bay *et al.*, 2006), Difference of Gaussian (Lowe, 1999) and the Hessian matrix to name a few. There are strong relations between scale-space theory and wavelet theory, although these two notions of multi-scale representation have been developed from somewhat different premises. Wavelets are multi scaled versions of a specific mother function, thus when convolving them with data, one can exploit the scale contents of that data, in a very similar way that the frequency contents of data can be expressed using the Fourier transform. A strong response to a wavelet function with a certain support and scale, suggests that there is significant information at that scale at that image location.

2.2. The Finsler-Haantjes Curvature

The most intuitive definition for curvature is the amount by which a geometric object deviates from being flat, or straight in the case of a line. It is natural to define the curvature of a straight line to be identically zero. The curvature of a circle of radius R should be large if R is small and small if R is large. Thus the curvature of a circle is defined to be the reciprocal of the squared radius (do Carmo, 1976).

The following metric definition for curvature is due to Haantjes, following an idea of Finsler (Blumenthal & Menger, 1970):

Definition 2.1. *Let (M,d) be a metric space, let* $c : I = [0,1] \tilde{\to} M$ *be a homeomorphism, and let* $p, q, r \in c(I),\ q, r \neq p$. *Denote by* $\widehat{qr}$ *the arc of* $c(I)$ *between* q *and* r, *and by* qr *the segment from* q *to* r. *We say that* c *has* Finsler-Haantjes curvature $\kappa_{FH}(p)$ *at the point* p *iff:*

$$\kappa_{FH}^2(p) = 24 \lim_{q,r \to p} \frac{l(\widehat{qr}) - d(q,r)}{(d(q,r))^3}\ ; \tag{2.1}$$

where "$l(\widehat{qr})$*" denotes the length, in intrinsic metric induced by* d, *of* $\widehat{qr}$ *– see Figure 1. (Here we assume the curve* $c(I)$ *is* rectifiable, *hence that, in particular, the arc* $\widehat{qr}$ *has finite length.)*

This definition of curvature represents, indeed, a proper adaptation, for an extensive class of curves in quite general metric spaces, of the classical notion of curvature, as proven by the following

Theorem 2.1. *Let* $c \in C^3(I)$ *be a smooth curve in* $\mathbb{R}^3$, *and let* $p \in c$ *be a regular point. Then* $\kappa_{FH}(p)$ *exists and, moreover,* $\kappa_{FH}(p) = k(p)$ *– the classical (differential) curvature of* c *at* p.

Remark. Originally the Finsler-Haantjes curvature is defined with $l(\widehat{qr})$ appearing in the denominator instead of $d(q,r)$, ((Blumenthal & Menger, 1970)). We have opted for the above definition

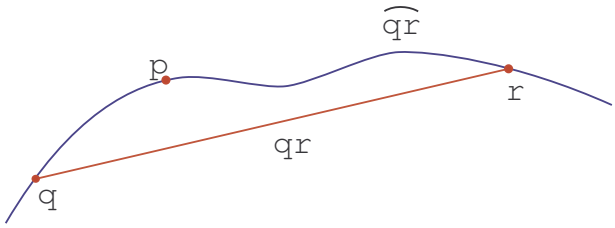

Figure 1. A (metric) arc and its corresponding chord (metric segment).

for practicality reasons. Moreover, in the setting of this work (and, in fact, in a much more general context) the above theorem still holds with our modified definition, therefore the definition used herein is interchangeable with the original one (see, again (Blumenthal & Menger, 1970)).

3. Finsler-Haantjes Curvature for Wavelets and Images

In this section we consider a semi-discrete (or semi-continuous) version of the Finsler-Haantjes curvature, and then introduce this curvature measure in the case of a wavelet function.

3.1. Semi-discrete Finsler-Haantjes Curvature

Consider a typical piecewise-linear wavelet φ, such as the one depicted in Figure 2, let $\widehat{AE}$ be the arc of curve between the points A and E, and let $d(A, E)$ is the length of the line-segment AE.

Then

$$l(\widehat{AE}) = a + b + c + d \ \ ; d(A, E) = e + f. \tag{3.1}$$

The following discretization of formula (2.1) is, therefore, natural:

$$\kappa^2_{FH}(\varphi) = 24[(a + b + c + d) - (e + f)]/(e + f)^3. \tag{3.2}$$

In addition to the total curvature of the wavelet φ, one can also compute the "local" curvatures of the partial wavelets $\varphi_1 = \widehat{ABC}$ and $\varphi_2 = \widehat{CDE}$, that is the curvatures at the "peaks" B and D:

$$\kappa^2_{FH}(B) = 24(a + b - e)/e^3 \ , \tag{3.3}$$

and

$$\kappa^2_{FH}(D) = 24(c + d - f)/f^3 \ , \tag{3.4}$$

as well as the mean curvature of these peaks:

$$H_{FH}(\widehat{AE}) = [\kappa_{FH}(B) + \kappa_{FH}(D)]/2. \tag{3.5}$$

Even though these variations may prove to be useful in certain applications, we believe that the correct approach, in the sense that it best corresponds to the scale of the wavelet, would be to compute the total curvature of φ. However, had the definition of Finsler-Haantjes curvature been limited solely to piecewise-linear wavelets, its applicability would have also been diminished. We show, however, that it is also definable for the "classical" Haar wavelets, in a rather straightforward manner.

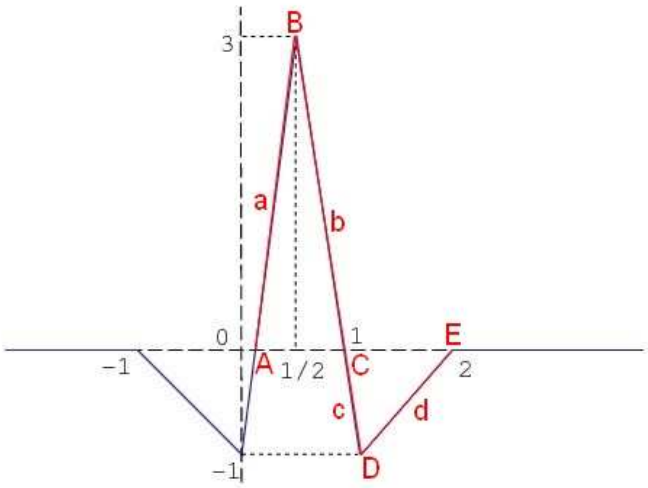

Figure 2. A typical piecewise-linear wavelet (red), part of the Meyer Wavelet (Meyer, 1993) (blue and red).

Remark. In the sequel we will therefore omit the coefficient $\sqrt{24}$ for convenience.

3.2. *Finsler-Haantjes curvature of Haar Wavelets*

For every $s \in \mathbb{Z}$ let $j = 2^s$, and let Ψ_j denote the Haar wavelet at scale j and with zero shift, where $\Psi_1 = \Psi$ is the mother wavelet of Haar basis, considered in the above example. Then Ψ_j can be presented as:

$$\Psi_j = \begin{cases} j^{-1}, & x \in (0, \frac{j}{2}); \\ -j^{-1}, & x \in (\frac{j}{2}, j); \\ 0 & otherwise. \end{cases} \tag{3.6}$$

Then, in the notations of Figure 2 we have that $A = 0, E = j$, so we have that $l(\widehat{AE}) = 4 \cdot j^{-1} + j$, and $d(\widehat{AE}) = j$, therefore for these wavelets the Finsler-Haantjes curvature satisfies:

$$\kappa^2_{FH}(\Psi_j) = \frac{(4 \cdot j^{-1} + j) - j}{j^3} = 4 \cdot j^{-4} \tag{3.7}$$

The Finsler-Haantjes curvature is certainly invariant under shifts therefore the same dependency of K_{FH} in scale is the same for shifted Haar wavelets as well.

3.3. *Finsler-Haantjes curvature of Walsh Basis*

Let R_s be the Rademacher function which takes the value $1, -1$ on the dyadic intervals $[\frac{j}{2^{s+1}}, \frac{j+1}{2^{s+1}})$, $j = 0, 1, ..., 2^{s+1}$ of the unit interval. Figure 3 shows the first four Rademacher functions.

Then for any $k \in \mathbb{N}$, if we take the binary expansion of k as a sum of powers of 2, $k = 2^{p_1} + 2^{p_2} + \cdots + 2^{p_m}$, and define the k_{th} Walsh function as ((Beauchamp, 1975)):

$$W_k = R_{p_1} \cdot R_{p_2} \cdots R_{p_m} \tag{3.8}$$

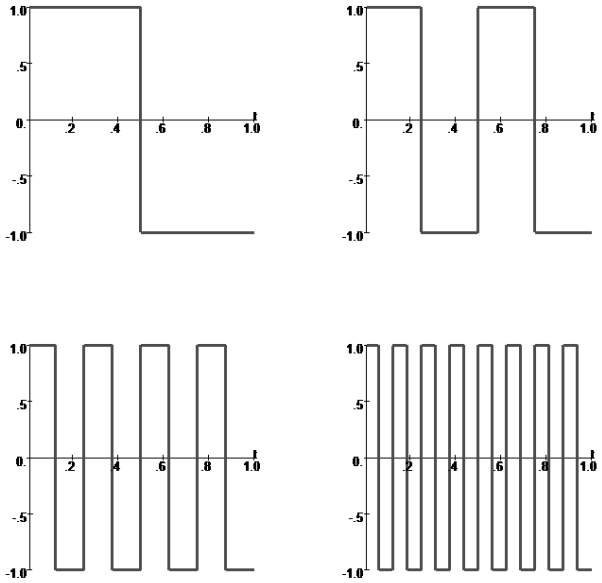

Figure 3. First four Rademacher functions.

Again, in the notations of Figure 2 we have that, $A = 0, E = 1, l(\widehat{AE}) = 2 \cdot 2^s + 1, d(\widehat{AE}) = 1$ which results with

$$\kappa^2_{FH}(W_s) = \frac{(2 \cdot 2^s + 1) - 1}{1^3} = 2^{s+1} \ . \tag{3.9}$$

Although the Walsh basis is not a wavelet basis (see (Beauchamp, 1975)), we can easily regard the function W_s as a function in a specific scale which is $j = \frac{1}{s+1}$ hence the curvature of the Walsh function at scale j is $2^{\frac{1}{j}}$.

For a smooth wavelet Ψ, compactly supported, we can of course define its Finsler-Haantjes, K_{FH} by taking $l(\widehat{AE})$ to be the usual arc length given by $\int_{\text{support}\Psi} \sqrt{1 + \Psi'^2}$.

3.4. Curvature vs. Scale

By an analysis similar to those in Sections 3.2 and 3.3, we will be able to compute a specific dependency of the Finsler-Haantjes curvature as a function of scale, for every family of piecewise constant wavelets. Moreover, with only a limited amount of additional effort, this goal is also achievable for the families of piecewise linear wavelets. This correlation most probably depends on the specific family under consideration. Indeed, as already noted above, Haar wavelets behave differently from the Walsh basis as far as the curvature vs. scale correspondence is concerned. To obtain a similar relation in the case of smooth wavelets, one should recall that if Ψ_j is a smooth wavelet function at some scale j, then it can be approximated, for instance, in the L_2-norm, by a sequence of Haar functions. More precisely, for every $\epsilon > 0$, there exists $k = k(j, \epsilon) \in \mathbb{N}$, such that

$$\int_{\text{supp}\Psi_j} |\Psi_j - \sum_i^k Haar_i|^2 < \epsilon \ . \tag{3.10}$$

Combining the inequality above with Equation (3.7) we obtain that the Finsler-Haantjes curvature of Ψ will display a scale-curvature relation similar with that observed for the Haar wavelet. Here, by "similar" we mean that it will decrease as curvature increases. However, we probably cannot expect in this case a simple analytic expression comparable with the one displayed in the case of Haar wavelets. The precise behavior, if can be derived at all, is left as an open question at this point. It would be reasonable to assume that it depends on the specific wavelet family Ψ, as well as on the proximity factor ϵ. Nevertheless, this behavior is indeed demonstrated in the numerical tests that were applied on a variety of wavelets families. For each type of wavelets, Haantjes curvature was computed for the wavelets families at different scales. The general behavior is similar in all different families and are shown in Figure 4. It is shown that, as expected, curvature decreases as scale increases. As indicated by Equation (3.7), we see that the decrease of curvature as a function of scale for the Haar wavelet is different then the one of classical differential geometry of smooth manifolds, where the decrease has a magnitude of $(scale)^{-2}$, while for the Haar wavelet it was shown to be in a magnitude of $(scale)^{-4}$. The difference evidently follows from the fact that we compute the Finsler-Haantjes curvature in a global way rather than locally, as usually curvature is computed in the classical differential geometric setting.

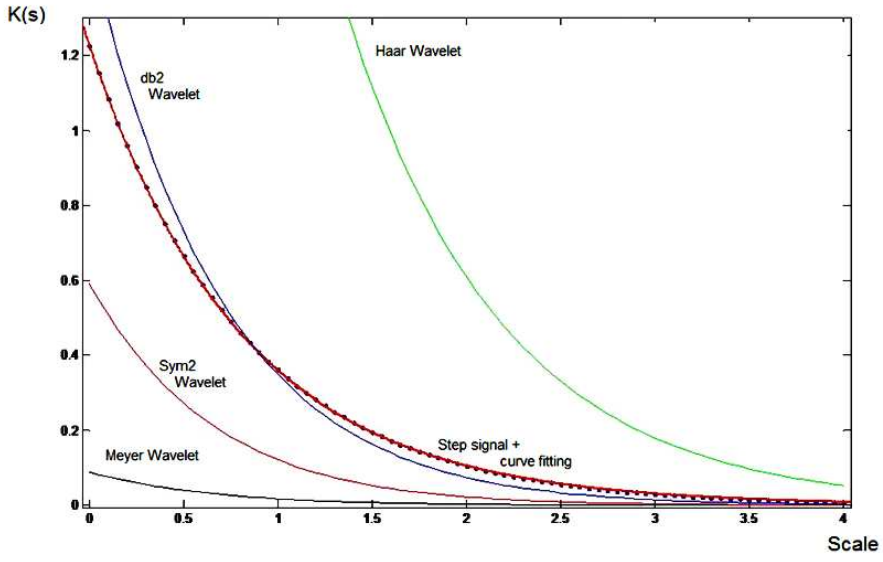

Figure 4. Curvature as a function of scale for a number of standard wavelets: The Haar wavelets, db2 wavelets, sym2 wavelets, the Meyer wavelets; as well as the step signal.

3.5. Curvature for images

From the definition of Finsler-Haatjes for curves we can easily define a discrete version of curvature for surfaces in general, and for images in particular. For say, a point x on a surface Σ, the most natural thing to do is to consider Fisler-Haantjes curvature in any of the directions emanating from x, then find the maximal and minimal curvatures, and then take either the mean of these two

values so to obtain a Finsler-Haantjes *mean curvature* or, alternatively take the multiplication of these two in order to obtain a Finsler-Haantjes version of the *Gaussian curvature* at x. We adopt this concept to images while we consider an image as a surface embedded in some $\mathbb{R}^n$. A gray scale image, for example, can naturally be considered as a surface in $\mathbb{R}^3$. In this case the Finsler-Haantjes curvature is computed at each pixel in four different directions and then the average of these four curvatures is taken. This is done in the framework that was defined in Equation 3.3 of localized curvature, where for images the localization is done by considering a window of some size $n \times n$ centered at the pixel. Each of the images shows the results of computing this version of mean curvature as computed for window sizes of 3×3, 5×5 and 7×7.

Before we proceed further, let us briefly discuss a limit case: If a signal (image) displays a unique scale, e.g. for periodic signals, for which there is a direct correlation between scale and the period T, one expects that to observe that the graph of the curvature function is the smoothest precisely in windows of size T. That this is indeed the case is illustrated in Figure 5.

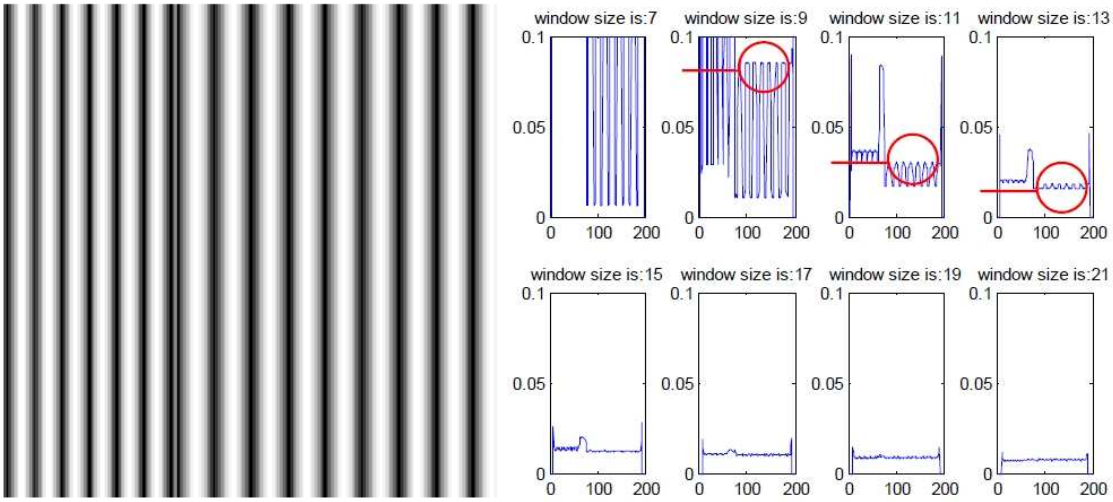

Figure 5. Left: A test image, consisting of two *sin* signals of different periods (11 pixels – left, and 15 pixels – right). Right: As expected, on the windows corresponding to the period of the signal (image) the curvature graph is the most smooth. (Notice the highlighted "windows".)

We clearly can see how Haanjes-Finsler curvature performs as an edge detector. This result is expected, since curvature, even its metric, abstract setting, still has qualities similar to those of a second derivative. This is clearly illustrated in Figure 6. This is further emphasized in the more challenging example in Figure 7, of a satellite image of the Egypt pyramids at Giza, as they lie against the background of sand dunes and opposed to the adjacent neighbourhood of Cairo. It should be noted that, curvature map in itself can serve as a good man made detection tool in arial and satellite images.

Figure 6. Haantjes-Finsler curvature of an image with respect to different scales. From top left in clockwise direction: original image, $3X3$, $7X7$ and $5X5$ window size.

4. Texture segmentation

As a possible application of the proposed method of indicating scale via curvature we look at the problem of image texture segmentation. The novel segmentation scheme yielded from this approach is outlined below.

1. At each pixel Haantjes-Finsler curvatures are computed at different scales and different orientations. For each window, curvatures are computed in 4 directions, horizontal vertical and two diagonal directions $\kappa_h, \kappa_v, \kappa_{d_1}, \kappa_{d_2}$. Finally, the average $\kappa_{Avg} = (\kappa_{Max}(pix) - \kappa_{min}(pix))/\kappa_{Max}(pix)$ of these four obtained curvatures is taken as the curvature at the pixel in the relevant scale. (The specific average considered here was inspired by the standard Image Processing definition of the contrast $C(I)$ of an image I, $C(I) = (I_{Max} - I_{min})/I_{Max}$.) This approximates the average curvature at each scale. The outcome of this step is a vector of length m where m is the number of different scales, $V(pix, scale)$ where pix denotes pixel, and each entry of the vector represents the average curvature at the corresponding scale.

2. Next, at each pixel, the gradient, with respect to scale $\nabla_{scale}V$, of this curvature vector is computed, and we look for the scales at which the gradient exceeds a predefined threshold. (Note that, at this point, curvature and scale are already interchangeable.) Afterwards, all scales which fulfill the threshold criteria are averaged in order to get a scalar value for each pix. The average scale is the outcome of this step. We consider this scale as the scale of important information at the relevant pixel.

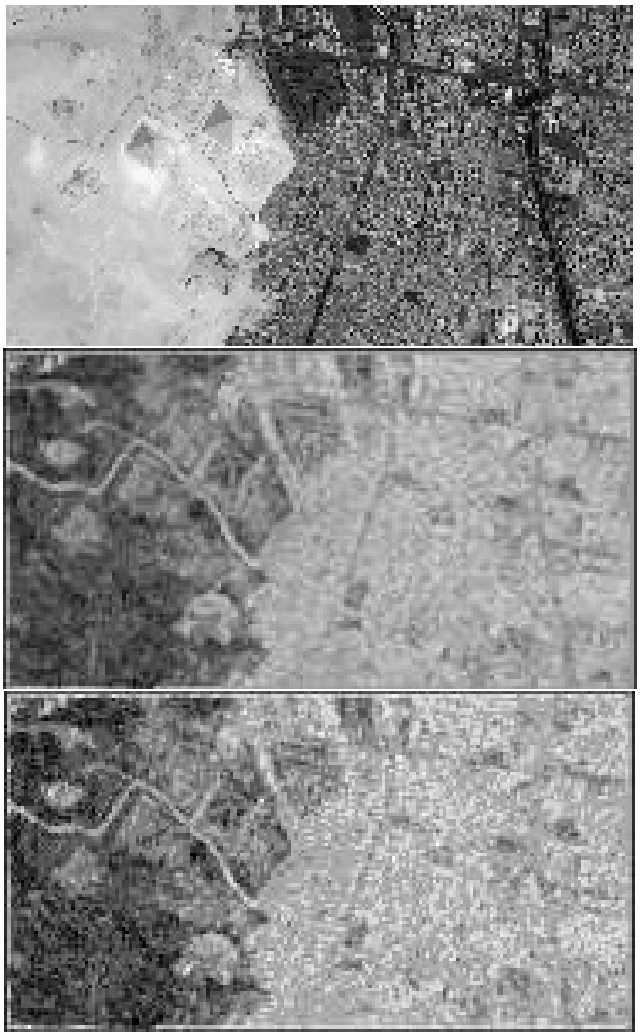

Figure 7. Haantjes-Finsler curvature of a satellite image with respect to different scales. From top to bottom: original image, curvature averaged on 3X3 windows, curvature averaged on 7X7 windows.

3. The output of previous step is a matrix in the same size as the image size, each entry of which is the scale of information at the relevant pixel. A smoothed version of this matrix is obtained by a linear filtering at size which is compatible with the amount of localized information one wishes to obtain. Segmentation to small textures will require small filtering support.

4. We segment the image according to the smoothed information scale computed in the previous step. Pixels with similar scales are grouped together to form different segments. The segmentation is done after curvature values are quantized to several levels. In the experiments shown herein quantization is taken into seven levels.

The procedure detailed above is summarized as Algorithm 1, which is divided into its four main constituent parts:

Input: Grayscale image I
Output: Vector $V(pix, scale)$ of length m = number of scales
foreach *pixel pix in I* **do**
  foreach *window of size* $\leq m$ **do**
    compute $\kappa_h(pix), \kappa_v(pix), \kappa_{d_1}(pix), \kappa_{d_2}(pix)$ and find $\kappa_{Max}(pix), \kappa_{min}(pix)$;
    compute $\kappa(pix) = \kappa_{Avg}(pix) = \frac{\kappa_{Max} - \kappa_{min}}{\kappa_{Max}}$;
  end
end

Input: $V(pix, scale)$
Output: Matrix $M(I)$ – The average scale matrix
foreach *pixel pix in I* **do**
  compute $\nabla_{scale} V$;
  choose scale threshold s_0;
  select scales s_i for which $V(pix, scale) > s_0$;
  compute $s_{Avg} = s_{Avg}(pix) = \frac{\sum s_i}{|\{s_i \,|\, V(pix,scale) > s_0\}|}$;
end

Input: $M(I)$
Output: Matrix $\widetilde{M}(I)$ – Smoothed version of $M(I)$
choose window size $w_0 = w_0(texture)$;
apply linear filter at size w_0;

Input: $\widetilde{M}(I)$
Output: Segmented image $\tilde{I}$
choose maximal number of quantization levels q_0;
foreach *pixel pix in I* **do**
  compute the quantized values $\bar{s}_{Avg}(pix)_j\,,\ j = 1, \ldots, q_0$;
end
group pixels in segments $\mathfrak{s}_l(j) = \{pix \,|\, \bar{s}_{Avg}(pix) = \bar{s}_{Avg}(pix)_j\}$;

Algorithm 1: Segmentation algorithm.

In the following figures, first results of the proposed method are shown for different images. Figure 8 shows the original synthetic image which is comprised of two different textures, the second image in the figure shows the gradient vector $\frac{\partial}{\partial scale} V(scale, pixel)$ of the scaled curvature vector V, while in the third image we see the gradient vector field after smoothing with a filter of size 3×3, and in the fourth image the outcome segmentation is shown after quantization of the smoothed gradient into 4 levels. In the segmented image we see intermediate texture around the internal circle. When one looks at the original image we can clearly see that this is caused by those pixels that are in the intersection of the two different ares of the images and indeed we cannot associate specific texture to these pixels.

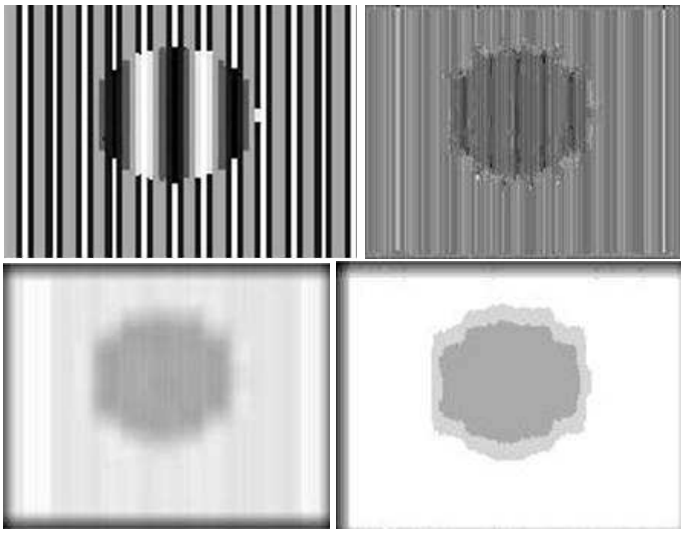

Figure 8. Segmentation of two synthetic textures: From top to bottom and from left to right: Original image, averaged information scales, smoothed gradient of the scaled curvature, the outcome of the segmentation process after quantization into 4 levels.

In Figure 9 from top to bottom we see the original image, averaged information scales as depicted in the second step of the algorithm described above and the outcome of the segmentation process after smoothed by $3X3$ window and quantized to 7 levels. Notice the sensitivity of segmentation to texture.

Figure 9. Segmentation of mandrill image. From left to tight: Original image, averaged information scales, the outcome of the segmentation process after smoothed by $3X3$ window and quantized to 7 levels.

Figure 10 shows similar phenomena on an image of fabric with several textures. The figure shows the original image and the segmented outcome of the process. We can see good separation between the different textures.

The efficiency of the proposed the segmentation algorithm is highlighted on what might be called the ”semi -synthetic” (due to the regularity and quasi-periodicity of this natural image) of

the stairs – see Figure 11.

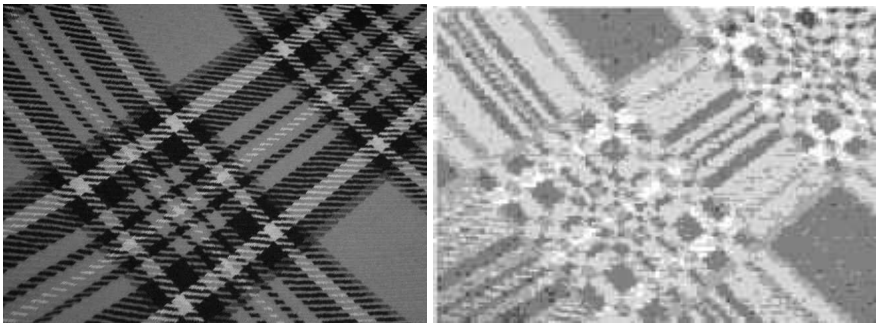

Figure 10. Segmentation of fabric image, window size and quantization level as in Figure 9. Although filter size is small one can easily see good differentiation between different structures along the fabric.

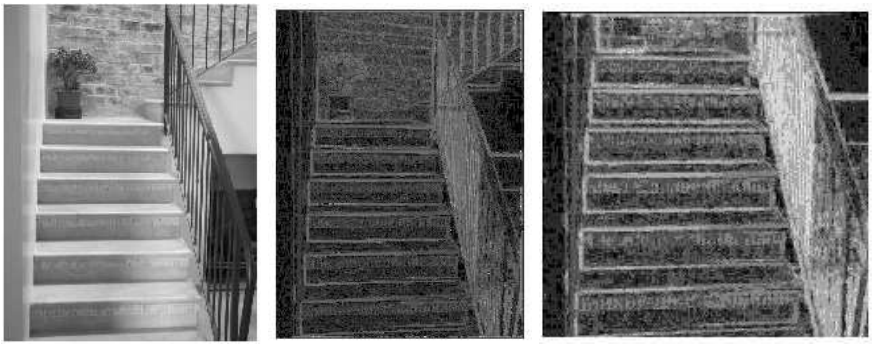

Figure 11. Segmentation of the stairs image: Original image (left), curvature computed using 3*X*3 windows (middle), detail of the segmented image using the same window size (right).

Finally, in Figure 12 the zebras are distinguished from the background of the image after their texture is segmented and separated from the texture of the background.

We conclude this Section with some preliminary comparison results. The briefness of this part is a direct consequence of the main goal of this paper, as stated in the introduction, and which we reiterate here briefly: Our essential objective is to continue and further develop the theoretical framework proposed in (Saucan *et al.*, 2010), that, in our opinion, allows, perhaps for the first time, to integrate, in a unique setting, the two common paradigms of Image Processing, namely the Harmonic Analysis/Wavelets and the Geometric (Graphics related) ones. Therefore, the present endeavor should be viewed rather as a feasibility check, rather that a bourn per se.

Nevertheless, some first comparisons were made, and we gaged our method by likening it with an established method for texture segmentation (Brox & Weickert, 2006) in conjunction with the use of the classical Gabor wavelets. Some of these results are presented in Figure 13.

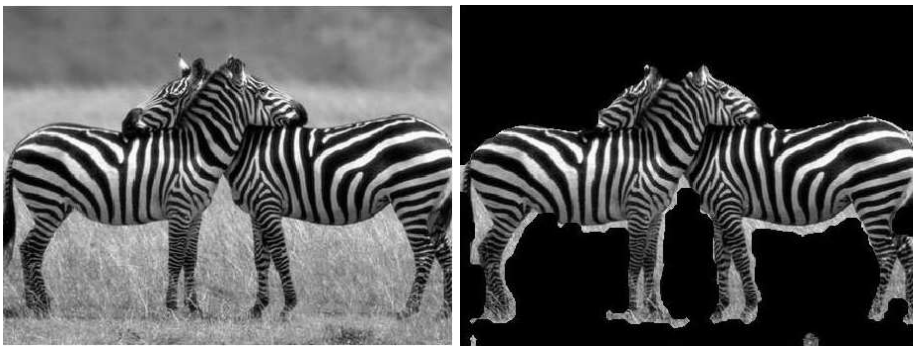

Figure 12. The zebras are extracted from the background of the original image. Extraction is based on the proposed texture segmentation.

5. Summary

The concept of scale is important for several image processing tasks. The calculation of scale on real life data usually relies on the convolution of the data with multi scale filter, where Gaussian derivatives are widespread. In this work we explored the relation between the concept of scale, to curvature. We have used the discrete definition proposed by Haantjes, and have established the theoretical exponential relation that is expected from geometry.

In addition, we propose to use the simpler curvature calculation as a means for automatic scale selection. In that respect, we show two interesting useful applications of the concept of curvature: as edge detectors and for the task of texture segmentation.

As we have noted in the introduction, scale and curvature are simply two manifests of the same physical phenomenon, it should evidently be that scale and curvature calculation can be inter-changed to accomplish the same tasks. However, while for scale only practical, intuitive, but not fully formalized definitions are given even in the most classical textbooks and other such authoritative sources, curvature – even metric one – is a classical, fully established and technical mathematical notion. We propose, therefore, in view of the remark above, to formally define scale by means of the Finsler-Haantjes curvature, at least in the purely theoretical setting. This is more relevant in the context of 2-dimensional (as well, of course, as higher dimensional ones), nonseparable signals, where a proper notion of scale is far less intuitive then in the 1-dimensional, classical, case.

Moreover, we suggest, to use this idea, not only for texture segmentation, but also in many other applications that make use of scale analysis of signals in general and of images in particular. Due to the efficiency of the computation of Haantjes curvature relative to, for instance, wavelets and Gabor functions computations in many scales, we can regard for applications both in image processing, as well as machine vision, where usually efficiency is essential. Just to name a few, we suggest the following,

a Compression and compress sensing.

b Detection of key points in images and registration.

c Scale space representation.

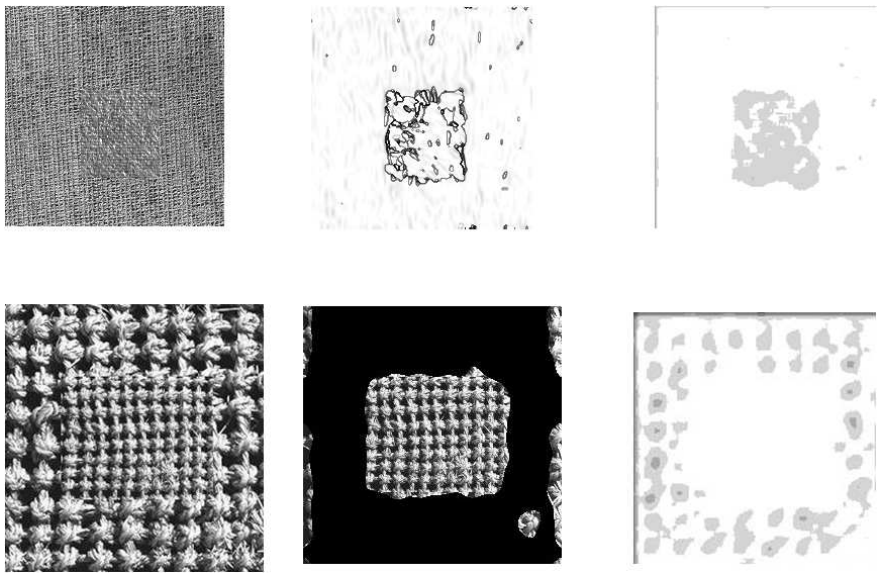

Figure 13. Texture segmentation: Gabor wavelets based segmentation (above) versus curvature based segmentation (below).

d Adaptive edge detection.

e Object recognition.

As for further possible research issues we believe that what we have presented in this paper is actually the tip of an iceberg as far the scale-curvature connection is concerned. Again, to name a few we can mention the following directions,

a Automatic scale selection in the sense of pointing out automatically a scale up to which one can apply analysis-synthesis process with a guaranteed accuracy

b Use additional information which is obtained during the process for additional tasks. As the curvature is computed we gain information about all scales at which, the curvature jumps above a predefined threshold. The method presented herein only makes use of the average of all these scales however one can employ this information for an adaptive scale selection making use of the relevant information of each of these.

c In addition to the above, there is also information about the various directions at which curvature is computed, which is obtained during the process and this information can certainly be exploited for a variety of implementations such as those mentioned above.

d Can we use the curvature-scale relation in order to gain information about the "adequacy" of a certain wavelet family to a given signal? For instance, it is often asked, is it beneficial, in any way, to decompose say, a natural image using a specific wavelets family over the others, say, for obtaining sparse representation? We hope that some answers can be given for this challenging question, via the scale-curvature analysis. We suggest to account for e.g., the exponential decay

of curvature as a function of scale, for the given signal, and then looking for the wavelet family with most similar behavior. In fact this particular question was the one that motivated this line of research.

Acknowledgments

Emil Saucan's research was partly supported by Israel Science Foundation Grants 221/07 and 93/11. and by European Research Council under the European Communitys Seventh Framework Programme (FP7/2007-2013) / ERC grant agreement nº [203134].

References

Antoine, J.P. and L. Jaques (2003). Measuring a curvature radius with directional wavletes. In: *GROUP 24: Physical and Mathematical Aspects of Symmetries, Inst. Phys. Conf. Series*. In J-P. Gazeau, R. Kerner, J-P. Antoine, S. Metens, J-Y. Thibon, (Eds.) **173**(8), 899–904.

Bay, H., T. Tuytelaars and L. Van Gool (2006). SURF: Speeded Up Robust Features. *Lecture Notes in Computer Science* **3951**, 404–417.

Beauchamp, K.G. (1975). *Walsh Functions and Their Applications*. London Academic Press.

Blumenthal, L.M. and K. Menger (1970). *Studies in Geometry*. Freeman & co., San Francisco.

Brox, T. and J. Weickert (2006). A TV flow based local scale estimate and its application to texture discrimination. *Journal of Visual Communication and Image Representation*. **17**(5), 1053–1073.

Cohen, L. (1993). The Scale Representation. *IEEE Trans. Signal Processing*. **41**(12), 3275–3292.

do Carmo, M.P (1976). *Differential Geometry of Curves and Surfaces*. Prentice-Hall, Englewood Cliffs, NJ.

Florack (1997). Image Structure. *Computational Imaging and Vision* **10**. Kluwer Academic Publishers, Dordrecht.

Florack, L., B.M. ter Haar Romeny, J.J. Koenderink and M.A. Viergever (1992). Scale and the differential structure of images. *Image Vision Comput.* **10**(6), 376–388.

Koenderink, J.J. (1984). The structure of images. *Biological Cybernetics*. **50**, 363–370.

Lindeberg, T. (1998). Feature detection with automatic scale selection. *International Journal of Computer Vision*. **30**, 77–116.

Lounsbery, J.M., A.D. DeRose and J. Warren (1997). Multiresolution Analysis For Surfaces Of Arbitrary Topological Type. *ACM Transactions on Graphics*. **16**(1), 34–73.

Lowe, D.G. (1999). Object recognition from local scale-invariant features. *ICCV '99*. **2**, 1150–1157.

Meyer, Y. (1993). *Wavelets : Algorithms & Applications*. SIAM, University of Michigan, MI.

Petersen, P. (1998). *Riemannian Geometry*. Springer-Verlag, New York.

Saucan, E. (2006). Curvature – Smooth, Piecewise-Linear and Metric. In: *What is Geometry?, Advanced Studies in Mathematics and Logic*. G. Sica, (Ed.), pp. 237-268

Saucan, E. and E. Appleboim (2005). Curvature Based Clustering for DNA Microarray Data Analysis. *Lecture Notes in Computer Science* **3523**, 405–412.

Saucan, E. and E. Appleboim (2009). Metric Methods in Surface Triangulation. *Lecture Notes in Computer Science* **5654**, 335–355.

Saucan, E., C. Sagiv and E. Appleboim (2010). Geometric Wavelets for Image Processing: Metric Curvature of Wavelets. In: *Proceedings of SampTA 2009, France, Marseille, May 18-22, 2009*. pp 85–89.

Strömberg, J.O. (1983). A modified Franklin system and high order spline systems on $\mathbb{R}^n$ as unconditional bases for Hardy spaces. In: *Conference on Harmonic Analysis in honor of A. Zygmund*. Wadeworth International Group, Belmont, CA. W. Beckner, (Ed.), pp 475-494.

Valette, S. and R. Prost (2004). Wavelet-Based Multiresolution Analysis Of Irregular Surface Meshes. *IEEE Transaction on Visualization and Computer Graphics*. **10**(2), 113–122.

Witkin, A.P. (1983). Scale-space filtering. In: *Proceedings of the Eighth international joint conference on Artificial intelligence*. Vol. 2, pp. 1019–1022.

Witkin, A.P. (1983). Scale Space Filtering: A New Approach to Multi-Scale Descriptions. In: *Proc. 8th Int. Joint Conf. Art. Intell., Germany, Karlsruhe*. pp. 1019–1022.

Theory and Applications of Mathematics & Computer Science

(ISSN 2067-2764)
http://www.uav.ro/applications/se/journal/index.php/tamcs

Theory and Applications of Mathematics & Computer Science 3 (1) (2013) 56–64

Third Order Boundary Value Problem with Integral Condition at Resonance

Assia Guezane-Lakoud[a,*], Assia Frioui[b]

[a]*Laboratory of Advanced Materials, Faculty of Sciences Badji Mokhtar-Annaba University P. O. Box 12, 23000 Annaba, Algeria*
[b]*Laboratory of applied mathematics and modeling, Department of Mathematics, University 08 Mai45-Guelma, P. O. Box 401, Guelma 24000, Algeria*

Abstract

This paper deals with a class of third order boundary value problem with integral condition at resonance. Some existence results are obtained by using the coincidence degree theory of Mawhin.

Keywords: Fixed point theorem, coincidence degree theory of Mawhin, third order boundary value problem, integral condition, Fredholm operators, resonance.
2010 MSC: 34B15, 34B18, 34G20.

1. Introduction

Let us consider the following third-order differential equation:

$$x'''(t) = f\left(t, x(t), x'(t)\right), 0 < t < 1, \tag{1.1}$$

subject to the following nonlocal conditions

$$x(0) = x''(0) = 0, x(1) = \frac{2}{\eta^2}\int_0^\eta x(t)\,dt, \eta \in (0,1), \tag{1.2}$$

where $f : [0,1] \times \mathbb{R}^2 \to \mathbb{R}$ is a Carathéodory function, and $\eta \in (0,1)$. We say that the boundary value problem (1.1), (1.2) is a resonance problem if the linear equation $Lx = x'''$, with the boundary value conditions (1.2) has a non-trivial solution i.e., $\dim \ker L \geq 1$.

*Corresponding author
Email addresses: a_guezane@yahoo.fr (Assia Guezane-Lakoud), frioui.assia@yahoo.fr (Assia Frioui)

The research of ordinary differential equations with nonlocal conditions plays a very important role in both theory and applications. It is widely used in describing a large number of physical, biological and chemical phenomena. Moreover, the theory of boundary-value problems with integral boundary conditions arises in different areas of applied mathematics and physics. For example, heat conduction, chemical engineering, underground water flow, thermo-elasticity, and plasma physics can be reduced to the nonlocal problems with integral boundary conditions. In recent years, the multi-point boundary value problems at resonance for second order, third order ordinary differential equations have been extensively studied and many excellent results have been obtained, for instance, see (Feng & Webb, 1997*a*), (Feng & Webb, 1997*b*), (Gupta, 1995), (Gupta & Tsamatos, 1994), (Liu & Yu, 2002), (Liu, 2003), (Liu & Zhao, 2007), (Kosmatov, 2006), (Du, 2008), (Du & Ge, 2005), (Ma, 2005), (Nagle & Pothoven, 1995), (Xue & Ge, 2004). (see, also, (Y. Liu, 2005), (X. Lin, 2009), (H Zhang & Chen, 2009)). However, to our knowledge, the corresponding results for third-order with integral boundary conditions, are rarely seen (see, for example, (X. Lin & Meng, 2011), (Karakostas & Tsamatos, 2002), (Yang, 2006); (A. Yang, 2011) and references therein). (Meng & Du, 2010) studied the following second-order multi-point boundary value problem at resonance:

$$\begin{cases} x''(t) = f(t, x(t), x'(t)) + e(t), t \in (0,1), \\ x(0) = \sum_{i=1}^{m} \alpha_i x(\xi_i), \ x'(1) = \sum_{j=1}^{n} \beta_j x\left(\eta_j\right), \end{cases}$$

where $f : [0,1] \times \mathbb{R}^2 \to \mathbb{R}$ is a Carathéodory function, $e \in L^1[0,1], 0 < \xi_1 < .... < \xi_m < 1$, $\alpha_i \in \mathbb{R}$, $i = 1, 2, ...m, m \geq 2$ and $0 < \eta_1 < ..... < \eta_n < 1, \beta_j \in \mathbb{R}$, $j = 1, ...n, n \geq 1$. By using coincidence degree of Mawhin the authors obtain many excellent results about the existence of solutions for the above problem under the resonance conditions $\sum_{i=1}^{m} \alpha_i = \sum_{j=1}^{n} \beta_j = 1$ and $\sum_{i=1}^{m} \alpha_i \xi_i = 0$.

By using coincidence degree of Mawhin (Lin & Meng, 2011), established the existence of solutions for the following third-order multi-point boundary value problem at resonance

$$\begin{cases} x'''(t) = f(t, x(t), x'(t), x''(t)), 0 < t < 1 \\ x''(0) = \sum_{i=1}^{m} \alpha_i x''(\xi_i), \quad x'(0) = 0, x(1) = \sum_{j=1}^{n} \beta_j x\left(\eta_j\right), \end{cases}$$

where $0 < \xi_1 < .... < \xi_m < 1$, $\alpha_i \in \mathbb{R}$, $i = 1, ...m, m \geq 1$ and $0 < \eta_1 < ..... < \eta_n < 1, \beta_j \in \mathbb{R}$, $j = 1, ...n, n \geq 2$, and $f : [0,1] \times \mathbb{R}^3 \to \mathbb{R}$ is a continuous function.

More recently, (X. Zhang & Ge, 2009) studied the following nonlocal boundary value problem:

$$\begin{cases} x''(t) = f(t, x(t), x'(t)) + e(t), t \in (0,1) \\ x'(0) = \int_0^1 h(t) x'(t)\, dt, x'(1) = \int_0^1 g(t) x'(t)\, dt, \end{cases}$$

where $f, g \in C([0,1], [0,\infty))$. Especially by using the coincidence degree of Mawhin, and under the resonance conditions $\int_0^1 h(t)\, dt = 1$, and $\int_0^1 g(t)\, dt = 1$, the authors proved at least one solution.of the boundary value problem.

The purpose of this paper is to study the existence of solutions for nonlocal boundary value problem $(1,1), (1,2)$ at resonance and establish an existence theorem . Our method is based upon the coincidence degree theory of (Mawhin, 1979).

2. Main results

We first recall some notation and an abstract existence result (Mawhin, 1979).

Let X, Y be two real Banach spaces and let $L : domL \subset X \to Y$ be a linear operator which is Fredholm map of index zero and $P : X \to X$, $Q : Y \to Y$ be continuous projectors such that $ImP = KerL$, $KerQ = ImL$ and $X = KerL \oplus KerP$, $Y = ImL \oplus ImQ$. It follows that $L|_{domL \cap KerP} : domL \cap KerP \to ImL$ is invertible, we denote the inverse of that map by K_P. Let Ω be an open bounded subset of X such that $domL \cap \Omega \neq \emptyset$, the map $N : X \to Y$ is said to be L-compact on $\overline{\Omega}$ if the map $QN\left(\overline{\Omega}\right)$ is bounded and $K_P(I - QN) : \overline{\Omega} \to X$ is compact. To obtain our existence results we use the following fixed point theorem of (Mawhin, 1979).

Theorem 2.1. *Let be L a Fredholm operator of index zero and N be L− compact on* $\overline{\Omega}$. *Assume that the following conditions are satisfied:*

i) $Lx \neq \lambda Nx$ *for every* $(x, \lambda) \in [(domL \backslash KerL) \cap \partial\Omega] \times (0, 1)$.

ii) $Nx \notin \text{Im } L$ *for every* $x \in KerL \cap \partial\Omega$.

iii) $\deg(QN|_{KerL}, \Omega \cap KerL, 0) \neq 0$, *where* $Q : Y \to Y$ *is a projection as above with* $\text{Im } L = KerQ$.

Then the equation $Lx = Nx$ *has at least one solution in* $domL \cap \overline{\Omega}$.

In the following, we shall use the classical spaces $C[0,1]$, $C^1[0,1]$, $C^2[0,1]$ and $L^1[0,1]$. For $x \in C^2[0,1]$, we use the norm $\|x\| = \max\{\|x\|_\infty, \|x'\|_\infty\}$ where $\|x\|_\infty = \max_{t\in[0,1]} |x(t)|$ and denote the norm in $L^1[0,1]$ by $\|\cdot\|_1$. We will use the Sobolev space $W^{3,1}(0,1)$ which is defined by $W^{3,1}(0,1) = \{x : [0,1] \to \mathbb{R} : x, x', x'' \text{ are absolutely continuous on } [0,1] \text{ with } x''' \in L^1[0,1]\}$.

Let $X = C^2[0,1]$, $Y = L^1[0,1]$, L is the linear operator from $domL \subset X$ to Y with $domL = \left\{x \in W^{3,1}(0,1) : x(0) = x''(0) = 0,\ x(1) = \frac{2}{\eta^2}\int_0^\eta x(t)\,dt\right\}$ and $Lx = x'''$, $x \in \text{dom } L$. We define $N : X \to Y$ by setting

$$Nx = f(t, x(t), x'(t)), t \in (0,1).$$

Then the BVP (1.1) and (1.2) can be written as $Lx = Nx$.

Theorem 2.2. *Assume that the following conditions are satisfied:*

1) There exists functions $\alpha, \beta, \gamma \in L^1[0,1]$, *such that for all* $(x, y) \in \mathbb{R}^2$, $t \in [0,1]$ *then*

$$|f(t,x,y)| \leq \alpha(t)|x| + \beta(t)|y| + \gamma(t). \tag{2.1}$$

2) There exists a constant $M > 0$, *such that for* $x \in domL$, *if* $|x'(t)| > M$ *for all* $t \in [0,1]$, *then*

$$\int_0^1 (1-s)^2 f(s, x(s), x'(s))\,ds - \frac{2}{3\eta^2}\int_0^\eta (\eta - s)^3 f(s, x(s), x'(s))\,ds \neq 0. \tag{2.2}$$

3) There exists a constant $M^* > 0$, *such that for any* $x(t) = bt \in KerL$ *with* $|b| > M^*$, *either*

$$b\left[\int_0^1 (1-s)^2 f(s, b(s), b)\,ds - \frac{2}{3\eta^2}\int_0^\eta (\eta - s)^3 f(s, b(s), b)\,ds\right] < 0, \tag{2.3}$$

or else

$$b\left[\int_0^1 (1-s)^2 f(s, b(s), b)\,ds - \frac{2}{3\eta^2}\int_0^\eta (\eta - s)^3 f(s, b(s), b)\,ds\right] > 0. \tag{2.4}$$

then BVP $(1,1)$ *and* $(1,2)$ *has at least one solution in* $C^2[0,1]$, *provided*

$$\|\alpha\| + \|\beta\| < \frac{1}{2}. \tag{2.5}$$

2.1. Proof of Theorem 2.2

For the proof of Theorem 2.2 we shall apply Theorem 2.1 and the following lemmas.

Lemma 2.1. *The operator $L : domL \subset X \to Y$ is a Fredholm operator of index zero. Furthermore, the linear projector operator $Q : Y \to Y$ can be definied by*

$$Qy(t) = k\left[\int_0^1 (1-s)^2 y(s)\,ds - \frac{2}{3\eta^2}\int_0^\eta (\eta - s)^3 y(s)\,ds\right]t,$$

where $k = 60/5 - 2\eta^3$ and the linear operator $K_P : \text{Im } L \to dom\, L \cap Ker\, P$ can be written by

$$K_p y(t) = \frac{1}{2}\int_0^t (t-s)^2 y(s)\,ds, \forall y \in \text{Im } L.$$

Furthermore

$$\left\|K_p y\right\| \le \|y\|_1, \forall y \in \text{Im } L.$$

Proof. It is clear that

$$kerL = \{x \in \text{dom } L : x = bt,\ b \in \mathbb{R},\ t \in [0,1]\} \simeq \mathbb{R}.$$

Now we show that

$$\text{Im } L = \left\{ y \in Y : \int_0^1 (1-s)^2 y(s)\,ds - \frac{2}{3\eta^2}\int_0^\eta (\eta - s)^3 y(s)\,ds = 0 \right\}. \tag{2.6}$$

The problem

$$x''' = y \tag{2.7}$$

has a solution $x(t)$ that satisfies the conditions $x(0) = x''(0) = 0,\ x(1) = \frac{2}{\eta^2}\int_0^\eta x(t)\,dt$, if and only if

$$\int_0^1 (1-s)^2 y(s)\,ds - \frac{2}{3\eta^2}\int_0^\eta (\eta - s)^3 y(s)\,ds = 0. \tag{2.8}$$

In fact from (2.7) we have

$$x(t) = x''(0)\frac{t^2}{2} + x'(0)t + x(0) + \frac{1}{2}\int_0^t (t-s)^2 y(s)\,ds = x'(0)t + \frac{1}{2}\int_0^t (t-s)^2 y(s)\,ds.$$

According to $x(1) = \frac{2}{\eta^2}\int_0^\eta x(t)\,dt$,we obtain

$$\int_0^1 (1-s)^2 y(s)\,ds - \frac{2}{3\eta^2}\int_0^\eta (\eta - s)^3 y(s)\,ds = 0.$$

On the other hand, if (2.8) holds, setting

$$x(t) = bt + \frac{1}{2}\int_0^t (t-s)^2 y(s)\,ds,$$

where b is an arbitrary constant, then $x(t)$ is a solution of (2.7). Hence (2.6) holds.
Setting

$$Ry = \int_0^1 (1-s)^2 y(s)\,ds - \frac{2}{3\eta^2}\int_0^\eta (\eta - s)^3 y(s)\,ds,$$

define $Qy(t) = k.(Ry).t$, it is clear that $\dim \mathrm{Im}Q = 1$. We have

$$Q^2 y = Q(Qy) = k(k.Ry)\left(\int_0^1 (1-s)^2 sds - \frac{2}{3\eta^2}\int_0^\eta (\eta - s)^3 sds\right)t = (kRy)\,t = Qy,$$

which implies that the operator Q is a projector. Furthermore, $\mathrm{Im}\,L = kerQ$.
Let $y = (y - Qy) + Qy$, where $y - Qy \in KerQ = \mathrm{Im}\,L$, $Qy \in \mathrm{Im}Q$. It follows from $KerQ = \mathrm{Im}\,L$ and $Q^2 y = Qy$ that $\mathrm{Im}\,Q \cap \mathrm{Im}\,L = \{0\}$. Then, we have $Y = \mathrm{Im}\,L \oplus \mathrm{Im}\,Q$. Since $\dim KerL = 1 = \dim \mathrm{Im}\,Q = co\dim \mathrm{Im}\,L = 1$, L is a Fredholm map of index zero.
Now we define a projector P from X to X by setting

$$Px(t) = x'(0)\,t.$$

Then the generalized inverse $K_P : \mathrm{Im}\,L \to domL \cap KerP$ of L can be written by

$$K_p = \frac{1}{2}\int_0^t (t-s)^2 y(s)\,ds.$$

Obviously, $\mathrm{Im}\,P = KerL$ and $P^2 x = Px$. It follows from $x = (x - Px) + Px$ that $X = KerP + KerL$. By simple calculation, we can get that $KerL \cap KerP = \{0\}$. Then $X = KerL \oplus KerP$. From the definitions of P and K_P it is easy to see that the generalized inverse of L is K_P. In fact, for $y \in \mathrm{Im}\,L$, we have

$$\left(LK_p\right)y(t) = \left[\left(K_p y\right)t\right]''' = y(t),$$

and for $x \in domL \cap kerP$, we know

$$\left(K_p L\right)x(t) = \left(K_p\right)x'''(t) = \frac{1}{2}\int_0^t (t-s)^2 x'''(s)\,ds = x(t) - x(0) - x'(0)\,t - \frac{1}{2}x''(0)\,t^2,$$

in view of $x \in domL \cap kerP$, $x(0) = x''(0) = 0$ and $Px = 0$, thus

$$\left(K_p L\right)x(t) = x(t).$$

This shows that $K_p = \left(L|_{\mathrm{dom}L \cap \mathrm{ker}P}\right)^{-1}$. Also we have

$$\left\|K_p y\right\|_\infty \le \int_0^1 (1-s)^2 |y(s)|\,ds \le \int_0^1 |y(s)|\,ds = \|y\|_1,$$

and from $\left(K_p y\right)'(t) = \int_0^1 (1-s)\, y(s)\, ds$, we obtain

$$\left\|\left(K_p y\right)'\right\|_\infty \leq \int_0^1 (1-s)\,|y(s)|\, ds \leq \int_0^1 |y(s)|\, ds = \|y\|_1$$

then $\left\|K_p y\right\| \leq \|y\|_1$. This completes the proof of Lemma 2.1. □

Lemma 2.2. *Let* $\Omega_1 = \{x \in domL \backslash KerL : Lx = \lambda Nx, for\ some\ \lambda \in [0,1]\}$. *Then* Ω_1 *is bounded.*

Proof. Suppose that $x \in \Omega_1$, and $Lx = \lambda Nx$. Thus $\lambda \neq 0$ and $QNx = 0$, so it yields

$$\int_0^1 (1-s)^2 f(s, x(s), x'(s))\, ds - \frac{2}{3\eta^2} \int_0^\eta (\eta - s)^3 f(s, x(s), x'(s))\, ds = 0.$$

Thus, by condition (2), there exists $t_0 \in [0,1]$, such that $|x'(t)| \leq M$. In view of

$$x'(0) = x'(t_0) - \int_0^{t_0} x''(t)\, dt, x''(t) = x''(0) + \int_0^t x'''(s)\, ds,$$

then, we have

$$|x'(0)| \leq M + \int_0^1 \left(\int_0^1 |x'''(s)\, ds| \right) dt = M + \|x'''\|_1 = M + \|Lx\|_1 \leq M + \|Nx\|_1 . \tag{2.9}$$

Again for $x \in \Omega_1$, $x \in domL \backslash KerL$, then $(I-P)x \in domL \cap KerP$ and $LPx = 0$, thus from Lemma 3, we know

$$\|(I-P)x\| = \left\|K_p L(I-Px)\right\| \leq \|L(I-Px)\|_1 = \|Lx\|_1 \leq \|Nx\|_1 . \tag{2.10}$$

From (2.9) and (2.10), we have

$$\|x\| \leq \|Px\| + \|(I-P)x\| = |x'(0)| + \|(I-P)x\| \leq M + 2\|Nx\|_1 . \tag{2.11}$$

From (2.1) and (2.11), we obtain

$$\|x\| \leq 2\left[\|\alpha\|_1 \|x\|_\infty + \|\beta\|_1 \|x'\|_\infty + \|\gamma\|_1 + \frac{M}{2}\right]. \tag{2.12}$$

Thus, from $\|x\|_\infty \leq \|x\|$ and (2.12) we have

$$\|x\|_\infty \leq \frac{2}{1 - 2\|\alpha\|_1}\left[\|\beta\|_1 \|x'\|_\infty + \|\gamma\|_1 + \frac{M}{2}\right]. \tag{2.13}$$

From $\|x'\|_\infty \leq \|x\|$, and (2.12) and (2.13), one has

$$\|x'\|_\infty \left[1 - \frac{2\|\beta\|_1}{1 - 2\|\alpha\|_1}\right] \leq \frac{2}{1 - 2\|\alpha\|_1}\left[\|\gamma\|_1 + \frac{M}{2}\right].$$

Therefore,

$$\|x'\|_\infty \left[\frac{1-2\|\alpha\|_1-2\|\beta\|_1}{1-2\|\alpha\|_1}\right] \leq \frac{1}{1-2\|\alpha\|_1}\left[2\|\gamma\|_1+M\right].$$

i.e.,

$$\|x'\|_\infty \leq \frac{2\left[\|\gamma\|_1+\frac{M}{2}\right]}{1-2\|\alpha\|_1-2\|\beta\|_1} = M_1. \tag{2.14}$$

From (2.14), there exists $M_1 > 0$, such that

$$\|x'\|_\infty \leq M_1, \tag{2.15}$$

thus from (2.15) and (2.13), there exists $M_2 > 0$, such that

$$\|x\|_\infty \leq M_2. \tag{2.16}$$

Hence

$$\|x\| = \max\{\|x\|_\infty, \|x'\|_\infty\} \leq \max\{M_1, M_2\}.$$

Again from (2.1), (2.15) and (2.16), we have

$$\|x'''\|_1 = \|Lx\|_1 \leq \|Nx\|_1 \leq \|\alpha\|_1 M_2 + \|\beta\|_1 M_1 + \|\gamma\|_1.$$

So Ω_1 is bounded. □

Lemma 2.3. *The set* $\Omega_2 = \{x \in KerL : Nx \in \text{Im } L\}$ *is bounded.*

Proof. Let $x \in \Omega_2$, then $x \in KerL = \{x \in domL : x = bt,\ b \in \mathbb{R},\ t \in [0,1]\}$, and $QNx = 0$, therefore

$$\int_0^1 (1-s)^2 f(s, bs, b)\, ds - \frac{2}{3\eta^2}\int_0^\eta (\eta - s)^3 f(s, bs, b)\, ds = 0.$$

From condition (2) of Theorem 2.2, $\|x\|_\infty = |b| \leq M$, so $\|x\| = |b| \leq M$, thus Ω_2 is bounded. □

Lemma 2.4. *If the first part of condition (3) of Theorem 2.2 holds, then*

$$b\frac{60}{5-2\eta^3}\left[\int_0^1 (1-s)^2 f(s, b(s), b)\, ds - \frac{2}{3\eta^2}\int_0^\eta (\eta - s)^3 f(s, b(s), b)\, ds\right] < 0, \tag{2.17}$$

for all $|b| > M^*$. *Let* $\Omega_3 = \{x \in KerL : -\lambda Jx + (1-\lambda)QNx = 0,\ \ \lambda \in [0,1]\ \}$ *where* $J : KerL \to$ Im Q *is the linear isomorphism given by* $J(bt) = bt$, $\forall b \in \mathbb{R}$, $t \in [0,1]$. *Then* Ω_3 *is bounded.*

Proof. Suppose that $x = b_0 t \in \Omega_3$, then we obtain

$$\lambda b_0 = (1-\lambda)\frac{60}{5-2\eta^3} \times \left(\int_0^1 (1-s)^2 f(s, b(s), b)\, ds - \frac{2}{3\eta^2}\int_0^\eta (\eta - s)^3 f(s, b(s), b)\, ds\right).$$

If $\lambda = 1$, then $b_0 = 0$. Otherwise, if $|b_0| > M^*$, then in view of (2.17) one has $\lambda b_0^2 = b_0(1-\lambda)\frac{60}{5-2\eta^3} \times \left(\int_0^1 (1-s)^2 f(s, b(s), b)\, ds - \frac{2}{3\eta^2}\int_0^\eta (\eta - s)^3 f(s, b(s), b)\, ds\right) < 0,$

which contradicts the fact that $\lambda b_0^2 \geq 0$. Then $|x| = |b_0 t| \leq |b_0| \leq M^*$, we obtain $\|x\| \leq M^*$, therefore $\Omega_3 \subset \{x \in KerL : \|x\| \leq M^*\}$ is bounded.

If $\lambda = 0$, it yields

$$\int_0^1 (1-s)^2 f(s, b(s), b)\, ds - \frac{2}{3\eta^2} \int_0^\eta (\eta - s)^3 f(s, b(s), b)\, ds = 0,$$

taking condition (2) of Theorem 2.2 into account, we obtain $\|x\| = |b| \leq M^*$. □

Lemma 2.5. *If the second part of condition (3) of Theorem 2.2 holds, then*

$$b \frac{60}{5 - 2\eta^3} \left[\int_0^1 (1-s)^2 f(s, b(s), b)\, ds - \frac{2}{3\eta^2} \int_0^\eta (\eta - s)^3 f(s, b(s), b)\, ds \right] > 0, \tag{2.18}$$

for all $|b| > M^*$. Let $\Omega_3 = \{x \in KerL : \lambda Jx + (1-\lambda) QNx = 0, \ \lambda \in [0,1]\}$, here J is defined as in Lemma 2.4. Similar to the above argument, we can verify that Ω_3 is bounded.

Now the proof of Theorem 2.2 is a consequence of Theorem 2.1 and the above lemmas.

Proof. **of Theorem 2.2**. Let Ω to be an open bounded subset of X such that $\cup_{i=1}^3 \overline{\Omega}_i \subset \Omega$. By using the Arzela- Ascoli theorem, we can prove that $K_P(I - QN) : \overline{\Omega} \to X$ is compact, thus N is L-compact on $\overline{\Omega}$. Then by Lemmas 2.2 and 2.3, we have

i) $Lx \neq \lambda Nx$ pour tout $(x, \lambda) \in [(domL \backslash KerL) \cap \partial\Omega] \times (0,1)$.

ii) $Nx \notin \text{Im } L$ pour tout $x \in KerL \cap \partial\Omega$.

iii) Let $H(x, \lambda) = \pm \lambda Jx + (1-\lambda) QNx = 0$.

According to Lemmas 2.4 and 2.5, we know that $H(x, \lambda) \neq 0$ for every $x \in KerL \cap \partial\Omega$. Thus, by the homotopy property of degree, $\deg(QN|_{KerL}, \Omega \cap KerL, 0) = \deg(H(\cdot, 0), \Omega \cap KerL, 0) = \deg(H(\cdot, 1), \Omega \cap KerL, 0) = \deg(\pm J, \Omega \cap KerL, 0) \neq 0$. Then by Theorem 2.1, $Lx = Nx$ has at least one solution in $domL \cap \overline{\Omega}$, so the BVP (1.1), (1, 2) has at least one solution in $C^2[0,1]$. The proof is complete. □

References

A. Yang, B. Sun, W. Ge (2011). Existence of positive solutions for self-adjiont boundary-value problems with integral boundary condition at resonance. *Electron. J. Differential Equations* **11**, 1–8.

Du, Z (2008). Solvability of functional differential equations with multi-point boundary value problem at resonance. *Comput. Math. Appl* **55**, 2653–2661.

Du, Z., X. Lin and W. Ge (2005). On a third-order multi-point boundary value problem at resonance. *J. Math. Anal. Appl* **302**, 217–229.

Feng, W. and J. R. L. Webb (1997*a*). Solvability of m-point boundary value problems with nonlinear growth. *J. Math. Anal. Appl* **212**, 467–480.

Feng, W. and J. R. L. Webb (1997*b*). Solvability of three-point boundary value problems at resonance. *Nonlinear Anal. Theory, Methods and Appl* **30**, 3227–3238.

Gupta, C.P (1995). A second order m-point boundary value problem at resonance. *Nonlinear Anal* **24**, 1036–1046.

Gupta, C.P., S.K. Ntouyas and P.Ch. Tsamatos (1994). On an m-point boundary-value problem for second-order ordinary differential equations. *Nonlinear Anal* **23**, 1427–1436.

H Zhang, W Liu, J Zhang and T Chen (2009). Existence of solutions for three- point boundary value problem. *J. Appl. Math. & Informatics* **27**(5-6), 35–51.

Karakostas, G. L. and P. Ch. Tsamatos (2002). Sufficient conditions for the existence of nonnegative solutions of a nonlocal boundary value problem. *Appl. Math. Letters* **15**(4), 401–407.

Kosmatov, N (2006). A multi-point boundary value problem with two critical conditions. *Nonlinear Analysis: Theory, Methods & Applications* **65**, 622–633.

Lin, X., Z. Du. and F. Meng (2011). A note on a third-order multi-point boundary value problem at resonance. *Math. Nachr.* **284**(13), 1690 – 1700.

Liu, B (2003). Solvability of multi-point boundary value problem at resonance (ii). *Appl. Math. Comput* **136**, 353–377.

Liu, B. and J. S. Yu (2002). Solvability of multi-point boundary value problems at resonance (i). *Indian J. Pure Appl. Math* **34**, 475–494.

Liu, B. and Z. Zhao (2007). A note on multi-point boundary value problems. *Nonlinear Anal* **67**, 2680–2689.

Ma, R (2005). Multiplicity results for a third order boundary value problem at resonance, nonlinear anal. *Nonlinear Anal* **32**, 493–499.

Mawhin, J. (1979). *Topological degree methods in nonlinear boundary value problems*. NSFCBMS Regional Conference Series in Mathematics, American Mathematical Society, Providence, RI.

Meng, F. and Z. Du (2010). Solvability of a second order multi-point boundary value problem at resonance. *Appl. Math. Comput* **208**, 23–30.

Nagle, R. K. and K. L. Pothoven (1995). On a third-order nonlinear boundary value problems at resonance. *J. Math. Anal. Appl* **195**, 148–159.

X. Lin, W. Liu (2009). A nonlinear third-order multi-point boundary value prob- lems in the resonance case. *J. App Math comput* **29**, 35–51.

X. Lin, Z. Du and F. Meng (2011). Existence of solutions to a nonlocal boundary value problem with nonlinear growth. *Boundary Value Problems* **2011**, 15pp.

X. Zhang, M. Feng and W. Ge (2009). Existence result of second-order differential equations with integral boundary conditions at resonance. *J. Math. Anal. Appl* **353**(1), 311–319.

Xue, C., Z. Du. and W. Ge (2004). Solutions to m-point boundary value problems of third order ordinary differential equations at resonance. *J. Appl. Math. Comput* **17**(1-2), 299–244.

Y. Liu, W Ge (2005). Solution of multi-point boundary value problems for higher-order differential equations at resonance(iii). *Tamkang Journal of Mathematics* **36**(2), 119–130.

Yang, Z. (2006). Positive solutions of a second-order integral boundary-value problem. *J. Math. Anal. Appl* **321**, 751–765.

Theory and Applications of Mathematics & Computer Science

(ISSN 2067-2764)
http://www.uav.ro/applications/se/journal/index.php/tamcs

Theory and Applications of Mathematics & Computer Science 3 (1) (2013) 65–84

The $(\mathcal{G}, \beta, \phi, h(\cdot,\cdot), \rho, \theta)$-Univexities of Higher-Orders with Applications to Parametric Duality Models in Minimax Fractional Programming

Ram U Verma[a,*]

[a]*International Publications USA, 3400 S Brahma Blvd Suite 31B, Kingsville, TX 78363, USA*

Abstract

Based on the recently introduced (see (Verma, 2012)) major higher order generalizations ($\mathcal{G}$, β, ϕ, $h(\cdot,\cdot)$, ρ, θ) - univexities, several second-order parametric duality models for a semiinfinite minimax fractional programming problem are developed with appropriate duality results under various generalized second-order ($\mathcal{G}$, β, ϕ, $h(\cdot,\cdot)$, ρ, θ) - univexity assumptions. The obtained results encompass a large variety of investigations on generalized univexities and their extensions in the literature.

Keywords: Semiinfinite programming, minimax fractional programming, generalized second-order univex functions, infinitely many equality and inequality constraints, dual problems, duality theorems.
2010 MSC: 49N15, 90C26, 90C30, 90C32, 90C45, 90C47.

1. Introduction

In this paper, we intend to establish some results on second-order duality under various generalized $(\mathcal{G}, \beta, \phi, h(\cdot,\cdot), \rho, \theta)$-univexity assumptions for the semiinfinite discrete minimax fractional programming problem of the form:

$$(P) \qquad \text{Minimize} \ \max_{1\le i\le p} \frac{f_i(x)}{g_i(x)}$$

subject to

$$G_j(x,t) \le 0 \ \text{ for all } t \in T_j, \quad j \in \underline{q} = \{1,2,\cdots,q\},$$
$$H_k(x,s) = 0 \ \text{ for all } s \in S_k, \quad k \in \underline{r} = \{1,2,\cdots,r\},$$
$$x \in X,$$

*Corresponding author
Email address: verma99@msn.com (Ram U Verma)

where p, q, and r are positive integers, X is a nonempty open convex subset of $\mathbb{R}^n$ (n-dimensional Euclidean space), for each $j \in \underline{q} = \{1, 2, \ldots, q\}$ and $k \in \underline{r} = \{1, 2, \ldots, r\}$, T_j and S_k are compact subsets of complete metric spaces, for each $i \in \underline{p}$, f_i and g_i are twice continuously differentiable real-valued functions defined on X, for each $j \in \underline{q}$, $z \to G_j(z, t)$ is a twice continuously differentiable real-valued function defined on X for all $t \in T_j$, for each $k \in \underline{r}$, $z \to H_k(z, s)$ is a twice continuously differentiable real-valued function defined on X for all $s \in S_k$, for each $j \in \underline{q}$ and $k \in \underline{r}$, $t \to G_j(x, t)$ and $s \to H_k(x, s)$ are continuous real-valued functions defined, respectively, on T_j and S_k for all $x \in X$, and for each $i \in \underline{p}$, $g_i(x) > 0$ for all x satisfying the constraints of (P). The present communication is concerned with the major generalization $(\mathcal{G}, \beta, \phi, h(\cdot, \cdot), \rho, \theta)$- univexity of the second order introduced by Verma (see (Verma, 2012)) that generalizes $(\mathcal{F}, \beta, \phi, \rho, \theta)$-univexity introduced by Zalmai (see (Zalmai, 2012)) and the first order univexity studied by Zalmai and Zhang (see (Zalmai & Zhang, 2007)) with its applications to parametric duality models in minimax fractional programming. The obtained results not only generalize the work of Zalmai on second order univexities, but also generalize other investigations on general invexities, including the valued-contributions of Jeyakumar (see (Jeyakumar *b*, 1985)), Liu (see (Liu, 1999)), Mangasarian (see (Mangasarian, 1975)), Mishra (see (Mishra, 1997), (Mishra, 2000)), Mishra and Rueda (see (Mishra & Rueda, 2000), (Mishra & Rueda, 2006)), Mond (see (Mond, 1974)) and others. Based on Mangasarian's second-order dual problem, Mond (see (Mond, 1974)) established some duality results under relatively simpler conditions involving a certain second-order generalization of the concept of convexity, while observed some possible computational advantages of second-order duality results, and also studied a pair of second-order symmetric dual problems. Mond's original notion of second-order convexity was followed by generalizations by other authors in different ways and applied establishing several second-order duality results for several classes of nonlinear programming problems. Although there exist various second-order duality results in the related literature for several classes of mathematical programming problems with a finite number of constraints, we feel our second-order duality results established in this paper are new and general in nature to the context of semiinfinite programming. For more details on second order duality results, we refer the reader (see (Aghezzaf, 2003) - (Zalmai & Zhang, 2007)), but more importantly, (see (Aghezzaf, 2003) - (Jeyakumar *b*, 1985), (Mond & Weir, 1981-1983), (Mond & Zhang, 1995) - (Zalmai & Zhang, 2007)).

Note that second-order duality for a conventional nonlinear programming problem is of the form

$$(P_0) \qquad \text{Minimize } f(x) \text{ subject to } g_i(x) \le 0, \quad i \in \underline{m}, \quad x \in \mathbb{R}^n,$$

where f and g_i, $i \in \underline{m}$, are twice differentiable real-valued functions defined on $\mathbb{R}^n$, was initially considered and studied by Mangasarian (see (Mangasarian, 1975)). The idea underlying his approach to constructing a second-order dual problem was based on taking linear and quadratic approximations of the objective and constraint functions about an arbitrary but fixed point, leading to the Wolfe dual of the approximated problem, and then allowing the fixed point to vary. Mangasarian (see (Mangasarian, 1975)), more specifically, formulated the following second-order dual problem for (P_0):

$$(D_0) \qquad \text{Maximize } f(y) + \sum_{i=1}^{m} u_i g_i(y) - \tfrac{1}{2}\left\langle z, \left[\nabla^2 f(y) + \sum_{i=1}^{m} u_i \nabla^2 g_i(y)\right] z\right\rangle$$

subject to

$$\nabla f(y) + \sum_{i=1}^{m} u_i \nabla g_i(y) + \Big[\nabla^2 f(y) + \sum_{i=1}^{m} u_i \nabla^2 g_i(y)\Big] z = 0,$$
$$y \in \mathbb{R}^n, \quad u \in \mathbb{R}^m, \quad u \geq 0, \quad z \in \mathbb{R}^n,$$

where $\nabla F(y)$ and $\nabla^2 F(y)$ denote, respectively, the gradient and Hessian of the function $F : \mathbb{R}^n \to \mathbb{R}$ evaluated at y and $\langle a, b\rangle$ denotes the inner product of the vectors a and b. Then, by imposing somewhat complicated conditions on f, g_i, $i \in \underline{m}$, and z, he proved weak, strong, and converse duality theorems for (P_0) and (D_0).

We observe that all the duality results established in this paper can easily be modified and restated for each one of the following classes of nonlinear programming problems, that are special cases of (P):

$(P1)$ Minimize $\dfrac{f_1(x)}{g_1(x)}$;

$(P2)$ Minimize $\max\limits_{1\leq i\leq p} f_i(x)$;

$(P3)$ $\underset{x\in\mathbb{F}}{\text{Minimize}}\ f_1(x)$,

where $\mathbb{F}$ (assumed to be nonempty) is the feasible set of (P), that is,

$$\mathbb{F} = \{x \in \mathbb{R}^n : G_j(x,t) \leq 0 \text{ for all } t \in T_j,\ j \in \underline{q}, \quad H_k(x,s) = 0 \text{ for all } s \in S_k,\ k \in \underline{r}\};$$

$(P4)$ Minimize $\max\limits_{1\leq i\leq p} \dfrac{f_i(x)}{g_i(x)}$

subject to

$$\tilde{G}_j(x) \leq 0, \quad j \in \underline{q}, \quad \tilde{H}_k(x) = 0, \quad k \in \underline{r}, \quad x \in \mathbb{R}^n,$$

where f_i and g_i, $i \in \underline{p}$, are as defined in the description of (P), and $\tilde{G}_j$, $j \in \underline{q}$, and $\tilde{H}_k$, $k \in \underline{r}$, are real-valued functions defined on X;

$(P5)$ $\underset{x\in\mathbb{G}}{\text{Minimize}}\ \dfrac{f_1(x)}{g_1(x)}$;

$(P6)$ $\underset{x\in\mathbb{G}}{\text{Minimize}}\ \max\limits_{1\leq i\leq p} f_i(x)$;

$(P7)$ $\underset{x\in\mathbb{G}}{\text{Minimize}}\ f_1(x)$,

where $\mathbb{G}$ is the feasible set of $(P4)$, that is,

$$\mathbb{G} = \{x \in \mathbb{R}^n : \tilde{G}_j(x) \leq 0,\ j \in \underline{q}, \quad \tilde{H}_k(x) = 0, \quad k \in \underline{r}\}.$$

2. Preliminaries

In this section we recall, the recently introduced major generalization $(\mathcal{G},\beta,\phi,h(\cdot,\cdot),\rho,\theta)-$ univexiity by Verma (see (Verma, 2012)) to the notion of the Zalmai type $(\mathcal{F},\beta,\phi,\rho,\theta)$-univexity of higher order (See (Zalmai, 2012)) to the context of parametric duality models in semiinfinite discrete minimax fractional programming. The obtained notion, in fact, reduces to most of the existing notions of invexities and univexities in the literature.

Recall that a function $\mathcal{G}:\mathbb{R}^n\to\mathbb{R}$ is said to be *sublinear*(*superlinear*) if

$$\mathcal{G}(x+y)\leq(\geq)\mathcal{G}(x)+\mathcal{G}(y)\;\forall\;x,y\in\mathbb{R}^n,$$

and $\mathcal{G}(ax)=a\mathcal{G}(x)$ for all $x\in\mathbb{R}^n$ and $a\in\mathbb{R}_+=[0,\infty)$.

Let $x^*\in X$ and let us assume that the function $f:X\to\mathbb{R}$ is twice continuously differentiable at x^*.

Definition 2.1. The function f is said to be *(strictly)* $(\mathcal{G},\beta,\phi,h(x^*,z),\rho,\theta)$-*univex* at x^* of higher order if there exist functions $\beta:X\times X\to\mathbb{R}_+\backslash\{0\}=(0,\infty)$, $\phi:\mathbb{R}\to\mathbb{R}$, $\rho:X\times X\to\mathbb{R}$, $\theta:X\times X\to\mathbb{R}^n$, and a sublinear function $\mathcal{G}(x,x^*;\cdot):\mathbb{R}^n\to\mathbb{R}$ such that for each $x\in X(x\neq x^*)$ and $z\in\mathbb{R}^n$,

$$\phi(f(x)-f(x^*)+\langle z,\nabla_z h(x^*,z)\rangle-h(x^*,z))(>)\geq\mathcal{G}(x,x^*;\beta(x,x^*)[\nabla_z h(x^*,z)]) + \rho(x,x^*)\|\theta(x,x^*)\|^2,$$

where $h:\mathbb{R}^n\times\mathbb{R}^n\to\mathbb{R}^n$ is differentiable with respect to the second component.

Definition 2.2. The function f is said to be *(strictly)* $(\mathcal{G},\beta,\phi,h(x^*,z),\rho,\theta)$-*pseudounivex* at x^* if there exist functions $\beta:X\times X\to\mathbb{R}_+\backslash\{0\}$, $\phi:\mathbb{R}\to\mathbb{R}$, $\rho:X\times X\to\mathbb{R}$, $\theta:X\times X\to\mathbb{R}^n$, and a sublinear function $\mathcal{G}(x,x^*;\cdot):\mathbb{R}^n\to\mathbb{R}$ such that for each $x\in X(x\neq x^*)$ and $z\in\mathbb{R}^n$,

$$\mathcal{G}(x,x^*;\beta(x,x^*)[\nabla_z h(x^*,z)])\geq-\rho(x,x^*)\|\theta(x,x^*)\|^2 \Rightarrow\quad\phi(f(x)-f(x^*)+\langle z,\nabla_z h(x^*,z)\rangle-h(x^*,z))(>)\geq 0,$$

equivalently,

$$\phi(f(x)-f(x^*)+\langle z,\nabla_z h(x^*,z)\rangle-h(x^*,z))(\leq)<0\Rightarrow \mathcal{G}(x,x^*;\beta(x,x^*)[\nabla_z h(x^*,z)])<-\rho(x,x^*)\|\theta(x,x^*)\|^2,$$

where $h:\mathbb{R}^n\times\mathbb{R}^n\to\mathbb{R}^n$ is differentiable with respect to the second component.

Definition 2.3. The function f is said to be *prestrictly* $(\mathcal{G},\beta,\phi,h(x^*,z),\rho,\theta)$-*pseudounivex* at x^* if there exist functions $\beta:X\times X\to\mathbb{R}_+\backslash\{0\}$, $\phi:\mathbb{R}\to\mathbb{R}$, $\rho:X\times X\to\mathbb{R}$, $\theta:X\times X\to\mathbb{R}^n$, and a sublinear function $\mathcal{G}(x,x^*;\cdot):\mathbb{R}^n\to\mathbb{R}$ such that for each $x\in X(x\neq x^*)$ and $z\in\mathbb{R}^n$,

$$\mathcal{G}(x,x^*;\beta(x,x^*)[\nabla_z h(x^*,z)])>-\rho(x,x^*)\|\theta(x,x^*)\|^2 \Rightarrow\quad\phi(f(x)-f(x^*)+\langle z,\nabla_z h(x^*,z)\rangle-h(x^*,z))\geq 0,$$

equivalently,

$$\phi(f(x) - f(x^*) + \langle z, \nabla_z h(x^*, z)\rangle - h(x^*, z)) < 0 \Rightarrow \\ \mathcal{G}(x, x^*; \beta(x, x^*)[\nabla_z h(x^*, z)]) \leq -\rho(x, x^*)\|\theta(x, x^*)\|^2,$$

where $h : \mathbb{R}^n \times \mathbb{R}^n \to \mathbb{R}^n$ is differentiable with respect to the second component.

Definition 2.4. The function f is said to be *(prestrictly)*$(\mathcal{G}, \beta, \phi, h(x^*, z), \rho, \theta)$*-quasiunivex* at x^* if there exist functions $\beta : X \times X \to \mathbb{R}_+\backslash\{0\}$, $\phi : \mathbb{R} \to \mathbb{R}$, $\rho : X \times X \to \mathbb{R}$, $\theta : X \times X \to \mathbb{R}^n$, and a sublinear function $\mathcal{G}(x, x^*; \cdot) : \mathbb{R}^n \to \mathbb{R}$ such that for each $x \in X$ and $z \in \mathbb{R}^n$,

$$\phi(f(x) - f(x^*) + \langle z, \nabla_z h(x^*, z)\rangle - h(x^*, z))(<) \leq 0 \\ \Rightarrow \quad \mathcal{G}(x, x^*; \beta(x, x^*)[\nabla_z h(x^*, z)]) \leq -\rho(x, x^*)\|\theta(x, x^*)\|^2,$$

equivalently,

$$\mathcal{G}(x, x^*; \beta(x, x^*)[\nabla_z h(x^*, z)]) > -\rho(x, x^*)\|\theta(x, x^*)\|^2 \Rightarrow \\ \phi(f(x) - f(x^*) + \langle z, \nabla_z h(x^*, z)\rangle - h(x^*, z))(\geq) > 0,$$

where $h : \mathbb{R}^n \times \mathbb{R}^n \to \mathbb{R}^n$ is differentiable with respect to the second component.

Definition 2.5. The function f is said to be *strictly* $(\mathcal{G}, \beta, \phi, h(x^*, z), \rho, \theta)$*-quasiunivex* at x^* if there exist functions $\beta : X \times X \to \mathbb{R}_+\backslash\{0\}$, $\phi : \mathbb{R} \to \mathbb{R}$, $\rho : X \times X \to \mathbb{R}$, $\theta : X \times X \to \mathbb{R}^n$, and a sublinear function $\mathcal{G}(x, x^*; \cdot) : \mathbb{R}^n \to \mathbb{R}$ such that for each $x \in X$ and $z \in \mathbb{R}^n$,

$$\phi(f(x) - f(x^*) + \langle z, \nabla_z h(x^*, z)\rangle - h(x^*, z)) \leq 0 \\ \Rightarrow \quad \mathcal{G}(x, x^*; \beta(x, x^*)[\nabla_z h(x^*, z)]) < -\rho(x, x^*)\|\theta(x, x^*)\|^2,$$

equivalently,

$$\mathcal{G}(x, x^*; \beta(x, x^*)[\nabla_z h(x^*, z)]) \geq -\rho(x, x^*)\|\theta(x, x^*)\|^2 \Rightarrow \\ \phi(f(x) - f(x^*) + \langle z, \nabla_z h(x^*, z)\rangle - h(x^*, z)) > 0,$$

where $h : \mathbb{R}^n \times \mathbb{R}^n \to \mathbb{R}^n$ is differentiable with respect to the second component.

We note that the generalized $(\mathcal{G}, \beta, \phi, h(\cdot, \cdot), \rho, \theta)$-univexities (see (Verma, 2012)) at x^* of higher order reduce to the Zalmai type $(\mathcal{F}, \beta, \phi, \rho, \theta)$-univexities (see (Zalmai, 2012)) of higher-order if we set

$$h(x^*, z) = \langle z, \nabla f(x^*)\rangle + \frac{1}{2}\langle z, \nabla^2 f(x^*)z\rangle.$$

Then, we have

$$\nabla_z h(x^*, z) = \nabla f(x^*) + \nabla^2 f(x^*)z$$

and

$$\langle z, \nabla_z h(x^*, z)\rangle - h(x^*, z) = \frac{1}{2}\langle z, \nabla^2 f(x^*)z\rangle.$$

We observe some of the implications from the above definitions as follows: if f is $(\mathcal{G}, \beta, \phi, h(\cdot,\cdot), \rho, \theta)$-univex at x^*, then it is both $(\mathcal{G}, \beta, \phi, h(\cdot,\cdot), \rho, \theta)$-pseudounivex and $(\mathcal{G}, \beta, \phi, h(\cdot,\cdot), \rho, \theta)$-quasiunivex at x^*, if f is $(\mathcal{G}, \beta, \phi, h(\cdot,\cdot), \rho, \theta)$-quasiunivex at x^*, then it is prestrictly $(\mathcal{G}, \beta, \phi, h(\cdot,\cdot), \rho, \theta)$-quasiunivex at x^*, and if f is strictly $(\mathcal{G}, \beta, \phi, h(\cdot,\cdot), \rho, \theta)$-pseudounivex at x^*, then it is $(\mathcal{G}, \beta, \phi, h(\cdot,\cdot), \rho, \theta)$-quasiunivex at x^*.

Note that during the proofs of the duality theorems, sometimes it may be more convenient to use certain alternative but equivalent forms of the above definitions. We conclude this section by recalling a set of parametric necessary optimality conditions for (P) based on the following result.

Theorem 2.1. *(See (Verma, 2013)) Let $x^* \in \mathbb{F}$ and $\lambda^* = \max_{1\le i\le p} f_i(x^*)/g_i(x^*)$, for each $i \in \underline{p}$, let f_i and g_i be twice continuously differentiable at x^*, for each $j \in \underline{q}$, let the function $z \to G_j(z,t)$ be twice continuously differentiable at x^* for all $t \in T_j$, and for each $k \in \underline{r}$, let the function $z \to H_k(z,s)$ be twice continuously differentiable at x^* for all $s \in S_k$. If x^* is an optimal solution of (P), if the second order generalized Abadie constraint qualification holds at x^*, and if for any critical direction y, the set cone*

$$\begin{aligned} &\{\Big(\nabla G_j(x^*,t), \langle y, \nabla^2 G_j(x^*,t)y\rangle\Big) : t \in \hat{T}_j(x^*), j \in \underline{q}\} \\ + \quad &span\{\Big(\nabla H_k(x^*,s), \langle y, \nabla^2 H_k(x^*,s)y\rangle\Big) : s \in S_k, k \in \underline{r}\}, \end{aligned}$$

where $\hat{T}_j(x^*) = \{t \in T_j : G_j(x^*,t) = 0\}$, is closed, then there exist $u^* \in U = \{u \in \mathbb{R}^p : u \ge 0, \sum_{i=1}^p u_i = 1\}$ and integers ν_0^* and ν^*, with $0 \le \nu_0^* \le \nu^* \le n+1$, such that there exist ν_0^* indices j_m, with $1 \le j_m \le q$, together with ν_0^* points $t^m \in \hat{T}_{j_m}(x^*)$, $m \in \underline{\nu_0^*}$, $\nu^* - \nu_0^*$ indices k_m, with $1 \le k_m \le r$, together with $\nu^* - \nu_0^*$ points $s^m \in S_{k_m}$ for $m \in \underline{\nu^*}\backslash\underline{\nu_0^*}$, and ν^* real numbers v_m^*, with $v_m^* > 0$ for $m \in \underline{\nu_0^*}$, with the property that

$$\sum_{i=1}^{p} u_i^*[\nabla f_i(x^*) - \lambda^*(\nabla g_i(x^*)] + \sum_{m=1}^{\nu_0^*} v_m^*[\nabla G_{j_m}(x^*, t^m) + \sum_{m=\nu_0^*+1}^{\nu^*} v_m^* \nabla H_k(x^*, s^m) = 0, \tag{2.1}$$

$$\langle y, \Big[\sum_{i=1}^{p} u_i^*[\nabla^2 f_i(x^*) - \lambda^* \nabla^2 g_i(x^*)] + \sum_{m=1}^{\nu_0^*} v_m^* \nabla^2 G_{j_m}(x^*, t^m) + \sum_{m=\nu_0^*+1}^{\nu^*} v_m^* \nabla^2 H_k(x^*, s^m)\Big] y\rangle \ge 0. \tag{2.2}$$

We shall call x a *normal* feasible solution of (P) if x satisfies all the constraints of (P), if the generalized Abadie constraint qualification holds at x, and if the set $cone\{\nabla G_j(x,t) : t \in \hat{T}_j(x), j \in \underline{q}\} + span\{\nabla H_k(x,s) : s \in S_k, k \in \underline{r}\}$ is closed.

The above theorem on the necessary optimality conditions provides us with clear guidelines for formulating numerous Wolfe-type duality models for (P). From now on, the functions f_i, g_i, $i \in \underline{p}$, $z \to G_j(z,t)$, and $z \to H_k(z,s)$ are twice continuously differentiable on X for all $t \in T_j$, $j \in \underline{q}$, and all $s \in S_k$, $k \in \underline{r}$.

3. Duality Models

In this section, we consider two duality models with special constraint structures that allow for a greater variety of generalized $(\mathcal{G}, \beta, \phi, h(x,z), \rho, \theta)$-univexity conditions under which duality can be established based on the following set:

$$\mathbb{H} = \Big\{(y, z, u, v, \lambda, \nu, \nu_0, J_{\nu_0}, K_{\nu\setminus\nu_0}, \bar{t}, \bar{s}) : \ y \in X;\ z \in \mathbb{R}^n;\ u \in U;\ 0 \le \nu_0 \le \nu \le n+1;$$
$$v \in \mathbb{R}^{\nu}, v_i > 0, 1 \le i \le \nu_0;\ \lambda \in \mathbb{R}_+;\ J_{\nu_0} = (j_1, j_2, \ldots, j_{\nu_0}),\ 1 \le j_i \le q;\ K_{\nu\setminus\nu_0} =$$
$$(k_{\nu_0+1}, \ldots, k_{\nu}), 1 \le k_i \le r;\ \bar{t} = (t^1, t^2, \ldots, t^{\nu_0}),\ t^i \in T_{j_i};\ \bar{s} = (s^{\nu_0+1}, \ldots, s^{\nu}),\ s^i \in S_{k_i}\Big\}.$$

Consider the following two problems:

(DI) $\sup_{(y,z,u,v,\lambda,\nu,\nu_0,J_{\nu_0},K_{\nu\setminus\nu_0},\bar{t},\bar{s})\in\mathbb{H}} \lambda$

subject to

$$\sum_{i=1}^{p} u_i[\nabla_z h_i(y,z) - \lambda\nabla_z \kappa_i(y,z)] + \sum_{m=1}^{\nu_0} v_m[\nabla_z \mu_{j_m}(y, t^m, z) + \sum_{m=\nu_0+1}^{\nu} v_m[\nabla_z \psi_{k_m}(y, s^m, z)] = 0, \tag{3.1}$$

$$f_i(y) - \lambda g_i(y) + \sum_{i=1}^{p} u_i[h_i(y,z) - \lambda\kappa_i(y,z) - \langle z, \nabla_z h_i(y,z) - \lambda\nabla_z \kappa_i(y,z)]\rangle \ge 0, \quad i \in \underline{p}, \tag{3.2}$$

$$G_{j_m}(y, t^m) + \mu_{j_m}(y, t^m, z) - \langle z, \nabla_z \mu_{j_m}(y, t^m, z)\rangle \ge 0, \quad m \in \underline{\nu_0}, \tag{3.3}$$

$$v_m H_{k_m}(y, s^m) + v_m \psi_{k_m}(y, s^m, z) - \langle z, v_m \nabla_z \psi_{k_m}(y, s^m, z)\rangle \ge 0, \quad m \in \underline{\nu}\setminus\underline{\nu_0}; \tag{3.4}$$

($\tilde{DI}$) $\sup_{(y,z,u,v,\lambda,\nu,\nu_0,J_{\nu_0},K_{\nu\setminus\nu_0},\bar{t},\bar{s})\in\mathbb{H}} \lambda$

subject to (3.2)-(3.4) and

$$\mathcal{G}\Big(x, y; \sum_{i=1}^{p} u_i[\nabla_z h_i(y,z)] - \sum_{i=1}^{p} u_i\lambda[\nabla_z \kappa_i(y,z)] + \sum_{m=1}^{\nu_0} v_m[\nabla_z \mu_{j_m}(y, z, t^m)] + \sum_{m=\nu_0+1}^{\nu} v_m[\nabla_z \psi_{k_m}(y, z, s^m)] \ge 0 \ \text{ for all } x \in \mathbb{F}, \tag{3.5}$$

where $\mathcal{G}(x, y; \cdot)$ is a sublinear function from $\mathbb{R}^n$ to $\mathbb{R}$.

Note that if we Compare (DI) and ($\tilde{DI}$), we see that ($\tilde{DI}$) is relatively more general than (DI) in the sense that any feasible solution of (DI) is also feasible for ($\tilde{DI}$), but the converse may not be necessarily true.

Lemma 3.1. *(See (Zalmai, 2012)) For each $x \in X$,*

$$\varphi(x) \equiv \max_{1\le i\le p} \frac{f_i(x)}{g_i(x)} = \max_{u\in U} \frac{\sum_{i=1}^{p} u_i f_i(x)}{\sum_{i=1}^{p} u_i g_i(x)}.$$

The next theorem shows that (DI) is a dual problem for primal (P).

Theorem 3.1. *(Weak Duality) Let x and $w = (y, z, u, v, \lambda, \nu, \nu_0, J_{\nu_0}, K_{\nu\setminus\nu_0}, \bar{t}, \bar{s})$ be arbitrary feasible solutions of (P) and (DI), respectively, and let us assume that any one of the following five sets of hypotheses is satisfied:*

(a) *(i) for each $i \in \underline{p}$, f_i is $(\mathcal{G}, \beta, \bar{\phi}, h_i(\cdot,\cdot), \bar{\rho}_i, \theta)$-univex and $-g_i$ is $(\mathcal{G}, \beta, \bar{\phi}, \kappa_i(\cdot,\cdot), \tilde{\rho}_i, \theta)$-univex at y, $\bar{\phi}$ is superlinear, and $\bar{\phi}(a) \ge 0 \Rightarrow a \ge 0$;*

(ii) the function $\xi \to G_{j_m}(\xi, t^m)$ is $(\mathcal{G}, \beta, \hat{\phi}_m, \mu_m(\cdot,\cdot), \hat{\rho}_m, \theta)$-quasiunivex at y, $\hat{\phi}_m$ is increasing, and $\hat{\phi}_m(0) = 0$ for each $m \in \underline{\nu_0}$;

(iii) the function $\xi \to \nu_m H_{k_m}(\xi, s^m)$ is $(\mathcal{G}, \beta, \breve{\phi}_m, \psi_m(\cdot,\cdot), \breve{\rho}_m, \theta)$- quasiunivex at y, $\breve{\phi}_m$ is increasing, and $\breve{\phi}_m(0) = 0$ for each $m \in \underline{\nu}\setminus\underline{\nu_0}$;

(iv) $\rho^*(x,y) + \sum_{m=1}^{\nu_0} \nu_m \hat{\rho}_m(x,y) + \sum_{m=\nu_0+1}^{\nu} \breve{\rho}_m(x,y) \ge 0$ where $\rho^*(x,y) = \sum_{i=1}^{p} u_i[\bar{\rho}_i(x,y) + \lambda\tilde{\rho}_i(x,y)]$;

(b) *(i) for each $i \in \underline{p}$, f_i is $(\mathcal{G}, \beta, \bar{\phi}, h_i(\cdot,\cdot), \bar{\rho}_i, \theta)$-univex and $-g_i$ is $(\mathcal{G}, \beta, \bar{\phi}, \kappa_i(\cdot,\cdot), \tilde{\rho}_i, \theta)$-univex at y, $\bar{\phi}$ is superlinear, and $\bar{\phi}(a) \ge 0 \Rightarrow a \ge 0$;*

(ii) the function $\xi \to \sum_{m=1}^{\nu_0} \nu_m G_{j_m}(\xi, t^m)$ is $(\mathcal{G}, \beta, \hat{\phi}, \mu_m(\cdot,\cdot), \hat{\rho}, \theta)$-quasiunivex at y, $\hat{\phi}$ is increasing, and $\hat{\phi}(0) = 0$;

(iii) the function $\xi \to \nu_m H_{k_m}(\xi, s^m)$ is $(\mathcal{G}, \beta, \breve{\phi}_m, \psi_m(\cdot,\cdot), \breve{\rho}_m, \theta)$-quasiunivex at y, $\breve{\phi}_m$ is increasing, and $\breve{\phi}_m(0) = 0$ for each $m \in \underline{\nu}\setminus\underline{\nu_0}$;

(iv) $\rho^*(x,y) + \hat{\rho}(x,y) + \sum_{m=\nu_0+1}^{\nu} \breve{\rho}_m(x,y) \ge 0$;

(c) *(i) for each $i \in \underline{p}$, f_i is $(\mathcal{G}, \beta, \bar{\phi}, h_i(\cdot,\cdot), \bar{\rho}_i, \theta)$-univex and $-g_i$ is $(\mathcal{G}, \beta, \bar{\phi}, \tilde{\rho}_i, \kappa_i(\cdot,\cdot), \theta)$-univex at y, $\bar{\phi}$ is superlinear, and $\bar{\phi}(a) \ge 0 \Rightarrow a \ge 0$;*

(ii) the function $\xi \to G_{j_m}(\xi, t^m)$ is $(\mathcal{G}, \beta, \hat{\phi}_m, \mu_m(\cdot,\cdot), \hat{\rho}_m, \theta)$-quasiunivex at y, $\hat{\phi}_m$ is increasing, and $\hat{\phi}_m(0) = 0$ for each $m \in \underline{\nu_0}$;

(iii) the function $\xi \to \sum_{m=\nu_0+1}^{\nu} \nu_m H_{k_m}(\xi, s^m)$ is $(\mathcal{G}, \beta, \breve{\phi}, \psi_m(\cdot,\cdot), \breve{\rho}, \theta)$-quasiunivex at y, $\breve{\phi}$ is increasing, and $\breve{\phi}(0) = 0$;

(iv) $\rho^*(x,y) + \sum_{m=1}^{\nu_0} \nu_m \hat{\rho}_m(x,y) + \breve{\rho}(x,y) \ge 0$;

(d) *(i) for each $i \in \underline{p}$, f_i is $(\mathcal{G}, \beta, \bar{\phi}, h_i(\cdot,\cdot), \bar{\rho}_i, \theta)$-univex and $-g_i$ is $(\mathcal{G}, \beta, \bar{\phi}, \kappa_i(\cdot,\cdot), \tilde{\rho}_i, \theta)$-univex at y, $\bar{\phi}$ is superlinear, and $\bar{\phi}(a) \ge 0 \Rightarrow a \ge 0$;*

(ii) *the function* $\xi \to \sum_{m=1}^{\nu_0} v_m G_{j_m}(\xi, t^m)$ *is* $(\mathcal{G}, \beta, \hat{\phi}, \mu_m(\cdot,\cdot), \hat{\rho}, \theta)$*-quasiunivex at* y, $\hat{\phi}$ *is increasing, and* $\hat{\phi}(0) = 0$*;*

(iii) *the function* $\xi \to \sum_{m=\nu_0+1}^{\nu} v_m H_{k_m}(\xi, s^m)$ *is* $(\mathcal{G}, \beta, \breve{\phi}, \psi_m(\cdot,\cdot), \breve{\rho}, \theta)$*-quasiunivex at* y, $\breve{\phi}$ *is increasing, and* $\breve{\phi}(0) = 0$*;*

(iv) $\rho^*(x,y) + \hat{\rho}(x,y) + \breve{\rho}(x,y) \geq 0$*;*

(e) *(i)* *for each* $i \in \underline{p}$, f_i *is* $(\mathcal{G}, \beta, \bar{\phi}, h_i(\cdot,\cdot), \bar{\rho}_i, \theta)$*-univex and* $-g_i$ *is* $(\mathcal{G}, \beta, \bar{\phi}, \kappa_i(\cdot,\cdot), \tilde{\rho}_i, \theta)$*-univex at* y, $\bar{\phi}$ *is superlinear, and* $\bar{\phi}(a) \geq 0 \Rightarrow a \geq 0$*;*

(ii) *the function* $\xi \to \sum_{m=1}^{\nu_0} v_m G_{j_m}(\xi, t^m) + \sum_{m=\nu_0+1}^{\nu} v_m H_{k_m}(\xi, s^m)$ *is* $(\mathcal{G}, \beta, \hat{\phi}, \tau_m, \hat{\rho}, \theta)$*-quasiunivex at* y, $\hat{\phi}$ *is increasing, and* $\hat{\phi}(0) = 0$*;*

(iii) $\rho^*(x,y) + \hat{\rho}(x,y) \geq 0$.

Then $\varphi(x) \geq \lambda$.

Proof. (a): Applying (i), we have the following inequality:

$$\begin{aligned}
&\bar{\phi}\Big(\sum_{i=1}^{p} u_i[f_i(x) - f_i(y)] + \Big\langle z, \sum_{i=1}^{p} u_i \nabla_z h_i(y,z) \Big\rangle - \sum_{i=1}^{p} u_i h_i(y,z) \\
&+ \lambda[\sum_{i=1}^{p} u_i[-g_i(x) + g_i(y)] - \Big\langle z, \sum_{i=1}^{p} u_i \nabla_z \kappa_i(y,z) \Big\rangle + \sum_{i=1}^{p} u_i \kappa_i(y,z)]\Big) \\
&\quad \geq \mathcal{G}\Big(x, y; \beta(x,y) \sum_{i=1}^{p} u_i\{\nabla_z h_i(y,z) - \lambda \nabla_z \kappa_i(y,z)\}\Big) + \sum_{i=1}^{p} u_i[\bar{\rho}_i(x,y) + \lambda \tilde{\rho}_i(x,y)]\|\theta(x,y)\|^2. \quad (3.6)
\end{aligned}$$

From the primal feasibility of x, dual feasibility of w, and (3.3), we find that

$$G_{j_m}(x, t^m) \leq 0 \leq G_{j_m}(y, t^m) + \mu_{j_m}(y, t^m, z) - \langle z, \nabla_z \mu_{j_m}(y, t^m, z)\rangle, \quad m \in \underline{\nu_0},$$

and hence using the properties of the functions $\hat{\phi}_m$, we have

$$\hat{\phi}_m(G_{j_m}(x, t^m) - [G_{j_m}(y, t^m) + \mu_{j_m}(y, t^m, z) - \langle z, \nabla_z \mu_{j_m}(y, t^m, z)\rangle]) \leq 0,$$

which from (ii) implies that $\mathcal{G}(x, y; \beta(x,y)[\nabla_z \mu_{j_m}(y, t^m, z)]) \leq -\hat{\rho}_m(x,y)\|\theta(x,y)\|^2$. As $v_m > 0$ for each $m \in \underline{\nu_0}$, the above inequality yield

$$\mathcal{G}\Big(x, y; \beta(x,y) \sum_{m=1}^{\nu_0} v_m[\langle z, \nabla_z \mu_{j_m}(y, t^m, z)\rangle]\Big) \leq -\sum_{m=1}^{\nu_0} v_m \hat{\rho}_m(x,y)\|\theta(x,y)\|^2. \quad (3.7)$$

Similarly, from the primal feasibility of x, dual feasibility of w, (3.4), and (iii) we deduce (since $v_m > 0$ for each $m \in \underline{\nu} \backslash \underline{\nu_0}$) that

$$\mathcal{G}\Big(x, y; \beta(x,y) \sum_{m=\nu_0+1}^{\nu} v_m[\nabla_z \psi_{j_m}(y, t^m, z)]\Big) \leq -\sum_{m=\nu_0+1}^{\nu} \breve{\rho}_m(x,y)\|\theta(x,y)\|^2. \quad (3.8)$$

Now, based on the positivity of $\beta(x,y)$, sublinearity of $\mathcal{G}(x,y;\cdot)$, and (3.1), we conclude that

$$\mathcal{G}\Big(x,y;\beta(x,y)\sum_{i=1}^{p}u_i\{\nabla_z h_i(y,z)-\lambda\nabla_z\kappa_i(y,z)\}\Big)+\mathcal{G}(x,y;\beta(x,y)\sum_{m=1}^{\nu_0}v_m[\nabla_z\mu_{j_m}(y,t^m,z)])$$
$$+\quad \mathcal{G}\Big(x,y;\beta(x,y)\sum_{m=\nu_0+1}^{\nu}v_m[\nabla_z\psi_{j_m}(y,t^m,z)]\Big)\geq 0. \tag{3.9}$$

Next, applying (3.9) to (3.6), and then combining with (3.7) and (3.8) and using (iv), we have

$$\bar{\phi}\Big(\sum_{i=1}^{p}u_i[f_i(x)-f_i(y)]+\Big\langle z,\sum_{i=1}^{p}u_i\nabla_z h_i(y,z)\Big\rangle-\sum_{i=1}^{p}u_i h_i(y,z)$$
$$+\quad \lambda[\sum_{i=1}^{p}u_i[-g_i(x)+g_i(y)]-\Big\langle z,\sum_{i=1}^{p}u_i\nabla_z\kappa_i(y,z)\Big\rangle+\sum_{i=1}^{p}u_i\kappa_i(y,z)]\Big)$$
$$\geq\quad \mathcal{G}\Big(x,y;\beta(x,y)\sum_{i=1}^{p}u_i\{\nabla_z h_i(y,z)-\lambda\nabla_z\kappa_i(y,z)\}\Big)$$
$$+\quad \sum_{i=1}^{p}u_i[\bar{\rho}_i(x,y)+\lambda\tilde{\rho}_i(x,y)]\|\theta(x,y)\|^2\geq-\Big[\mathcal{G}(x,y;\beta(x,y)\sum_{m=1}^{\nu_0}v_m[\nabla_z\mu_{j_m}(y,t^m,z)])$$
$$+\quad \mathcal{G}\Big(x,y;\beta(x,y)\sum_{m=\nu_0+1}^{\nu}v_m[\nabla_z\psi_{j_m}(y,t^m,z)]\Big)\Big]\geq\sum_{m=1}^{\nu_0}v_m\hat{\rho}_m(x,y)\|\theta(x,y)\|^2+\sum_{m=\nu_0+1}^{\nu}\breve{\rho}_m(x,y)\|\theta(x,y)\|^2$$
$$+\quad \sum_{i=1}^{p}u_i[\bar{\rho}_i(x,y)+\lambda\tilde{\rho}_i(x,y)]\|\theta(x,y)\|^2=\sum_{m=1}^{\nu_0}v_m\hat{\rho}_m(x,y)\|\theta(x,y)\|^2$$
$$+\quad \sum_{m=\nu_0+1}^{\nu}\breve{\rho}_m(x,y)\|\theta(x,y)\|^2+\rho^*(x,y)\|\theta(x,y)\|^2\geq 0.$$

But $\bar{\phi}(a)\geq 0 \;\Rightarrow\; a\geq 0$ and hence because of (3.2) the above inequality reduces to

$$\sum_{i=1}^{p}u_i[f_i(x)-\lambda g_i(x)]\geq 0.$$

Finally, this inequality using Lemma 3.1 leads to the weak duality inequality as follows:

$$\varphi(x)=\max_{1\leq i\leq p}\frac{f_i(x)}{g_i(x)}=\max_{u\in U}\frac{\sum_{i=1}^{p}u_i f_i(x)}{\sum_{i=1}^{p}u_i g_i(x)}\geq\lambda.$$

(b) - (e) : The proofs are similar to that of part (a). □

The following theorem is based on the $(\mathcal{G},\beta,h_i(\cdot,\cdot),\tilde{\rho}_i,\theta)$-univexities and quasiunivexities.

Theorem 3.2. *(Weak Duality) Let x and $w=(y,z,u,v,\lambda,\nu,\nu_0,J_{\nu_0},K_{\nu\setminus\nu_0},\bar{t},\bar{s})$ be arbitrary feasible solutions of (P) and (DI), respectively, and let us assume that any one of the following five sets of hypotheses is satisfied:*

(a) (i) for each $i \in \underline{p}$, f_i is $(\mathcal{G}, \beta, h_i(\cdot,\cdot), \bar{\rho}_i, \theta)$-univex and $-g_i$ is $(\mathcal{G}, \beta, \kappa_i(\cdot,\cdot), \tilde{\rho}_i, \theta)$-univex at y,

(ii) the function $\xi \to G_{j_m}(\xi, t^m)$ is $(\mathcal{G}, \beta, \mu_m(\cdot,\cdot), \hat{\rho}_m, \theta)$-quasiunivex at y, for each $m \in \underline{\nu_0}$;

(iii) the function $\xi \to \nu_m H_{k_m}(\xi, s^m)$ is $(\mathcal{G}, \beta, \psi_m(\cdot,\cdot), \breve{\rho}_m, \theta)$-quasi univex at y, for each $m \in \underline{\nu} \backslash \underline{\nu_0}$;

(iv) $\rho^*(x,y) + \sum_{m=1}^{\nu_0} \nu_m \hat{\rho}_m(x,y) + \sum_{m=\nu_0+1}^{\nu} \breve{\rho}_m(x,y) \geq 0$ where $\rho^*(x,y) = \sum_{i=1}^{p} u_i[\bar{\rho}_i(x,y) + \lambda \tilde{\rho}_i(x,y)]$;

(b) (i) for each $i \in \underline{p}$, f_i is $(\mathcal{G}, \beta, h_i(\cdot,\cdot), \bar{\rho}_i, \theta)$-univex and $-g_i$ is $(\mathcal{G}, \beta, \kappa_i(\cdot,\cdot), \tilde{\rho}_i, \theta)$-univex at y, $\bar{\phi}$ is superlinear, and $\bar{\phi}(a) \geq 0 \Rightarrow a \geq 0$.

(ii) the function $\xi \to \sum_{m=1}^{\nu_0} \nu_m G_{j_m}(\xi, t^m)$ is $(\mathcal{G}, \beta, \mu_m(\cdot,\cdot), \hat{\rho}, \theta)$-quasiunivex at y.

(iii) the function $\xi \to \nu_m H_{k_m}(\xi, s^m)$ is $(\mathcal{G}, \beta, \breve{\phi}_m, \psi_m(\cdot,\cdot), \breve{\rho}_m, \theta)$-quasiunivex at y.

(iv) $\rho^*(x,y) + \hat{\rho}(x,y) + \sum_{m=\nu_0+1}^{\nu} \breve{\rho}_m(x,y) \geq 0$;

(c) (i) for each $i \in \underline{p}$, f_i is $(\mathcal{G}, \beta, h_i(\cdot,\cdot), \bar{\rho}_i, \theta)$-univex and $-g_i$ is $(\mathcal{G}, \beta, \tilde{\rho}_i, \kappa_i(\cdot,\cdot), \theta)$-univex at y.

(ii) the function $\xi \to G_{j_m}(\xi, t^m)$ is $(\mathcal{G}, \beta, \mu_m(\cdot,\cdot), \hat{\rho}_m, \theta)$-quasiunivex at y.

(iii) the function $\xi \to \sum_{m=\nu_0+1}^{\nu} \nu_m H_{k_m}(\xi, s^m)$ is $(\mathcal{G}, \beta, \psi_m(\cdot,\cdot), \breve{\rho}, \theta)$-quasiunivex at y.

(iv) $\rho^*(x,y) + \sum_{m=1}^{\nu_0} \nu_m \hat{\rho}_m(x,y) + \breve{\rho}(x,y) \geq 0$;

(d) (i) for each $i \in \underline{p}$, f_i is $(\mathcal{G}, \beta, h_i(\cdot,\cdot), \bar{\rho}_i, \theta)$-univex and $-g_i$ is $(\mathcal{G}, \beta, \kappa_i(\cdot,\cdot), \tilde{\rho}_i, \theta)$-univex at y.

(ii) the function $\xi \to \sum_{m=1}^{\nu_0} \nu_m G_{j_m}(\xi, t^m)$ is $(\mathcal{G}, \beta, \hat{\phi}, \mu_m(\cdot,\cdot), \hat{\rho}, \theta)$-quasiunivex at y.

(iii) the function $\xi \to \sum_{m=\nu_0+1}^{\nu} \nu_m H_{k_m}(\xi, s^m)$ is $(\mathcal{G}, \beta, \breve{\phi}, \psi_m(\cdot,\cdot), \breve{\rho}, \theta)$-quasiunivex at y.

(iv) $\rho^*(x,y) + \hat{\rho}(x,y) + \breve{\rho}(x,y) \geq 0$;

(e) (i) for each $i \in \underline{p}$, f_i is $(\mathcal{G}, \beta, h_i(\cdot,\cdot), \bar{\rho}_i, \theta)$-univex and $-g_i$ is $(\mathcal{G}, \beta, \kappa_i(\cdot,\cdot), \tilde{\rho}_i, \theta)$-univex at y.

(ii) the function $\xi \to \sum_{m=1}^{\nu_0} \nu_m G_{j_m}(\xi, t^m) + \sum_{m=\nu_0+1}^{\nu} \nu_m H_{k_m}(\xi, s^m)$ is $(\mathcal{G}, \beta, \tau_m, \hat{\rho}, \theta)$-quasiunivex at y.

(iii) $\rho^*(x,y) + \hat{\rho}(x,y) \geq 0$.

Then $\varphi(x) \geq \lambda$.

Proof. (a): Applying (i), we have the following inequality:

$$\begin{aligned}
&\sum_{i=1}^{p} u_i[f_i(x) - f_i(y)] + \Big\langle z, \sum_{i=1}^{p} u_i \nabla_z h_i(y,z)\Big\rangle - \sum_{i=1}^{p} u_i h_i(y,z) \\
&+ \lambda[\sum_{i=1}^{p} u_i[-g_i(x) + g_i(y)] - \Big\langle z, \sum_{i=1}^{p} u_i \nabla_z \kappa_i(y,z)\Big\rangle + \sum_{i=1}^{p} u_i \kappa_i(y,z)] \\
&\geq \mathcal{G}\Big(x,y;\beta(x,y)\sum_{i=1}^{p} u_i\{\nabla_z h_i(y,z) - \lambda\nabla_z \kappa_i(y,z)\}\Big) + \sum_{i=1}^{p} u_i[\bar{\rho}_i(x,y) + \lambda\tilde{\rho}_i(x,y)]\|\theta(x,y)\|^2. \quad (3.10)
\end{aligned}$$

From the primal feasibility of x, dual feasibility of w, and (3.3), we find that

$$G_{j_m}(x,t^m) \leq 0 \leq G_{j_m}(y,t^m) + \mu_{j_m}(y,t^m,z) - \langle z, \nabla_z \mu_{j_m}(y,t^m,z)\rangle, \quad m \in \underline{\nu_0}.$$

Then we have $G_{j_m}(x,t^m) - [G_{j_m}(y,t^m) + \mu_{j_m}(y,t^m,z) - \langle z, \nabla_z \mu_{j_m}(y,t^m,z)\rangle] \leq 0$, which from (ii) implies that $\mathcal{G}(x,y;\beta(x,y)[\nabla_z \mu_{j_m}(y,t^m,z)]) \leq -\hat{\rho}_m(x,y)\|\theta(x,y)\|^2$. As $\nu_m > 0$ for each $m \in \underline{\nu_0}$, the above inequalities yield

$$\mathcal{G}\Big(x,y;\beta(x,y)\sum_{m=1}^{\nu_0} \nu_m[\langle z, \nabla_z \mu_{j_m}(y,t^m,z)\rangle]\Big) \leq -\sum_{m=1}^{\nu_0} \nu_m \hat{\rho}_m(x,y)\|\theta(x,y)\|^2. \quad (3.11)$$

Similarly, from the primal feasibility of x, dual feasibility of w, (3.4), and (iii) we deduce that

$$\mathcal{G}\Big(x,y;\beta(x,y)\sum_{m=\nu_0+1}^{\nu} \nu_m[\nabla_z \psi_{j_m}(y,t^m,z)]\Big) \leq -\sum_{m=\nu_0+1}^{\nu} \breve{\rho}_m(x,y)\|\theta(x,y)\|^2. \quad (3.12)$$

Now, based on the positivity of $\beta(x,y)$, sublinearity of $\mathcal{G}(x,y;\cdot)$, and applying (3.1), we conclude that

$$\begin{aligned}
&\mathcal{G}\Big(x,y;\beta(x,y)\sum_{i=1}^{p} u_i\{\nabla_z h_i(y,z) - \lambda\nabla_z \kappa_i(y,z)\}\Big) + \mathcal{G}(x,y;\beta(x,y)\sum_{m=1}^{\nu_0} \nu_m[\nabla_z \mu_{j_m}(y,t^m,z)]) \\
+ \quad &\mathcal{G}\Big(x,y;\beta(x,y)\sum_{m=\nu_0+1}^{\nu} \nu_m[\nabla_z \psi_{j_m}(y,t^m,z)]\Big) \geq 0. \quad (3.13)
\end{aligned}$$

Next, applying (3.13) to (3.10), and then combining with (3.11) and (3.12) and using (iv), we have

$$\begin{aligned}
&\Big(\sum_{i=1}^{p} u_i[f_i(x) - f_i(y)] + \Big\langle z, \sum_{i=1}^{p} u_i \nabla_z h_i(y,z)\Big\rangle - \sum_{i=1}^{p} u_i h_i(y,z) \\
+ \quad &\lambda[\sum_{i=1}^{p} u_i[-g_i(x) + g_i(y)] - \Big\langle z, \sum_{i=1}^{p} u_i \nabla_z \kappa_i(y,z)\Big\rangle + \sum_{i=1}^{p} u_i \kappa_i(y,z)]\Big) \\
\geq \quad &\Big(\rho^*(x,y) + \sum_{m=1}^{\nu_0} \nu_m \hat{\rho}_m(x,y) + \sum_{m=\nu_0+1}^{\nu} \breve{\rho}_m(x,y)\Big)\|\theta(x,y)\|^2 \geq 0.
\end{aligned}$$

Hence because of (3.2) the above inequality reduces to

$$\sum_{i=1}^{p} u_i[f_i(x) - \lambda g_i(x)] \geq 0.$$

Finally, this inequality using Lemma 3.1 leads to the weak duality inequality as follows:

$$\varphi(x) \equiv \max_{1\leq i\leq p} \frac{f_i(x)}{g_i(x)} = \max_{u\in U} \frac{\sum_{i=1}^{p} u_i f_i(x)}{\sum_{i=1}^{p} u_i g_i(x)} \geq \lambda.$$

(b) - (e) : The proofs are similar to that of part (a). □

Theorem 3.3. *(Strict Converse Duality) Let x^* be a normal optimal solution of (P), let $\tilde{w} = (\tilde{x}, \tilde{z}, \tilde{u}, \tilde{v}, \tilde{\lambda}, \tilde{\nu}, \tilde{\nu}_0, J_{\tilde{\nu}_0}, K_{\tilde{\nu}\setminus\tilde{\nu}_0}, \tilde{\bar{t}}, \tilde{\bar{s}})$ be an optimal solution of (DI), and assume that any one of the following five sets of conditions is satisfied:*

(a) The assumptions specified in part (a) of Theorem 3.2 are satisfied for the feasible solution $\tilde{w}$ of (DI). Moreover, $\bar{\phi}(a) > 0 \Rightarrow a > 0$, f_i is strictly $(\mathcal{G}, \beta, \bar{\phi}, h(\cdot,\cdot), \bar{\rho}_i, \theta)$-univex at $\tilde{x}$ for at least one $i \in \underline{p}$ with the corresponding component $\tilde{u}_i$ of $\tilde{u}$ positive, or $-g_i$ is strictly $(\mathcal{G}, \beta, \bar{\phi}, \kappa(\cdot,\cdot), \tilde{\rho}_i, \theta)$-univex at $\tilde{x}$ for at least one $i \in \underline{p}$ with the corresponding component $\tilde{u}_i$ of $\tilde{u}$ positive (and $\tilde{\lambda} > 0$), or $\xi \to G_{j_m}(\xi, \tilde{t}^m)$ is strictly $(\mathcal{G}, \beta, \hat{\phi}_m, \mu(\cdot,\cdot), \hat{\rho}_m, \theta)$-pseudounivex at $\tilde{x}$ for at least one $m \in \underline{\tilde{\nu}_0}$, or $\xi \to \tilde{\nu}_m H_{k_m}(\xi, \tilde{s}^m)$ is strictly $(\mathcal{G}, \beta, \breve{\phi}_m, \psi(\cdot,\cdot), \breve{\rho}_m, \theta)$-pseudounivex at $\tilde{x}$ for at least one $m \in \underline{\tilde{\nu}}\setminus\underline{\tilde{\nu}_0}$, or

$$\rho^*(x^*, \tilde{x}) + \sum_{m=1}^{\tilde{\nu}_0} \tilde{\nu}_m \hat{\rho}_m(x^*, \tilde{x}) + \sum_{m=\tilde{\nu}_0+1}^{\tilde{\nu}} \tilde{\nu}_m \breve{\rho}_m(x^*, \tilde{x}) > 0,$$

where $\rho^*(x^*, \tilde{x}) = \sum_{i=1}^{p} \tilde{u}_i[\bar{\rho}_i(x^*, \tilde{x}) + \tilde{\lambda}\tilde{\rho}_i(x^*, \tilde{x})]$.

(b) The assumptions specified in part (b) of Theorem 3.2 are satisfied for the feasible solution $\tilde{w}$ of (DI). Moreover, $\bar{\phi}(a) > 0 \Rightarrow a > 0$, f_i is strictly $(\mathcal{G}, \beta, \bar{\phi}, h(\cdot,\cdot), \bar{\rho}_i, \theta)$-univex at $\tilde{x}$ for at least one $i \in \underline{p}$ with the corresponding component $\tilde{u}_i$ of $\tilde{u}$ positive, or $-g_i$ is strictly $(\mathcal{G}, \beta, \bar{\phi}, \kappa(\cdot,\cdot), \tilde{\rho}_i, \theta)$-univex at $\tilde{x}$ for at least one $i \in \underline{p}$ with the corresponding component $\tilde{u}_i$ of $\tilde{u}$ positive (and $\tilde{\lambda} > 0$), or $\xi \to \sum_{m=1}^{\tilde{\nu}_0} \tilde{\nu}_m G_{j_m}(\xi, \tilde{t}^m)$ is strictly $(\mathcal{G}, \beta, \hat{\phi}, \mu(\cdot,\cdot), \hat{\rho}, \theta)$-pseudounivex at $\tilde{x}$, or $\xi \to \tilde{\nu}_m H_{k_m}(\xi, \tilde{s}^m)$ is strictly $(\mathcal{G}, \beta, \breve{\phi}_m, \psi(\cdot,\cdot), \breve{\rho}_m, \theta)$-pseudounivex at $\tilde{x}$ for at least one $m \in \underline{\tilde{\nu}}\setminus\underline{\tilde{\nu}_0}$, or $\rho^*(x^*, \tilde{x}) + \hat{\rho}(x^*, \tilde{x}) + \sum_{m=\tilde{\nu}_0+1}^{\tilde{\nu}} \tilde{\nu}_m \breve{\rho}_m(x^*, \tilde{x}) > 0$.

(c) The assumptions specified in part (c) of Theorem 3.2 are satisfied for the feasible solution $\tilde{w}$ of (DI). Moreover, $\bar{\phi}(a) > 0 \Rightarrow a > 0$, f_i is strictly $(\mathcal{G}, \beta, \bar{\phi}, h(\cdot,\cdot), \bar{\rho}_i, \theta)$-univex at $\tilde{x}$ for at least one $i \in \underline{p}$ with the corresponding component $\tilde{u}_i$ of $\tilde{u}$ positive, or $-g_i$ is strictly $(\mathcal{G}, \beta, \bar{\phi}, \kappa(\cdot,\cdot), \tilde{\rho}_i, \theta)$-univex at $\tilde{x}$ for at least one $i \in \underline{p}$ with the corresponding component $\tilde{u}_i$ of $\tilde{u}$ positive (and $\tilde{\lambda} > 0$), or $\xi \to G_{j_m}(\xi, \tilde{t}^m)$ is strictly $(\mathcal{G}, \beta, \hat{\phi}_m, \mu(\cdot,\cdot), \hat{\rho}_m, \theta)$-pseudounivex at $\tilde{x}$ for at least one $m \in \underline{\tilde{\nu}_0}$, or $\xi \to \sum_{m=\tilde{\nu}_0+1}^{\tilde{\nu}} \tilde{\nu}_m H_{j_m}(\xi, \tilde{s}^m)$ is strictly $(\mathcal{G}, \beta, \breve{\phi}, \psi(\cdot,\cdot), \breve{\rho}, \theta)$-pseudounivex at $\tilde{x}$, or $\rho^*(x^*, \tilde{x}) + \sum_{m=1}^{\tilde{\nu}_0} \tilde{\nu}_m \hat{\rho}_m(x^*, \tilde{x}) + \tilde{\nu}_m \breve{\rho}(x^*, \tilde{x}) > 0$.

(d) The assumptions specified in part (d) of Theorem 3.2 are satisfied for the feasible solution $\tilde{w}$ of (DI). Moreover, $\bar{\phi}(a) > 0 \Rightarrow a > 0$, f_i is strictly $(\mathcal{G}, \beta, \bar{\phi}, h(\cdot,\cdot), \bar{\rho}_i, \theta)$-univex at $\tilde{x}$ for at least one $i \in \underline{p}$ with the corresponding component $\tilde{u}_i$ of $\tilde{u}$ positive, or $-g_i$ is strictly $(\mathcal{G}, \beta, \bar{\phi}, \kappa(\cdot,\cdot), \tilde{\rho}_i, \theta)$-univex at $\tilde{x}$ for at least one $i \in \underline{p}$ with the corresponding component $\tilde{u}_i$ of $\tilde{u}$ positive (and $\tilde{\lambda} > 0$), or $\xi \to \sum_{m=1}^{\tilde{\nu}_0} \tilde{\nu}_m G_{j_m}(\xi, \tilde{t}^m)$ is strictly $(\mathcal{G}, \beta, \hat{\phi}, \mu(\cdot,\cdot), \hat{\rho}, \theta)$-pseudounivex at $\tilde{x}$, or $\xi \to \sum_{m=\tilde{\nu}_0+1}^{\tilde{\nu}} \tilde{\nu}_m H_{k_m}(\xi, \tilde{s}^m)$ is strictly $(\mathcal{G}, \beta, \breve{\phi}, \psi(\cdot,\cdot), \breve{\rho}_m, \theta)$-pseudounivex at $\tilde{x}$, or $\rho^*(x^*, \tilde{x}) + \hat{\rho}(x^*, \tilde{x}) + \breve{\rho}(x^*, \tilde{x}) > 0$.

(e) The assumptions specified in part (e) of Theorem 3.2 are satisfied for the feasible solution $\tilde{w}$ of (DI). Moreover, $\bar{\phi}(a) > 0 \Rightarrow a > 0$, f_i is strictly $(\mathcal{G}, \beta, \bar{\phi}, h(\cdot,\cdot), \bar{\rho}_i, \theta)$-univex at $\tilde{x}$ for at least one $i \in \underline{p}$ with the corresponding component $\tilde{u}_i$ of $\tilde{u}$ positive, or $-g_i$ is strictly $(\mathcal{G}, \beta, \bar{\phi}, \kappa(\cdot,\cdot), \tilde{\rho}_i, \theta)$-univex at $\tilde{x}$ for at least one $i \in \underline{p}$ with the corresponding component $\tilde{u}_i$ of $\tilde{u}$ positive (and $\tilde{\lambda} > 0$), or $\xi \to \sum_{m=1}^{\tilde{\nu}_0} \tilde{\nu}_m G_{j_m}(\xi, \tilde{t}^m) + \sum_{m=\tilde{\nu}_0+1}^{\tilde{\nu}} \tilde{\nu}_m H_{k_m}(\xi, \tilde{s}^m)$ is strictly $(\mathcal{G}, \beta, \hat{\phi}, \tau(\cdot,\cdot), \hat{\rho}, \theta)$-pseudounivex at $\tilde{x}$, or $\rho^*(x^*, \tilde{x}) + \hat{\rho}(x^*, \tilde{x}) > 0$.

Then $\tilde{x} = x^*$ and $\varphi(x^*) = \tilde{\lambda}$.

Proof. The proof is similar to that of Theorem 3.2. □

4. Specialization I

In this section, we consider two duality models with special constraint structures that allow the generalized $(\mathcal{G}, \beta, \phi, h(\cdot,\cdot), \rho, \theta)$-univexity reduce to second order generalized $(\mathcal{F}, \beta, \phi, \rho, \theta)$-univexity introduced and studied by Zalmai (see (Zalmai, 2012)) under which duality can be established.

Consider the following two problems:

(DII) $\sup_{(y,z,u,v,\lambda,\nu,\nu_0,J_{\nu_0},K_{\nu\setminus\nu_0},\bar{t},\bar{s})\in\mathbb{H}} \lambda$

subject to

$$\sum_{i=1}^{p} u_i[\nabla f_i(y) - \lambda \nabla g_i(y)] + \sum_{m=1}^{\nu_0} v_m \nabla G_{j_m}(y, t^m) + \sum_{m=\nu_0+1}^{\nu} v_m \nabla H_{k_m}(y, s^m)$$
$$+ \Big\{ \sum_{i=1}^{p} u_i[\nabla^2 f_i(y) - \lambda \nabla^2 g_i(y)] + \sum_{m=1}^{\nu_0} v_m \nabla^2 G_{j_m}(y, t^m) + \sum_{m=\nu_0+1}^{\nu} v_m \nabla^2 H_{k_m}(y, s^m) \Big\} z = 0, \quad (4.1)$$

$$f_i(y) - \lambda g_i(y) - \frac{1}{2}\langle z, [\nabla^2 f_i(y) - \lambda \nabla^2 g_i(y)] z\rangle \geq 0, \quad i \in \underline{p}, \quad (4.2)$$

$$G_{j_m}(y, t^m) - \frac{1}{2}\langle z, \nabla^2 G_{j_m}(y, t^m) z\rangle \geq 0, \quad m \in \underline{\nu_0}, \quad (4.3)$$

$$v_m H_{k_m}(y, s^m) - \frac{1}{2}\langle z, v_m \nabla^2 H_{k_m}(y, s^m) z\rangle \geq 0, \quad m \in \underline{\nu}\setminus\underline{\nu_0}; \quad (4.4)$$

$$(\tilde{D}II) \qquad \sup_{(y,z,u,v,\lambda,\nu,\nu_0,J_{\nu_0},K_{\nu\setminus\nu_0},\bar{t},\bar{s})\in\mathbb{H}} \lambda \text{ subject to (3.3) and (4.2) - (4.4).}$$

The next theorem shows that (DII) is a dual problem for (P).

Theorem 4.1. *(Weak Duality) Let x and $w = (y, z, u, v, \lambda, \nu, \nu_0, J_{\nu_0}, K_{\nu\setminus\nu_0}, \bar{t}, \bar{s})$ be arbitrary feasible solutions of (P) and (DII), respectively, and assume that any one of the following five sets of hypotheses is satisfied:*

(a) *(i) for each $i \in \underline{p}$, f_i is $(\mathcal{F}, \beta, \bar{\phi}, \bar{\rho}_i, \theta)$-sounivex and $-g_i$ is $(\mathcal{F}, \beta, \bar{\phi}, \tilde{\rho}_i, \theta)$-sounivex at y, $\bar{\phi}$ is superlinear, and $\bar{\phi}(a) \geq 0 \Rightarrow a \geq 0$;*

(ii) the function $\xi \to G_{j_m}(\xi, t^m)$ is $(\mathcal{F}, \beta, \hat{\phi}_m, \hat{\rho}_m, \theta)$-quasisounivex at y, $\hat{\phi}_m$ is increasing, and $\hat{\phi}_m(0) = 0$ for each $m \in \underline{\nu_0}$;

(iii) the function $\xi \to v_m H_{k_m}(\xi, s^m)$ is $(\mathcal{F}, \beta, \breve{\phi}_m, \breve{\rho}_m, \theta)$-quasisounivex at y, $\breve{\phi}_m$ is increasing, and $\breve{\phi}_m(0) = 0$ for each $m \in \underline{\nu}\setminus\underline{\nu_0}$;

(iv) $\rho^*(x, y) + \sum_{m=1}^{\nu_0} v_m\hat{\rho}_m(x, y) + \sum_{m=\nu_0+1}^{\nu} v_m\breve{\rho}_m(x, y) \geq 0$, where $\rho^*(x, y) = \sum_{i=1}^{p} u_i[\bar{\rho}_i(x, y) + \lambda\tilde{\rho}_i(x, y)]$;

(b) *(i) for each $i \in \underline{p}$, f_i is $(\mathcal{F}, \beta, \bar{\phi}, \bar{\rho}_i, \theta)$-sounivex and $-g_i$ is $(\mathcal{F}, \beta, \bar{\phi}, \tilde{\rho}_i, \theta)$-sounivex at y, $\bar{\phi}$ is superlinear, and $\bar{\phi}(a) \geq 0 \Rightarrow a \geq 0$;*

(ii) the function $\xi \to \sum_{m=1}^{\nu_0} v_m G_{j_m}(\xi, t^m)$ is $(\mathcal{F}, \beta, \hat{\phi}, \hat{\rho}, \theta)$-quasisounivex at y, $\hat{\phi}$ is increasing, and $\hat{\phi}(0) = 0$;

(iii) the function $\xi \to v_m H_{k_m}(\xi, s^m)$ is $(\mathcal{F}, \beta, \breve{\phi}_m, \breve{\rho}_m, \theta)$-quasisounivex at y, $\breve{\phi}_m$ is increasing, and $\breve{\phi}_m(0) = 0$ for each $m \in \underline{\nu}\setminus\underline{\nu_0}$;

(iv) $\rho^*(x, y) + \hat{\rho}(x, y) + \sum_{m=\nu_0+1}^{\nu} \breve{\rho}_m(x, y) \geq 0$;

(c) *(i) for each $i \in \underline{p}$, f_i is $(\mathcal{F}, \beta, \bar{\phi}, \bar{\rho}_i, \theta)$-sounivex and $-g_i$ is $(\mathcal{F}, \beta, \bar{\phi}, \tilde{\rho}_i, \theta)$-sounivex at y, $\bar{\phi}$ is superlinear, and $\bar{\phi}(a) \geq 0 \Rightarrow a \geq 0$;*

(ii) the function $\xi \to G_{j_m}(\xi, t^m)$ is $(\mathcal{F}, \beta, \hat{\phi}_m, \hat{\rho}_m, \theta)$-quasisounivex at y, $\hat{\phi}_m$ is increasing, and $\hat{\phi}_m(0) = 0$ for each $m \in \underline{\nu_0}$;

(iii) the function $\xi \to \sum_{m=\nu_0+1}^{\nu} v_m H_{k_m}(\xi, s^m)$ is $(\mathcal{F}, \beta, \breve{\phi}, \breve{\rho}, \theta)$-quasisounivex at y, $\breve{\phi}$ is increasing, and $\breve{\phi}(0) = 0$;

(iv) $\rho^*(x, y) + \sum_{m=1}^{\nu_0} v_m\hat{\rho}_m(x, y) + \breve{\rho}(x, y) \geq 0$;

(d) *(i) for each $i \in \underline{p}$, f_i is $(\mathcal{F}, \beta, \bar{\phi}, \bar{\rho}_i, \theta)$-sounivex and $-g_i$ is $(\mathcal{F}, \beta, \bar{\phi}, \tilde{\rho}_i, \theta)$-sounivex at y, $\bar{\phi}$ is superlinear, and $\bar{\phi}(a) \geq 0 \Rightarrow a \geq 0$;*

(ii) the function $\xi \to \sum_{m=1}^{\nu_0} v_m G_{j_m}(\xi, t^m)$ is $(\mathcal{F}, \beta, \hat{\phi}, \hat{\rho}, \theta)$-quasisounivex at y, $\hat{\phi}$ is increasing, and $\hat{\phi}(0) = 0$;

(iii) *the function* $\xi \to \sum_{m=\nu_0+1}^{\nu} v_m H_{k_m}(\xi, s^m)$ *is* $(\mathcal{F}, \beta, \breve{\phi}, \breve{\rho}, \theta)$*-quasisounivex at* y, $\breve{\phi}$ *is increasing, and* $\breve{\phi}(0) = 0$*;*

(iv) $\rho^*(x, y) + \hat{\rho}(x, y) + \breve{\rho}(x, y) \geq 0$*;*

(e) *(i) for each* $i \in \underline{p}$, f_i *is* $(\mathcal{F}, \beta, \bar{\phi}, \bar{\rho}_i, \theta)$*-sounivex and* $-g_i$ *is* $(\mathcal{F}, \beta, \bar{\phi}, \tilde{\rho}_i, \theta)$*-sounivex at* y, $\bar{\phi}$ *is superlinear, and* $\bar{\phi}(a) \geq 0 \Rightarrow a \geq 0$*;*

(ii) the function $\xi \to \sum_{m=1}^{\nu_0} v_m G_{j_m}(\xi, t^m) + \sum_{m=\nu_0+1}^{\nu} v_m H_{k_m}(\xi, s^m)$ *is* $(\mathcal{F}, \beta, \hat{\phi}, \hat{\rho}, \theta)$*-quasisounivex at* y, $\hat{\phi}$ *is increasing, and* $\hat{\phi}(0) = 0$*;*

(iii) $\rho^*(x, y) + \hat{\rho}(x, y) \geq 0$.

Then $\varphi(x) \geq \lambda$.

Proof. The poof is similar to that of Theorem 3.2. □

5. Specializations II

In this section, we consider certain specializations of the $(\mathcal{G}, \beta, \phi, h(\cdot, \cdot), \rho, \theta)$-univexity to first order univexity under which first order duality (see (Zalmai & Zhang, 2007)) can be established. These duality models have the following forms:

$(DIII)$ $\sup_{(y,u,v,\lambda,\nu,\nu_0,J_{\nu_0},K_{\nu\setminus\nu_0},\bar{t},\bar{s})\in\mathbb{H}} \lambda$

subject to

$$\sum_{i=1}^{p} u_i[\nabla f_i(y) - \lambda \nabla g_i(y)] + \sum_{m=1}^{\nu_0} v_m \nabla G_{j_m}(y, t^m) + \sum_{m=\nu_0+1}^{\nu} v_m \nabla H_{k_m}(y, s^m) = 0, \tag{5.1}$$

$$u_i[f_i(y) - \lambda g_i(y)] \geq 0, \quad i \in \underline{p}, \tag{5.2}$$

$$G_{j_m}(y, t^m) \geq 0, \quad m \in \underline{\nu_0}, \tag{5.3}$$

$$v_m H_{k_m}(y, s^m) \geq 0, \quad m \in \underline{\nu}\setminus\underline{\nu_0}; \tag{5.4}$$

$(\tilde{D}III)$ $\sup_{(y,u,v,\lambda,\nu,\nu_0,J_{\nu_0},K_{\nu\setminus\nu_0},\bar{t},\bar{s})\in\mathbb{H}} \lambda$

subject to (3.3) and (5.2) - (5.4).

Theorem 5.1. *(see (Zalmai & Zhang, 2007)) (Weak Duality) Let* x *and* $(y, u, v, \lambda, \nu, \nu_0, J_{\nu_0}, K_{\nu\setminus\nu_0}, \bar{t}, \bar{s})$ *be arbitrary feasible solutions of (P) and (DIII), respectively, and assume that any one of the following five sets of hypotheses is satisfied:*

(a) *(i) for each* $i \in \underline{p}$, f_i *is* $(\mathcal{F}, \beta, \bar{\phi}, \bar{\rho}_i, \theta)$*-univex and* $-g_i$ *is* $(\mathcal{F}, \beta, \bar{\phi}, \tilde{\rho}_i, \theta)$*-univex at* y, $\bar{\phi}$ *is superlinear, and* $\bar{\phi}(a) \geq 0 \Rightarrow a \geq 0$*;*

(ii) *the function* $z \to G_{j_m}(z, t^m)$ *is* $(\mathcal{F}, \beta, \hat{\phi}_m, \hat{\rho}_m, \theta)$*-quasiunivex at* y, $\hat{\phi}_m$ *is increasing, and* $\hat{\phi}_m(0) = 0$ *for each* $m \in \underline{\nu_0}$*;*

(iii) *the function* $z \to \nu_m H_{k_m}(z, s^m)$ *is* $(\mathcal{F}, \beta, \breve{\phi}_m, \breve{\rho}_m, \theta)$*-quasiunivex at* y, $\breve{\phi}_m$ *is increasing, and* $\breve{\phi}_m(0) = 0$ *for each* $m \in \underline{\nu} \backslash \underline{\nu_0}$*;*

(iv) $\rho^* + \sum_{m=1}^{\nu_0} \nu_m \hat{\rho}_m + \sum_{m=\nu_0+1}^{\nu} \nu_m \breve{\rho}_m \geq 0$*, where* $\rho^* = \sum_{i=1}^{p} u_i(\bar{\rho}_i + \lambda \tilde{\rho}_i)$*;*

(b) *(i)* *for each* $i \in \underline{p}$, f_i *is* $(\mathcal{F}, \beta, \bar{\phi}, \bar{\rho}_i, \theta)$*-univex and* $-g_i$ *is* $(\mathcal{F}, \beta, \bar{\phi}, \tilde{\rho}_i, \theta)$*-univex at* y, $\bar{\phi}$ *is superlinear, and* $\bar{\phi}(a) \geq 0 \Rightarrow a \geq 0$*;*

(ii) *the function* $z \to \sum_{m=1}^{\nu_0} \nu_m G_{j_m}(z, t^m)$ *is* $(\mathcal{F}, \beta, \hat{\phi}, \hat{\rho}, \theta)$*-quasiunivex at* y, $\hat{\phi}$ *is increasing, and* $\hat{\phi}(0) = 0$*;*

(iii) *the function* $z \to \nu_m H_{k_m}(z, s^m)$ *is* $(\mathcal{F}, \beta, \breve{\phi}_m, \breve{\rho}_m, \theta)$*-quasiunivex at* y, $\breve{\phi}_m$ *is increasing, and* $\breve{\phi}_m(0) = 0$ *for each* $m \in \underline{\nu} \backslash \underline{\nu_0}$*;*

(iv) $\rho^* + \hat{\rho} + \sum_{m=\nu_0+1}^{\nu} \breve{\rho}_m \geq 0$*;*

(c) *(i)* *for each* $i \in \underline{p}$, f_i *is* $(\mathcal{F}, \beta, \bar{\phi}, \bar{\rho}_i, \theta)$*-univex and* $-g_i$ *is* $(\mathcal{F}, \beta, \bar{\phi}, \tilde{\rho}_i, \theta)$*-univex at* y, $\bar{\phi}$ *is superlinear, and* $\bar{\phi}(a) \geq 0 \Rightarrow a \geq 0$*;*

(ii) *the function* $z \to G_{j_m}(z, t^m)$ *is* $(\mathcal{F}, \beta, \hat{\phi}_m, \hat{\rho}_m, \theta)$*-quasiunivex at* y, $\hat{\phi}_m$ *is increasing, and* $\hat{\phi}_m(0) = 0$ *for each* $m \in \underline{\nu_0}$*;*

(iii) *the function* $z \to \sum_{m=\nu_0+1}^{\nu} \nu_m H_{k_m}(z, s^m)$ *is* $(\mathcal{F}, \beta, \breve{\phi}, \breve{\rho}, \theta)$*-quasiunivex at* y, $\breve{\phi}$ *is increasing, and* $\breve{\phi}(0) = 0$*;*

(iv) $\rho^* + \sum_{m=1}^{\nu_0} \nu_m \hat{\rho}_m + \breve{\rho} \geq 0$*;*

(d) *(i)* *for each* $i \in \underline{p}$, f_i *is* $(\mathcal{F}, \beta, \bar{\phi}, \bar{\rho}_i, \theta)$*-univex and* $-g_i$ *is* $(\mathcal{F}, \beta, \bar{\phi}, \tilde{\rho}_i, \theta)$*-univex at* y, $\bar{\phi}$ *is superlinear, and* $\bar{\phi}(a) \geq 0 \Rightarrow a \geq 0$*;*

(ii) *the function* $z \to \sum_{m=1}^{\nu_0} \nu_m G_{j_m}(z, t^m)$ *is* $(\mathcal{F}, \beta, \hat{\phi}, \hat{\rho}, \theta)$*-quasiunivex at* y, $\hat{\phi}$ *is increasing, and* $\hat{\phi}(0) = 0$*;*

(iii) *the function* $z \to \sum_{m=\nu_0+1}^{\nu} \nu_m H_{k_m}(z, s^m)$ *is* $(\mathcal{F}, \beta, \breve{\phi}, \breve{\rho}, \theta)$*-quasiunivex at* y, $\breve{\phi}$ *is increasing, and* $\breve{\phi}(0) = 0$*;*

(iv) $\rho^* + \hat{\rho} + \breve{\rho} \geq 0$*;*

(e) *(i)* *for each* $i \in \underline{p}$, f_i *is* $(\mathcal{F}, \beta, \bar{\phi}, \bar{\rho}_i, \theta)$*-univex and* $-g_i$ *is* $(\mathcal{F}, \beta, \bar{\phi}, \tilde{\rho}_i, \theta)$*-univex at* y, $\bar{\phi}$ *is superlinear, and* $\bar{\phi}(a) \geq 0 \Rightarrow a \geq 0$*;*

(ii) *the function* $z \to \sum_{m=1}^{\nu_0} \nu_m G_{j_m}(z, t^m) + \sum_{m=\nu_0+1}^{\nu} \nu_m H_{k_m}(z, s^m)$ *is* $(\mathcal{F}, \beta, \hat{\phi}, \hat{\rho}, \theta)$*-quasiunivex at* y, $\hat{\phi}$ *is increasing, and* $\hat{\phi}(0) = 0$*;*

(iii) $\rho^* + \hat{\rho} \geq 0$*.*

Then $\varphi(x) \geq \lambda$*.*

6. Concluding Remarks

The duality results established in this communication encompass a fairly large number of second-order dual problems and duality theorems that were investigated previously for several classes of nonlinear programming problems. Furthermore, the methods utilized in this paper could lead to extend and generalize results to other classes of mathematical programming problems based on general univexity assumptions.

Acknowledgment

The author is greatly indebted to the reviewer for all highly constructive comments and valuable suggestions leading to the revised version.

References

Aghezzaf, B. (2003). Second order mixed type duality in multiobjective programming problems, *J. Math. Anal. Appl.* **285**, 97–106.

Ahmad, I. and Z. Husain (2005). Nondifferentiable second-order symmetric duality, *Asia-Pacific J. Oper. Res.* **22**, 19–31.

Ahmad, I., Z. Husain and S. Sharma (2007). Higher-order duality in nondifferentiable multiobjective programming, *Numer. Func. Anal. Optim.* **28**, 989–1002.

Ahmad, I. and S. Sharma (2007). Second-order duality for nondifferentiable multiobjective programming problems, *Numer. Func. Anal. Optim.* **28**, 975–988.

Bector, C. R. and B. K. Bector (1986). Generalized bonvex functions and second-order duality for a nonlinear programming problem, *Congressus Numer.* **22**, 37–52.

Bector, C. R. and B. K. Bector (1986). On various duality theorems for second-order duality in nonlinear programming, *Cahiers du Centre d'Etudes de Rechereche Opér.* **28**, 283–292.

Bector, C. R. and S. Chandra (1986). Second-order duality for generalized fractional programming, *Methods Oper. Res.* **56**, 11–28.

Bector, C. R. and S. Chandra (1986). Second order symmetric and self dual programs, *Opsearch* **23**, 89–95.

Bector, C. R. and S. Chandra (1986). First and second order duality for a class of nondifferentiable fractional programming problems, *J. Inform. Optim. Sci.* **7**, 335–348.

Bector, C. R. and S. Chandra (1987). Generalized bonvexity and higher order duality for fractional programming, *Opsearch* **24**, 143–154.

Bector, C. R., S. Chandra and I. Husain (1991). Second-order duality for a minimax programming problem, *Opsearch* **28**, 249–263.

Chen, X. (2008). Sufficient conditions and duality for a class of multiobjective fractional programming problems with higher-order (F, α, ρ, d)-convexity, *J. Appl. Math. Comput.* **28**, 107–121.

Egudo, R. R. and M. A. Hanson (1993). Second order duality in multiobjective programming, *Opsearch* **30**, 223–230.

Gulati, T. R. and D. Agarwal (2007). Second-order duality in multiobjective programming involving (F, α, ρ, d)-V-type I functions, *Numer. Funct. Anal. Optim.* **28**, 1263–1277.

Gulati, T. R. and D. Agarwal (2007). On Huard type second-order converse duality in nonlinear programming, *Appl. Math. Lett.* **20**, 1057–1063.

Gulati, T. R. and D. Agarwal (2008). Optimality and duality in nondifferentiable multiobjective mathematical programming involving higher order (F, α, ρ, d)-type I functions, *J. Appl. Comput.* **27**, 345–364.

Gulati, T. R. and I. Ahmad (1997). Second order symmetric duality for nonlinear minimax mixed integer programming problems, *European J. Oper. Res.* **101**, 122–129.

Gulati, T.R., I. Ahmad and I. Husain (2001). Second order symmetric duality with generalized convexity, *Opsearch* **38**, 210–222.

Gulati, T. R. and Geeta (2010). Mond-Weir type second-order symmetric duality in multiobjective programming over cones, *Appl. Math. Lett.* **23**, 466–471.

Gulati, T. R. and S. K. Gupta (2007). Second-order symmetric duality for minimax integer programs over cones, *Internat. J. Oper. Res.* **4**, 181–188.

Gulati, T. R. and S. K. Gupta (2007). Higher-order nondifferentiable symmetric duality with generalized F-convexity, *J. Math. Anal. Appl.* **329**, 229–237.

Gulati, T. R. and S. K. Gupta (2007). A note on Mond-Weir type second-order symmetric duality, *Asia-Pac. J. Oper. Res.* **24**, 737–740.

Gulati, T. R. and S. K. Gupta (2009). Higher-order symmetric duality with cone constraints, *Appl. Math. Lett.* **22**, 776–781.

Gulati, T. R., S. K. Gupta and I. Ahmad (2008). Second-order symmetric duality with cone constraints, *J. Comput. Appl. Math.* **220**, 347–354.

Gulati, T. R. and G. Mehndiratta (2010). Nondifferentiable multiobjective Mond-Weir type second-order symmetric duality over cones, *Optim. Lett.* 4, 293–309.

Gulati, T. R., H. Saini and S. K. Gupta (2010). Second-order multiobjective symmetric duality with cone constraints, *European J. Oper. Res.* **205**, 247–252.

Gupta, S. K. and N. Kailey (2010). A note on multiobjective second-order symmetric duality, *European J. Oper. Res.* **201**, 649–651.

Hachimi, M. and B. Aghezzaf (2004). Second order duality in multiobjective programming involving generalized type-I functions, *Numer. Funct. Anal. Optim.* **25**, 725–736.

Hanson, M. A. (1993). Second order invexity and duality in mathematical programming, *Opsearch* **30**, 313–320.

Hou, S. H. and X. M. Yang (2002). On second-order symmetric duality in nondifferentiable programming, *J. Math. Anal. Appl.* **255**, 491–498.

Husain, Z., I. Ahmad and S. Sharma (2009). Second order duality for minmax fractional programming, *Optim. Lett.* **3**, 277–286.

Husain, I., A. Goyel and M. Masoodi (2007). Second order symmetric and maxmin symmetric duality with cone constraints, *Internat. J. Oper Res.* **4**, 199–205.

Husain, I. and Z. Jabeen (2004). Second order duality for fractional programming with support functions, *Opsearch* **41**, 121–134.

Jeyakumar, V. (1985). ρ-Convexity and second order duality, *Utilitas Math.* **29**, 71–85.

Jeyakumar, V. (1985). First and second order fractional programming duality, *Opsearch* **22**, 24–41.

Liu, J. C. (1999). Second order duality for minimax programming, *Utilitas Math.* **56**, 53–63

Mangasarian, O. L. (1975). Second- and higher-order duality theorems in nonlinear programming, *J. Math. Anal. Appl.* **51**, 607–620.

Mishra, S. K. (1997). Second order generalized invexity and duality in mathematical programming, *Optimization* **42**, 51–69.

Mishra, S. K. (2000). Second order symmetric duality in mathematical programming with F-convexity, *European J. Oper. Res.* **127**, 507–518.

Mishra, S. K. and N. G. Rueda (2000). Higher-order generalized invexity and duality in mathematical programming, *J. Math. Anal. Appl.* **247**, 173–182.

Mishra, S. K. and N. G. Rueda (2006). Second-order duality for nondifferentiale minimax programming involving generalized type I functions, *J. Optim. Theory Appl.* **130**, 477–486.

Mond, B. (1974). Second order duality for nonlinear programs, *Opsearch* **11**, 90–99.

Mond, B. and T. Weir (1981–1983). Generalized convexity and higher-order duality, *J. Math. Sci.* **16-18**, 74–94.

Mond, B. and T. Weir (1981). Generalized concavity and duality, in *Generalized Concavity in Optimization and Economics* (S. Schaible and W. T. Ziemba, eds.), *Academic Press, New York,* 1981, pp. 263–279.

Mond, B. and J. Zhang (1995). Duality for multiobjective programming involving second-order V-invex functions, in *Proceedings of the Optimization Miniconference II* (B. M. Glover and V. Jeyakumar, eds.), University of New South Wales, Sydney, Australia, 1995, pp. 89–100.

Mond, B. and J. Zhang (1998). *Higher order invexity and duality in mathemaical programming*, in Generalized Convexity, Generalized Monotonicity : Recent Results (J. P. Crouzeix, *et al.*, eds.), Kluwer Academic Publishers, printed in the Netherlands, 1998, pp. 357–372.

Patel, R. B. (1997). Second order duality in multiobjective fractional programming, *Indian J. Math.* **38**, 39–46.

Srivastava, M. K. and M. Bhatia (2006). Symmetric duality for multiobjective programming using second order (F,ρ)-convexity, *Opsearch* **43**, 274–295.

Srivastava, S. K. and M. G. Govil (2000). Second order duality for multiobjective programming involving (F,ρ,σ)-type I functions, *Opsearch* **37**, 316–326.

Suneja, C. S. K., S. Lalitha and S. Khurana (2003). Second order symmetric duality in multiobjective programming, *European J. Oper. Res.* **144**, 492–500.

Suneja, S. K., M. K. Srivastava and M. Bhatia (2008). Higher order duality in multiobjective fractional programming with support functions, *J. Math. Anal. Appl.* **347**, 8–17.

Verma, R. U. (2012). A generalization to Zalmai type univexities and applications to parametric Duality models in discrete minimax fractional programming, *Advances in Nonlinear Variational Inequalities* **15**(2), 113–123.

Verma, R. U. (2013). Generalized $(\mathcal{G},b,\beta,\phi,h,\rho,\theta)$-univexities with applications to parametric duality models for discrete minimax fractional programming, *Transactions on Mathematical Programming and Applications* **1**(1), 1–14.

Zalmai, G. J. (2012).Generalized second-order $(\mathcal{F},\beta,\phi,\rho,\theta)-$univex functions and parametric duality models in semi-infinite discrete minmax fractional programming, *Advances in Nonlinear Variational Inequalities* **15**(2), 63–91.

Zalmai, G. J. (1999). Optimality conditions and duality for constrained measurable subset selection problems with minmax objective functions, *Optimization* **2**, 377–395.

Zalmai, G. J. and Q. Zhang (2007). Generalized $(\mathcal{F},\beta,\phi,\rho,\theta)$-univex functions and parametric duality models in semiinfinite discrete minmax fractional programming, *Advances in Nonlinear Variational Inequalities* **10**, 21–42.

Theory and Applications of Mathematics & Computer Science

(ISSN 2067-2764)
http://www.uav.ro/applications/se/journal/index.php/tamcs

Theory and Applications of Mathematics & Computer Science 3 (1) (2013) 85–89

On Univalent Functions with Logarithmic Coefficients by Using Convolution

Sh. Najafzadeh[a,*], A. Ebadian[a]

[a]*Department of Mathematics, Payame Noor University, Iran*

Abstract

The purpose of this present paper is to derive some inclusion results and coefficient estimates for certain analytic functions with logarithmic coefficients by using Hadamard product. Relevant connections of the results with various known properties are also investigated.

Keywords: Convolution, univalent function, logarithmic coefficient, coefficient bounds, extreme point, convex set.
2010 MSC: 30C45, 30C50.

1. Introduction and Motivation

let A denote the class of normalized functions $f(z)$ of the from

$$f(z) = z + \sum_{n=2}^{+\infty} a_n z^n, \tag{1.1}$$

which are holomorphic in the open unit disk $\Delta = \{z : |z| < 1\}$. Let N denote the subclass of A consisting of functions $f(z)$ of the form

$$f(z) = z - \sum_{n=2}^{+\infty} a_n z^n. \quad (a_n \geq 0). \tag{1.2}$$

Associated with each f in A is a well defined logarithmic function

$$\log \frac{f(z)}{z} = 2 \sum_{n=1}^{+\infty} \gamma_n z^n. \ z \in \Delta. \tag{1.3}$$

*Corresponding author
Email addresses: najafzadeh1234@yahoo.ie (Sh. Najafzadeh), aebadian@yahoo.com (A. Ebadian)

The numbers γ_n are called the logarithmic coefficients of $f(z)$. See (Girela, 2000). For $\log \frac{f(z)}{z}$ given by (1.3) and $G(z) \in N$ given by

$$G(z) = z - \sum_{n=2}^{+\infty} b_n z^n, \tag{1.4}$$

the convolution (or Hadamard product) of

$$F(z) = -(\log \frac{f(z)}{z}) + (1 + 2\gamma_1)z, \tag{1.5}$$

and $G(z)$ denoted by $F * G$, is defined by

$$H(z) = F * G := z - \sum_{n=2}^{+\infty} 2\gamma_n b_n z^n. \tag{1.6}$$

We denote by $\Pi(\eta, \beta)$ and $Q(\eta, \beta)$ consisting of the functions $H(z) = F * G$ in N which satisfy

$$Re\{\frac{\frac{zH'(z)}{H(z)}}{\eta\frac{zH'(z)}{H(z)} + (1-\eta)}\} > \beta \tag{1.7}$$

and

$$Re\{\frac{1 + \frac{zH''(z)}{H'(z)}}{1 + \eta\frac{zH''(z)}{H'(z)}}\} > \beta\,, \quad 0 \le \beta < 1, 0 \le \eta < 1, \tag{1.8}$$

respectively. Also the functions $H(z)$ in N are said to be in the class $\Lambda(\eta, \beta, \psi)$, if there exists a function $\psi(z) \in N$ such that

$$Re\{\frac{\frac{zH'(z)}{\psi(z)}}{\eta\frac{zH'(z)}{\psi(z)} + (1-\eta)}\} > \beta. \tag{1.9}$$

For these subclassess we prove some interesting theorems include coefficient bounds, inclusion results, extreme points and property of convex sets.

Several other interesting subclasses of univalent functions were investigated recently, for example, by Ghanim and Darus (Ghanim & Darus, 2008), Prajapat and Goyal (Prajapat & Goyal, 2009), Acu and Owa (Acu & Owa, 2000) and etc. See also (Najafzadeh & Kulkarni, 2006) and (Najafzadeh & Ebadian, 2009).

2. Main result

Theorem 2.1. *If $H(z) \in \Lambda(\eta, \beta, \psi)$, then*

$$\sum_{n=2}^{+\infty} [2\gamma_n b_n(1 - \eta\beta) - \beta(1-\eta)c_n] \le 1 - \beta. \tag{2.1}$$

Proof. Since $H(z) \in \Lambda(\eta,\beta,\psi)$, then there exists a function $\psi(z) = z - \sum_{n=2}^{+\infty} c_n z^n \in N$ such that (1.9) holds true. By putting (1.6) and $H'(z) = (F * g)' = 1 - \sum_{n=2}^{+\infty} 2\gamma_n b_n z^n$ in (1.9) we get $Re\{\frac{1-\sum_{n=2}^{+\infty} 2\gamma_n b_n z^{n-1}}{1-\sum_{n=2}^{+\infty}(2\eta\gamma_n b_n+(1-\eta)c_n)z^{n-1}}\} > \beta$. By choosing the values of z on the real axis so that $\frac{z(F*G)'}{\psi(z)}$ is real and letting $r \to 1^-$ through real values, we have $\frac{1-\sum_{n=2}^{+\infty} 2\gamma_n b_n}{1-\sum_{n=2}^{+\infty}(2\eta\gamma_n b_n+(1-\eta)c_n)} \geq \beta$, or equivalently $\sum_{n=2}^{+\infty}[2\gamma_n b_n(1-\eta\beta) - \beta(1-\eta)c_n] \leq 1-\beta$. Now the proof is complete. □

Theorem 2.2. *If $H(z) \in Q(\eta,\beta)$, then $\sum_{n=2}^{+\infty} 2\gamma_n b_n(1+\eta(n-1)+\beta n^2) \leq 1-\beta$.*

Proof. Since $H(z) \in Q(\eta,\beta)$, then by (1.6) and (1.8) we get $Re\{\frac{1-\sum_{n=2}^{+\infty} 2n^2\gamma_n b_n z^{n-1}}{1-\sum_{n=2}^{+\infty} 2n\gamma_n(1+\eta(n-1))z^{n-1}}\} > \beta$. By choosing the values of z on the real axis so that $\frac{z(F*G)''}{(F*G)'}$ is real and letting $r \to 1^-$ though real values we have $\frac{1-\sum_{n=2}^{+\infty} 2n^2\gamma_n b_n}{1-\sum_{n=2}^{+\infty} 2n\gamma_n b_n(1+\eta(n-1))} > \beta$. The above inequality gives the required result. □

Definition 2.1. A function $H(z) \in N$ is said to be in $W(\eta,\beta)$, if there exists a function $\psi(z) = z - \sum_{n=2}^{+\infty} c_n z^n$ such that

(a) The condition (2.1) holds true;

(b) For every n, $2\gamma_n b_n - c_n \geq 0$.

In the next theorem we prove an inclusion property.

Theorem 2.3. *$W(\eta,\beta) \subseteq \Lambda(\eta,\beta,\psi)$.*

Proof. Let $H(z) \in W(\eta,\beta)$, we must show that $H(z) \in \Lambda(\eta,\beta,\psi)$ or equivalently the condition (1.9) holds. But

$$\left|\frac{\frac{z(F*G)'}{\psi(z)}}{\eta\frac{z(F*G)'}{\psi(z)}+(1-\eta)}-1\right| = \left|\frac{1-\sum_{n=2}^{+\infty} 2\gamma_n b_n z^{n-1}}{1-\sum_{n=2}^{+\infty}(2\eta\gamma_n b_n+(1-\eta)c_n)z^{n-1}}-1\right| = \left|\frac{(\eta-1)\sum_{n=2}^{+\infty}(2\gamma_n b_n - c_n)z^{n-1}}{1-\sum_{n=2}^{+\infty}(2\eta\gamma_n b_n+(1-\eta)c_n)z^{n-1}}\right|$$

$$\leq \frac{(1-\eta)\sum_{n=2}^{+\infty}(2\gamma_n b_n - c_n)}{1-\sum_{n=2}^{+\infty}(2\eta\gamma_n b_n+(1-\eta)c_n)}.$$

If (a) holds , above fraction is bounded above by $1-\alpha$ and hence (1.9) is satisfied. So $H(z) \in \Lambda(\eta,\beta,\psi)$. □

Remark. By putting $\psi(z) = G(z)$, in the last Theorem we obtain $\Pi(\eta,\beta) \subseteq W(\eta,\beta)$, and also by putting $\psi(z) = G(z)$ in (2.1) we have $\sum_{n=2}^{+\infty}[2\gamma_n(1-\eta\beta) - \beta(1-\eta)]b_n \leq 1-\beta$. This is the necessary and sufficient condition for functions $H(z) \in N$ to be in the class $\Pi(\eta,\beta)$.

3. Coefficient estimates and Distortion bounds for functions in $W(\eta,\beta)$

In this section we find coefficient bounds and verify distortion Theorem for the class $W(\eta,\beta)$.

Remark. If $H(z)$ be in the class $W(\eta,\beta)$, then

$$\sum_{n=2}^{+\infty}\gamma_n b_n \leq \frac{n(1-\beta)+\beta(1-\eta)}{2(1-\eta\beta)}. \tag{3.1}$$

Proof. From definition of $W(\eta,\beta)$ and taking $\psi(z)=z-\sum_{n=2}^{+\infty}c_n z^n$, we have $\sum_{n=2}^{+\infty}(1-\eta\beta)(2\gamma_n b_n)\leq 1-\beta+\beta(1-\eta)c_n$. If $c_n\leq\frac{1}{n}$ $(\forall n)$, thus we have $\sum_{n=2}^{+\infty}\gamma_n b_n\leq\frac{n(1-\beta)+\beta(1-\eta)}{2(1-\eta\beta)}$. □

Remark. The function $H_n(z)=z-\frac{n(1-\beta)+\beta(1-\eta)}{2(1-\eta\beta)}z^n$ is an extremal function for the class $W(\eta,\beta)$.

Theorem 3.1. *Let $H(z)=F*G$ be in the class $W(\eta,\beta)$, then for $|z|\leq r<1$*

$$r-\frac{2-\beta-\beta\eta}{4(1-\eta\beta)}r^2\leq|F*G|\leq r+\frac{2-\beta-\beta\eta}{4(1-\eta\beta)}r^2 \tag{3.2}$$

Proof. Since

$$H(z)=F*G=z-\sum_{n=2}^{+\infty}2\gamma_n b_n z^n, \tag{3.3}$$

so by (2.1) we get $\sum_{n=2}^{+\infty}2\gamma_n b_n(1-\eta\beta)-\beta(1-\eta)c_n\leq 1-\beta$. Since $c_n\leq\frac{1}{n}\leq\frac{1}{2}$ we have $\sum_{n=2}^{+\infty}2n\gamma_n b_n(1-\eta\beta)\leq\frac{\beta(1-\eta)}{2}+1-\beta$, or $2\sum_{n=2}^{+\infty}2n\gamma_n b_n(1-\eta\beta)\leq 2-\beta-\beta\eta$, or $2\sum_{n=2}^{+\infty}2\gamma_n b_n\leq 2\sum_{n=2}^{+\infty}n\gamma_n b_n\leq\frac{2-\beta-\beta\eta}{2(1-\eta\beta)}$, or $\sum_{n=2}^{+\infty}2\gamma_n b_n\leq\frac{2-\beta-\beta\eta}{4(1-\eta\beta)}$. From this inequality and (3.3) we have $|F*G|\leq|z|+\sum_{n=2}^{+\infty}2\gamma_n b_n|z|^n$ $\leq r+\frac{2-\beta-\beta\eta}{4(1-\eta\beta)}r^2$, and $|F*G|\geq r-\frac{2-\beta-\beta\eta}{4(1-\eta\beta)}r^2$. □

Theorem 3.2. *The class $W(\eta,\beta)$ is convex.*

Proof. Let $H_1(z)$ and $H_2(z)$ be in the class $W(\eta,\beta)$ with respect to functions $\psi_1(z)=z-\sum_{n=2}^{+\infty}c_n z^n$ and $\psi_2(z)=z-\sum_{n=2}^{+\infty}c'_n z^n$. For $0\leq j\leq 1$ we must show that $H(z)=jH_1(z)+(1-j)H_2(z)$ belongs to $W(\eta,\beta)$ with respect to $\psi(z)=j\psi_1(z)+(1-j)\psi_2(z)$. But $H_1(z)=z-\sum_{n=2}^{+\infty}2\gamma_n b_n z^n$, $H_2(z)=z-\sum_{n=2}^{+\infty}2\gamma_n b'_n z^n$, and $H(z)=z-\sum_{n=2}^{+\infty}s_n(j)z^n$, where $s_n(j)=2\gamma_n(jb_n+(1-j)b'_n)$. Also $\psi(z)=z-\sum_{n=2}^{+\infty}r_n(j)z^n$ where $r_n(j)=jc_n+(1-j)c'_n$.

The function $H(z)$ will belong to $W(\eta,\beta)$ if

(i) $\sum_{n=2}^{+\infty}[s_n(j)(1-\eta\beta)-\beta(1-\eta)r_n(j)]\leq 1-\beta$,

(ii) $s_n(j)-r_n(j)\geq 0$ for every n.

Since H_1 and H_2 are in $W(\eta,\beta)$ then $2\gamma_n b_n-c_n\geq 0$ and $2\gamma_n b'_n-c'_n\geq 0$, for all n. With direct calculation since $0\leq j\leq 1$ we have, $s_n(j)-r_n(j)=2\gamma_n(jb_n+(1-j)b'_n)-(jc_n+(1-j)c'_n)=j(2\gamma_n b_n-c_n)+(1-j)(2\gamma_n b'_n-c'_n)\geq 0$. Also $\sum_{n=2}^{+\infty}[s_n(j)(1-\eta\beta)-\beta(1-\eta)r_n(j)]=j\sum_{n=2}^{+\infty}2\gamma_n b_n(1-\eta\beta)-\beta(1-\eta)c_n+(1-j)\sum_{n=2}^{+\infty}2\gamma_n b'_n(1-\eta\beta)-\beta(1-\eta)c'_n\leq j(1-\beta)+(1-j)(1-\beta)=1-\beta$. Now the proof is complete. □

References

Acu, M. and S. Owa (2000). On some subclass of univalent functions. *Journal of Inequalities in Pure and Applied Mathematics* **6**(3), 1–14.

Ghanim, F. and M. Darus (2008). On new subclass of analytic univalent function with negative coefficient I. *Int. J. Contemp. Math. Sciences* **3**(27), 1317–1329.

Girela, D. (2000). Logarithmic coefficients of univalent functions. *Annals Acad. Sci. Fenn. Math. Series 1, Mathematica* **25**(2), 337–350.

Najafzadeh, Sh. and A. Ebadian (2009). Neighborhood and partial sum property for univalent holomorphic functions in terms of Komatu operator. *Acta Universitatis Apulensis* **25**(19), 81–90.

Najafzadeh, Sh. and S. R. Kulkarni (2006). Convex subclass of starlike functions in terms of combination of integral operators. *Int. Review of pure and appl. Math.* **2**(1), 25–34.

Prajapat, J. K. and S. P. Goyal (2009). Application of Srivastava-Attiya operator to the classes of strongly starlike and strongly convex functions. *J. Math. Ineq.* **3**(1), 129–137.

Theory and Applications of Mathematics & Computer Science

(ISSN 2067-2764, EISSN 2247-6202)
http://www.uav.ro/applications/se/journal/index.php/tamcs

Theory and Applications of Mathematics & Computer Science 3 (2) (2013) 1–35

Semitopological Vector Spaces and Hyperseminorms

Mark Burgin[a,*]

[a] *University of California, Los Angeles 405 Hilgard Ave. Los Angeles, CA 90095.*

Abstract

In this paper, we introduce and study semitopological vector spaces. The goal is to provide an efficient base for developing the theory of extrafunction spaces in an abstract setting of algebraic systems and topological spaces. Semitopological vector spaces are more general than conventional topological vector spaces, which proved to be very useful for solving many problems in functional analysis. To study semitopological vector spaces, hypermetrics and hyperpseudometrics are introduced and it is demonstrated that hyperseminorms, studied in previous works of the author, induce hyperpseudometrics, while hypernorms induce hypermetrics. Sufficient and necessary conditions for a hyperpseudometric (hypermetric) to be induced by a hyperseminorm (hypernorm) are found. We also show that semitopological vector spaces are closely related to systems of hyperseminorms. Then defining boundedness and continuity relative to associated systems of hyperseminorms, we study relations between relative boundedness and relative continuity for mappings of vector spaces with systems of hyperseminorms and systems of hypernorms.

Keywords: Functional analysis, topological vector space, norm, seminorm, hyperseminorm, boundedness, continuity, extrafunction.
2010 MSC: 47L10, 46A19, 46S60.

1. Introduction

The concept of a real or complex extrafunction essentially extends the concept of a real or complex function, encompassing, in particular, the concept of a distribution, i.e., distributions are a kind of extrafunctions (Burgin, 2012). Extrafunctions have many advantages in comparison with functions and distributions. For instance, integration of extrafunctions is more powerful than integration of functions allowing integration of a much larger range of functions as it is demonstrated in (Burgin, 2012).

At the same time, spaces of extrafunctions have a more sophisticated structure in comparison with spaces of functions, which are topological vector spaces and have a highly advanced theory (cf., for example, (Bourbaki, 1953-1955); (Robertson & Robertson, 1964); (Riez & Sz.-Nagy,

*Corresponding author
Email address: markburg@cs.ucla.edu (Mark Burgin)

1955); (Rudin, 1991); (Grothendieck, 1992); (Kolmogorov & Fomin, 1999)). In particular, it has been demonstrated that topological vector spaces provide an efficient context for the development of integration and are very useful for solving many problems in functional analysis in general (Choquet, 1969); (Edwards & Wayment, 1970); (Shuchat, 1972); (Kurzweil, 2000). In addition, locally convex topological vector spaces offer a convenient structure for studies of summation, which is integration of functions on natural numbers (Pietsch, 1965).

In this paper we introduce and study semitopological vector spaces, operators in these spaces and their mappings. It provides a base for the theory of extrafunction spaces in an abstract setting of algebraic systems and topological spaces. Semitopological vector spaces are more general than conventional topological vector spaces. To study semitopological vector spaces, hypermetrics and hyperpseudometrics are introduced and it is demonstrated that hyperseminorms induce hyperpseudometrics, while hypernorms induce hypermetrics. Norms are special cases of hypernorms, while seminorms are special cases of hyperseminorms. Sufficient and necessary conditions for a hyperpseudometric (hypermetric) to be induced by a hyperseminorm (hypernorm) are found. We also show that semitopological vector spaces are closely related to systems of hyperseminorms.

An essential property of operators in mathematics is continuity (cf. (Dunford & Schwartz, 1958); (Rudin, 1991); (Kolmogorov & Fomin, 1999)). One of the central results of functional analysis is the theorem that establishes equivalence between continuity and boundedness for linear operators. Here we extend the concepts of boundedness and continuity for operators and mappings of semitopological vector spaces with systems of hyperseminorms and seminorms, differentiating between different types of boundedness and continuity and making these concepts relative to systems of hyperseminorms and seminorms. Then we study these concepts, proving a series of theorems, which establish equivalence between a type of relative continuity and the corresponding type of relative boundedness for linear operators in semitopological vector spaces with systems of hyperseminorms or seminorms. Classical results describing continuous operators in convex spaces become direct corollaries of theorems proved in this paper. In conclusion, several problems for further research are formulated.

I would like to express my gratitude to the anonymous reviewer for useful remarks and observations.

2. Semitopological vector spaces

The concept of a semitopological vector space is an extension of the concept of a topological vector space.

Definition 2.1. *A semitopological vector space* L over a field $\mathbf{F}$ is a vector space over $\mathbf{F}$ with a topology in which addition is continuous, while scalar multiplication by elements from $\mathbf{F}$ is continuous with respect to L, i.e., the scalar multiplication mapping $m : \mathbf{F} \times L \to L$ is continuous in the second coordinate.

When the multiplication mapping $m : \mathbf{F} \times L \to L$ is continuous, then L is a topological vector space over the field $\mathbf{F}$. Some authors (cf., for example, (Rudin, 1991)) additionally demand that the point $\mathbf{0}$ in a topological vector space is closed. This condition results in the Hausdorff topology in topological vector spaces.

In what follows, **F** stands either for the field $\mathbb{R}$ of all real numbers or for the field $\mathbb{C}$ of all complex numbers or for a subfield of $\mathbb{C}$ that contains $\mathbb{R}$, while **0** denotes the zero element of any vector space.

Semitopological vector spaces are closely related to hypernorms and hyperseminorms.

Let $\mathbb{R}_\omega$ be the set of all real hypernumbers and $\mathbb{R}^+_\omega$ be the set of all non-negative real hypernumbers (Burgin, 2012).

Definition 2.2. a) A mapping $q : L \to \mathbb{R}^+_\omega$ is called a *hypernorm* if it satisfies the following conditions:

N1 . For any x from L, $q(x) = 0$ if and only if $x = \mathbf{0}$.

N2 . $q(ax) = |a| \cdot q(x)$ for any x from L and any number a from **F**.

N3 . (the triangle inequality or subadditivity).

$$q(x + y) \leq q(x) + q(y) \quad \text{for any } x \text{ and } y \text{ from } L$$

b) A vector space L with a norm is called a *hypernormed vector space* or simply, a *hypernormed space*.

c) The real hypernumber $q(x)$ is called the *hypernorm* of an element x from the hypernormed space L.

Note that *norms* in vector spaces coincide with hypernorms that take values only in the set of real numbers.

Example 2.1. As it is proved in (Burgin, 2012), the set of all real hypernumbers $\mathbb{R}_\omega$ is a hypernormed space where the hypernorm $\| \cdot \|$ is defined by the following formula:

If α is a real hypernumber, i.e.,$\alpha = \mathrm{Hn}(a_i)_{i\in\omega}$ with $a_i \in \mathbb{R}$ for all $i \in \omega$, then $\|\alpha\| = \mathrm{Hn}(|a_i|)_{i\in\omega}$.

Note that this hypernorm coincides with the conventional norm on real numbers but it is impossible get the same topology by means of a conventional finite norm.

Example 2.2. As it is proved in (Burgin, 2002), the set of all complex hypernumbers $\mathbb{C}_\omega$ of all complex hypernumbers is a hypernormed space where the hypernorm $\| \cdot \|$ is defined by the following formula:

If α is a complex hypernumber,i.e., $\alpha = \mathrm{Hn}(a_i)_{i\in\omega}$ with $a_i \in \mathbb{C}$ for all $i \in \omega$, then $\|\alpha\| = \mathrm{Hn}(|a_i|)_{i\in\omega}$.

Note that this hypernorm coincides with the conventional norm on complex numbers but it is impossible get the same topology by means of a conventional finite norm.

There are hypernormed spaces that are not normed spaces.

Example 2.3. The set $C(\mathbb{R}, \mathbb{R})$ of all continuous real functions is a hypernormed space where the hypernorm $\| \cdot \|$ is defined by the following formula:

If $f : \mathbb{R} \to \mathbb{R}$, then $\|f\| = \mathrm{Hn}(a_i)_{i\in\omega}$ where $a_i = max\{|f(x)|; a_i = [-i, i]\}$.

At the same time, it is known that $C(\mathbb{R}, \mathbb{R})$ is not a normed space (Robertson & Robertson, 1964).

There are natural relations between hypernorms and semitopological vector spaces.

Theorem 2.1. *Any hypernormed space is a Hausdorff semitopological vector space.*

Proof. Let us consider a vector space L with a hypernorm q. Taking an element x from L and a positive real number k, we define the neighborhood $O_k x$ of x by the following formula

$$O_k x = \{y \in L;\ q(x - y) < k\}.$$

At first, we show that the system of so defined neighborhoods determines a topology in L. To do this, it is necessary to check the following neighborhood axioms (Kuratowski, 1966):

NB1. Any neighborhood of a point $x \in X$ contains this point.

NB2. For any two neighborhoods $O_1 x$ and $O_2 x$ of a point $x \in X$, there is a neighborhood Ox of x that is a subset of the intersection $O_1 x \cap O_2 x$.

NB3. For any neighborhood Ox of a point $x \in X$ and a point $y \in Ox$, there is a neighborhood Oy of y that is a subset of Ox.

Let us consider a point x from X.

NB1: The point x belongs to $O_k x$ because $q(x - x) = q(\mathbf{0}) = 0 < k$ for any positive real number k.

NB2: Taking two positive real numbers k and h, we see that the intersection $O_k x \cap O_h x = O_l x$ also is a neighborhood of x where $l = \min\{k, h\}$.

NB3: Let $y \in O_k x$. Then $q(x - y) < k$ and by properties of real numbers, there is a positive real number t such that $q(x - y) < k - t$. Then $O_t x \subseteq O_k x$. Indeed, if $z \in O_t x$, then $q(y - z) < t$. Consequently,

$$q(x - z) = q((x - y) + (y - z)) \leq q(x - y) + q(y - z) < (k - t) + t = k.$$

It means that $z \in O_k x$.

Thus, we have a topology in L, and this topology is Hausdorff because any hypernorm separates points, i.e., if $x \neq y$, then $q(x - y) \neq 0$.

Now we show that addition is continuous and scalar multiplication is continuous in the second coordinate with respect to this topology.

Let us consider a sequence $\{x_i;\ i = 1, 2, 3, \dots\}$ that converges to x, a sequence $\{y_i;\ i = 1, 2, 3, \dots\}$ that converges to y, and the sequence $\{z_i = x_i + y_i;\ i = 1, 2, 3, \dots\}$. Convergence of these two sequences means that for any $k > 0$, there are a natural number n such that $q(x_i - x) < k$ for any $i > n$ and a natural number m such that $q(y_i - y) < k$ for any $i > m$. Then by properties of a hypernorm, we have

$$q(z_i - (x + y)) = q((x_i + y_i) - (x + y)) = q((x_i - x) + (y_i - y)) \leq q(x_i - x) + q(y_i - y) < k + k = 2k$$

when $i > \max\{n, m\}$. As k is an arbitrary positive real number, this means that the sequence $\{z_i = x_i + y_i;\ i = 1, 2, 3, \dots\}$. converges to $x + y$. Consequently, addition is continuous in L.

In addition, for any number a from $\mathbf{F}$, we have

$$q(u_i - ax) = q(ax_i - ax) = q(a(x_i - x)) \leq |a|q(x_i - x) < |a|k$$

where $u_i = ax_i$. As k is an arbitrary positive real number and $|a|$ is a constant, this means that the sequence $\{u_i = ax_i;\ i = 1, 2, 3, \dots\}$ converges to ax. Consequently, scalar multiplication is continuous in the second coordinate. Theorem is proved. □

Hypernormed spaces are also hypermetric spaces.

Definition 2.3. a) A mapping $\mathbf{d} : X \times X \to \mathbb{R}^+_\omega$ is called a *hypermetric* (or a *hyperdistance function*) in a set X if it satisfies the following axioms:

M1. For any x and y from X, $\mathbf{d}(x, y) = 0$ if and only if $x = y$.

M2. (Symmetry). $\mathbf{d}(x, y) = \mathbf{d}(y, x)$ for all $x, y \in X$.

M3. (the triangle inequality or subadditivity).

$$\mathbf{d}(x, y) \leq \mathbf{d}(x, z) + \mathbf{d}(z, y) \text{ for all } x, y, z \in X.$$

b) A set X with a hypermetric $\mathbf{d}$ is called a *hypermetric space*.

c) The real hypernumber $\mathbf{d}(x, y)$ is called the *distance* between x and y in the hypermetric space X.

Note that the distance between two elements in a hypermetric space can be a real number, finite hypernumber or infinite hypernumber. When the distance between two elements of X is always a real number, $\mathbf{d}$ is a metric.

Lemma 2.1. *a) A hypernorm q in a vector space L induces a hypermetric $\mathbf{d}_q$ in this space.*

b) If q is a norm in L, then $\mathbf{d}_q$ is a metric.

Indeed, if $q : X \to R^+_\omega$ is a hypernorm in L and x and y are elements from L, then we can define $\mathbf{d}_q(x, y) = q(x - y)$. Properties of a hypernorm imply that $\mathbf{d}_q$ satisfies all axioms M1- M3. The statement (b) directly follows from definitions.

Theorem 2.1 and Lemma 2.1 imply the following result.

Corollary 2.1. *$\mathbb{R}_\omega$ and $\mathbb{C}_\omega$ are hypermetric spaces.*

It is interesting to find what hypermetrics in vector spaces are induced by hypernorms and what metrics in vector spaces are induced by norms. To do this, let us consider additional properties of hypermetrics and metrics.

Definition 2.4. A hypermetric (metric) in a vector space L is called *linear* if it satisfies the following axioms:

LM1. $\mathbf{d}(x + z, y + z) = \mathbf{d}(x, y)$ for any $x, y, z \in L$.

LM2. $\mathbf{d}(ax, ay) = |a| \cdot \mathbf{d}(x, y)$ for all $x, y \in L$ and $a \in \mathbf{F}$.

Example 2.4. Let us take the space of all real numbers $\mathbb{R}$ as the space L. The natural metric in this space is defined as $\mathbf{d}(x, y) = |x - y|$. This metric is linear. Indeed,

$$\mathbf{d}(x + z, y + z) = |(x + z) - (y + z)| = |x - y| = \mathbf{d}(x, y)$$

and

$$\mathbf{d}(ax, ay) = |ax - ay| = |a(x - y)| = |a| \cdot |x - y| = |a| \cdot \mathbf{d}(x, y).$$

Example 2.5. Let us take the two-dimensional real vector space $\mathbb{R}^2$ as the space L. The natural metric in this space is defined by the conventional formula

$$\text{If} \quad x = (x_1, x_2) \text{ and } y = (y_1, y_2)\,, \text{ then } \mathbf{d}(x, y) = \sqrt{(x_1 - y_1)^2 + (x_2 - y_2)^2}.$$

This metric is also linear. Indeed,

$$\mathbf{d}(x+z, y+z) = \sqrt{((x_1 + z_1) - (y_1 + z_1))^2 + ((x_2 + z_2) - (y_2 + z_2))^2} = \sqrt{(x_1 - y_1)^2 + (x_2 - y_2)^2} = \mathbf{d}(x, y)$$

and

$$\mathbf{d}(ax, ay) = \sqrt{(ax_1 - ay_1)^2 + (ax_2 - ay_2)^2} = \sqrt{a^2(x_1 - y_1)^2 + a^2(x_2 - y_2)^2} =$$
$$= |a| \sqrt{(x_1 - y_1)^2 + (x_2 - y_2)^2} = |a| \cdot \mathbf{d}(x, y).$$

Example 2.6. Let us take the two-dimensional real vector space $\mathbb{R}^2$ as the space L. The natural metric in this space is defined by the conventional formula

$$\text{If } x = (x_1, x_2) \text{ and } y = (y_1, y_2), \text{ then } \mathbf{d}(x, y) = (x_1 - y_1)^2 + (x_2 - y_2)^2.$$

This metric is not linear. Indeed, let us take $x = (3, 3)$, $y = (1, 1)$, and $a = 2$. Then $\mathbf{d}(x, y) = 8$, while $\mathbf{d}(2x, 2y) = 32$.

These examples show that there are linear metrics (hypermetrics) in vector spaces and there are metrics (hypermetrics) in vector spaces that are not linear. The majority of popular metrics are induced by norms and thus, they are linear as the following result demonstrates.

Theorem 2.2. *A hypermetric* $\mathbf{d}$ *is induced by a hypernorm if and only if* $\mathbf{d}$ *is linear.*

Proof. Necessity. Let us consider a vector space L with a hypernorm q. By Lemma 2.1, it induces the hypermetric $\mathbf{d}_q(x, y) = q(x-y)$. Then $\mathbf{d}_q(x+z, y+z) = q((x+z)(y+z)) = q(x-y) = \mathbf{d}_q(x, y)$, i.e., Axiom LM1 is true. In addition, $\mathbf{d}_q(ax, ay) = q(ax-ay) = q(a(x-y)) = |a| \cdot q(x-y) = |a| \cdot \mathbf{d}_q(x, y)$, i.e., Axiom LM2 is also true.

Necessity. Let us consider a vector space L with a linear hypermetric $\mathbf{d}$. We define the hypernorm $q_{\mathbf{d}}$ by the following formula

$$q_{\mathbf{d}}(x) = \mathbf{d}(\mathbf{0}, x).$$

We show that $q_{\mathbf{d}}$ is a hypernorm. Indeed, $q_{\mathbf{d}}(\mathbf{0}) = \mathbf{d}(\mathbf{0}, \mathbf{0}) = 0$. Besides, if $q_d(x) = \mathbf{d}(\mathbf{0}, x) = 0$, then $x = 0$ by Axiom **M1**. This gives us Axiom **N1** for $q_{\mathbf{d}}$.

In addition,

$$q_{\mathbf{d}}(ax) = \mathbf{d}(\mathbf{0}, ax) = \mathbf{d}(a\mathbf{0}, ax) = \mathbf{d}(a(\mathbf{0}, x)) = |a| \cdot \mathbf{d}(\mathbf{0}, x) = |a| \cdot q_{\mathbf{d}}(x)$$

by Axiom LM2. This gives us Axiom N2 for $q_{\mathbf{d}}$.

Likewise, by Axioms M3 and LM1, we have

$$q_{\mathbf{d}}(x + y) = \mathbf{d}(\mathbf{0}, x + y) \leq \mathbf{d}(\mathbf{0}, x) + \mathbf{d}(x, x + y) = \mathbf{d}(\mathbf{0}, x) + \mathbf{d}(\mathbf{0}, y) = q_{\mathbf{d}}(x) + q_{\mathbf{d}}(y).$$

This gives us the triangle inequality (Axiom N3) for $q_{\mathbf{d}}$.

Theorem is proved. □

Corollary 2.2. *A metric* **d** *is induced by a norm if and only if* **d** *is linear.*

Taking only a part of the hypernorm properties, we come to the concept of a hyperseminorm.

Definition 2.5. a) A mapping $q : L \to \mathbb{R}^+_\omega$ is called a *hyperseminorm* if it satisfies the following conditions:

N2. $q(ax) = |a| \cdot q(x)$ for any x from L and any number a from $\mathbb{R}$.

N3. (the triangle inequality or subadditivity).

$$q(x + y) \leq q(x) + q(y) \text{ for any } x \text{ and } y \text{ from } L.$$

b) A vector space L with a norm is called a *hyperseminormed vector space* or simply, a *hyperseminormed space*.

c) The real hypernumber $q(x)$ is called the *hyperseminorm* of an element x from the hyperseminormed space L.

d) A set $X \subseteq L$ is called q - bounded if there is a positive real number h such that for any element a from X, the inequality $q(a) < h$ is true.

e) A set $X \subseteq L$ is called weakly q - *bounded* if there is a positive real hypernumber α such that for any element a from X, the inequality $q(a) < \alpha$ is true.

Note that any seminorm is a hyperseminorm that takes values only in the set of real numbers.

Proposition 2.1. *If $q : L \to \mathbb{R}$ is a hyperseminorm, then it has the following properties:*

(1) $q(x) \geq 0$ *for any* $x \in L$.
(2) $q(x - y) = q(y - x)$ *for any* $x, y \in L$.
(3) $q(\mathbf{0}) = 0$.
(4) $|q(x)q(y)| = q(x - y)$ *for any* $x, y \in L$.
(5) $q(x) - q(y) \leq q(x + y)$ *for any* $x, y \in L$.

Proof. (1) By Axiom N3, we have

$$q(x) + q(-x) \geq q(x + (-x)) = q(\mathbf{0}).$$

At the same time, by N2, we have $q(\mathbf{0}) = 0 \cdot q(\mathbf{0}) = 0$ and $q(-x) = q(x)$. This gives us

$$q(x) + q(-x) = q(x) + q(x) = 2q(x) \geq q(x + (-x)) = q(\mathbf{0}) = 0$$

and thus, $q(x) \geq 0$.

(2) By Axiom N2, we have

$$q(x - y) = q(-(y - x)) = |-1| \cdot q(y - x) = q(y - x).$$

(3) By Axiom N2, we have

$$q(\mathbf{0}) = q(0 \cdot \mathbf{0}) = |0| \cdot q(\mathbf{0}) = 0.$$

(4) By Axiom N3, we have

$$q(x) = q(x - y + y) \leq q(x - y) + q(y).$$

Thus,

$$q(x) - q(y) \leq q(x - y).$$

As q is symmetric (property (2)), we have

$$q(y) - q(x) \leq q(x - y).$$

Consequently,

$$|q(x) - q(y)| = q(x - y).$$

Property (5) is a consequence of property (4).

Proposition is proved. □

There are intrinsic relations between hyperseminorms and semitopological vector spaces.

Theorem 2.3. *Any hyperseminormed space is a semitopological vector space, which is Hausdorff if and only if it is a hypernormed space.*

Proof. Let us consider a vector space L with a hyperseminorm q. Taking an element x from L and a positive real number k, we define the neighborhood $O_k x$ of x by the following formula

$$O_k x = \{y \in L; q(x - y) < k\}.$$

To show that the system of so defined neighborhoods determines a topology in L, we check the neighborhood axioms (Kuratowski, 1966).

NB1: The point x belongs to $O_k x$ because by Proposition 1, $q(x - x) = q(\mathbf{0}) = 0 < k$ for any positive real number k.

NB2: Taking two positive real numbers k and h, we see that the intersection $O_k x \cap O_h x = O_l x$ is also a neighborhood of x where $l = \min\{k, h\}$.

NB3: Let $y \in O_k x$. Then $q(x - y) < k$ and by properties of real numbers, there is a positive real number t such that $q(x - y) < k - t$. Then $O_t x \subseteq O_k x$. Indeed, if $z \in O_t x$, then $q(y - z) < t$. Consequently,

$$q(x - z) = q((x - y) + (y - z)) \leq q(x - y) + q(y - z) < (k - t) + t = k.$$

It means that $z \in O_k x$.

Now we show that addition is continuous and scalar multiplication is continuous in the second coordinate with respect to this topology.

Let us consider a sequence $\{x_i;\ i = 1, 2, 3, \dots\}$ that converges to x, a sequence $\{y_i;\ i = 1, 2, 3, \dots\}$ that converges to y, and the sequence $\{z_i = x_i + y_i;\ i = 1, 2, 3, \dots\}$. Convergence of these two sequences means that for any $k > 0$, there are a natural number n such that $q(x_i - x) < k$ for any $i > n$ and a natural number m such that $q(y_i - y) < k$ for any $i > m$. Then by properties of a hyperseminorm, we have

$$q(z_i - (x + y)) = q((x_i + y_i) - (x + y)) = q((x_i - x) + (y_i - y)) \leq q(x_i - x) + q(y_i - y) < k + k = 2k,$$

when $i > \max\{n, m\}$. As k is an arbitrary positive real number, this means that the sequence $\{z_i = x_i + y_i;\ i = 1, 2, 3, \dots\}$ converges to $x + y$. Consequently, addition is continuous in L.

In addition, for any number a from $\mathbf{F}$, we have

$$q(u_i - ax) = q(ax_i - ax) = q(a(x_i - x)) = |a| q(x_i - x) < |a| k,$$

where $u_i = ax_i$. As k is an arbitrary positive real number and $|a|$ is a constant, this means that the sequence $\{u_i = ax_i;\ i = 1, 2, 3, \dots\}$ converges to ax. Consequently, scalar multiplication is continuous in the second coordinate.

By Theorem 2.2, if q is a hypernorm, then the space L is Hausdorff. At the same time, if q is not a hypernorm, then there are x and y from L such that $x \neq y$ but $q(x - y) = 0$. According to definition, these points x and y cannot be separated in the topology defined above. Thus, the space L is not Hausdorff.

Theorem is proved. □

Hyperseminormed spaces are also hyperpseudometric spaces.

Definition 2.6. A *hyperpseudometric* in a set X is a mapping $\mathbf{d} : X \times X \to \mathbb{R}^+_\omega$ that satisfies the following axioms:

P1. $\mathbf{d}(x, y) = 0$ if $x = y$,
i.e., the distance between an element and itself is equal to zero.

M2. (Symmetry). $d(x, y) = d(y, x)$ for all $x, y \in X$,
i.e., the distance between x and y is equal to the distance between y and x.

M3. (the triangle inequality or subadditivity).

$$\mathbf{d}(x, y) \leq \mathbf{d}(x, z) + \mathbf{d}(z, y) \text{ for all } x, y, z \in X.$$

When the distance between two elements of X is always a real number, $\mathbf{d}$ is a *pseudometric* (Kuratowski, 1966).

Note that although it would look natural, we do not use terms semimetric and hypersemimetric because according to the mathematical convention, semimetric is defined by a distance that satisfies only axioms M1 and M2.

Lemma 2.2. *a) A hyperseminorm in a vector space L induces a hyperpseudometric in this space.*

b) If q is a seminorm in L, then $\mathbf{d}_q$ is a pseudometric.

Indeed, if $q : X \times \mathbb{R}^+_\omega$ is a hyperseminorm in L and x and y are elements from L, then we can define $\mathbf{d}_q(x, y) = q(x - y)$. Properties of a hyperseminorm imply that $\mathbf{d}_q$ satisfies all axioms P1, M2 and M3. In addition, if q takes values only in $\mathbb{R}$, then the same is true for $\mathbf{d}_q$, i.e., $\mathbf{d}_q$ is a pseudometric.

It is interesting to find what hyperpseudometrics in vector spaces are induced by hyperseminorms and what pseudometrics in vector spaces are induced by seminorms. To do this, let us consider additional properties of hypermetrics and metrics.

Definition 2.7. A hyperpseudometric (metric) in a vector space L is called *linear* if it satisfies the Axioms LM1 and LM2.

Examples 2.4 - 2.6 show that there are linear pseudometrics (hyperpseudometrics) in vector spaces and there are pseudometrics (hyperpseudometrics) in vector spaces that are not linear. The majority of popular pseudometrics are induced by seminorms and thus, they are linear as the following result demonstrates.

Theorem 2.4. *A hyperpseudometric* $\mathbf{d}$ *is induced by a hyperseminorm if and only if* $\mathbf{d}$ *is linear. Proof is similar to the proof of Theorem 2.2.*

Corollary 2.3. *A pseudometric* $\mathbf{d}$ *is induced by a seminorm if and only if* $\mathbf{d}$ *is linear. We define the kernel* $\operatorname{Ker} q$ *of a hyperseminorm q in L as*

$$\operatorname{Ker} q = \{x \in L;\ q(x) = 0\}.$$

Theorem 2.5. *The kernel* $\operatorname{Ker} q$ *of a hyperseminorm q in L is a vector subspace of L.*

Indeed, if $q(x) = 0$ and $a \in \mathbf{F}$, then by Axiom N2,

$$q(ax) = |a| \cdot q(x) = |a| \cdot 0 = 0$$

i.e., $ax \in \operatorname{Ker} q$. In addition, $q(x) = 0$ and $q(y) = 0$, then by Axiom N3,

$$q(x + y) \leq q(x) + q(y) = 0 + 0 = 0$$

and $q(x + y) = 0$ because by Proposition 2.1, $q(x + y) \geq 0$.

Theorem 2.5 allows factorization of the hyperseminormed space L by its subspace $\operatorname{Ker} q$, obtaining the quotient space L_q . The hyperseminorm q induces the hypernorm p_q in the space L_q . This gives us the natural projection $\tau : L \to L_q$, which preserves the hyperseminorm q.

Example 2.7. Let us consider the set $C^\infty(\mathbb{R}, \mathbb{R})$ of all smooth real functions. The following seminorms are considered in is the set $C^\infty(\mathbb{R}, \mathbb{R})$. For each point $a \in \mathbb{R}$, and $f \in C^\infty(\mathbb{R}, \mathbb{R})$, we define

$$q_k(f) = (f(a))^2 + (f'(a))^2 + (f''(a))^2 + \ldots + (f^{(k)}(a))^2.$$

The factorization of the space by its subspace $\operatorname{Ker} q$ is called the k - th order jet space $J^k_a(\mathbb{R}, \mathbb{R})$ of $C^\infty(\mathbb{R}, \mathbb{R})$ at the point a. Jet spaces were introduced by Ehresmann (Ehresmann, 1952, 1953) and have various applications in the theory of differential equations and differential relations, as well as in the theory of manifolds (Gromov, 1986), (Krasilshchik *et al.*, 1986).

It is possible to get the same quotient space using the following seminorm

$$m_k(f) = \max\{|f(a)|, |f'(a)|, |f''(a)|, \ldots, |f^{(k)}(a)|\}.$$

Let us consider a Hausdorff space X that is a quotient space of L with the projection $\eta : L \to X$, preserves the hyperseminorm q. Then it is possible to define a projection $\nu : L_q \to X$ preserves the hyperseminorm q and for which $\eta = \nu\tau$, i.e., the following diagram is commutative:

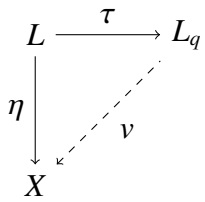

This gives us the following result.

Theorem 2.6. *a) L_q is the largest Hausdorff quotient space of the topological space L that preserves the hyperseminorm q.*

b) L_q is the largest quotient space of the topological space L in which the hyperseminorm q induces the hypernorm p_q.

It is possible to define two basic operators in a vector space L.

1. If z is an element from $\mathbf{L}$, then the translation operator T_z is defined by the formula:

$$T_z(x) = x + z \text{ where } x, z \in L.$$

2. If $a \neq 0$ is an element from $\mathbf{F}$, then the multiplication operator M_a is defined by the formula:

$$M_a(x) = ax \text{ where } x \in L.$$

Proposition 2.2. *Operators T_z and M_a are homeomorphisms of the semitopological vector space L.*

Proof. The axioms of a vector space imply that T_z and M_a are one-to-one mappings and their inverses are T_{-z} and M_{-a} , respectively. As addition is continuous in L, the operator T_z is also continuous. As scalar multiplication is continuous with respect to L, the operator M_a is also continuous. Proposition is proved. □

Corollary 2.4. *The topology of a semitopological vector space L is translation-invariant, or simply invariant, i.e., a subset A from L is open if and only if any its translation $A + a$ is open.*

As a result, such a topology is completely determined by any local base and thus, by any local base at $\mathbf{0}$.

Let us consider two subsets K and C of a semitopological vector space L.

Theorem 2.7. *If C is compact, K is closed and $K \cap C = \varnothing$, then $\mathbf{0}$ has a neighborhood V such that*

$$(K + V) \cap (C + V) = \varnothing.$$

Proof Proof is similar to the proof of Theorem 1.10 from (Rudin, 1991) because it uses only the first property of semitopological vector spaces.

As topological vector spaces are special cases of semitopological vector spaces, Theorem 1.10 from (Rudin, 1991) is a corollary of Theorem 2.7.

In a topological space X, the weakest separation axiom is $\mathbf{T}_0$ (Kelly, 1955) where:

$$\mathbf{T}_0 \text{ (the } \textit{Kolmogorov Axiom}). \forall x, y \in X \, (\exists Ox(y \notin Ox) \vee \nexists Oy(x \notin Oy)).$$

Lemma 2.3. *In a topological space X, all points are closed if and only if X satisfies the axiom $\mathbf{T}_0$.*

Proof. Sufficiency. If X satisfies the axiom $\mathbf{T}_0$ and x is a point from X, then each point from the complement Cx of x has a neighborhood that does not contain x. Thus, all these neighborhoods are subsets of Cx. By definition, Cx is an open set (Kuratowski, 1966) and consequently, its complement x is a closed set.

Necessity. If $x, y \in X$ and the point x is closed, then y belongs to the complement Cx of x, which is open as the complement of a closed set (Kuratowski, 1966). Thus, y has a neighborhood Oy that is a subset of Cx. Consequently, Oy does not contain x. As points x and y are arbitrary, X satisfies the axiom $\mathbf{T}_0$.

Lemma is proved. □

We remind (Alexandroff, 1961) that T_3 - *spaces*, or *regular spaces*, are topological spaces in which satisfy Axiom $\mathbf{T}_3$:

$\mathbf{T}_3$ *For every point a and closed set B, there exist disjoint open sets which separately contain a and B.*

It means that points and closed sets are separated.

Note that there are semitopological vector spaces in which not all points are closed. The space $\mathbb{R}^\omega$ of all sequences of real numbers is an example of such a semitopological vector space. Moreover, in $\mathbb{R}^\omega$, there are no closed points.

As a point is a compact space, Theorem 2.5 implies the following result.

Corollary 2.5. *Every semitopological vector space L in which all points are closed is a regular space.*

Lemma 2.3 and Corollary 2.5 imply the following result.

Corollary 2.6. *In semitopological vector spaces, L axiom* $\mathbf{T}_0$ *implies axiom* $\mathbf{T}_3$.

As any regular space is a Hausdorff space (Alexandroff, 1961), we have the following result.

Corollary 2.7. *Every semitopological vector space L in which all points are closed is a Hausdorff space.*

Lemma 2.3 and Corollary 2.7 imply the following result.

Corollary 2.8. *In semitopological vector spaces, L axiom* $\mathbf{T}_0$ *implies axiom* $\mathbf{T}_2$.

As both sets $K + V$ and $C + V$ in Theorem 2.7 are open, the closure of $K + V$ does not intersect $C + V$, while the closure of $C + V$ does not intersect $K + V$. As any point a from L is a compact space, we can take $K = \{a\}$. Applying Theorem 2.7 to this situation, we obtain the result, which has a considerable interest according to (Rudin, 1991).

Corollary 2.9. *Any neighborhood* O_a *of any point a in a semitopological vector space L contains the closure of some neighborhood* V_a *of the same point a.*

As topological vector spaces are special cases of semitopological vector spaces, Theorem 1.11 from (Rudin, 1991) is a corollary of Corollary 2.9.

3. Mappings of hyperseminormed vector spaces

Let us consider a hyperseminormed vector space L, i.e., a vector space L with a system of hyperseminorms Q, a hyperseminormed vector space M with a system of hyperseminorms P, a hyperseminorm q from Q, a hyperseminorm p from P, and a subset V of the space L.

Vector spaces with systems of hyperseminorms (of hypernorms) will be called *polyhyperseminormed spaces (polyhypernormed spaces)* because vector spaces over $\mathbb{R}$ with systems of norms or seminorms are called *polynormed spaces* (see (Helemski, 1989); (Dosi, 2011)).

Definition 3.1. a) An operator (mapping) $A : L \to M$ is called (q, p) - *bounded at a point a* from L if for any positive real number k, there is a positive real number h such that for any element b from L, the inequality $q(a - b) < k$ implies the inequality $p(A(b) - A(a)) < h$.

b) An operator (mapping) $A : L \to M$ is called (q, p) - *bounded* if it is (q, p) - bounded at all points of L.

c) An operator (mapping) $A : L \to M$ is called V - *uniformly* (q, p) - *bounded* if for any positive real number k, there is a positive real number h such that for any element a from V and any element b from L, the inequality $q(a - b) < k$ implies the inequality $p(A(b) - A(a)) < h$.

d) An operator (mapping) $A : L \to M$ is called *uniformly* (q, p) - bounded in V if for any positive real number k, there is a positive real number h such that for any elements a and b from V, the inequality $q(a - b) < k$ implies the inequality $p(A(b) - A(a)) < h$.

Note that when the set V contains only one point (say a), then V - uniform (q, p) - boundedness coincides with (q, p) - boundedness at the point a.

Definitions imply the following result.

Lemma 3.1. *Any uniformly* (q, p) *- bounded in L operator is L - uniformly* (q, p) *- bounded and any L - uniformly* (q, p) *- bounded operator is* (q, p) *- bounded.*

At the same time, as the following example demonstrates, there are (q, p) - bounded operators that are not L - uniformly (q, p) - bounded.

Example 3.1. Let us take $L = M = \mathbb{R}$ and assume that q and p are both equal to the absolute value, while $A(x) = x^2$. This mapping (operator) is (q, p) - bounded but not L - uniformly (q, p) - bounded.

However, for linear operators, the inverse of Lemma 3.1 is also true.

Proposition 3.1. *The following conditions are equivalent for a linear operator (mapping) A:*

(1) A is (q, p) *- bounded.*

(2) A is uniformly (q, p) *- bounded in L.*

(3) For some point a, A is uniformly (q, p) *- bounded at the point a.*

(4) A is L - uniformly (q, p) *- bounded.*

Proof. Implications (2) $\Rightarrow$ (1) $\Rightarrow$ (3) directly follow from definitions. So, we need to prove only (3) $\Rightarrow$ (2), namely, if $A : L \to M$ is (q, p) - bounded at a point a from L, then it is uniformly (q, p) - bounded.

Let us consider another point b from L and assume that $q(b - c) < k$ for some c from L. Then taking $d = c - (b - a)$, we have

$$q(a - d) = q(a - (c - (b - a)) = q(b - c) < k.$$

As A is (q, p) - bounded at a, there is a positive real number h such that $p(A(a) - A(d)) < h$. As A is linear operator, we have

$$p(A(b) - A(c)) = p(A(b - c)) = p(A(a - (c - (b - a)) = p(A(a - d)) = p(A(a) - A(d)) < h.$$

This shows that A is (q, p) - bounded at the point b because c is an arbitrary point for which $q(b - c) < k$. Thus, A is uniformly (q, p) - bounded in L because for a fixed number k, we have the same number h for all points in L.

In addition, we see that by definition, properties (2) and (4) always coincide.

Proposition is proved. □

Corollary 3.1. *A linear operator (mapping) A is* (q, p) *- bounded if and only if it is* (q, p) *- bounded at* $\mathbf{0}$.

The above proof of Proposition 3.1 gives us the following result.

Corollary 3.2. *Any* (q, p) *- bounded linear operator (mapping)* $A : L \to M$ *is* L *- uniformly* (q, p) *- bounded.*

These results show that for linear operators, the concepts of a (q, p) - bounded at a point operator and of a (q, p) - bounded operator coincide.

For operators that are not linear, these results are true as the following examples demonstrate.

Example 3.2. Let us assume that $L = M = \mathbb{R}_\omega$ is the space of all real hypernumbers (cf. Example 2.1), while both hyperseminorms q and p are both equal to the absolute value $\| \cdot \|$ of real hypernumbers. Actually the absolute value $\| \cdot \|$ is a norm in the space $\mathbb{R}_\omega$ (Burgin, 2012).

For the operator A, we define $A(x) = x$ for all real hypernumbers x but the hypernumber $\nu = \mathrm{Hn}(i)_{i\in\omega}$ and put $A(\nu) = 1$. Then $\|\nu - (\nu + 1)\| = 1$ but $\|A(\nu) - A(\nu + 1)\| = \|1 - (\nu + 1)\| = \|\nu\| = \nu$ and this hypernumber is larger than any positive real number (Burgin, 2012). Thus, operator A is (q, p) - bounded at any real number but it is not (q, p) - bounded at the hypernumbers ν.

This shows that an operator can be (q, p) - bounded at one point and not (q, p) - bounded at another point of L.

Example 3.3. Let us take $L = M = C(\mathbb{R}, \mathbb{R})$, while the space $C(\mathbb{R}, \mathbb{R})$ of all continuous real functions is a hypernormed space (cf. Example 2.1) where the hypernorm $\| \cdot \|$ is defined by the following formula:

$$\text{If } f : \mathbb{R} \to \mathbb{R}, \text{ then } \|f\| = \mathrm{Hn}(a_i)_{i\in\omega} \text{ where } a_i = max\{|f(x)|;\ a_i \in [-i, i]\}.$$

We define $A(f) = f$ for all real functions f but the function $\nu(x) = x^2$ and put $A(x^2) = e(x)$ where $e(x) = 1$ for all $x \in \mathbb{R}$. This operator A is (q, p) - bounded at any constant function from L but it is not (q, p) - bounded at ν. At the same time, taking $u(x) = x^2 + 1$, we have $\|\nu - u\| = 1$, while $\|A(\nu) - A(u)\| = \|e - u\| = \mathrm{Hn}(i)_{i\in\omega}$ and this hypernumber is larger than any positive real number (Burgin, 2011).

This also shows that an operator can be (q, p) - bounded at one point and not (q, p) - bounded at another point of L.

However, for norms and seminorms, we do not need additional conditions to establish the result of Proposition 3.1.

Proposition 3.2. *If q is a seminorm, then an operator (mapping) $A : L \to M$ is (q, p) - bounded if and only if it is (q, p) - bounded, at least, at one point.*

Proof. Let us consider two points a and c from L and assume that an operator $A : L \to M$ is (q, p) - bounded at the point a. Then taking a point b such that $q(c - b) < u$ where u is a positive real number.

As q is a seminorm, $q(a - c)$ is equal to some positive real number w. Thus, by properties of seminorms, we have

$$q(a - b) = q(a - c + c - b) \leq q(a - c) + q(c - b) < w + u.$$

As the operator A is (q, p) - bounded at the point a and $q(a - c) < w + 1$, we have a positive real number h such that $p(A(a) - A(b)) < h$ and a positive real number k such that $p(A(a) - A(c)) < k$. Consequently,

$$p(A(c) - A(b)) \leq p(A(a) - A(c)) + p(A(a) - A(b)) < k + h.$$

As b is an arbitrary point from L, A is (q, p) - bounded at the point c.

As c is an arbitrary point from L, the operator A is (q, p) - bounded.

Proposition is proved. □

Proposition 3.2 implies the following results.

Corollary 3.3. *The concepts of a (q, p) - bounded at a point operator and of a (q, p) - bounded operator coincide when q is a seminorm.*

Note that Examples 3.2 and 3.3 show this is not true for the general case of hyperseminorms.

Corollary 3.4. *When q is a seminorm, an operator (mapping) A is (q, p) - bounded if and only if it is (q, p) - bounded at $\mathbf{0}$.*

The above proof of Proposition 3.2 gives us the following result.

Corollary 3.5. *If q is a seminorm, then any (q, p) - bounded operator (mapping) $A : L \to M$ is L - uniformly (q, p) - bounded.*

Proposition 3.3. *If q is a seminorm and there is a (q, p) - bounded operator (mapping) A of the linear space L onto the linear space M, then p is a finite hyperseminorm.*

Proof. Let us take a point u from M. As A is a projection (surjection), there are points a and b such that $A(a) = \mathbf{0}$ and $A(b) = u$. As q is a seminorm, $q(b - a)$ is less than some positive real number w. As the operator A is (q, p) - bounded, there is a positive real number h such that $p(A(a) - A(b)) < h$

$$p(u) = p(u - \mathbf{0}) = p(A(b) - A(a)) < h.$$

As u is an arbitrary point from M, the hyperseminorm p is finite.

Proposition is proved. □

Note that a finite hyperseminorm is not always a seminorm and a finite hypernorm is not always a norm.

Definition 3.2. (Burgin, 2012). A real hypernumber is called *monotone* is it has a monotone representative.

For instance, all real numbers are monotone hypernumbers (Burgin, 2012). At the same time, all finite monotone real hypernumbers are real numbers (Burgin, 2012). Thus, Proposition 3.3 implies the following result.

Corollary 3.6. *If q is a seminorm, there is a (q, p) - bounded operator (mapping)A of the linear space L onto the linear space M and all values of p are monotone hypernumbers, then p is a seminorm.*

Definitions imply the following results.

Lemma 3.2. *If $W \subseteq V \subseteq L$, then any V - uniformly (q, p) - bounded operator is W - uniformly (q, p) - bounded and any uniformly (q, p) - bounded in V operator is uniformly (q, p) - bounded in W.*

Lemma 3.3. *Any V - uniformly (q, p) - bounded operator is (q, p) - bounded in V.*

Let us consider a binary relation u between the system of hyperseminorms Q, the system of hyperseminorms P and a subset V of the space L.

Definition 3.3. a) An operator (mapping) $A : L \to M$ is called (Q, u, P) - *bounded at a point a* from L if for any hyperseminorms q and p such that $(q, p) \in u$, the operator (mapping) A is (q, p) - bounded at the point a.

b) An operator (mapping) $A : L \to M$ is called V - *uniformly* (Q, u, P) - *bounded* if for any hyperseminorms q and p with $(q, p) \in u$ and any positive real number k, there is a positive real number h such that for any element a from V and any element b from L, the inequality $q(a - b) < k$ implies the inequality $p(A(b) - A(a)) < h$.

c) An operator (mapping) $A : L \to M$ is called *uniformly* (Q, u, P) - *bounded* in V if for any hyperseminorms q and p with $(q, p) \in u$ and any positive real number k, there is a positive real number h such that for any elements a and b from V, the inequality $q(a - b) < k$ implies the inequality $p(A(b) - A(a)) < h$.

d) An operator (mapping) $A : L \to M$ is called (Q, u, P) - *bounded* if it is (Q, u, P) - bounded at all points of L.

It means that an operator (mapping) A is (Q, u, P) - bounded if for any hyperseminorms q and p such that $(q, p) \in u$, the operator (mapping) A is (q, p) - bounded.

Note that when the set V contains only one point (say a), then V - uniform (Q, u, P) - boundedness coincides with (Q, u, P) - boundedness at the point a.

Lemma 3.1 implies the following result.

Lemma 3.4. *Any uniformly (Q, u, P) - bounded operator in L is L - uniformly (Q, u, P) - bounded, while any L - uniformly (Q, u, P) - bounded operator is (Q, u, P) - bounded.*

At the same time, taking $L = M = \mathbb{R}$, $Q = \{q\}$, $P = \{p\}$, and assuming that q and p are both equal to the absolute value and $u = \{(q, p)\}$, we see that Example 3.1 demonstrates that there are (Q, u, P) - bounded operators that are not L - uniformly (Q, u, P) - bounded.

However, for linear operators, the inverse of Lemma 3.4 is also true because Proposition 3.1 implies the following result.

Proposition 3.4. *The following conditions are equivalent for a linear operator (mapping) A:*

(1) A is (Q, u, P) - bounded.

(2) A is uniformly (Q, u, P) - bounded in L.

(3) For some point a, A is uniformly (Q, u, P) - bounded at the point a.

(4) A is L - uniformly (Q, u, P) - bounded.

Corollary 3.7. *A linear operator (mapping) A is (Q, u, P) - bounded if and only if it is (Q, u, P) - bounded at $\mathbf{0}$.*

Corollary 3.2 implies the following result.

Corollary 3.8. *Any (Q, u, P) - bounded linear operator (mapping) $A : L \to M$ is L - uniformly (Q, u, P) - bounded.*

These results show that for linear operators, the concepts of a (Q, u, P) - bounded at a point operator and a (Q, u, P) - bounded operator coincide.

At the same time, taking $L = M = \mathbb{R}$, $Q = \{q\}$, $P = \{p\}$, and assuming that q and p are both equal to the absolute value and $u = \{(q, p)\}$, we see that Examples 3.2 and 3.3 demonstrate that there are operators that are (Q, u, P) - bounded at one point and not (Q, u, P) - bounded at another point.

However, for norms and seminorms, we do not need additional conditions to establish the result of Proposition 3.4. We remind that the definability domain of the relation u is defined as

$$Du = \{q;\ \text{there is a pair } (q, p) \text{ that belongs to } u\}.$$

Then Proposition 3.2 implies the following result.

Proposition 3.5. *If all q from the definability domain Du of u are seminorms, then an operator (mapping) $A : L \to M$ is (Q, u, P) - bounded if and only if it is (Q, u, P) - bounded, at least, at one point.*

Proposition 3.5 implies the following result.

Corollary 3.9. *The concepts of (Q, u, P) - bounded at a point operators and (Q, u, P) - bounded operator coincide when all q from the definability domain Du of u are seminorms.*

Note that Examples 3.2 and 3.3 show this is not true for the general case of hyperseminorms.

Corollary 3.10. *When all q from the definability domain Du of u are seminorms, an operator (mapping) A is (Q, u, P) - bounded if and only if it is (Q, u, P) - bounded at $\mathbf{0}$.*

The above proof of Proposition 3.2 gives us the following result.

Corollary 3.11. *If all q from the definability domain Du of u are seminorms, then any (Q, u, P) - bounded operator (mapping) $A : L \to M$ is L - uniformly (Q, u, P) - bounded.*

Proposition 3.3 implies the following result.

Proposition 3.6. *If all q from the definability domain Du of u are seminorms and there is a (Q, u, P) - bounded operator (mapping) A of the linear space L onto the linear space M, then all p from the range $Rg\ u$ of u are finite hyperseminorms.*

Corollary 3.12. *If all q from the definability domain Du of u are seminorms and there is a (Q, u, P) - bounded operator (mapping) A of the linear space L onto the linear space M, and all values of all p from the range $Rg\ u$ are monotone hypernumbers, then all such p are seminorms.*

Definitions imply the following results.

Lemma 3.5. *If $W \subseteq V \subseteq L$, then any V - uniformly (Q, u, P) - bounded operator is W - uniformly (q, p) - bounded and any uniformly (Q, u, P) - bounded in V operator is uniformly (q, p) - bounded in W.*

Lemma 3.6. *Any V - uniformly (Q, u, P) - bounded operator is (Q, u, P) - bounded in V.*

Let us take a subset V of the space L.

Definition 3.4. a) An operator (mapping) $A : L \to M$ is called *uniformly (Q, u, P) - bounded at a point a* from L if for any positive real number k, there is a positive real number h such that for any hyperseminorms q and p with $(q, p) \in u$, and any element b from L, the inequality $q(a - b) < k$ implies the inequality $p(A(b) - A(a)) < h$.

b) An operator (mapping) $A : L \to M$ is called *u - uniformly (Q, u, P) - bounded* if it is uniformly (Q, u, P) - bounded at all points of L.

c) An operator (mapping) $A : L \to M$ is called u - *uniformly* (Q, u, P) - *bounded* in V if for any positive real number k, there is a positive real number h such that for any hyperseminorms q and p with $(q, p) \in u$, and any elements a and b from V, the inequality $q(a - b) < k$ implies the inequality $p(A(b) - A(a)) < h$.

d) An operator (mapping) $A : L \to M$ is called uV - *uniformly* (Q, u, P) - *bounded* in V if for any positive real number k, there is a positive real number h such that for any hyperseminorms q and p with $(q, p) \in u$, and any elements a from V and b from L, the inequality $q(a - b) < k$ implies the inequality $p(A(b) - A(a)) < h$.

Asking whether any (Q, u, P) - bounded at a point operator (mapping) is uniformly (Q, u, P) - bounded at the same point, we find that the answer is negative.

Example 3.4. Let us take $L = M = C(\mathbb{R}, \mathbb{R})$, while the space $C(\mathbb{R}, \mathbb{R})$ of all continuous real functions. It is possible (Burgin, 2012) for all real numbers x, to define seminorms $q_{ptx} = p_{ptx}$ by the following formula

$$q_{ptx}(f) = p_{ptx}(f) = |f(x)|.$$

We define $A(f) = xf(x)$ for all real functions f and $u = \{(q_{ptx}, p_{ptx}); x \in \mathbb{R}\}$. Taking the function $f(x) = x$ as the point a from L, we see that $A(f) = x^2$. Thus, taking some positive real number k, e.g., $k = 1$, the corresponding h from Definition 3.2 always exists but it grows with the growth of x. For instance, when $k = 1$, we have

$$q_{pt1}(f - g) < 1 \text{ implies } p_{pt1}(A(f) - A(g)) = p_{pt1}(xf - xg) < 1.$$

At the same time, $q_{pt10}(f - g) < 1$ does not imply $p_{pt10}(A(f) - A(g)) < 1$. It only implies $p_{pt10}(A(f) - A(g)) = p_{pt10}(xf - xg) < 10$. This means that for any pair (q_{ptx}, p_{ptx}) of seminorms and a number k, we need to find a specific number h to satisfy Definition 3.3 a. Consequently, the operator A is (Q, u, P) - bounded at f but it is not uniformly (Q, u, P) - bounded at f.

The same example shows that there are (Q, u, P) - bounded operators that are not uniformly (Q, u, P) - bounded.

It is also possible to ask whether Propositions 3.4 and 3.5 remain true for uniformly (Q, u, P) - bounded operators. In this case, the answer is positive.

Proposition 3.7. *If all q from the definability domain Du of the relation u are seminorms, then an operator (mapping) $A : L \to M$ is uniformly (Q, u, P) - bounded if and only if it is uniformly (Q, u, P) - bounded, at least, at one point.*

Indeed, Proposition 3.7 is a direct corollary of Proposition 3.5 because any uniformly (Q, u, P) - bounded at a point operator is (Q, u, P) - bounded at the same point and any uniformly (Q, u, P) - bounded operator is (Q, u, P) - bounded.

Proposition 3.7 implies the following result.

Corollary 3.13. *The concepts of uniformly (Q, u, P) - bounded at a point operators and uniformly (Q, u, P) - bounded operators coincide when all q from the definability domain Du of u are seminorms.*

Note that Examples 3.2 and 3.3 show this is not true for the general case of hyperseminorms.

Proposition 3.8. *If all q from the definability domain Du of u are seminorms and there is a uniformly (Q, u, P) - bounded operator (mapping) A of the linear space L onto the linear space M, then all p from the range $Rg\ u$ of u are finite hyperseminorms.*

Indeed, Proposition 3.8 is a direct corollary of Proposition 3.6 because any uniformly (Q, u, P) - bounded operator is (Q, u, P) - bounded.

Corollary 3.14. *If all q from the definability domain Du of u are seminorms and there is a uniformly (Q, u, P) - bounded operator (mapping) A of the linear space L onto the linear space M, and all values of all p from the range $Rg\ u$ are monotone hypernumbers, then all such p are seminorms.*

Definitions imply the following results.

Lemma 3.7. *a) Any uniformly (Q, u, P) - bounded at a point a operator A is (Q, u, P) - bounded at the point a.*

b) Any u-uniformly (Q, u, P) - bounded operator A is $((Q, u, P)$ - bounded.

Lemma 3.8. *Any u-uniformly (Q, u, P) - bounded in L operator is u-uniformly (Q, u, P) - bounded.*

At the same time, taking $L = M = \mathbb{R}$, $Q = \{q\}$, $P = \{p\}$, and assuming that hyperseminorms q and p are both equal to the absolute value and $u = \{(q, p)\}$, we see that Example 3.1 demonstrates that there are u-uniformly (Q, u, P) - bounded operators that are not uniformly (Q, u, P) - bounded because if Q has only one hyperseminorm q, P also has only one hyperseminorm p and u is a complete relation, then any (Q, u, P) - bounded operator is u-uniformly (Q, u, P) - bounded.

However, for linear operators, this is impossible as Proposition 3.1 allows us to prove the following result.

Proposition 3.9. *The following conditions are equivalent for a linear operator (mapping) A:*

(1) A is u-uniformly (Q, u, P) - bounded.

(2) A is u-uniformly (Q, u, P) - bounded in L.

(3) For some point a, A is uniformly (Q, u, P) - bounded at the point a.

Proof. Implications (2) $\Rightarrow$ (1) $\Rightarrow$ (3) directly follow from definitions. So, we need to prove only (3) $\Rightarrow$ (2), namely, if $A : L \to M$ is uniformly (Q, u, P) - bounded at a point a from L, then it is uniformly (Q, u, P) - bounded in L.

Let us consider another point b from L, take two hyperseminorms q and p with $(q, p) \in u$, and assume that $q(b - c) < k$ for some c from L. Then taking $d = c - (b - a)$, we have

$$q(a - d) = q(a - (c - (b - a))) = q(b - c) < k.$$

As A is uniformly (Q, u, P) - bounded at a, it is also (q, p) - bounded at a. Thus, there is a positive real number h such that $p(A(a) - A(d)) < h$. As A is linear operator, we have

$$p(A(b) - A(c)) = p(A(b - c)) = p(A(a - (c - (b - a)))) = p(A(a - d)) = p(A(a) - A(d)) < h.$$

This shows that A is (q, p) - bounded at the point b because c is an arbitrary point for which $q(b - c) < k$ and thus, A is u-uniformly (Q, u, P) - bounded because q and p are arbitrary hyperseminorms with $(q, p) \in u$. In addition, A is uniformly (q, p) - bounded in L because for a fixed number k, we have the same number h for all points in L.

Proposition is proved. □

Corollary 3.15. *A linear operator (mapping) $A : L \to M$ is u-uniformly (Q, u, P) - bounded if and only if it is uniformly (Q, u, P) - bounded at* $\mathbf{0}$.

Corollary 3.2 implies the following result.

Corollary 3.16. *Any u-uniformly (Q, u, P) - bounded linear operator (mapping) A is u-uniformly (Q, u, P) - bounded in L.*

These results show that for linear operators, different types of uniformly bounded operators coincide.

Proposition 3.10. *If the relation u is finite, then an operator (mapping) $A : L \to M$ is uniformly (Q, u, P) - bounded (at a point a) if and only if it is (Q, u, P) - bounded (at the point a).*

Proof. As any uniformly (Q, u, P) - bounded (at a point a) operator is (Q, u, P) - bounded (at the same point), we need only to show that when the relation u is finite, a (Q, u, P) - bounded (at a point a) operator $A : L \to M$ is uniformly (Q, u, P) - bounded (at the point a). At first, we consider local boundedness.

Indeed, by Definition 3.3, for any hyperseminorms q and p such that $(q, p) \in u$, the operator (mapping) A is (q, p)-bounded at the point a, that is, by Definition 3.1, the following condition is true:

Condition 1. For any positive real number k, there is a positive real number h such that for any element b from L, the inequality $q(a - b) < k$ implies the inequality $p(A(b) - A(a)) < h$.

This number h can be different for different pairs (q, p), but because u is finite, there is only a finite number of these pairs. So, we can take

$$l = max\{h; h \text{ satisfies Condition 1 for a pair } (q, p) \in u\}$$

and this number l will satisfy the condition from Definition 3.4. Thus, the operator A is uniformly (Q, u, P) - bounded at the point a.

The global case is proved in a similar way.

Proposition is proved. □

Corollary 3.17. *If systems of hyperseminorms Q and P are finite, then an operator (mapping) A is uniformly (Q, u, P) - bounded (at a point a) if and only if it is (Q, u, P) - bounded (at the point a).*

Now let us study different types of continuity in polyhyperseminormed vector spaces.

Definition 3.5. a) An operator (mapping) $A : L \to M$ is called (q, p) - *continuous at a point a* from L if for any positive real number k, there is a positive real number h such that for any element b from L, the inequality $q(a - b) < h$ implies the inequality $p(A(b) - A(a)) < k$.

b) An operator (mapping) $A : L \to M$ is called (q, p) - *continuous* if it is (q, p) - continuous at all points of L.

c) An operator (mapping) $A : L \to M$ is called *uniformly* (q, p) - *continuous in $V \subseteq L$* if for any positive real number k, there is a positive real number h such that for any elements a and b from V, the inequality $q(a - b) < h$ implies the inequality $p(A(b) - A(a)) < k$.

d) An operator (mapping) $A : L \to M$ is called V - *uniformly* (q, p) - *continuous* if for any positive real number k, there is a positive real number h such that for any element a from $V \subseteq L$ and any element b from L, the inequality $q(b - a) < h$ implies the inequality $p(A(b) - A(a)) < k$.

Note that when the set V contains only one point (say a), then V - *uniform* (q, p) - *continuity* coincides with (q, p) - continuity at the point a. Besides, to be L - *uniformly* (q, p) - *continuous* or to be *uniformly* (Q, u, P) - *continuous* in L means the same for all operators.

Definitions imply the following results.

Lemma 3.9. *For any $V \subseteq L$, any V - uniformly (q, p) - continuous operator is (q, p) - continuous in V.*

Lemma 3.10. *Any L - uniformly (q, p) - continuous operator is (q, p) - continuous.*

At the same time, as the following example demonstrates, there are (q, p) - continuous operators that are not L - uniformly (q, p) - continuous.

Example 3.5. Let us take $L = M = \mathbb{R}$ and assume that q and p are both equal to the absolute value, while $A(x) = x^2$. This mapping (operator) is (q, p) - continuous but not L - uniformly (q, p) - continuous.

However, for linear operators, the inverse of Lemma 3.9 is also true.

Proposition 3.11. *The following conditions are equivalent for a linear operator (mapping) A:*

(1) A is (q, p) - continuous.

(2) A is uniformly (q, p) - continuous in L.

(3) For some point a, A is uniformly (q, p) - continuous at the point a.

(4) A is L - uniformly (q, p) - continuous.

Proof. Implications (2) $\Rightarrow$ (1) $\Rightarrow$ (3) directly follow from definitions. So, we need to prove only (3) $\Rightarrow$ (2), namely, if $A : L \to M$ is (q, p) - continuous at a point a from L, then it is uniformly (q, p) - continuous in L.

Let us consider a positive real number k. Then because A is (q, p) - continuous at the point a, there is a positive real number h, such that the inequality $q(a - b) < h$ implies the inequality $p(A(b) - A(a)) < k$.

Let us take another point b from L and assume that $q(b-c) < h$ for some c from L. Then taking $d = c - (b - a)$, we have

$$q(a - d) = q(a - (c - (b - a))) = q(b - c) < h.$$

As A is (q, p) - continuous at a, we have $p(A(a) - A(d)) < k$. As A is linear operator, we have

$$p(A(b) - A(c)) = p(A(b - c)) = p(A(a - (c - (b - a)))) = p(A(a - d)) = p(A(a) - A(d)) < k.$$

This shows that A is (q, p) - continuous at the point b because c is an arbitrary point for which $q(b - c) < h$. Thus, A is uniformly (q, p) - continuous in L because for a fixed number k, we have the same number h for all points in L.

In addition, we see that by definition, properties (2) and (4) always coincide.

Proposition is proved. □

Corollary 3.18. *A linear operator (mapping) A is (q, p) - continuous if and only if it is (q, p) - continuous at* $\mathbf{0}$.

The above proof of Proposition 3.4 gives us the following result.

Corollary 3.19. *Any (q, p) - continuous linear operator (mapping) $A : L \to M$ is L - uniformly (q, p) - continuous.*

These results show that for linear operators, the concepts of (q, p) - continuous at a point operators and (q, p) - continuous operators coincide.

For operators that are not linear, these results are not true as the following examples demonstrate.

Example 3.6. Let us take $L = M = \mathbb{R}_\omega$ (cf. Example 2.1) and assume that q and p are both equal to the absolute value $\|\cdot\|$ of real hypernumbers. We define $A(x) = x$ for all real hypernumbers x but the hypernumber $\nu = Hn(i)_{i\in\omega}$ and put $A(\nu) = 1$. Then $\|\nu - (\nu + 1)\| = 1$ but $\|A(\nu) - A(\nu + 1)\| = \|1 - (\nu + 1)\| = \|\nu\| = \nu$ and this hypernumber is larger than any positive real number (Burgin, 2012). Thus, operator A is (q, p) - continuous at any real number but it is not (q, p) - continuous at ν.

This shows that an operator can be (q, p) - continuous at one point and not (q, p) - continuous at another point of L and thus not (q, p) - continuous in L, as well as not L - uniformly (q, p) - continuous.

Example 3.7. Let us take $L = M = C(\mathbb{R}, \mathbb{R})$, while the space $C(\mathbb{R}, \mathbb{R})$ of all continuous real functions is a hypernormed space (cf. Example 2.1) where the hypernorm $\| \cdot \|$ is defined by the following formula:

$$\text{If } f : \mathbb{R} \to \mathbb{R}, \text{ then } \|f\| = Hn(a_i)_{i\in\omega} \text{ where } a_i = max\{|f(x)|; a_i \in [-i, i]\}.$$

We define $A(f) = f$ for all real functions f but the function $v(x) = x^2$ and put $A(x^2) = e(x)$ where $e(x) = 1$ for all $x \in \mathbb{R}$. This operator A is (q, p) - continuous at any constant function from L, but it is not (q, p) - continuous at v. At the same time, taking $u(x) = x^2 + 1$, we have $\|v - u\| = 1$, while $\|A(v) - A(u)\| = \|e - u\| = Hn(i)_{i\in\omega}$ and this hypernumber is larger than any positive real number (Burgin, 2012).

This also shows that an operator can be (q, p) - continuous at one point and not (q, p) - continuous at another point of L and thus not (q, p) - continuous in L, as well as not L - uniformly (q, p) - continuous.

Definitions imply the following result.

Lemma 3.11. *If $W \subseteq V \subseteq L$, then any V - uniformly (q, p) - continuous operator is W - uniformly (q, p) - continuous.*

Now let us consider continuity with respect to a binary relation u between systems of hyperseminorms.

Definition 3.6. a) An operator (mapping) $A : L \to M$ is called (Q, u, P) - *continuous at a point* a from L if for any hyperseminorms q and p such that $(q, p) \in u$, the operator (mapping) A is (q, p) - continuous at the point a.

b) An operator (mapping) $A : L \to M$ is called (Q, u, P) - *continuous* if it is (Q, u, P) - continuous at all points of L.

c) An operator (mapping) $A : L \to M$ is called *uniformly* (Q, u, P) - *continuous in* $V \subseteq L$ if for any hyperseminorms q and p such that $(q, p) \in u$ and any positive real number k, there is a positive real number h such that for any elements a and b from V, the inequality $q(a - b) < h$ implies the inequality $p(A(b) - A(a)) < k$.

d) An operator (mapping) $A : L \to M$ is called V - *uniformly* (Q, u, P) - *continuous* if for any hyperseminorms q and p such that $(q, p) \in u$ and for any positive real number k, there is a positive real number h such that for any element a from $V \subseteq L$ and any element b from L, the inequality $q(b - a) < h$ implies the inequality $p(A(b) - A(a)) < k$.

Note that to be L - *uniformly* (Q, u, P) - *continuous* or to be *uniformly* (Q, u, P) - *continuous in* L means the same for all operators.

Lemma 3.10 implies the following result.

Lemma 3.12. *Any uniformly (Q, u, P) - continuous in L operator is (Q, u, P) - continuous.*

At the same time, taking $L = M = \mathbb{R}$, $Q = \{q\}$, $P = \{p\}$, and assuming that q and p are both equal to the absolute value and $u = \{(q, p)\}$, we see that Example 3.5 demonstrates that there are (Q, u, P) - continuous operators that are not L - uniformly (Q, u, P) - continuous.

However, for linear operators, the inverse of Lemma 3.12 is also true as Proposition 3.11 implies the following result.

Proposition 3.12. *The following conditions are equivalent for a linear operator (mapping) A:*

(1) A is (Q, u, P) - continuous.

(2) A is uniformly (Q, u, P) - continuous in L.

(3) For some point a, A is uniformly (Q, u, P) - continuous at the point a.

(4) A is L - uniformly (Q, u, P) - continuous.

Corollary 3.20. *A linear operator (mapping) A is (Q, u, P) - continuous if and only if it is (Q, u, P) - bounded at* $\mathbf{0}$.

Corollary 3.19 implies the following result.

Corollary 3.21. *Any (Q, u, P) - continuous linear operator (mapping) $A : L \to M$ is L - uniformly (Q, u, P) - continuous.*

These results show that for linear operators, the concepts of (Q, u, P) - continuous at a point operators and (Q, u, P) - continuous operators coincide.

At the same time, taking $L = M = \mathbb{R}_\omega$, $Q = \{q\}$, $P = \{p\}$, and assuming that q and p are both equal to the absolute value of real hypernumbers and $u = \{(q, p)\}$, we see that Example 3.6 demonstrates that there are operators that are (Q, u, P) - continuous at one point and not (Q, u, P) - continuous at another point. A similar situation is also presented in Example 3.7.

Definitions and Lemma 3.10 imply the following result.

Lemma 3.13. *If $W \subseteq V \subseteq L$, then any V - uniformly (Q, u, P) - continuous operator is W - uniformly (Q, u, P) - continuous.*

Lemma 3.9 imply the following result.

Lemma 3.14. *For any $V \subseteq L$, any V - uniformly (Q, u, P) - continuous operator is (Q, u, P) - continuous in V.*

Let us study relations between relative continuity and relative boundedness.

Theorem 3.1. *A linear operator (mapping) $A : L \to M$ is (Q, u, P) - continuous if and only if it is (Q, u, P) - bounded.*

Proof. Sufficiency. Let us consider a (Q, u, P) - bounded linear operator (mapping) $A : L \to M$ and suppose that A is not (Q, u, P) - continuous. It means that for some pair $(q, p) \in u$ of hyperseminorms q and p, the operator A is not (q, p) - continuous. By Corollary 3.9, A is not (q, p) - continuous at $\mathbf{0}$. Consequently, there is a positive real number k such that for any natural number n, there is an element x_n from L for which $q(x_n) < 1/n$ while $p(A(x_n)) > k$.

Let us consider the set $Z = \{z_n; n = 1, 2, 3, \ldots\}$ where $z_n = n \cdot x_n$ for all $n = 1, 2, 3, \ldots$ Then

$$q(z_n) = q(n \cdot x_n) = n \cdot q(x_n) < 1,$$

i.e., Z is a q - bounded set. At the same time, as A is a linear operator, we have

$$p(A(z_n)) = p(A(n \cdot x_n)) = n \cdot p(A(x_n)) > kn.$$

Thus, the image of Z is not a p - bounded set and A is not a (Q, u, P) - bounded operator. This contradicts our assumption and by *reductio ad absurdum*, A is (Q, u, P) - continuous.

Necessity. Let us consider a (Q, u, P) - continuous linear operator (mapping) $A : L \to M$ and suppose that A is not (Q, u, P) - bounded. It means that for some pair $(q, p) \in u$ of hyperseminorms q and p, the operator A is not (q, p) - bounded. By Corollary 3.3, A is not (q, p) - bounded at $\mathbf{0}$. Consequently, there is a positive real number k such that for any natural number n, there is an element x_n from L for which $q(x_n) < k$ while $p(A(x_n)) > n$.

Let us consider the set $Z = \{z_n; n = 1, 2, 3, \ldots\}$ where $z_n = (1/n) \cdot x_n$ for all $n = 1, 2, 3, \ldots$ Then

$$q(z_n) = q((1/n) \cdot x_n) = (1/n) \cdot q(x_n) < k/n.$$

It means that the sequence $\{z_n; n = 1, 2, 3, \ldots\}$ q - converges to $\mathbf{0}$.

At the same time, as A is a linear operator, we have

$$p(A(z_n)) = p(A((1/n) \cdot x_n)) = (1/n) \cdot p(A(x_n)) > k.$$

It means that the sequence $\{A(z_n); n = 1, 2, 3, \ldots\}$ does not p - converge to $\mathbf{0}$. This violates conditions from Definition 3.5 and shows A is not a (Q, u, P) - continuous operator. Thus, we have a contradiction with our assumption that A is a (Q, u, P) - continuous operator. By *reductio ad absurdum*, A is (Q, u, P) - bounded.

Theorem is proved. □

Corollary 3.22. *A linear operator (mapping) $A : L \to M$ is (q, p) - continuous if and only if it is (q, p) - bounded.*

Corollary 3.22 implies the following result.

Corollary 3.23. *A linear operator (mapping) $A : L \to M$ is L - uniformly (Q, u, P) - continuous if and only if it is L - uniformly (Q, u, P) - bounded.*

As topology of topological vector spaces is determined by system of seminorms (Rudin, 1991), Theorem 3.1 gives us the following classical result ((Dunford & Schwartz, 1958); (Rudin, 1991)).

Corollary 3.24. *A linear mapping A of a topological vector space L into a topological vector space M is continuous if and only if it is bounded.*

As for linear operators (mappings) continuity at a point coincides with continuity and boundedness at a point coincides with boundedness, we have the following results.

Corollary 3.25. *A linear operator (mapping) $A : L \to M$ is (q, p) - continuous at a point a if and only if it is (q, p) - bounded at a.*

Corollary 3.26. *A linear operator (mapping) $A : L \to M$ is (Q, u, P) - continuous at a point a if and only if it is (Q, u, P) - bounded at a.*

Let us take a vector subspace V of L and consider uniform (Q, u, P) - continuity in V.

Theorem 3.2. *A linear operator (mapping) $A : L \to M$ is uniformly (Q, u, P) - continuous in V if and only if it is uniformly (Q, u, P) - bounded in V.*

Proof. Sufficiency. Let us consider a vector subspace V of L and a uniformly (Q, u, P) - bounded in V linear operator (mapping) $A : L \to M$ and suppose that A is not uniformly (Q, u, P) - continuous in V. It means that for some pair $(q, p) \in u$ of hyperseminorms q and p, the operator A is not uniformly (q, p) - continuous. Consequently, there is a positive real number k such that for any natural number n, there are elements x_n and y_n from V for which $q(x_n - y_n) < 1/n$ while $p(A(x_n) - A(y_n)) > k$.

Let us consider two sets $Z = \{z_n;\ n = 1, 2, 3, \ldots\}$ and $U = \{u_n;\ n = 1, 2, 3, \ldots\}$ where $z_n = n \cdot x_n$ and $u_n = n \cdot y_n$ for all $n = 1, 2, 3, \ldots$ As V is a vector subspace of L, then Z and U are subsets of V. Besides,

$$q(z_n - u_n) = q(n \cdot x_n - n \cdot y_n) = q(n \cdot (x_n - y_n)) = n \cdot q(x_n - y_n) < 1.$$

It means that the set $\{z_n - u_n;\ n = 1, 2, 3, \ldots\}$ is q - bounded.

At the same time, as A is a linear operator, we have

$$p(A(z_n - u_n)) = p(A(n \cdot x_n - n \cdot y_n)) = n \cdot p(A(x_n) - A(y_n)) > kn.$$

It means that the set $\{A(z_n - u_n);\ n = 1, 2, 3, \ldots\}$ is not p - bounded. Thus, A is not a uniformly (Q, u, P) - bounded in V operator. This contradicts our assumption and by *reductio ad absurdum*, A is uniformly (Q, u, P) - continuous in V.

Necessity. Let us consider a uniformly (Q, u, P) - continuous in V linear operator (mapping) $A : L \to M$ and suppose that A is not uniformly (Q, u, P) - bounded in V. It means that for some pair $(q, p) \in u$ of hyperseminorms q and p, the operator A is not uniformly (q, p) - bounded in V. By Corollary 3.3, A is not (q, p) - bounded in V at $\mathbf{0}$ as V is a vector subspace of L. Consequently, there is a positive real number k such that for any natural number n, there is an element x_n from V for which $q(x_n) < k$ while $p(A(x_n)) > n$.

Let us consider the set $Z = \{z_n;\ n = 1, 2, 3, \ldots\}$ where $z_n = (1/n) \cdot x_n$ for all $n = 1, 2, 3, \ldots$ Then

$$q(z_n) = q((1/n) \cdot x_n) = (1/n) \cdot q(x_n) < k/n.$$

It means that the sequence $\{z_n;\ n = 1, 2, 3, \ldots\}$ q - converges to $\mathbf{0}$.

At the same time, as A is a linear operator, we have

$$p(A(z_n)) = p(A((1/n) \cdot x_n)) = (1/n) \cdot p(A(x_n)) > k.$$

It means that the sequence $\{A(z_n);\ n = 1, 2, 3, \ldots\}$ does not p - converge to $\mathbf{0}$. This violates conditions from Definition 3.5 and shows A is not a uniformly (Q, u, P) - continuous in V operator. Thus, we have a contradiction with our assumption that A is a uniformly (Q, u, P) - continuous in V operator. By *reductio ad absurdum*, A is uniformly (Q, u, P) - bounded in V.

Theorem is proved. □

Corollary 3.27. *For any vector subspace V of L, a linear operator (mapping) $A : L \to M$ is uniformly (q, p) - continuous in V if and only if it is uniformly (q, p) - bounded in V.*

As before, V is a vector subspace of L and we study V - uniform (Q, u, P) - continuity.

Theorem 3.3. *A linear operator (mapping) $A : L \to M$ is V - uniformly (Q, u, P) - continuous if and only if it is V - uniformly (Q, u, P) - bounded.*

Proof. Sufficiency. Let us consider a vector subspace V of L and a V - uniformly (Q, u, P) - bounded linear operator (mapping) $A : L \to M$ and suppose that A is not V - uniformly (Q, u, P) - continuous. It means that for some pair $(q, p) \in u$ of hyperseminorms q and p, the operator A is not V - uniformly (q, p) - continuous. Consequently, there is a positive real number k such that for any natural number n, there are elements x_n from V and y_n from L for which $q(x_n - y_n) < 1/n$ while $p(A(x_n) - A(y_n)) > k$.

Let us consider two sets $Z = \{z_n;\ n = 1, 2, 3, \ldots\}$ and $U = \{u_n;\ n = 1, 2, 3, \ldots\}$ where $z_n = n \cdot x_n$ and $u_n = n \cdot y_n$ for all $n = 1, 2, 3, \ldots$ As V is a vector subspace of L, then Z is a subset of V. Besides,

$$q(z_n - u_n) = q(n \cdot x_n - n \cdot y_n) = q(n \cdot (x_n - y_n)) = n \cdot q(x_n - y_n) < 1.$$

It means that the set $\{z_n - u_n;\ n = 1, 2, 3, \ldots\}$ is q - bounded.

At the same time, as A is a linear operator, we have

$$p(A(z_n - u_n)) = p(A(n \cdot x_n - n \cdot y_n)) = n \cdot p(A(x_n) - A(y_n)) > kn.$$

It means that the set $\{A(z_n - u_n);\ n = 1, 2, 3, \ldots\}$ is not p - bounded. Thus, A is not a V - uniformly (Q, u, P) - bounded operator. This contradicts our assumption and by *reductio ad absurdum*, A is V - uniformly (Q, u, P) - continuous.

Necessity. Let us consider a V - uniformly (Q, u, P) - continuous linear operator (mapping) $A : L \to M$ and suppose that A is not V - uniformly (Q, u, P) - bounded. It means that for some pair $(q, p) \in u$ of hyperseminorms q and p, the operator A is not V - uniformly (q, p) - bounded. By Corollary 3.3, A is not (q, p) - bounded at $\mathbf{0}$. Consequently, there is a positive real number k such that for any natural number n, there is an element x_n from L for which $q(x_n) < k$ while $p(A(x_n)) > n$.

Let us consider the set $Z = \{z_n;\ n = 1, 2, 3, \ldots\}$ where $z_n = (1/n) \cdot x_n$ for all $n = 1, 2, 3, \ldots$ Then

$$q(z_n) = q((1/n) \cdot x_n) = (1/n) \cdot q(x_n) < k/n.$$

It means that the sequence $\{z_n;\ n = 1, 2, 3, \ldots\}$ q - converges to $\mathbf{0}$.

At the same time, as A is a linear operator, we have

$$p(A(z_n)) = p(A((1/n) \cdot x_n)) = (1/n) \cdot p(A(x_n)) > k.$$

It means that the sequence $\{A(z_n);\ n = 1, 2, 3, \ldots\}$ does not p - converge to $\mathbf{0}$. This violates conditions from Definition 3.6 and shows A is not a V - uniformly (Q, u, P) - continuous operator. Thus, we have a contradiction with our assumption that A is a V - uniformly (Q, u, P) - continuous operator. By *reductio ad absurdum*, A is V - uniformly (Q, u, P) - bounded.

Theorem is proved. □

Corollary 3.28. *For any subset V of L, a linear operator (mapping) $A : L \to M$ is V - uniformly (q, p) - continuous if and only if it is V - uniformly (q, p) - bounded.*

Let us take a subset V of the space L.

Definition 3.7. a) An operator (mapping) $A : L \to M$ is called uniformly (Q, u, P) - *continuous at a point a* from L if for any positive real number k, there is a positive real number h such that for any hyperseminorms q and p with $(q, p) \in u$, for any element b from L, the inequality $q(a - b) < h$ implies the inequality $p(A(b) - A(a)) < k$.

b) An operator (mapping) $A : L \to M$ is called u - *uniformly* (Q, u, P) - *continuous* if it is uniformly (Q, u, P) - continuous at all points of L.

c) An operator (mapping) $A : L \to M$ is called u - *uniformly* (Q, u, P) - *continuous in V* if for any positive real number k, there is a positive real number h such that for any elements a and b from V and any hyperseminorms q and p with $(q, p) \in u$, the inequality $q(a - b) < h$ implies the inequality $p(A(b) - A(a)) < k$.

d) An operator (mapping) $A : L \to M$ is called uV - *uniformly* (Q, u, P) - *continuous* if for any positive real number k, there is a positive real number h such that for any elements a from V and b from L, and any hyperseminorms q and p with $(q, p) \in u$, the inequality $q(a - b) < h$ implies the inequality $p(A(b) - A(a)) < k$.

Note that to be uL - *uniformly* (Q, u, P) - *continuous* or to be u - *uniformly* (Q, u, P) - *continuous in L* means the same for all operators.

It it possible to ask a question how u - uniform (Q, u, P) - continuity is connected to (Q, u, P) - continuity. The following example and Lemma 3.5 clarify this situation.

Example 3.8. Let us take $L = M = C(\mathbb{R}, \mathbb{R})$, while the space $C(\mathbb{R}, \mathbb{R})$ of all continuous real functions. It is possible (Burgin, 2012) for all real numbers x, to define seminorms $q_{ptx} = p_{ptx}$ by the following formula

$$q_{ptx}(f) = p_{ptx}(f) = |f(x)|.$$

We define $A(f) = xf(x)$ for all real functions f and $u = \{(q_{ptx}, p_{ptx});\ x \in \mathbb{R}\}$. Taking the function $f(x) = x$ as the point a from L, we see that $A(f) = x^2$. Thus, taking some positive real

number k, e.g., $k = 1$, the corresponding h from Definition 3.2 always exists but it decreases with the growth of x. For instance, when $k = 1$, we have

$$q_{pt1}(f - g) < 1 \text{ implies } p_{pt1}(A(f) - A(g)) = p_{pt1}(xf - xg) < 1.$$

At the same time, $q_{pt10}(f - g) < 1$ does not imply $p_{pt10}(A(f) - A(g)) < 1$. It only implies $p_{pt10}(A(f)-A(g)) = p_{pt10}(xf-xg) < 10$. To have $p_{pt10}(A(f)-A(g)) < 1$, we need $q_{pt10}(f-g) < 0.1$.

It means that for any pair (q_{ptx}, p_{ptx}) of seminorms and a number k, we need to find a specific number h to satisfy Definition 3.7.a. Consequently, the operator A is (Q, u, P) - continuous at $f = x$ but it is not uniformly (Q, u, P) - continuous at f.

The same example shows that there are (Q, u, P) - continuous operators that are not u - uniformly (Q, u, P) - continuous.

Definitions imply the following result.

Lemma 3.15. *a) Any uniformly (Q, u, P) - continuous at a point a operator A is (Q, u, P) - continuous at the point a.*

b) Any u - uniformly (Q, u, P) - continuous operator A is (Q, u, P) - continuous.

Lemma 3.16. *Any u - uniformly (Q, u, P) - continuous in L operator is u - uniformly (Q, u, P) - continuous.*

For linear operators, the inverse of Lemma 3.15 is also true.

Proposition 3.13. *The following conditions are equivalent for a linear operator (mapping) A:*

(1) A is u - uniformly (Q, u, P) - continuous.

(2) A is u - uniformly (Q, u, P) - continuous in L.

(3) For some point a, A is uniformly (Q, u, P) - continuous at the point a.

(4) A is uL - uniformly (Q, u, P) - continuous.

Corollary 3.29. *A linear operator (mapping) A is u - uniformly (Q, u, P) - continuous in L if and only if it is (Q, u, P) - continuous at $\mathbf{0}$.*

Corollary 3.20 implies the following result.

Corollary 3.30. *Any u - uniformly (Q, u, P) - continuous linear operator (mapping) $A : L \to M$ is u - uniformly (Q, u, P) - continuous in L.*

These results show that for linear operators, the concepts of uniformly (Q, u, P) - continuous at a point operators and u - uniformly (Q, u, P) - continuous operators coincide.

At the same time, taking $L = M = \mathbb{R}_\omega$, $Q = \{q\}$, $P = \{p\}$, and assuming that q and p are both equal to the absolute value of real hypernumbers and $u = \{(q, p)\}$, we see that Example 3.6 demonstrates that there are operators that are (Q, u, P) - continuous at one point and not (Q, u, P) - continuous at another point. A similar situation is also presented in Example 3.7.

Definitions and Lemma 3.9 imply the following result.

Lemma 3.17. *If $W \subseteq V \subseteq L$, then any u - uniformly (Q, u, P) - continuous in V operator is u - uniformly (Q, u, P) - continuous in W.*

For finite relations u, different concepts of uniform continuity coincide.

Proposition 3.14. *If the relation u is finite, then, an operator (mapping) $A : L \to M$ is u - uniformly (Q, u, P) - continuous (u - uniformly (Q, u, P) - continuous at a point a) if and only if it is (Q, u, P) - continuous ((Q, u, P) - continuous at a point a).*

Proof. As any u - uniformly (Q, u, P) - continuous (u - uniformly (Q, u, P) - continuous at a point a) operator is (Q, u, P) - continuous ((Q, u, P) - continuous at the same point), we need only to show that when the relation u is finite, a (Q, u, P) - continuous (at a point a) operator $A : L \to M$ is uniformly (Q, u, P) - continuous (at the point a). At first, we consider local boundedness.

Indeed, by Definition 3.6, for any hyperseminorms q and p such that $(q, p) \in u$, the operator (mapping) A is (q, p) - continuous at the point a, that is, by Definition 3.4, the following condition is true:

Condition 2. For any positive real number k, there is a positive real number h such that for any element b from L, the inequality $q(a - b) < h$ implies the inequality $p(A(b) - A(a)) < k$.

This number h can be different for different pairs (q, p), but because u is finite, there is only a finite number of these pairs. So, we can take

$$l = min\{h : h \text{ satisfies Condition 2 for a pair } (q, p) \in u\},$$

and this number l will satisfy the condition from Definition 3.7 Thus, the operator A is u - uniformly (Q, u, P) - continuous at the point a.

The global case is proved in a similar way.

Proposition is proved. □

Corollary 3.31. *If systems of hyperseminorms Q and P are finite, then an operator (mapping) A is uniformly (Q, u, P) - continuous if and only if it is (Q, u, P) - continuous.*

There are connections between uniform with respect to systems of hyperseminorms continuity and uniform boundedness that are similar to the connections between nonuniform with respect to systems of hyperseminorms continuity and nonuniform boundedness described in Theorems 3.1 - 3.3. Namely, we have the following results.

Theorem 3.4. *A linear operator (mapping) $A : L \to M$ is uniformly (Q, u, P) - continuous at a point a if and only if it is uniformly (Q, u, P) - bounded at a.*

Proof is similar to the proof of Theorem 3.1.

Let us take a vector subspace V of the space L.

Theorem 3.5. *A linear operator (mapping) $A : L \to M$ is u - uniformly (Q, u, P) - continuous in V if and only if it is u - uniformly (Q, u, P) - bounded in V.*

Proof is similar to the proof of Theorem 3.2.

Theorem 3.6. *A linear operator (mapping) $A : L \to M$ is uV - uniformly (Q, u, P) - continuous if and only if it is uV - uniformly (Q, u, P) - bounded.*

Proof is similar to the proof of Theorem 3.3.

4. Conclusion

Semitopological vector spaces are introduced and studied. Semitopological vector spaces are more general than conventional topological vector spaces, which have been very useful for solving many problems in functional analysis. Thus, we come to the following problems.

Problem 1. Study topology in semitopological vector spaces.

Problem 2. Study applications of semitopological vector spaces.

In addition, hypernorms and hyperseminorms are introduced and studied. In this paper, it is demonstrated that hyperseminormed and hypernormed spaces are semitopological vector spaces.

These results bring us to the following problems.

Problem 3. Study what kinds of topology it is possible to define with systems of seminorms, hypernorms or hyperseminorms.

It is proved (cf. (Rudin, 1991)) that systems of seminorms characterize locally convex spaces and thus, there are topological vector spaces topology in which is not defined by systems of seminorms. It is possible to ask if the same is true for semitopological vector spaces. Namely, we have the following problem.

Problem 4. Is the topology in a semitopological vector space always defined by a system of seminorms?

In this paper, hypermetrics and hyperpseudometrics are also introduced and it is demonstrated that hyperseminorms induce hyperpseudometrics, while hypernorms induce hypermetrics. Sufficient and necessary conditions for a hyperpseudometric (hypermetric) to be induced by a hyperseminorm (hypernorm) are found. Hyperpseudometrics and hypermetrics define definite topologies in vector spaces.

Problem 5. Study what kinds of topology it is possible to define with hyperpseudometrics and hypermetrics.

In this paper, boundedness and continuity are defined relative to systems of hyperseminorms or hypernorms. Inclusion of hyperseminorm sets is reflected in the strength of corresponding topologies, namely, the larger is the set Q of hyperseminorms (hypernorms), the weaker topology it defines. In such a way, we obtain a definite scalability of spaces ((Burgin, 2004); (Burgin, 2006)) with systems of hyperseminorms (hypernorms), coming to the following problem.

Problem 6. Study scalability of topological spaces defined by systems of hyperseminorms and hypernorms.

Topological vector spaces provide an efficient context for the development of integration (Choquet, 1969); (Edwards & Wayment, 1970); (Shuchat, 1972); (Kurzweil, 2000).

Problem 7. Study integration in semitopological (polyhyperseminormed) vector spaces.

At the same time, integration and hyperintegration in bundles with a hyperspace base are defined and studied in (Burgin, 2010) where the hyperspace is built by means of seminorms. The goal of this paper is to provide a base for developing the theory of extrafunction spaces in an abstract setting of algebraic systems and topological spaces, where integration plays an important role (Burgin, 2012). So, we naturally come to the following problem.

Problem 8. Study integration and hyperintegration in bundles with a hyperspace base where the hyperspace is built by means of hyperseminorms.

It is possible to define norms and seminorms with values not only in number or hypernumber spaces but in more general spaces, e.g., operator spaces.

Problem 9. Study vector spaces that have norms or/and seminorms with values in general spaces.

Problem 10. Study continuity of non-linear operators in (mappings of) polyhyperseminormed (semitopological) vector spaces.

Here we have proved (Theorem 2.3) that any hyperseminormed vector space is a semitopological vector space. It would be interesting to find if a more general statement is also true.

Problem 11. Is any polyhyperseminormed vector space a semitopological vector space?

Thus, the theory of semitopological vector spaces opens many new opportunities for research in mathematics.

References

Alexandroff, P. (1961). *Elementary Concepts of Topology*. Dover Publications, New York.

Bourbaki, N. (1953-1955). *Espaces Vectoriels Topologiques*. Hermann, Paris.

Burgin, M. (2002). Theory of hypernumbers and extrafunctions: Functional spaces and differentiation. *Discrete Dynamics in Nature and Society* **7**, 201–212.

Burgin, M. (2004). Discontinuity structures in topological spaces. *International Journal of Pure and Applied Mathematics* **16**(4), 485–513.

Burgin, M. (2006). Scalable topological spaces. In: 5^{th} *Annual International Conference on Statistics, Mathematics and Related Fields, 2006 Conference Proceedings, Honolulu, Hawaii*. pp. 1865–1896.

Burgin, M. (2010). Integration in bundles with a hyperspace base: Indefinite integration. *Integration* **2**(4), 39–79.

Burgin, M. (2011). Differentiation in bundles with a hyperspace base. *Preprint in Mathematics, math.CA/1112.3421, 27 p.*

Burgin, M. (2012). *Hypernumbers and Extrafunctions: Extending the Classical Calculus*. Springer, New York.

Choquet, G. (1969). *Lectures on Analysis*. W.A. Benjamin, Inc., New York/Amsterdam.

Dosi, A. (2011). Local operator algebras, fractional positivity and the quantum moment problem. *Transactions of the American Mathematical Society* **363**(2), 801–856.

Dunford, N. and J. Schwartz (1958). *Linear Operators*. Interscience Publishers, New York.

Edwards, J. R. and S. G. Wayment (1970). A v-integral representation for linear operators on spaces of continuous functions with values in topological vector spaces. *Pacific J. Math.* **35**(2), 327–330.

Ehresmann, Ch. (1952). Introduction à la théorie des structures infinitésimales et des pseudogroupes de lie. *Colloque de Topologie et Géométrie Différentielle, Strasbourg* (11), 327–330.

Ehresmann, Ch. (1953). *Introduction à la théorie des structures infinitésimales et des pseudogroupes de Lie*. Géométrie Différentielle, Colloques Internationaux du Centre National de la Recherche Scientifique, Centre National de la Recherche Scientifique, Paris.

Gromov, M. (1986). *Partial differential relations*. Springer-Verlag, Berlin.

Grothendieck, A. (1992). *Topological Vector Spaces*. Gordon and Breach, New York.

Helemski, A. Ya. (1989). *The Homology of Banach and Topological Algebras*. Kluwer Academic Publishers, Dordrecht.

Kelly, J.L. (1955). *General Topology*. Van Nostrand Co., Princeton/New York.

Kolmogorov, A.N. and S.V. Fomin (1999). *Elements of the Theory of Functions and Functional Analysis*. Dover Publications, New York.

Krasilshchik, S., V. V. Lychagin and A. M. Vinogradov (1986). *Geometry of jet spaces and nonlinear partial differential equations*. Gordon and Breach, New York.

Kuratowski, K. (1966). *Topology*. Vol. 1. Academic Press, Warszawa.

Kurzweil, J. (2000). *Henstock-Kurzweil Integration: Its Relation to Topological Vector Spaces*. World Scientific Pub Co.

Pietsch, A. (1965). *Nukleare Lokalkonvexe Räume*. Akademie-Verlag, Berlin.

Riez, F. and B. Sz.-Nagy (1955). *Functional Analysis*. Frederik Ungar P.C., New York.

Robertson, A. P. and W. Robertson (1964). *Topological Vector Spaces*. Cambridge University Press, New York.

Rudin, W. (1991). *Functional Analysis*. McGrow-Hill, New York.

Shuchat, A.H. (1972). Integral representation theorems in topological vector spaces. *Trans. Amer. Math. Soc.* **172**, 373–397.

Theory and Applications of Mathematics & Computer Science

(ISSN 2067-2764, EISSN 2247-6202)
http://www.uav.ro/applications/se/journal/index.php/tamcs

Theory and Applications of Mathematics & Computer Science 3 (1) (2013) 90–98

On Ideal Convergent Difference Double Sequence Spaces in n-Normed Spaces Defined by Orlicz Function

Vakeel A. Khan[a,*], Sabiha Tabassum[a]

[a]*Department of Mathematics A.M.U. Aligarh-202002, India*

Abstract

The main aim of this paper is to define the generalized difference double sequence spaces ${}_2W^I(M, \|.,...,.\|, \Delta_m^n, p)$, ${}_2W_0^I(M, \|.,...,.\|, \Delta_m^n, p)$ and ${}_2W_\infty^I(M, \|.,...,.\|, \Delta_m^n, p)$ defined over a n-normed space $(X, \|.,...,.\|)$. Here we also study their properties and establish some inclusion relations.

Keywords: Double sequence spaces, n-norm, Orlicz Function, difference sequence spaces, I convergence.
2010 MSC: 46E30, 46E40, 46B20.

1. Introduction

The notion of ideal convergence was introduced first by Kostyrko et-al- (Kostyrko *et al.*, 2000) as an interesting generalization of statistical convergence (Khan & Tabassum, 2012) which was further studied in topological spaces. A family $I \subset 2^Y$ of subsets of a nonempty set Y is said to be an ideal in Y if

1. $\emptyset \in I$;
2. $A, B \in I$ imply $A \cup B \in I$;
3. $A \in I, B \subset A$ imply $B \in I$,

while an admissible ideal I further satisfies $\{x\} \in I$ for each $x \in Y$ (Kostyrko *et al.*, 2000, 2005; Savas, 2010).
Given $I \subset 2^{\mathbb{N}}$ be a nontrivial ideal in $\mathbb{N}$. Let X be a normed space. The sequence (x_j) in X is said to be $I-$*convergent* to $\xi \in X$, if for each $\varepsilon > 0$ the set $A(\varepsilon) = \{j \in \mathbb{N} : \|x_j - \xi\| \geq \varepsilon\}$ belongs to I (Khan & Tabassum, 2010).

*Corresponding author
Email addresses: vakhanmaths@gmail.com (Vakeel A. Khan), sabihatabassum@math.com (Sabiha Tabassum)

The concept of 2-normed spaces was initially introduced by G̈ahler (Gähler, 1963) in the mid of 1960's as an interesting nonlinear generalization of a normed linear space. Since then, many researchers have studied this concept and obtained various results, see for instance (Gunawan & Mashadi, 2001; Khan & Tabassum, 2010; Savas, 2010).

Recall (Khan & Tabassum, 2012) that an *Orlicz Function* is a function $M : [0, \infty) \to [0, \infty)$ which is continuous, nondecreasing and convex with $M(0) = 0$, $M(x) > 0$ for $x > 0$ and $M(x) \to \infty$, as $x \to \infty$. If convexity of M is replaced by $M(x+y) \leq M(x)+M(y)$, then it is called a *Modulus funtion* (Maddox, 1986).

Let w be the space of all sequences. Lindenstrauss and Tzafriri (Lindenstrauss & Tzafiri, 1971) used the idea of Orlicz sequence space. Let

$$l_M := \left\{x \in w : \sum_{k=1}^{\infty} M\left(\frac{|x_k|}{\rho}\right) < \infty, \text{ for some } \rho > 0\right\}$$

is Banach space with respect to the norm

$$\|x\|_M := \inf\left\{\rho > 0 : \sum_{k=1}^{\infty} M\left(\frac{|x_k|}{\rho}\right) \leq 1\right\}.$$

Orlicz function has been studied by V. A. Khan (Khan, 2008*a*,*b*) and many others.

Let $n \in \mathbb{N}$ and X be a real vector space of dimension d, where $n \leq d$. An n-norm on X is a function $\|., ..., .\| : X \times X \times ... \times X \to \mathbb{R}$ which satisfies the following four conditions:

1. $\|x_1, x_2, ..., x_n\| = 0$ if and only if $x_1, x_2, ..., x_n$ are linearly dependent,
2. $\|x_1, x_2, ..., x_n\|$ is invariant under permutation,
3. $\|\alpha x_1, x_2, ..., x_n\| = |\alpha|\|x_1, x_2, ..., x_n\|$, for any $\alpha \in \mathbb{R}$,
4. $\|x + x', x_2, ..., x_n\| \leq \|x, x_2, ..., x_n\| + \|x', x_2, ..., x_n\|$.

The pair $(X, \|., ., ..., .\|)$ is called an n-normed space (Savas, 2011).

Example 1.1. (see (Savas, 2011)). As a standard example of a n-normed space we may take R^n being equipped with the n-norm $\|x_1, x_2, ..., x_n\|_E$ = the volume of the n-dimensional parallelopiped spaned by the vectors $x_1, x_2, ..., x_{n-1}, x_n$ which may be given explicitly by the formula

$$\|x_1, x_2, ..., x_n\|_E = \begin{vmatrix} \langle x_1, x_2\rangle & ... & \langle x_1, x_n.\rangle \\ . & ... & \\ . & ... & \\ \langle x_n, x_1\rangle & ... & \langle x_n, x_n\rangle \end{vmatrix}.$$

where $\langle ., .\rangle$ denotes inner product.

Example 1.2. (see (Savas, 2011)). Let $(X, \|., ., ..., .\|)$ be an n-normed space of dimension $d \geq n \geq 2$ and $\{a_1, a_2, ..., a_n\}$ be a linearly independent set in X. Then the following function $\|., ., ..., .\|_\infty$ defined by

$$\|x_1, x_2, ..., x_{n-1}, x_n\|_\infty = \max\{\|x_1, x_2, ..., x_{n-1}, a_i\| : i = 1, 2, ..., n\}$$

defines an $(n-1)$−norm on X with respect to $\{a_1, a_2, ..., a_n\}$.

Definition 1.1. (see (Savas, 2011)). A sequence (x_j) in an n-normed space $(X, \|., ., ..., .\|)$ is said to be converge to some $L \in X$ in the n-norm if

$$\lim_{j\to\infty} \|x_j - L, x_1, ..., x_{n-1}\| = 0, \quad \text{for every } x_1, ..., x_{n-1} \in X.$$

Example 1.3. (see (Khan & Tabassum, 2010)). A sequence (x_j) in an n-normed space $(X, \|., ., ..., .\|)$ is said to be Cauchy with respect to the n-norm if

$$\lim_{j,k\to\infty} \|x_j - x_k, x_1, ..., x_{n-1}\| = 0, \quad \text{for every } x_1, ..., x_{n-1} \in X.$$

If every Cauchy sequence in X converges to some $L \in X$, then X is said to be complete with respect to the n-norm. Any complete n-normed space is said to be n-Banach space.

Let w, l_∞, c and c_0 denote the spaces of all, bounded, convergent and null sequences $x = (x_k)$ with complex terms, respectively, normed by

$$\|x\| = \sup_k |x_k|.$$

Kizmaz (Kizmaz, 1981), defined the difference sequences $l_\infty(\Delta), c(\Delta)$ and $c_0(\Delta)$ as follows:

$$Z(\Delta) = \{x = (x_k) : (\Delta x_k) \in Z\},$$

for $Z = l_\infty, c$ and c_0, where $\Delta x = (\Delta x_k) = (x_k - x_{k+1})$, for all $k \in \mathbb{N}$.

The above spaces are Banach spaces, normed by

$$\|x\|_\Delta = |x_1| + \sup_k |\Delta x_k|.$$

The notion of difference sequence spaces was generalized by Et. and Colak (Et & Colak, 1995) as follows:

$$Z(\Delta^n) = \{x = (x_k) : (\Delta^n x_k) \in Z\},$$

for $Z = l_\infty, c$ and c_0, where $n \in \mathbb{N}, (\Delta^n x_k) = (\Delta^{n-1} x_k - \Delta^{n-1} x_{k+1})$ and so that

$$\Delta^n x_k = \sum_{v=0}^{n} (-1)^v \binom{n}{v} x_{k+v}.$$

In 2005, Tripathy and Esi (Tripathy & Esi, 2006), introduced the following new type of difference sequence spaces:

$$Z(\Delta_m) = \{x = (x_k) \in w : \Delta_m x \in Z\}, \text{ for } Z = l_\infty, c \text{ and } c_0$$

where $\Delta_m x = (\Delta_m x_k) = (x_k - x_{k+m})$, for all $k \in \mathbb{N}$.

Later on, Tripathy, Esi and Tripathy (B. C. Tripathy & Tripathy, 2005), generalized the above notions and unified these as follows:
Let m, n be non negative integers, then for Z a given sequence space we have

$$Z(\Delta_m^n) = \{x = (x_k) \in w : (\Delta_m^n x_k) \in Z\}$$

where $\Delta_m^n x = (\Delta_m^n x_k) = (\Delta_m^{n-1} x_k - \Delta_m^{n-1} x_{k+m})$ and $\Delta_m^\circ x_k = x_k$ for all $k \in \mathbb{N}$. The difference operator is equivalent to the binomial representation

$$\Delta_m^n x_k = \sum_{v=0}^{n} (-1)^v \binom{n}{v} x_{k+mv}.$$

A *paranorm* is a function $g : X \to \mathbb{R}$ which satisfies the following axioms:
For any $x, y, x_0 \in X$, $\lambda, \lambda_0 \in \mathbb{C}$:

(i) $g(\theta) = 0$;
(ii) $g(x) = g(-x)$;
(iii) $g(x + y) \leq g(x) + g(y)$
(iv) the scalar multiplication is continuous, that is $\lambda \to \lambda_0$, $x \to x_0$ imply $\lambda x \to \lambda_0 x_0$.

Throughout, a double sequence $x = (x_{jk})$ is a double infinite array of elements x_{jk}. for $j, k \in \mathbb{N}$. Double sequences have been studied by V. A. Khan and S. Tabassum (Khan & Tabassum, 2012; V. & Tabassum, 2011; Khan & Tabassum, 2011, 2010), Moricz and Rhoades (Moricz & Rhoades, 1952) and many others.

Definition 1.2. (see (Khan & Tabassum, 2010)). A double sequence space X is said to be *Solid (Normal)*, if $(\alpha_{jk} x_{jk}) \in X$ whenever $(x_{jk}) \in X$ and for all double sequence (α_{jk}) of scalars with $|\alpha_{jk}| \leq 1$ for all $j, k \in \mathbb{N}$.

2. Main Results

In 2010 E. Savas (Savas, 2010) introduced certain new sequence spaces using ideal convergence in 2-normed spaces. Later on V. A. Khan and S. Tabassum (Khan & Tabassum, 2010) introduced similar kind of double sequence spaces using difference operator in 2-normed spaces. In this paper we generalized these sequence spaces in n-normed spaces.

Let $p = (p_{jk})$ be any bounded sequence of positive numbers, m, n be non-negative integers and let I be an admissible ideal of $\mathbb{N}$. Let ${}_2W(n - X)$ be the space of X-valued double sequence spaces defined over a n-normed space $(X, \|., ..., .\|)$. Then for an Orlicz function M we define the following sequence spaces:

$${}_2W^I(M, \|., ..., .\|, \Delta_m^n, p) = \Big\{x = (x_{jk}) \in {}_2W(n - X) : \forall \varepsilon > 0 \text{ the set } \Big\{(j, k) \in N \times N :$$

$$\lim_{j,k \to \infty} \left(M\left(\left\|\frac{\Delta_m^n x_{jk} - L}{\rho}, z_1, z_2, ..., z_{n-1}\right\|\right)\right)^{p_{jk}} \geq \varepsilon\Big\} \in I, \text{ for some } \rho > 0, L \in X, z_1, z_2, ..., z_{n-1} \in X\Big\}.$$

$${}_2W_0^I(M, \|., ..., .\|, \Delta_m^n, p) = \Big\{x = (x_{jk}) \in {}_2W(n - X) : \forall \varepsilon > 0 \text{ the set}\Big\{(j, k) \in N \times N :$$

$$\lim_{j,k\to\infty}\left(M\left(\left\|\frac{\Delta_m^n x_{jk}}{\rho}, z_1, z_2, ..., z_{n-1}\right\|\right)\right)^{p_{jk}} \geq \varepsilon\Big\} \in I, \text{ for some } \rho > 0, z_1, z_2, ..., z_{n-1} \in X\Big\}.$$

$${}_2W_\infty^I(M, \|., ..., .\|, \Delta_m^n, p) = \Big\{x = (x_{jk}) \in {}_2W(n-X) : \exists K > 0 \text{ s.t. } \Big\{(j,k) \in N \times N :$$

$$\sup_{j,k\geq 1}\left(M\left(\left\|\frac{\Delta_m^n x_{jk}}{\rho}, z_1, z_2, ..., z_{n-1}\right\|\right)\right)^{p_{jk}} \geq K\Big\} \in I, \text{ for some } \rho > 0, z_1, z_2, ..., z_{n-1} \in X\Big\}$$

where

$$(\Delta_m^n x_{jk}) = (\Delta_m^{n-1} x_{jk} - \Delta_m^{n-1} x_{j+1,k} - \Delta_m^{n-1} x_{j,k+1} + \Delta_m^{n-1} x_{j+1,k+1})$$

and

$$(\Delta_m^0 x_{jk}) = x_{jk} \quad \text{for all } \ j,k \in \mathbb{N},$$

which is equivalent to the following binomial representation:

$$\Delta_m^n x_{jk} = \sum_{u=0}^{n}\sum_{v=0}^{n}(-1)^{u+v}\binom{n}{u}\binom{n}{v}x_{j+mu,k+mv}.$$

and $\Delta x_{j,k} = x_{j,k} - x_{j+1,k} - x_{j,k+1} + x_{j+1,k+1}$.
The following inequality will be used throughout the paper. Let $p_{j,k}$ be a double sequence of positive real numbers with $0 < p_{jk} \leq \sup_{j,k} p_{jk} = H$, and let $D = \max\{1, 2^{H-1}\}$. Then for the factorable sequences (a_{jk}) and (b_{jk}) in the complex plane, we have

$$|a_{jk} + b_{jk}|^{q_{jk}} \leq D(|a_{jk}|^{q_{jk}} + |b_{jk}|^{q_{jk}})$$

Theorem 2.1. *If* $\{\Delta_m^n x_{jk}, z_1, z_2, ..., z_{n-1}\}$ *is a linearly independent set in* $(X.\|., ..., .\|)$ *for all but finite* j,k *where* $x = (x_{jk}) \in {}_2W(n-X)$ *and* $\inf_{j,k} p_{jk} > 0$, *then*

(i) $\lim_{j,k\to\infty}\left[M\left(\left\|\frac{\Delta_m^n x_{jk}}{\rho}, z_1, z_2, ..., z_{n-1}\right\|\right)\right]^{p_{jk}} = 0$, for every $\rho > 0$,

(ii) $\lim_{j,k\to\infty}\left[M\left(\left\|\frac{\Delta_m^n x_{jk}-L}{\rho}, z_1, z_2, ..., z_{n-1}\right\|\right)\right]^{p_{jk}} < \infty$, for every $\rho > 0$.

Proof. **(i).** Assume that $\{\Delta_m^n x_{jk}, z_1, z_2, ..., z_{n-1}\}$ is a linearly independent set in $(X.\|., ..., .\|)$ for all but finite j,k. Then we have $\|\Delta_m^n x_{jk}, z_1, z_2, ..., z_{n-1}\| \to 0$ as $j,k \to \infty$.
Since M is continuous and $0 < p_{jk} \leq \sup p_{jk} < \infty$, for each j,k, we have

$$\lim_{j,k\to\infty}\left[M\left(\left\|\frac{\Delta_m^n x_{jk}}{\rho}, z_1, z_2, ..., z_{n-1}\right\|\right)\right]^{p_{jk}} = 0, \text{ for every } \rho > 0.$$

(ii). Proof of this part is similar to part **(i)**. □

Theorem 2.2. ${}_2W^I(M, \|., ..., .\|, \Delta_m^n, p)$, ${}_2W_0^I(M, \|., ..., .\|, \Delta_m^n, p)$ *and* ${}_2W_\infty^I(M, \|., ..., .\|, \Delta_m^n, p)$ *are linear spaces.*

Proof. We prove the assertion for ${}_2W_0^I(M, \|.,...,.\|, \Delta_m^n, p)$ the others can be proved similarly. Assume that $x = (x_{jk})$ and $y = (y_{jk}) \in {}_2W_0^I(M, \|.,...,.\|, \Delta_m^n, p)$ and $\alpha, \beta \in \mathbb{R}$, so

$$\left\{(j,k) \in N \times N : \lim_{j,k\to\infty} \left(M\left(\left\|\frac{\Delta_m^n x_{jk}}{\rho_1}, z_1, z_2, ..., z_{n-1}\right\|\right)\right)^{p_{jk}} \geq \varepsilon\right\} \in I, \text{ for some } \rho_1 > 0, \tag{2.1}$$

$$\left\{(j,k) \in N \times N : \lim_{j,k\to\infty} \left(M\left(\left\|\frac{\Delta_m^n y_{jk}}{\rho_2}, z_1, z_2, ..., z_{n-1}\right\|\right)\right)^{p_{jk}} \geq \varepsilon\right\} \in I, \text{ for some } \rho_2 > 0, \tag{2.2}$$

Since $\|.,...,.\|$ is a n-norm, and M is an Orlicz function the following inequality holds:

$$\begin{aligned}
&\lim_{j,k\to\infty} \left(M\left(\left\|\tfrac{\Delta_m^n(\alpha x_{jk}+\beta y_{jk})}{|\alpha|\rho_1+|\beta|\rho_2}, z_1, z_2, ..., z_{n-1}\right\|\right)\right)^{p_{jk}} \\
&\leq D \lim_{j,k\to\infty} \left[\tfrac{|\alpha|\rho_1}{|\alpha|\rho_1+|\beta|\rho_2} M\left(\left\|\tfrac{\Delta_m^n x_{jk}}{\rho_1}, z_1, z_2, ..., z_{n-1}\right\|\right)\right]^{p_{jk}} \\
&+D \lim_{j,k\to\infty} \left[\tfrac{|\beta|\rho_2}{|\alpha|\rho_1+|\beta|\rho_2} M\left(\left\|\tfrac{\Delta_m^n y_{jk}}{\rho_2}, z_1, z_2, ..., z_{n-1}\right\|\right)\right]^{p_{jk}} \\
&\leq DF \lim_{j,k\to\infty} \left[M\left(\left\|\tfrac{\Delta_m^n x_{jk}}{\rho_1}, z_1, z_2, ..., z_{n-1}\right\|\right)\right]^{p_{jk}} \\
&+DF \lim_{j,k\to\infty} \left[M\left(\left\|\tfrac{\Delta_m^n y_{jk}}{\rho_2}, z_1, z_2, ..., z_{n-1}\right\|\right)\right]^{p_{jk}}
\end{aligned} \tag{2.3}$$

where

$$F = \max\left[1, \left(\frac{|\alpha|}{\alpha\rho_1 + |\beta|\rho_2}\right)^H, \left(\frac{|\beta|}{\alpha\rho_1 + |\beta|\rho_2}\right)^H\right] \tag{2.4}$$

From the above inequality, we get

$$\begin{aligned}
&\left\{(j,k) \in N \times N : \lim_{j,k\to\infty} \left(M\left(\left\|\tfrac{\Delta_m^n \alpha x_{jk}+\Delta_m^n \beta y_{jk}}{|\alpha|\rho_1+|\beta|\rho_2}, z_1, z_2, ..., z_{n-1}\right\|\right)\right)^{p_{jk}} \geq \varepsilon\right\} \\
&\subseteq \left\{(j,k) \in N \times N : DF \lim_{j,k\to\infty} \left(M\left(\left\|\tfrac{\Delta_m^n x_{jk}}{\rho_1}, z_1, z_2, ..., z_{n-1}\right\|\right)\right)^{p_{jk}} \geq \tfrac{\varepsilon}{2}\right\} \\
&\cup\left\{(j,k) \in N \times N : DF \lim_{j,k\to\infty} \left(M\left(\left\|\tfrac{\Delta_m^n y_{jk}}{\rho_2}, z_1, z_2, ..., z_{n-1}\right\|\right)\right)^{p_{jk}} \geq \tfrac{\varepsilon}{2}\right\}.
\end{aligned} \tag{2.5}$$

The sets on the right hand side belong to I and this completes the proof. □

Theorem 2.3. *For any fixed $(j,k) \in N \times N$, ${}_2W_\infty^I(M, \|.,...,.\|, \Delta_m^n, p)$ is paranomed space with respect to the paranorm defined by:*

$$g(x) = \inf_{j,k}\left\{\rho^{\frac{p_{jk}}{H}} : \left(\sup_{j,k\geq 1}\left(M\left(\left\|\frac{\Delta_m^n x_{jk}}{\rho}, z_1, z_2, ..., z_{n-1}\right\|\right)\right)^{p_{jk}}\right)^{\frac{1}{H}} \leq 1, \forall z_1, z_2, ..., z_{n-1} \in X\right\}. \tag{2.6}$$

Proof. (**i**) $x = \theta$ implies that then $\|0, z_1, z_2..., z_{n-1}\| = 0$ since the set containing 0 is linearly dependent. Also $M(0) = 0$ implies that $g(\theta) = 0$.

(ii) $g(x) = g(-x)$

(iii) Let $x = (x_{jk}), y = (y_{jk}) \in {}_2W_\infty^I(M, \|., ..., .\|, \Delta_m^n, p)$.

Then there exists $\rho_1, \rho_2 > 0$ such that: $\sup_{j,k\geq 1}\left(M\left(\left\|\frac{\Delta_m^n x_{jk}}{\rho_1}, z_1, z_2, ..., z_{n-1}\right\|\right)\right)^{p_{jk}} \leq 1$ and

$$\sup_{j,k\geq 1}\left(M\left(\left\|\frac{\Delta_m^n y_{jk}}{\rho_2}, z_1, z_2, ..., z_{n-1}\right\|\right)\right)^{p_{jk}} \leq 1 \tag{2.7}$$

for each $z_1, z_2, ..., z_{n-1} \in X$.

Let $\rho = \rho_1 + \rho_2$. Then by convexity of Orlicz function we have:

$$\begin{aligned}\sup_{j,k\geq 1}\left(M\left(\left\|\frac{\Delta_m^n x_{jk}+\Delta_m^n y_{jk}}{\rho}, z_1, z_2, ..., z_{n-1}\right\|\right)\right) &\leq \left(\frac{\rho_1}{\rho_1+\rho_2}\right)\sup_{j,k\geq 1} M\left(\left\|\frac{\Delta_m^n x_{jk}}{\rho_1}, z_1, z_2, ..., z_{n-1}\right\|\right)\\ &+\left(\frac{\rho_2}{\rho_1+\rho_2}\right)\sup_{j,k\geq 1} M\left(\left\|\frac{\Delta_m^n y_{jk}}{\rho_2}, z_1, z_2, ..., z_{n-1}\right\|\right).\end{aligned} \tag{2.8}$$

Thus $\sup_{j,k\geq 1} M\left(\left\|\frac{\Delta_m^n x_{jk}+\Delta_m^n y_{jk}}{\rho_1+\rho_2}, z_1, z_2, ..., z_{n-1}\right\|\right)^{p_{jk}} \leq 1$ and hence

$$\begin{aligned}g(x+y) \leq \inf_{j,k}\left\{\rho_1^{\frac{p_{jk}}{H}} : \sup_{j,k\geq 1}\left(M\left(\left\|\frac{\Delta_m^n x_{jk}}{\rho_1}, z_1, z_2, ..., z_{n-1}\right\|\right)\right)^{p_{jk}} \leq 1\right\}\\ + \inf_{j,k}\left\{\rho_2^{\frac{p_{jk}}{H}} : \sup_{j,k\geq 1}\left(M\left(\left\|\frac{\Delta_m^n y_{jk}}{\rho_2}, z_1, z_2, ..., z_{n-1}\right\|\right)\right)^{p_{jk}} \leq 1\right\}.\end{aligned} \tag{2.9}$$

The arbitrary ρ_1 and ρ_2 implies that $g(x + y) \leq g(x) + g(y)$.

(iv) Let $\alpha \to 0$ and $g(x^n - x) \to 0 \quad (n \to \infty)$

$$g(\alpha x) = \inf\left\{\left(\frac{\rho}{|\alpha|}\right)^{\frac{p_{jk}}{H}} : \sup_{j,k\geq 1}\left(M\left(\left\|\frac{\Delta_m^n \alpha x_{jk}}{\rho}, z_1, z_2, ..., z_{n-1}\right\|\right)\right)^{p_{jk}} \leq 1\right\}. \tag{2.10}$$

□

Theorem 2.4. *Let M, M_1, M_2, be Orlicz functions. Then we have*

(i) ${}_2W_0^I(M_1, \|., ..., .\|, \Delta_m^n, p) \subseteq {}_2W_0^I(M \circ M_1, \|., ..., .\|, \Delta_m^n, p)$
provided (p_{jk}) is such that $H_0 = \inf p_{jk} > 0$.

(ii) ${}_2W_0^I(M_1, \|., ..., .\|, \Delta_m^n, p) \cap {}_2W_0^I(M_2, \|., ..., .\|, \Delta_m^n, p) \subseteq {}_2W_0^I(M_1 + M_2, \|., ..., .\|, \Delta_m^n, p)$.

Proof. **(i).** For given $\varepsilon > 0$, first choose $\varepsilon_0 > 0$ such that $\max\{\varepsilon_0^H, \varepsilon_0^{H_0}\} < \varepsilon$. Now using the continuity of M choose $0 < \delta < 1$ such that $0 < t < \delta$, implies that $M(t) < \varepsilon_0$, Let $(x_{jk}) \in {}_2W_0^I(M_1, \|., .\|, \Delta_m^n, p)$. Now by definition:

$$A(\delta) = \left\{(j,k) \in N \times N : \lim_{j,k\to\infty}\left(M_1\left(\left\|\frac{\Delta_m^n x_{jk}}{\rho}, z_1, z_2, ..., z_{n-1}\right\|\right)\right)^{p_{jk}} \geq \delta^H\right\} \in I. \tag{2.11}$$

Thus if $(j,k) \notin A(\delta)$ then

$$\left(M_1\left(\left\|\frac{\Delta_m^n x_{jk}}{\rho}, z_1, z_2, ..., z_{n-1}\right\|\right)\right)^{p_{jk}} \leq \delta^H, \qquad \forall j,k \in \mathbb{N}. \tag{2.12}$$

That is

$$\left(M_1\left(\left\|\frac{\Delta_m^n x_{jk}}{\rho}, z_1, z_2, ..., z_{n-1}\right\|\right)\right)^{p_{jk}} < \delta, \qquad \forall j,k \in \mathbb{N}. \tag{2.13}$$

Hence from above using continuity of M we must have

$$M\left(M_1\left(\left\|\frac{\Delta_m^n x_{jk}}{\rho}, z_1, z_2, ..., z_{n-1}\right\|\right)\right)^{p_{jk}} < \varepsilon_0, \qquad \forall j,k \in \mathbb{N} \tag{2.14}$$

Which consequently implies that

$$\lim_{j,k\to\infty}\left[M\left(M_1\left(\left\|\frac{\Delta_m^n x_{jk}}{\rho}, z_1, z_2, ..., z_{n-1}\right\|\right)\right)\right]^{p_{jk}} < \max\{\varepsilon_0^H, \varepsilon_0^{H_0}\} < \varepsilon. \tag{2.15}$$

This shows that

$$\left\{(j,k) \in N \times N : \lim_{j,k\to\infty}\left[M\left(M_1\left(\left\|\frac{\Delta_m^n x_{jk}}{\rho}, z_1, z_2, ..., z_{n-1}\right\|\right)\right)\right]^{p_{jk}} \geq \varepsilon\right\} \subset A(\delta) \tag{2.16}$$

and so belongs to I. This completes the result.
(ii). Let $x_{jk} \in {}_2W_0^I(M_1, \|.,...,.\|, \Delta_m^n, p) \cap {}_2W_0^I(M_2, \|.,...,.\|, \Delta_m^n, p)$
Then the fact that

$$\begin{aligned}&\lim_{j,k\to\infty}\left[(M_1 + M_2)\left(\left\|\tfrac{\Delta_m^n x_{jk}}{\rho}, z_1, z_2, ..., z_{n-1}\right\|\right)\right]^{p_{jk}} \leq D \lim_{j,k\to\infty}\left[M_1\left(\left\|\tfrac{\Delta_m^n x_{jk}}{\rho}, z_1, z_2, ..., z_{n-1}\right\|\right)\right]^{p_{jk}} \\ &+D \lim_{j,k\to\infty}\left[M_2\left(\left\|\tfrac{\Delta_m^n x_{jk}}{\rho}, z_1, z_2, ..., z_{n-1}\right\|\right)\right]^{p_{jk}}.\end{aligned} \tag{2.17}$$

This gives the result. □

Theorem 2.5. *The sequence space* ${}_2W_0^I(M, \|.,...,.\|, \Delta_m^n, p), {}_2W_\infty^I(M, \|.,...,.\|, \Delta_m^n, p)$ *are Solid.*

Proof. We give the proof for ${}_2W_0^I(M, \|.,...,.\|, \Delta_m^n, p)$ only.

Let $(x_{jk}) \in {}_2W_0^I(M, \|.,...,.\|, \Delta_m^n, p)$ and let (α_{jk}) be a double sequence of scalars such that $|\alpha_{jk}| \leq 1$ for all $j,k \in \mathbb{N}$. Then we have

$$\begin{aligned}&\left\{(j,k) \in N \times N : \lim_{j,k\to\infty}\left[M\left(\left\|\tfrac{\Delta_m^n(\alpha_{jk}x_{jk})}{\rho}, z_1, z_2, ..., z_{n-1}\right\|\right)\right]^{p_{jk}} \geq \varepsilon\right\} \\ &\subseteq \left\{(j,k) \in N \times N : E \lim_{j,k\to\infty}\left[M\left(\left\|\tfrac{\Delta_m^n x_{jk}}{\rho}, z_1, z_2, ..., z_{n-1}\right\|\right)\right]^{p_{jk}} \geq \varepsilon\right\} \in I.\end{aligned} \tag{2.18}$$

Where $E = \max_{j,k}\{1, |\alpha_{jk}|^H\}$. Hence $(\alpha_{jk}x_{jk}) \in {}_2W_0^I(M, \|.,...,.\|, \Delta_m^n, p)$ for all double sequence of scalars (α_{jk}) with $|\alpha_{jk}| \leq 1$ for all $j,k \in \mathbb{N}$ whenever $(x_{jk}) \in {}_2W_0^I(M, \|.,...,.\|, \Delta_m^n, p)$. □

Acknowledgments. The authors would like to record their gratitude to the reviewer for his careful reading and making some useful corrections which improved the presentation of the paper.

References

B. C. Tripathy, A. Esi and B. K. Tripathy (2005). A new type of generalized difference cesáro sequence spaces. *Soochow J. of Math.* **31**(03), 333–340.

Et, M. and R. Colak (1995). On generalized difference sequence spaces. *Soochow Jour. Math.* **21**(4), 377–386.

Gähler, S. (1963). 2-merische räme und ihre topological struktur. *Math. Nachr.* **28**(4), 115–148.

Gunawan, H. and Mashadi (2001). On finite dimensional 2-normed spaces. *Soochow Jour. Math.,* **27**(3), 631–639.

Khan, V. A. (2008*a*). On a new sequence space defined by Orlicz functions. *Commun. Fac. Sci. Univ. Ank. Series Al* **57**(2), 25–33.

Khan, V. A. (2008*b*). On a new sequence space related to the Orlicz sequence space. *J. Mathematics and its applications* **30**, 61–69.

Khan, V. A. and S. Tabassum (2010). On ideal convergent difference double sequence spaces in 2-normed spaces defined by Orlicz function. *JMI International Journal of Mathematical Sciences* **1**(2), 26–34.

Khan, V. A. and S. Tabassum (2011). Statistically convergent double sequence spaces in 2-normed spaces defined by Orlicz function. *Applied Mathematics* **2**(4), 398–402.

Khan, V. A. and S. Tabassum (2012). Statistically Pre-Cauchy double sequences and Orlicz functions. *Southeast Asian Bull.Math.* **36**(2), 61–69.

Kizmaz, H. (1981). On certain sequence spaces. *Canad. Math. Bull.*

Kostyrko, P., M. Ňacaj, T. Šalát and M.Sleziak (2005). *i*-convergence and extremal *i*-limit points. *Math. Slovaco*.

Kostyrko, P., T. Šalát and W. Wilczynski (2000). Lectures on analysis. *Canad. Math. Bull.*

Lindenstrauss, J. and L. Tzafiri (1971). On Orlicz sequence spaces. *Math. Slovaco* **10**, 379– 390.

Maddox, I. J (1986). Sequence spaces defined by modulus. *Math. Proc. Camb. Soc.* **100**(2), 161–166.

Moricz, F. and B. E. Rhoades (1952). Almost convergence of double sequences and strong regularity of summability matrices. *Math.Proc.Camb.Phil.Soc.* **104**, 283–294.

Savas, E. (2010). On some new sequence spaces in 2-normed spaces using ideal convergence and an Orlicz function. *Journal of Inequalities and Applications* **104**, 283–294.

Savas, E. (2011). Some new double sequence spaces defined by Orlicz function in n-normed space. *Journal of Inequalities and Applications* **104**, 283–294.

Tripathy, B. C. and A. Esi (2006). A new type of difference sequence spaces. *International Journal of Science and Technology* **01**(01), 11–14.

V., A., Khan and S. Tabassum (2011). On some new quasi almost δ^m–lacunary strongly p-convergent double sequences defined by Orlicz functions. *Journal of Mathematics and ApplicationsSoutheast Asian Bull.Math.* **34**, 45–52.

Theory and Applications of Mathematics & Computer Science

(ISSN 2067-2764, EISSN 2247-6202)
http://www.uav.ro/applications/se/journal/index.php/tamcs

Theory and Applications of Mathematics & Computer Science 3 (1) (2013) 99–106

Satellite Constellation Reconfiguration Using the Approximating Sequence Riccati Equations

Ashraf H. Owis[a]

[a]*Department of Astronomy, Space and Meteorology Cairo University*

Abstract

In this work we study the reconfiguration of a constellation of satellite. In this work we consider the non-linear feedback optimal control of the motion of a spacecraft under the influence of the gravitational attraction of a central body, the Earth in our case, and we would like to transfer the spacecraft from lower circular orbit to a higher one. Both orbits around the Earth are assumed to be circular and coplanar. We use both radial and tangential thrust control. The nonlinear dynamics of the system will be factorized in such a way that the new factorized system is accessible. The problem is tackled using the Approximating Sequence Riccati Equations (ASRE) method. The technique is based on Linear Quadratic Regulator (LQR) with fixed terminal state, which guarantees closed loop solution. The method is tested through GNSS circular constellation.

Keywords: Nonlinear feedback, linear quadratic regulator, approximation sequence Riccati equation, GNSS satellite.
2010 MSC: 49.

1. Introduction

In some instances, it is desirable to deploy a constellation in stages to gradually expand its capacity. This requires launching additional satellites and reconfiguring the existing on-orbit satellites (de Weck *et al.*, 2008). Also, a constellation might be re-structured and reconfigured after it is initially set for operational reasons.

The most common way of raising or lowering the orbit of a spacecraft is the low thrust orbit rendezvous approach, which is a nonlinear optimal control problem. Historically, there are several method to solve the nonlinear optimal control problem in both open and closed loop contexts. In the open loop context the problem can be solved via indirect and then direct method. The indirect method was developed through Pontryagin Maximum Principle (PMP) (Bryson & Ho, 1975),

*Corresponding author
Email address: aowis@eun.eg (Ashraf H. Owis)

(Pontryagin *et al.*, 1952). The direct method was developed using the Karush-Kuhn-Tucker(KKT) algebric equation (Enright & Conway, 1992).

One of the most common methods for solving the nonlinear optimal control problem in the closed loop context is the State Dependent Riccati Equations (SDRE) (Cimen, 2006), (Owis, 2013). The Approximating Sequence of Riccati Equations (ASRE) (Cimen, 2004) technique is an iterative approach to solve the nonlinear optimal control problem. The ASRE is developed (Topputo & Bernelli-Zazzera, 2012) using the state transition matrix. The guidance designed with these methods is obtained in an open-loop context. In other words, the optimal path, even if minimizing the prescribed performance index, is not able to respond to any perturbation that could alter the state of the spacecraft. Furthermore, if the initial conditions are slightly varied (e.g. the launch date changes), the optimal solution needs to be recomputed again. The outcome of the classical problem is in fact a guidance law expressed as a function of the time, the initial and final time, and u the control vector, respectively. We develop a closed loop approach. With this approach the solutions that minimize the performance index are also functions of the generic initial state x_0; the outcome is in fact a guidance law written as $u = u(x_0, t_0, t)$, $t \in [t_0, t_f]$. This represents a closed-loop solution: given the initial conditions (t_0, x_0) it is possible to extract the optimal control law that solves the optimal control problem. Moreover, if for any reason the state is perturbed and assumes the new value $(t_0^{'}, x_0^{'}) = (x_0 + \delta x, t_0 + \delta t)$, we are able to compute the new optimal solution by simply evaluating so avoiding the solution of another optimal control problem. This property holds by virtue of the closed loop characteristics of the control law that can be viewed as a one-parameter family of solutions. Due to such property, a trajectory designed in this way has the property to respond to perturbations acting during the transfer that continuously alter the state of the spacecraft. The optimal feedback control for linear systems with quadratic objective functions is addressed through the matrix Riccati equation: this is a matrix differential equation that can be integrated backward in time to yield the initial value of the Lagrange multipliers (Bryson & Ho, 1975). Recently, the nonlinear feedback control of circular coplanar low-thrust orbital transfers has been faced using continuous orbital elements feedback and Lyapunov functions (Chang & Marsden, 2002) and proved optimal by (Alizadah & Villac, 2011). Later on the problem has been solved using the primer vector approximation method (Haung, 2012).

The analytical low-thrust optimal feedback control problem is solved, with modulated inverse-square-distance, in the frame of a nonlinear vector field, the two-body dynamics, supported by a nonlinear objective function by applying a globally diffeomorphic linearizing transformation that rearranges the original problem into a linear system of ordinary differential equations and a quadratic objective function written in a new set of variables with radial thrust (Topputo *et al.*, 2008). In this work we consider the nonlinear feedback optimal control of the motion of a spacecraft under the influence of the gravitational attraction of a central body, the Earth in our case, and we would like to transfer the spacecraft from lower to higher orbit. Both lower and higher orbits around the Earth are assumed to be circular and coplanar. We use both radial and tangential thrust control. The nonlinear dynamics of the system will be factorized in such a way that the new factorized system is accessible. The problem is tackled using the Approximating Sequence Riccati Equation (ASRE) method. The technique is based on Linear Quadratic Regulator (LQR) with fixed terminal state. The method is applied to GNSS circular constellation Figure 1.

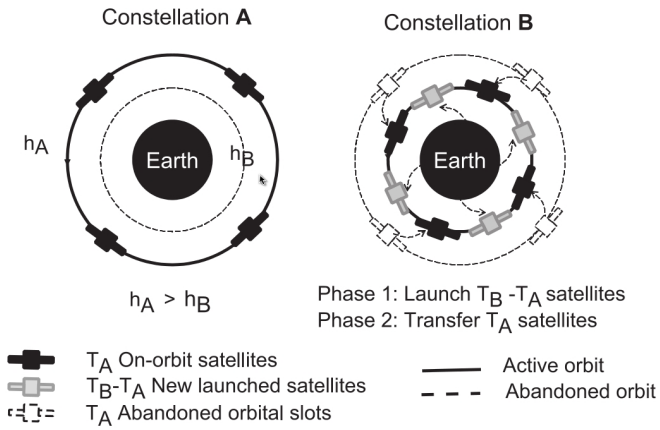

Figure 1. Constellation reconfiguration.

Linear Quadratic Regulator(LQR) with Fixed Terminal State.

Consider the following system with linear dynamics and quadratic performance index as follows:

$$\dot{X} = AX + BU, \qquad X(t_0) = X_0 \in \mathbb{R}^n, \tag{1.1}$$

the following performance index

$$J = X_f^T Q_f X_f + \frac{1}{2}\int_{t_0}^{t_f} [X^T QX + U^T RU]dt, \tag{1.2}$$

where A , B , Q , and R are constant coefficients matrices of the suitable dimensions. we have to find the m-dimensional control functions $U(t)$, $t \in [t_0\ t_f]$ which minimizes the J, which is an open loop (with t_0 fixed) optimal control. We optimize the performance index J, by adjoining the dynamics and the performance index (integrand) to form the Hamiltonian:

$$H(X, \lambda, U, t) = \frac{1}{2}(X^T QX + U^T RU) + \lambda^T (A(t)X + B(t)U),$$

where the Lagrange multiplier λ is called the adjoint variable or the costate. The necessary conditions for optimality are:

1. $\dot{X} = H_\lambda = A(t)X + B(t)U, \qquad X(t_0) = X_0,$
2. $\dot{\lambda} = -H_x = -QX - A^T\lambda, \qquad \lambda(t_f) = Q_f X_f,$
3. $H_u = 0 \Longrightarrow RU + B^T\lambda = 0 \Longrightarrow U^\star = -R^{-1}B^T\lambda.$

To find the minimum solution we have to check for $H_{uu} = \dfrac{\partial^2 H}{\partial \lambda^2} > 0$ or equivalently $R > 0$. Now we have that $\dot{X} = AX + BU^\star = AX - BR^{-1}B^T\lambda$, which can be combined to the the equation of the costate as follows

$$\begin{bmatrix} \dot{X} \\ \dot{\lambda} \end{bmatrix} = \begin{bmatrix} A & -BR^{-1}B^T \\ -Q & -A^T \end{bmatrix} \begin{bmatrix} X \\ \lambda \end{bmatrix}, \tag{1.3}$$

which is called the Hamiltonian matrix, it represents a $2n$ boundary value problem with $X(t_0) = X_0$ and, $\lambda(t_f) = Q_f X_f$.

We can solve this $2n$ boundary value problem using the transition matrix method as follows. Let's define a transition matrix

$$\phi_(t_1, t_0) = \begin{bmatrix} \phi_{11}(t_1, t_0) & \phi_{12}(t_1, t_0) \\ \phi_{21}(t_1, t_0) & \phi_{22}(t_1, t_0) \end{bmatrix},$$

we use this matrix to relate the current values of X and λ to the final values X_f and λ_f as follows

$$\begin{bmatrix} X \\ \lambda \end{bmatrix} = \begin{bmatrix} \phi_{11}(t, t_f) & \phi_{12}(t, t_f) \\ \phi_{21}(t, t_f) & \phi_{22}(t, t_f) \end{bmatrix} \begin{bmatrix} X(t_f) \\ \lambda(t_f) \end{bmatrix},$$

so we have $X = \phi_{11}(t, t_f)X(t_f) + \phi_{12}(t, t_f)\lambda(t_f) = [\phi_{11}(t, t_f) + \phi_{12}(t, t_f)Q_f]X(t_f)$, we can eliminate $X(t_f)$ to get $X = [\phi_{11}(t, t_f) + \phi_{12}(t, t_f)Q_f][\phi_{11}(t_0, t_f) + \phi_{12}(t_0, t_f)Q_f]^{-1}X(t_0) = X(t, X_0, t_0)$, now we can find $\lambda(t)$ in terms of $X(t_f)$ as $\lambda(t) = [\phi_{21}(t, t_f) + \phi_{22}(t, t_f)Q_f]X(t_f)$, then we can eliminate $X(t_f)$ to get $\lambda(t) = [\phi_{21}(t, t_f) + \phi_{22}(t, t_f)Q_f][\phi_{11}(t, t_f) + \phi_{12}(t, t_f)Q_f]^{-1}X(t) = \phi_{\lambda x}X(t)$. Now we search a solution for $\phi_{\lambda x}$. By differentiating $\lambda(t)$ we get $\dot{\lambda}(t) = \dot{\phi}_{\lambda x}X(t) + \phi_{\lambda x}\dot{X}(t)$. Comparing the last equation with the Hamiltonian matrix we get $-QX(t) - A^T\lambda(t) = \dot{\phi}_{\lambda x}X(t) + \phi_{\lambda x}\dot{X}(t)$, then we have

$$\begin{aligned} -\dot{\phi_{\lambda x}}(t)X(t) &= QX(t) + A^T\lambda(t) + \phi_{\lambda x}\dot{X}(t) \\ &= QX(t) + A^T\lambda(t) + \phi_{\lambda x}(AX - BR^{-1}B^T\lambda(t)) \\ &= (Q + \phi_{\lambda x}A)X(t) + (A^T - \phi_{\lambda x}BR^{-1}B^T)\lambda(t) \\ &= (Q + \phi_{\lambda x}A)X(t) + (A^T - \phi_{\lambda x}BR^{-1}B^T)\phi_{\lambda x}X(t) \\ &= [Q + \phi_{\lambda x}A + A^T\phi_{\lambda x} - \phi_{\lambda x}BR^{-1}B^T\phi_{\lambda x}]X(t). \end{aligned}$$

Since this is true for arbitrary $X(t)$, $\phi_{\lambda x}$ must satisfy

$$-\dot{\phi}_{\lambda x}(t) = Q + \phi_{\lambda x}A + A^T\phi_{\lambda x} - \phi_{\lambda x}BR^{-1}B^T\phi_{\lambda x}, \tag{1.4}$$

which is the matrix differential Riccati Equation . We can solve for $\phi_{\lambda x}$ by solving Riccati Equation backwards in time from t_f with $\phi_{\lambda x}(t_f) = Q_f$. The optimal control is then given by

$$U^\star = -R^{-1}B^T\lambda(t) = -R^{-1}B^T\phi_{\lambda x}X = -K(t)X(t, X_0, t_0). \tag{1.5}$$

From 1.5 we notice that the optimal control is a linear full-state feedback control, therefore the linear quadratic terminal controller is feedback by default.

2. The Approximating Sequence of Riccati Equations(ASRE)

Assume that we have the following nonlinear system

$$\dot{X} = f(X, U, t) \tag{2.1}$$

$$X(t_0) = X_0, \quad X(t_f) = X_f \in R^n \tag{2.2}$$

with performance index

$$J = \phi(X_f, t_f) + \int_{t_0}^{t_f} L(X, U, t)dt. \tag{2.3}$$

This system can be rewritten in the state dependent quasi-linear system as follows

$$\dot{X}^i = A(X^{i-1})X^i + B(X^{i-1})U^i \tag{2.4}$$
$$X(t_0) = X_0^0, \quad X(t_f) = X_f^n \in R^n \tag{2.5}$$

$$J = {X_f^i}^T Q(X_f^{i-1})X_f^i + \frac{1}{2}\int_{t_0}^{t_f} [{X^i}^T Q(X^{i-1})X^i + {U^i}^T R(X^{i-1})U^i]dt, \tag{2.6}$$

where i represents the iteration step over the time interval $[t_i - 1, t_i]$ Figure 2, the technique is based of the previously introduced Linear Quadratic Regulator with fixed terminal state, which is a full state feedback and therefore the obtained solution will be a closed loop one, i.e. able to respond to the unexpected change in the inputs. The technique works as follows: the initial state is used to compute A_0, and B_0 and we solve for the first LQR iteration and compute X^1 and then used to compute new value of A_1, and B_1 for the second iteration until the final state error reaches a value below a set threshold.

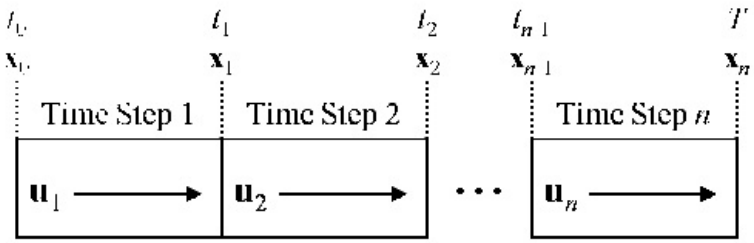

Figure 2. Time Interval Disecretization.

3. Optimal Orbit Transfer

The equations of motion are written in polar coordinates (r, θ), in the inertial Earth-Centered frame. In order to transfer the spacecraft between two circular coplanar orbits two components of the thrust control are used. The tangential component T_θ, and the radial component T_r.

The equations of motion are:

$$\begin{aligned} \ddot{r} - r\dot{\theta}^2 &= T_r - \frac{\mu}{r^2} \\ r\ddot{\theta} + 2\dot{r}\dot{\theta} &= T_\theta \end{aligned} \tag{3.1}$$

where μ is the gravitational constant of the Earth ($3.986005 \times 10^{14} m^3/s^2$) In this system of units the gravitational constant μ is unity, and equations (3.1) are rewritten as:

$$\begin{aligned} \ddot{r} - r\dot{\theta}^2 &= T_r - \frac{1}{r^2} \\ \ddot{\theta} + 2\frac{\dot{r}\dot{\theta}}{r} &= \frac{T_\theta}{r} \end{aligned} \tag{3.2}$$

Equations of motion in state variable form, equations (3.2), are then written in state variable form. The state vector $\mathbf{x}$ is chosen to be:

$$\mathbf{x} = \begin{bmatrix} x_1 \\ x_2 \\ x_3 \\ x_4 \end{bmatrix} = \begin{bmatrix} r \\ \theta \\ \dot{r} \\ \dot{\theta} \end{bmatrix} \tag{3.3}$$

and the control vector is :

$$\mathbf{u} = \begin{bmatrix} u_1 \\ u_2 \end{bmatrix} = \begin{bmatrix} T_r \\ T_\theta \end{bmatrix}. \tag{3.4}$$

Then equation (3.2) can be written in the form :

$$\dot{\mathbf{x}} = \mathbf{f}(\mathbf{x}) + \mathbf{B}(\mathbf{x})\mathbf{u}. \tag{3.5}$$

Choosing a suitable factorization equation (3.5) is rewritten in the factored state variable form :

$$\dot{\mathbf{x}} = \mathbf{A}(\mathbf{x})\mathbf{x} + \mathbf{B}(\mathbf{x})\mathbf{u}, \tag{3.6}$$

where :

$$\mathbf{A}(\mathbf{x}) = \begin{bmatrix} 0 & 0 & 1 & 0 \\ 0 & 0 & 0 & 1 \\ x_4^2 & -\frac{1}{x_1^2 x_2} & 0 & 0 \\ -\frac{2x_4}{x_1^2} & 0 & 0 & 0 \end{bmatrix}, \tag{3.7}$$

$$\mathbf{B}(\mathbf{x}) = \begin{bmatrix} 0 & 0 \\ 0 & 0 \\ 1 & 0 \\ 0 & \frac{1}{x_1} \end{bmatrix}. \tag{3.8}$$

4. Factored Controllability

For the factored system (3.6) the controllability is established by verifying that the controllability matrix $\mathbf{M}_{cl} = [\mathbf{B}\ \mathbf{AB}\ \mathbf{A}^2\mathbf{B}\ \mathbf{A}^3\mathbf{B}]$ has a rank equals to $n = 4\ \forall x$ in the domain.

Since $\mathbf{A}$ and $\mathbf{B}$ have nonvanishing rows the controllability matrix $\mathbf{M}_{cl}$ for the System (3.6) is of rank 4.

Nondimensionalization of the problem in order to simplify the calculation we dimensionalize the system by removing the units from the equations of motion via multiplying or dividing some

constants. The two constant we divide by are the radial distance of the initial orbit and the gravitational constant μ in this case the radius of the initial orbit is unity and velocity is divided by the circular velocity of the initial orbit $\sqrt{\frac{\mu}{r_0^2}}$ and the time is multiplied by $\sqrt{\frac{\mu}{r_0^3}}$. In the first two example we would like to make an optimal orbit transfer (i.e. from $(r = 1)$ to $(r = 1.2)$ in time $t_f = 4.469, 5.2231$ (time unit) Figure 3 with an optimal control function of both radial and tangential components Figure 4. The initial angle is $(\theta_0 = \frac{\pi}{2})$ and the final angle is $(\theta_f = \frac{3\pi}{2})$. $\dot{r}_0 = 0$ and $\dot{r}_f = 0$ for the initial and final orbits. $\dot{\theta}_0 = \sqrt{\frac{1}{r_0^3}} = 1$ and $\dot{\theta}_f = \sqrt{\frac{1}{r_f^3}} = 0.54433105395$. In the second $\theta_f = \frac{5\pi}{2}$ with $t_f = 6.866$. In both examples the matrices **Q** and **R** are the identity matrices:

$$\mathbf{Q} = \begin{bmatrix} 1 & 0 & 0 & 0 \\ 0 & 1 & 0 & 0 \\ 0 & 0 & 1 & 0 \\ 0 & 0 & 0 & 1 \end{bmatrix}, \mathbf{R} = \begin{bmatrix} 1 & 0 \\ 0 & 1 \end{bmatrix}.$$

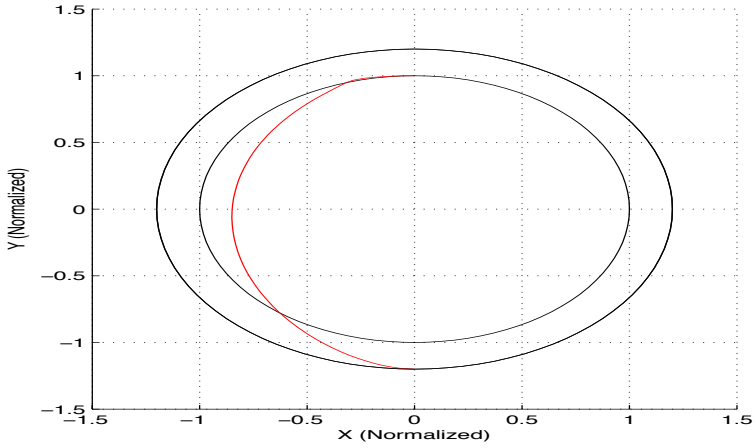

Figure 3. Trajectory of orbit transfer in polar coordinates, from $[r_0 = 1,\ \theta_0 = \pi/2\ , \dot{r}_0 = 0,\ \dot{\theta}_0 = 1]$ to $[r_f = 1.2,\ \theta_f = 3\pi/2,\ \dot{r}_f = 0,\ \dot{\theta}_f = 0.72213]$

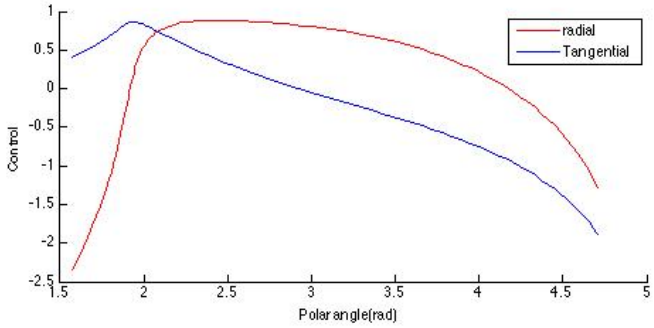

Figure 4. Control function in polar coordinates, from $[r_0 = 1,\ \theta_0 = \pi/2,\ \dot{r}_0 = 0,\ \dot{\theta}_0 = 1]$ to $[r_f = 1.2,\ \theta_f = 3\pi/2, \dot{r}_f = 0,\ \dot{\theta}_f = 0.54433]$.

5. Conclusion

The nonlinear feedback optimal control can be solved by factorizing the original nonlinear dynamics into accessible (weakly controllable) linear dynamics of state dependent factors. The factorized problem has been solved using the the Approximating Sequence Riccati Equations (ASRE) method. The technique is based on Linear Quadratic Regulator (LQR) with fixed terminal state, which guarantees closed loop solution. The method is tested through reconfiguration of a GNSS circular constellation. The result is valid for any circular orbit transfer.

6. Acknowledgments

This project was supported financially by the Science and Technology Development Fund (STDF), Egypt, Grant No 1834.

References

Alizadah, I. and B. F. Villac (2011). Static solutions of the Hamilton-Jacobi-Bellman equation for circular orbit transfer. *Jounal of Guidance, Control and Dynamics* **34**(5), 1584–1588.

Bryson, A. J. and Y. C. Ho (1975). *Applied Optimal Control: Optimization, Estimation and Control*. Taylor and Francis Group. NY.

Chang, D. E. and D. F. Marsden (2002). Lyapunov based transfer between elliptic keplerian orbits. *Discrete and Continuos Dynamical Systems. Series B* **2**, 57–67.

Cimen, T. (2004). Global optimal feedback control for general nonlinear systems with nonquadratic performance criteria. *Systems & Control Letters* **53**(5), 327–346.

Cimen, T. (2006). Recent advances in nonlinear optimal feedback control design. In: *9th WSEAS International Conference on Applied Mathematics, Anonymous ROKETSAN Missiles Industries Inc*.

de Weck, O. L., U. Scialom and A. Siddiqi (2008). Optimal reconfiguration of satellite constellations with the auction algorithm. *Acta Astronautica* **12**, 112–130.

Enright, P. and B. Conway (1992). Discrete approximations to optimal trajectories using direct transcription and nonlinear programming. *Journal of Guidance, Control, and Dynamic* **15**, 994–1002.

Haung, W. (2012). Solving coplanar power-limited orbit transfer probelm by primer vector approximation method. *Internation Journal of Aerospace Engineering*.

Owis, A. (2013). Feedback optimal control of low-thrust orbit transfer in central gravity field. *International Journal of Advanced Computer Science and Applications* **4**(4), 158–162.

Pontryagin, L., V. Boltyanskii, R. Gamkrelidze and E. Mishchenko (1952). *The Mathematical Theory of Optimal Processes*. 2nd ed.. John Wiley & Sons, New York. New York.

Topputo, F., A. Owis and F. Bernelli-Zazzera (2008). Analytical solution of the feedback optimal control for radially accelerated orbits. *Journal of Guidance, Control and Dynamics* **31**(5), 1352–1359.

Topputo, F. and F. Bernelli-Zazzera (2012). A method to solve the nonlinear optimal control problem in astrodynamics. In: *The 1St IAA Conference on Dynamics and Control of Space Systems*. Porto, Portugal.

Theory and Applications of Mathematics & Computer Science

(ISSN 2067-2764, EISSN 2247-6202)
http://www.uav.ro/applications/se/journal/index.php/tamcs

Theory and Applications of Mathematics & Computer Science 3 (2) (2013) 36–58

Visual Motif Patterns in Separation Spaces

James Peters[a,b,*], Randima Hettiarachichi[a]

[a] *Computational Intelligence Laboratory, University of Manitoba,Winnipeg, Manitoba R3T 5V6 Canada*
[b] *School of Mathematics & Computer / Information Sciences, University of Hyderabad, Central Univ. P.O., Hyderabad 500046, India*

Abstract

This article introduces descriptive separation spaces useful in the discovery of what are known as motif patterns. The proposed approach presents the separation axioms in terms of descriptive proximities. Asymmetries arise naturally in the form of the separation of neighbourhoods of descriptively distinct points in what are known as Leader uniform topological spaces. A practical application of the proposed approach is given in terms of visual motif patterns, identification of nearness structures and pattern stability analysis in digital images.

Keywords: Descriptive proximity, near sets, visual motif patterns, separation spaces.
2010 MSC: Primary 26A21, Secondary 26A24, 54D35, 54A20, 54E99, 18B30.

1. Introduction

This article introduces separation spaces, useful in the study of set patterns. Various forms of separation in topological spaces are defined by what are known as separation axioms. The main purpose of a separation axiom is to make the points and sets in a space topologically distinguishable (Thron, 1966, §14.1). The earliest of such spaces comes from F. Hausdorff, where distinct points belong to disjoint neighbourhoods (Hausdorff, 1957*a*, §40.II). In this article, traditional separation spaces are extended to description-based separation spaces. The practical benefit of considering descriptive separation spaces is the generation of multiple patterns that are descriptively distinguishable. In a Hausdorff space, for example, a pair of descriptively distinct points become generators of distinguishable set patterns.

A form of set pattern (Grenander, 1993, §17.5) of particular interest in an approach to pattern recognition is given in terms of what are known as descriptive motif patterns. A *descriptive motif pattern* is a collection of sets such that each member of the collection is descriptively close to a motif. A *motif* is a set with members that are near one or more members of other sets. Motifs

*Corresponding author
Email address: james.peters3@ad.umanitoba.ca (James Peters)

are a particular form set pattern generators. Visual motif patterns are found in pictures, geometric structures, and digital images. A *visual motif pattern* is a particular form of descriptive motif pattern that is a collection of sets such that each member of the collection is visually close to a set that is a motif. Visual motif patterns have a number of important applications (Naimpally & Peters, 2013; Peters, 2013*a*).

The study of visual patterns includes a consideration of S. Leader's uniform topology[1] in a metric space (Leader, 1959) and its extension to descriptive uniform topologies that provide a basis for new forms of asymmetric spaces. A *descriptive uniform topology* is determined by finding the collection of all sets that are descriptively near a given set.

Set descriptions result from the introduction of feature vectors that describe members of sets such as sets of pixels in digital images. These considerations lead in a straightforward way to a form of topology of digital images with considerable practical importance in solving image analysis and image classification problems. Since we are interested in patterns in separation spaces, we introduce stability criteria for the generation of multiple set patterns. A visual pattern is considered *stable*, provided the members of the pattern do not wander away from the pattern generator, neither spatially nor descriptively.

2. Preliminaries

Let X be a nonempty set of points, $\mathcal{P}(X)$ the powerset of X, $\mathcal{P}^2(X)$ the set of all collections of subsets of X. A single point $x \in X$ is denoted by a lowercase letter, a subset $A \in \mathcal{P}(X)$ by an uppercase letter, collection of subsets in $\mathcal{P}^2(X)$ by a round letter such as $\mathcal{B} \in \mathcal{P}^2(X)$. The *closure* of a subset $A \in \mathcal{P}(X)$ (denoted by cl$A$) is defined by

$$\mathrm{cl}A = \{x \in X : x \,\delta\, A\},$$

i.e., cl$A$ is the set of all points x in X that are near A. Let δ on a nonempty set X denote a spatial nearness (proximity) relation. For $A, B \in \mathcal{P}(X)$, $A \,\delta\, B$ (reads A is spatially near B), provided $A \cap B \neq \emptyset$, *i.e.*, the intersection of A and B is not empty (cl$A$ and cl$B$ have at least one point in common). The spatial proximity (nearness) relation δ is defined by

$$\delta = \{(A, B) \in \mathcal{P}(X) \times \mathcal{P}(X) : \mathrm{cl}A \cap \mathrm{cl}B \neq \emptyset\}.$$

$A \,\underline{\delta}\, B$ (reads A far (remote) from B), provided cl$A$ and cl$B$ have no points in common such that $\underline{\delta} = \mathcal{P}(X) \times \mathcal{P}(X) \setminus \delta$. Sets that are far from each other relative to the locations of the points in the sets (the points in one set are not among the points of the other set) are called *spatially remote* sets. The complement of a set $C \in \mathcal{P}(X)$ is denoted by C^c.

In the study of patterns, a descriptive form of EF-proximity is useful (Peters & Naimpally, 2012). Let X be a nonempty set endowed with a descriptive proximity relation δ_Φ, $x \in X$, $A, B \in \mathcal{P}(X)$, and let $\Phi = \{\phi_1, \ldots, \phi_i, \ldots, \phi_n\}$, a set of probe functions $\phi_i : X \to \mathbb{R}$ that represent features

[1] Metric space uniformity is logically equivalent to EF-proximity and the axioms given by Efremovič (Efremovič, 1951) (see Theorem 1.15, one of the most beautiful results in set-theoretic topology (Naimpally & Peters, 2013, §1.11, p. 27)). Many thanks to Som Naimpally for pointing this out.

of each x, where $\phi_i(x)$ equals a feature value of x. Let $\Phi(x)$ denote a feature vector for the object x, *i.e.*, a vector of feature values that describe x, where

$$\Phi(x) = (\phi_1(x), \ldots, \phi_i(x), \ldots, \phi_n(x)) .$$

A feature vector provides a description of an object. Let $A, B \in \mathcal{P}(X)$. Let $\mathcal{Q}(A), \mathcal{Q}(B)$ denote sets of descriptions of points in A, B, respectively. For example,

$$\mathcal{Q}(A) = \{\Phi(a) : a \in A\} .$$

The expression $A \; \delta_\Phi \; B$ reads *A is descriptively near B*. The descriptive proximity of A and B is defined by

$$A \; \delta_\Phi \; B \Leftrightarrow \mathcal{Q}(\mathrm{cl}A) \cap \mathcal{Q}(\mathrm{cl}B) \neq \emptyset.$$

Descriptive remoteness of A and B (denoted by $A \; \underline{\delta}_\Phi \; B$) is defined by

$$A \; \underline{\delta}_\Phi \; B \Leftrightarrow \mathcal{Q}(\mathrm{cl}A) \cap \mathcal{Q}(\mathrm{cl}B) = \emptyset.$$

Early informal work on the descriptive intersection of disjoint sets based on the shapes and colours of objects in the disjoint sets is given by N. Rocchi (Rocchi, 1969, p.159). The *descriptive intersection* $\underset{\Phi}{\cap}$ of A and B is defined by

$$A \underset{\Phi}{\cap} B = \{x \in A \cup B : \Phi(x) \in \mathcal{Q}(\mathrm{cl}A) \text{ and } \Phi(x) \in \mathcal{Q}(\mathrm{cl}B)\} .$$

The descriptive intersection will be nonempty, provided there is at least one element of cl$A$ with a description that matches the description of a least one element of cl$B$. That is, a nonempty descriptive intersection of sets A and B is a set containing $a \in \mathrm{cl}A$ and $b \in \mathrm{cl}B$ such that $\Phi(a) = \Phi(b)$. Observe that A and B can be disjoint and yet $A \underset{\Phi}{\cap} B$ can be nonempty. In finding subsets $A, B \in \mathcal{P}(X)$ that are descriptively near, one considers descriptive intersection of the closure of A and the closure of B. That is, cl$A \underset{\Phi}{\cap}$ cl$B$ implies $A \; \delta_\Phi \; B$. The descriptive proximity (nearness) relation δ_Φ is defined by

$$\delta_\Phi = \left\{(A, B) \in \mathcal{P}(X) \times \mathcal{P}(X) : \mathrm{cl}A \underset{\Phi}{\cap} \mathrm{cl}B \neq \emptyset\right\} .$$

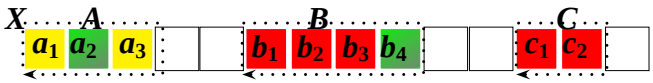

Figure 1. $\Phi = \{\text{colour probe fns}\}$, cl$A \underset{\Phi}{\cap}$ cl$B = \{a_2, b_4\}$, cl$A \underset{\Phi}{\cap}$ cl$C = \emptyset$.

Example 2.1. Descriptive intersection of disjoint sets
The coloured and white squares in Figure 1 represent cells in a weave. A *cell* in a fabric is that part of a weave strand that overlaps another weave strand. The parallel strands of each layer in a weave are perpendicular to those strands in the other layer, making the cells square (Thomas, 2009). Choose Φ to be a set of probe functions representing weave cell colours. Let the set of cells X in Figure 1 be endowed with δ_Φ. Notice that sets $A, B \in \mathcal{P}(X)$ are disjoint but the descriptive intersection is nonempty. That is, cl$A \underset{\Phi}{\cap}$ cl$B = \{a_2, b_4\}$. Similarly, for $B, C \in \mathcal{P}(X)$, cl$B \underset{\Phi}{\cap}$ cl$C = \{b_1, b_2, b_3, c_1, c_2\}$. ■

The descriptive remoteness of A and B (denoted by $A \underline{\delta}_\Phi B$) such that $\underline{\delta}_\Phi = \mathcal{P}(X) \times \mathcal{P}(X) \setminus \delta_\Phi$ is defined by

$$A \underline{\delta}_\Phi B \Leftrightarrow \mathrm{cl}A \underset{\Phi}{\cap} \mathrm{cl}B = \emptyset.$$

Example 2.2. Descriptively remote disjoint sets
Choose Φ to be a set of probe functions representing weave cell colours. In Figure 1, sets $A, C \in \mathcal{P}(X)$ are disjoint. In addition, there are no cells in A with descriptions that resemble cells in C. Hence, the descriptive intersection is empty. That is, $A \underline{\delta}_\Phi C$ (A and C are remote), since $\mathrm{cl}A \underset{\Phi}{\cap} \mathrm{cl}C = \emptyset$. ■

2.1. Descriptive EF-proximity

A binary relation δ_Φ is a *descriptive EF-proximity*, provided the following axioms are satisfied for $A, B, C \in \mathcal{P}^2(X)$.

($\boldsymbol{EF_\Phi}$.1) $A \delta_\Phi B$ implies $A \neq \emptyset, B \neq \emptyset$.
($\boldsymbol{EF_\Phi}$.2) $A \underset{\Phi}{\cap} B \neq \emptyset$ implies $A \delta_\Phi B$.
($\boldsymbol{EF_\Phi}$.3) $A \delta_\Phi B$ implies $B \delta_\Phi A$ (descriptive symmetry).
($\boldsymbol{EF_\Phi}$.4) $A \delta_\Phi (B \cup C)$, if and only if, $A \delta_\Phi B$ or $A \delta_\Phi C$.
($\boldsymbol{EF_\Phi}$.5) Descriptive Efremovič axiom:

$$A \underline{\delta}_\Phi B \text{ implies } A \underline{\delta}_\Phi C \text{ and } B \underline{\delta}_\Phi C^c \text{ for some } C \in \mathcal{P}(X).$$

The structure (X, δ_Φ) is a *descriptive EF-proximity space* (or, briefly, *descriptive EF space*).

Theorem 2.1. *Let $(X, \delta), (X, \delta_\Phi)$ be spatial and descriptive EF-spaces, respectively, with nonempty sets $A, B \in \mathcal{P}(X)$, $A \cap B \neq \emptyset$. Then $A \cap B \subseteq A \underset{\Phi}{\cap} B$.*

Proof. Let $A, B \in \mathcal{P}(X)$ and assume $A \cap B \neq \emptyset$. If $x \in A \cap B$, then, by definition, $\Phi(x) \in \mathcal{Q}(A)$ and $\Phi(x) \in \mathcal{Q}(B)$. By assumption $x \in A \cap B \subseteq A \cup B$. Then, $x \in A \underset{\Phi}{\cap} B$. Hence, $A \cap B \subseteq A \underset{\Phi}{\cap} B$. □

Descriptive EF-proximity is useful in describing, analysing and classifying the parts within a single digital image or the parts in either near or remote sets in separate digital images. The basic approach to the study of set patterns introduced in this article reflects recent work on descriptively near sets (see, *e.g.*, (Peters & Naimpally, 2012; Peters, 2012; Peters *et al.*, 2013)). Applications of descriptive EF-proximity are numerous (see, *e.g.*, (Naimpally & Peters, 2013; Peters, 2013*c*)).

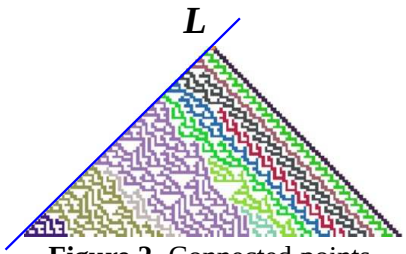

Figure 2. Connected points.

2.2. Shape set patterns

Shape descriptors are useful in representing, extracting and quantifying shape information from images. In general, a digital image *shape descriptor* is an expression that describes, identifies or indexes an image region. Shape descriptors are usually mathematical expressions used to extract

image region shape feature values. In this section, we briefly consider picture points in terms of adjacency, connectedness, and edges.

Let $p, q \in \mathbb{Z} \times \mathbb{Z}$ be points in a grid X. Points p and q are *spatially adjacent*, provided they are joined by an edge (Klette & Rosenfeld, 2004). For example, pairs of magenta pixels in the grid in Figure 2 are spatially adjacent, since each pair of magenta pixels is joined by an edge.

Remark 2.1. Points vs. cells.
Points are the standard elements in standard topological spaces. In some discrete cases, the base elements are *cells* (indivisible collections of points) (Düntsch & Vakarelov, 2007). ■

In keeping with an interest in descriptive proximity, points p, q in a grid are *descriptively adjacent*, provided p, q have matching descriptions and there is an edge connecting p, q such that the description of the points on a connecting edge match the descriptions of p, q. For example, for the blue line $L \subset X$ along the northwest edge of the weave in Figure 2, each pair of pixels $p, q \in L$ are descriptively adjacent but pixels below L are not descriptively adjacent to any pixel in L, since L contains only blue pixels in Figure 2. Let p, q be magenta points, then the descriptive closure of L is descriptively far from p, q and the closure of any point $r \in L$ is descriptively far from either p or q, *i.e.*,

$$
\begin{aligned}
\Phi &= \{\phi : \phi(x) = \text{ colour brightness of } x \text{ for } x \in X\},\\
\mathrm{cl}_\Phi L &= \left\{x \in X : x \underset{\Phi}{\cap} L \neq \emptyset\right\},\\
\mathrm{cl}_\Phi r &= \{y \in X : \Phi(y) = \Phi(r)\},\\
\mathrm{cl}_\Phi L \ \underline{\delta}_\Phi \ &\{p, q\},\\
\mathrm{cl}_\Phi r \ \underline{\delta}_\Phi \ &p,\\
\mathrm{cl}_\Phi r \ \underline{\delta}_\Phi \ &q.
\end{aligned}
$$

Descriptive adjacency is the heartbeat (main influence) in the study of visual motif patterns in pictures that are descriptive proximity spaces (Peters *et al.*, 2013; Peters, 2013*a*,*c*; Peters & Naimpally, 2012; Naimpally & Peters, 2013) (for the underlying near set theory, see, also, (Peters, 2013*b*; Henry, 2010)).

A 2D digital image (also called a picture) is defined on a finite, rectangular array of point samples called a *grid*. An element of a grid is a point sample or pixel. In terms of a digitized optical sensor value, a *point sample* (briefly, point) is a single number in a greyscale image or a set of 3 numbers in a colour image (Smith, 1995). In a 2D model of an image, a pixel is a point sample that exists only at a point in the plane. For a colour image, each pixel is defined by three point samples, one for each colour channel.

Let M be a set of grid points in a picture and let

$$S = p_0, p_1, \ldots, p_{i-1}, p_i, \ldots, p_n$$

be a sequence of points in M. The sequence S is called a *path*. Further, let $p = p_0, q = p_n$. Then M is *connected*, provided, for all points $p, q \in M$, point p_i is adjacent to p_{i-1} in a path between p

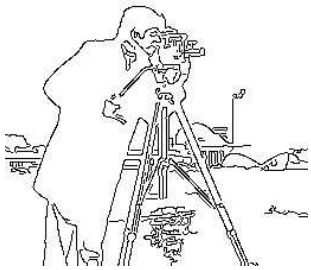

Figure 3. Sample straight edges.

and q in M. Maximally connected subsets of M are called *connected components* of M (Klette & Rosenfeld, 2004, §1.1.4).

The set of points in L in Figure 2 are connected and the remainder of the points in this weave are also connected. Let $X = L \cup W$, where W is the set of points in the threads in the weave in Figure 2. The set X is not a connected component, since there are pairs of points in separate threads with no path between the points. However, taken separately, any thread W containing pixels with the same colour is a connected component.

Let M be a grid that is connected and let points $p, q \in M$. A path between p and q defines an *edge*. A path between p and q defines a *straight edge*, provided every point in the path has the same gradient orientation. The penultimate example of a picture edge is a straight line segment such as the edges along the contour of the camera tripod legs in Figure 3. Hence, straight edges in a picture are distinguished from ridges, valleys and, in general, arcs, where the points in the paths defining non-straight edges have unequal gradient orientation.

A *shape set pattern* is a set pattern that results from the choices of shape descriptors used in comparing descriptions of picture elements. For example, the pairs of points along the diagonal in the northeast corner of Figure 2 are both spatially adjacent (each pair points along the upper northeast diagonal are joined by an edge) and descriptively adjacent (each pair points p, q along the diagonal are joined by an edge containing points that descriptively match p, q). Spatial adjacency and descriptive adjacency shape descriptors are important in separating spatially connected points from descriptively connected points in a picture and deriving spatial and descriptive set patterns in pictures.

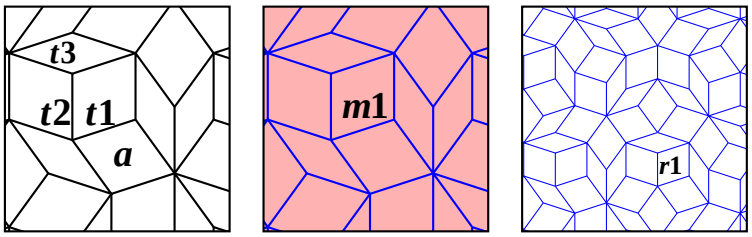

Figure 4. Spatial $\mathfrak{P}(t1) = \{t1, t2, t3, a\}$ & descriptive $\mathfrak{P}_\Phi(t1) = \{t1, m1, r1\}$.

Example 2.3. Descriptive penrose tiling shape pattern.
Choose Φ to be a set of probe functions representing shape features such as connected, edge gradient, and edge gradient orientation as well as colour and intensity features. Also, for example, choose tile $t1$ in Figure 4 as a shape pattern generator[2]. Tile $t1$ in the penrose tiling in Figure 4 is descriptively near tiles $m1$ (in the middle tiling) and $r1$ (in the righthand tiling) as well as a number of other unlabelled tiles that are descriptively near some part of $t1$. In generating descriptive shape patterns, we use the descriptive closure of a set A in a picture X (denoted by $\mathrm{cl}_\Phi A$), defined by

$$\mathrm{cl}_\Phi A = \left\{ x \in X : \{x\}\ \delta_\Phi\ A,\ i.e., \{x\} \underset{\Phi}{\cap} A \neq \emptyset \right\}.$$

In effect, $x\ \mathrm{cl}_\Phi A$ for $x \in X$ means $\Phi(x) \in \mathcal{Q}(A)$. Then

$$\mathfrak{P}_\Phi(t1) = \{t1, m1, r1, \dots\}.$$

For example, $\mathrm{cl}_\Phi t1 \cap \mathrm{cl}_\Phi m1 \neq \emptyset$, since the gradient orientation of edges along the border of $t1$ match the gradient orientation of the edges along the border of $m1$. Similarly, $\mathrm{cl}_\Phi t1 \cap \mathrm{cl}_\Phi r1 \neq \emptyset$, and so on. ■

3. Descriptive uniform topology on digital images

It was S. Leader who pointed out in 1959 that it is possible to determine what he called a uniform topology in a metric space (Leader, 1959). By introducing a metric on a nonempty set of points, one obtains a metric space. Then a topology in the metric space results from observing which points are close to each given set of points. A point x in a set X is *close* to a set A, provided the distance between x and A is zero. A *digital uniform topology* in a metric space on a digital image is determined by observing which sets of pixels are close to a given set of pixels.

A useful alternative form of uniform topology (called a discrete uniform topology) arises in a proximity space by defining the nearness of sets in terms of set intersection. A discrete uniform topology in a proximity space is determined by observing which sets have nonempty intersection with a given set. In a discrete uniform topology, sets that are close to a given set are called *near sets*.

A descriptive form of either the Leader form of uniform topology or discrete uniform topology arises when the nearness of sets is based on the descriptions of members of one set matching the descriptions of members of another set. A *descriptive uniform topology* in a metric space is determined by finding which sets are descriptively close to each given set. In a descriptive uniform topology, nonempty disjoint sets can be descriptively near each other. The introduction of a uniform topology in a metric space or discrete uniform topology or descriptive uniform topology on a digital image provides a basis for the study of visual patterns in a image. In the sequel, it is assumed that each of the traditional separation spaces is defined in the context of a discrete uniform topology and that each descriptive separation space is defined in the context of a descriptive uniform topology on a nonempty set. From an application point-of-view, the focus in this article is on the introduction of uniform topologies that provide a basis for the introduction of asymmetric spaces on digital images.

[2]Regular structures known as *pattern generators* in pattern theory, are described in U. Grenander (Grenander, 1993, 1996), in building patterns from simple building blocks.

4. Antisymmetric spaces

During the 1930s, separation axioms were discovered and called *Trennungsaxiome* (*Trennung* is German for *separation*) by P. Alexandroff and H. Hopf (Alexandroff & Hopf, 1935, 58ff, §4). Hence, these axioms are named with a subscripted T as $T_n, n = 0, 1, 2, 3, 4, 5$. Often these axioms have alternate names such as Hausdorff, normal, regular, Tychonoff, and so on and there is no unanimity in the nomenclature. In this article, we consider only axioms T_0, T_1, T_2. Each of these separation axioms concern the distinctness of points.

Remark 4.1. Distinct points.
Let X be a nonempty set endowed with a proximity relation δ. Points $x, y \in X$ are *spatially distinct*, provided the closures of x and y are not near, *i.e.*, $\text{cl}\{x\} \underline{\delta} \text{cl}\{y\}$. ■

The anti-symmetric axiom T_0 (discovered by A. Kolmogorov) is defined as follows.

> $\boldsymbol{T_0}$: (a) For every pair of distinct points, at least one of them is far from the other, or
> (b) For every pair of distinct points in a topological space X, there exists an open set containing one of the points but not the other point (*cf.* (Alexandroff & Hopf, 1935, p. 58)).

The discovery of T_0 topologies in digital images hinges on what is meant by the observation that points are descriptively distinct.

Remark 4.2. Descriptively distinct points.
Let Φ be a set of probe functions that represent features of points x in a nonempty set X. Then let X be endowed with a descriptive proximity relation δ_Φ. Points x, y are *descriptively distinct*, provided x and y are spatially distinct and the feature vectors $\Phi(x)$ and $\Phi(y)$ are not equal. For example, points x, y in a digital image X are descriptively distinct (*descriptively far*), provided x and y are spatially distinct and have different descriptions, *i.e.*, $x \underline{\delta}_\Phi y$. ■

Let Φ be a set of probe functions representing features of members of a set and let $\varepsilon > 0$. There is a descriptive form of T_0 space (denoted by T_0^Φ). Let a *descriptive open neighbourhood* $N_{\Phi(x)}$ be defined by

$$N_{\Phi(x)} = \{y \in X : \Phi(x) = \Phi(y) \text{ and } |x - y| < \varepsilon\}.$$

That is, the description of each point in $N_{\Phi(x)}$ matches the description of x. Due to the spatial restriction $|x - y| < \varepsilon$, $N_{\Phi(x)}$ is also called a *bounded descriptive neighbourhood* (Peters, 2013*d*, §1.19.3).

> $\boldsymbol{T_0^\Phi}$: For every pair x, y of descriptively distinct points in a topological space X, there exists a descriptive open neighbourhood containing one of the points but not the other point.

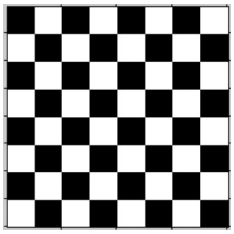

Figure 5. Sample visual space.

Example 4.1. T_0^Φ Visual space.
Let X be represented by the checkerboard in Figure 5 and let x, y be black and white points in X. It is easily verified that X is a topological space. Then let $N_{\Phi(x)}$ be a descriptive open neighbourhood of x. The point y is excluded from $N_{\Phi(x)}$, since $\Phi(x) \neq \Phi(y)$. This is true for every pair of descriptively distinct points in X. Hence, X is a T_0^Φ space. ■

> $\boldsymbol{T_1}$: A topological space is T_1 if, and only if, distinct points are not near.

> $\boldsymbol{T_1^\Phi}$: A topological space is T_1^Φ if, and only if, descriptively distinct points are not descriptively near.

Example 4.2. Checkerboard T_1^Φ space. Choose Φ to be a set of probe functions that represent greyscale and colour intensities of points in an image. Let a topological space X be represented by the checkerboard in Figure 5. X is an example of a visual T_1^Φ space. To see this, let $x, y \in X$ be points in black and white squares, respectively. The points x and y are descriptively distinct and $x \underline{\delta}_\Phi y$. In general, black and white pixels in X are descriptively distinct and not near, descriptively. Hence, the checkerboard is an example of a T_1^Φ space. ■

Lemma 4.1. *A digital image X endowed with a descriptive proximity δ_Φ such that X contains descriptively distinct points is a T_1^Φ space.*

Proof. Let X be a digital image (a set of points called pixels) endowed with a descriptive proximity δ_Φ. Choose Φ, a set of probe functions that represent features of points in X. Let points $x, y \in X$ be descriptively distinct. Then $x \underline{\delta}_\Phi y$, *i.e.*, x is descriptively not near y. Hence, X is a T_1^Φ space. □

Hausdorff observed that it is possible for a pair of distinct points to have distinct neighbourhoods and used this axiom in his work. The corresponding space with *pairs of distinct points belong to disjoint neighbourhoods* (Hausdorff, 1957*b*, §40.II) is now named after him and is called the T_2 or Hausdorff space.

T_2: A topological space is T_2, if and only if, distinct points have disjoint neighbourhoods (distinct points live in disjoint *houses*[4]).

There is a descriptive counterpart of a traditional T_2 space (denoted by T_2^{Φ}), introduced in (Peters, 2013*a*) (see, also, (Naimpally & Peters, 2013)). In a T_2^{Φ} space, one can observe that descriptively distinct points belong to disjoint descriptive neighbourhoods.

T_2^{Φ}: A topological space is T_2^{Φ} if, and only if, descriptively distinct points have disjoint descriptive neighbourhoods.

Example 4.3. A T_2^{Φ} Visual space. Choose Φ to be a set of probe functions that represent greyscale and colour intensities of points in an image. Let a topological space X again be represented by the checkerboard in Figure 5. X is an example of a visual T_2^{Φ} space. To see this, let $x, y \in X$ be points in black and white squares, respectively. Then consider a pair of descriptive neighbourhoods $N_{\Phi(x)}, N_{\Phi(y)}$ of x and y, respectively. Neighbourhood $N_{\Phi(x)}$ contains only points with descriptions that match the description of x, *i.e.*, $N_{\Phi(x)}$ contains only black points. Similarly, neighbourhood $N_{\Phi(y)}$ contains only points with descriptions that match the description of y, *i.e.*, $N_{\Phi(y)}$ contains only white points. Hence, $N_{\Phi(x)}, N_{\Phi(y)}$ are disjoint. ■

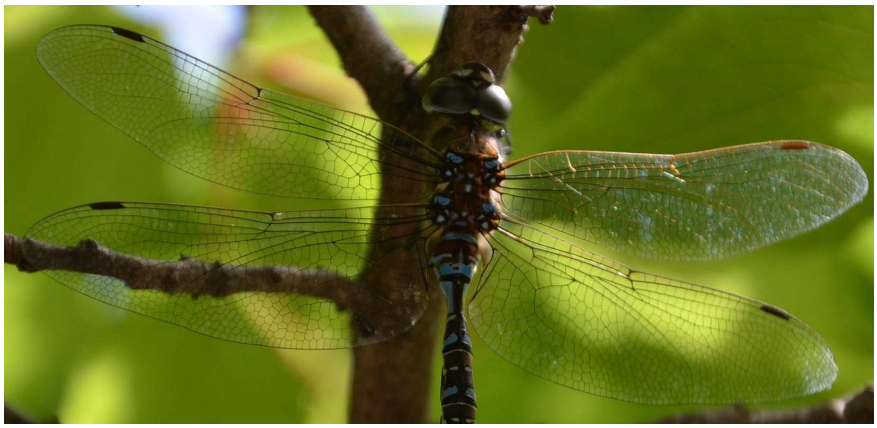

Figure 6. Manitoba dragonfly.

Observe that a T_2^{Φ} space is also a T_1^{Φ} space, since, by definition, descriptively distinct points are not near. The dragonfly in Figure 6 provides an illustration of a biology-based T_2^{Φ} space (see Example 4.4 for details). Also observe that a T_1^{Φ} space is also a T_0^{Φ} space, since, for every pair of descriptively distinct points, one can find a descriptive open set containing of the points and not containing the other point. The penultimate example of a T_1^{Φ} space that is also a T_0^{Φ} space is a

[4]A partition is a T_2 space if, and only if, every class has no more than one point, *i.e.*, every class is single tenant "house".

space where descriptively distinct points belong to open descriptive neighbourhoods. From these observations, observe that $T_2^\Phi \Rightarrow T_1^\Phi \Rightarrow T_0^\Phi$.

Let $\varepsilon \in \mathbb{R}$ such that $\varepsilon > 0$. A *bounded descriptive neighbourhood* $N_{\Phi(x)}$ of a point x in a set X is defined by

$$N_{\Phi(x)} = \{y \in X : d(\Phi(x), \Phi(y)) = 0 \text{ and } |x - y| < \varepsilon\},$$

where d is the taxicab distance between the descriptions of x and y, *i.e.*,

$$d(\Phi(x), \Phi(y)) = \sum_{i=1}^{n} |\phi_i(x) - \phi_i(y)| : \phi_i \in \Phi.$$

Theorem 4.1. *A digital image X endowed with a descriptive proximity δ_Φ such that X contains two or more descriptively distinct points is a T_2^Φ space.*

Proof. Let X be a digital image (a set of points called pixels) endowed with a descriptive proximity δ_Φ. Choose Φ, a set of probe functions that represent features of points in X. Let points $x, y \in X$ be descriptively distinct. Let $N_{\Phi(x)}, N_{\Phi(y)}$ be descriptive neighbourhoods of x, y, respectively. If $a \in N_{\Phi(x)}$, then $d(\Phi(a), \Phi(x)) = 0$, *i.e.*, each member of $N_{\Phi(x)}$ must descriptively match x. Similarly, each $b \in N_{\Phi(y)}$ descriptively matches y. Then, $N_{\Phi(x)} \cap N_{\Phi(y)} = \emptyset$. Hence, X is a T_2^Φ space. □

Figure 7. Dragonfly edges.

Example 4.4. Dragonfly T_2^Φ Shape space.
Choose Φ to be a set of probe functions that represent the gradient orientation of the points in an image. Let a topological space X be represented by the dragonfly in Figure 6, endowed with a descriptive proximity relation δ_Φ. X is an example of a complex visual T_2^Φ shape space. To see this, let $x, y \in X$ be points along the edges of the filtered dragonfly image in Figure 7. The points x and y are descriptively distinct, since these points have different gradient orientations. In addition, points x, y are centers of disjoint descriptive neighbourhoods $N_{\Phi(x)}, N_{\Phi(y)}$, respectively, in a T_2^Φ Shape Space.

Proof. We assume that $\Phi(x) \neq \Phi(y)$, *i.e.*, x and y have different gradient orientations in Figure 7. The descriptive neighbourhood $N_{\Phi(x)}$ of point x (with no spatial restriction) is defined by

$$N_{\Phi(x)} = \{a \in X : \Phi(x) = \Phi(a)\},$$

i.e., the gradient orientation of x matches the gradient orientation of each point a in $N_{\Phi(x)}$. Hence, $y \notin N_{\Phi(x)}$, since the gradient orientation of y does not match the gradient orientation of x. Similarly, observe that $x \notin N_{\Phi(y)}$. Then $N_{\Phi(x)}, N_{\Phi(y)}$ are disjoint. This is true of every pair of points in X that have unequal gradient orientations. Hence, X is an example of a descriptive T_2^{Φ} shape space. □

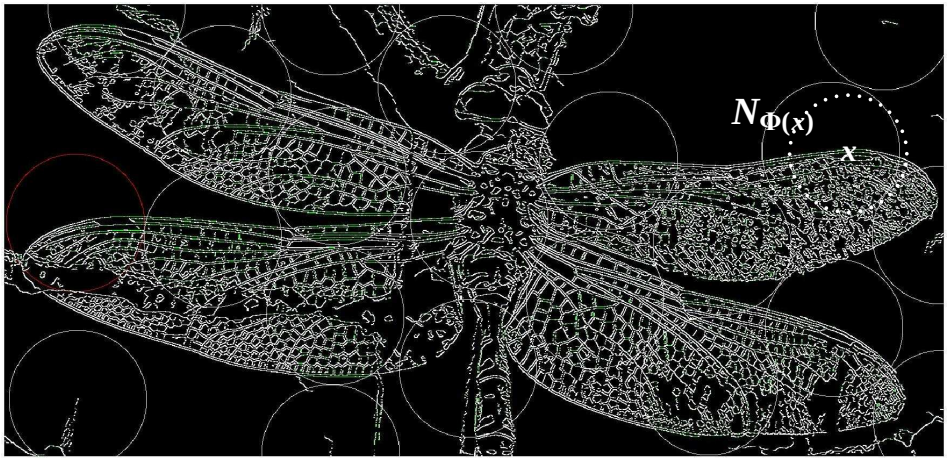

Figure 8. T_2^{Φ} Shape space.

Remark 4.3. $N_{\Phi(x)}$, T_2^{Φ} **Implementation details**.
A Matlab® 7.10.0 (R2010a) script written by C. Uchime has been used on the dragonfly image in Figure 6 to extract the edges shown in Figure 7. From Example 4.4, we know that the dragonfly in Figure 7 provides a basis for a T_2^{Φ} shape space. Next, bounded descriptive neighbourhoods $N_{\Phi(x)}, N_{\Phi(y)}$ of points x, y, respectively, are found by selecting x, y, radius ε, and pixel gradient orientation as the shape descriptor. For simplicity, only $N_{\Phi(x)}$ is shown in Figure 8.

Using C. Uchime's Matlab script, the selection of x, y is done manually by clicking on two points of interest on the dragonfly wings (see Figure 8). Starting with $N_{\Phi(x)}$, for example, the construction of the shape pattern $\mathfrak{P}_{\Phi}(N_{\Phi(x)})$ is carried out by using Matlab to search through the image for points (outside the motif neighbourhood) with gradient orientations that match the gradient orientation of x. For each pixel $x' \notin N_{\Phi(x)}$ such that $\Phi(x') = \Phi(x)$, a new neighbourhood is constructed. In practice, only a restricted number of neighbourhoods are found, namely, those neighbourhoods with centers that are reasonably close to the motif neighbourhood center x. ■

4.1. Descriptive nearness structures

Herrlich nearness structures are extended to descriptive nearness structures in this section. One begins the study of such structures by choosing Φ, a set of probe functions that represent features of members of a nonempty set X. Let X be endowed with a descriptive proximity relation Φ. By way of illustration, the honey bee in Figure 9 provides a basis for a shape nearness space relative to the bee image edges shown in Figure 10 (see Example 4.5 for details).

Figure 9. Bee

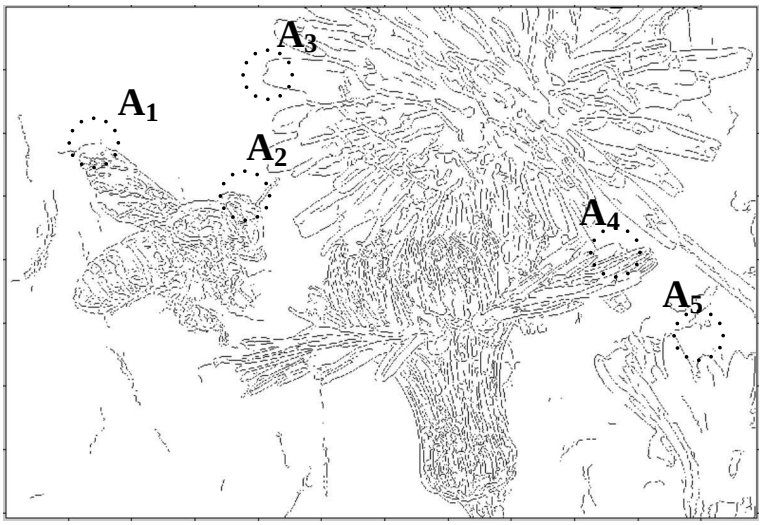

Figure 10. $\xi_\Phi = \{A_1, \ldots, A_5\}$

For descriptive nearness, we use the following notation.

$$
\begin{aligned}
X &= \text{ nonempty set of points,}\\
\Phi &= \{\text{probe functions representing features of } x \in X\},\\
\mathcal{A}, \mathcal{B} &\text{ denote collections of subsets in } X, \textit{ i.e.}, \mathcal{A}, \mathcal{B} \in \mathcal{P}^2(X),\\
Q(\mathcal{A}) &= \{Q(A) : A \in \mathcal{A}\},\\
\eta_\Phi \mathcal{A}, &\text{ or } \mathcal{A} \in \eta, \textit{ i.e.}, \text{ members of } \mathcal{A} \text{ are descriptively near,}\\
\underset{\Phi}{\eta}\, \mathcal{A}, &\textit{ i.e.}, \text{ members of } \mathcal{A} \text{ are not descriptively near,}\\
A\, \eta_\Phi\, B &= \eta_\Phi\{A, B\} \ (A \text{ descriptively near } B),\\
\mathcal{A} \vee \mathcal{B} &= \{A \cup B : A \in \mathcal{A}, B \in \mathcal{B}\},\\
cl_{\eta_\Phi} E &= \{x \in X : \{x, E\} \in \eta_\Phi\} \ (x \text{ descriptively near } E),\\
cl_{\eta_\Phi} \mathcal{A} &= \{cl_\eta A : Q(A) \in Q(\mathcal{A})\}.
\end{aligned}
$$

A descriptive nearness structure (denoted by ξ_Φ) is defined by

$$
\xi_\Phi = \left\{ \mathcal{A} \in \mathcal{P}^2(X) : \bigcap_\Phi \{A : A \in \mathcal{A}\} \neq \emptyset \right\}.
$$

In the following axioms, let $\mathcal{A} \in \xi_\Phi$. It can be shown that the descriptive nearness structure ξ_Φ satisfies (dN.1)-(dN.5):

(dN.1) $\bigcap_\Phi \{A : A \in \mathcal{A}\} \neq \emptyset \Rightarrow \eta_\Phi \mathcal{A}$ is not empty,
(dN.2) $\underset{\Phi}{\eta}\, \mathcal{A}$ and $\underset{\Phi}{\eta}\, \mathcal{B} \Rightarrow \underset{\Phi}{\eta}(\mathcal{A} \vee \mathcal{B})$,
(dN.3) $\eta_\Phi \mathcal{A}$ and, for each $B \in \mathcal{B}$, there is an $A \in \mathcal{A} : A \subset B \Rightarrow \eta_\Phi \mathcal{B}$,

(dN.4) $\emptyset \in \mathcal{A} \Rightarrow \underline{\eta}_{\Phi}\ \mathcal{A}$,
(dN.5) $\eta_{\Phi}(cl_{\eta}\mathcal{A}) \Rightarrow \eta_{\Phi}\mathcal{A}$ (descriptive Herrlich axiom).

Example 4.5. Descriptive Herrlich nearness.
Let the set X be represented by the set of edge pixels in Figure 10 and let Φ contain a single probe function representing pixel orientation. Each member of the collection of subsets $\mathcal{A}$ contains ridge pixels, where

$$\xi_{\Phi} = \mathcal{A} = \{A_1, A_2, A_3, A_4, A_5\},$$

since each pair of sets in $\mathcal{A}$ contain pixels with matching orientation. Observe that there are other collections of subsets $\mathcal{B}$ in Figure 10 containing pixels with matching orientations that are not the same as the pixels orientations in the subsets in $\mathcal{A}$. Hence, ξ_{Φ} contains more collections of descriptively near subsets that are not shown in Figure 10. ■

5. Visual patterns in descriptive separation spaces

Figure 11. T_2^{Φ}.

Visual patterns arise naturally from the different forms of descriptive separation spaces. We illustrate this in terms of patterns that naturally occur in T_1^{Φ} and T_2^{Φ} spaces. Let $\mathcal{P}^2(X)$ denote the set of collections of subsets in X and let pattern $\mathfrak{P} \in \mathcal{P}^2(X)$, motif $M \in \mathcal{P}(X)$. Let Φ be a set of probe functions that represent features of members of X and let X be endowed with a descriptive proximity δ_{Φ}. For example, the 1870 Punch dancing delivery boy image in Figure 11 provides a basis for a visual pattern (see Example 5.2 for details). Further, a visual pattern $\mathfrak{P}_{\Phi}$ is a descriptive motif pattern, provided the following axioms are satisfied.

(**motif**.1) Sets in $\mathfrak{P}_{\Phi}$ are pairwise disjoint.
(**motif**.2) A is descriptively near M ($A\ \delta_{\Phi}\ M$) for each $A \in \mathfrak{P}_{\Phi}$.
(**motif**.3) If there are pairs $A, B \in \mathfrak{P}_{\Phi}$ that are copies of M, there is an isometry[5] of the plane that maps A onto B.

A descriptive motif pattern is an example of what is known as a discrete pattern in the study of patterns in tilings and weaving (see, *e.g.*, (Grünbaum & Shepard, 1987)). Observing visual patterns in an image is aided by various forms of image filtering, sharpening the features of pixel neighbourhoods, making it more possible to detect those parts of an image that are either close or remote from each other.

[5]Let A and B be sets of pixels in digital images endowed with metrics d_X and d_Y. An *isometry* is a distance-preserving map (Beckman & Quarles, 1953). For any pair pixels $x, y \in A$ with descriptions $\Phi(x), \Phi(y)$ found in B (*i.e.*, $f(\Phi(x)), f(\Phi(y)) \in B$), a map $f : A \to B$ is an isometry, provided

$$d_Y(f(\Phi(x)), f(\Phi(y))) = d_X(\Phi(x), \Phi(y)).$$

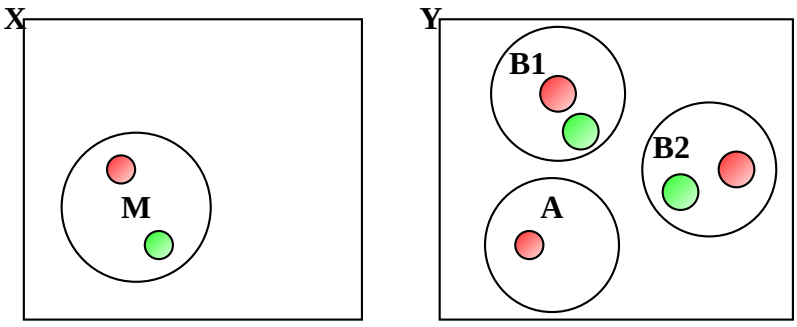

Figure 12. $\mathfrak{P}_\Phi = \{A, B1, B2\}$.

Example 5.1. Sample descriptive motif pattern.
Let sets of points X, Y endowed with a proximity relation δ be represented by Figure 12. Choose Φ to be a set of probe functions that represent greyscale and colour features of points in X, Y. The set M in Figure 12 represents a motif in a set pattern. Observe that $A, B1, B2$ are pairwise disjoint and each of the sets $A, B1, B2$ is descriptively near M. For example, M is descriptively near $B1$, since M and $B1$ contain subsets with red and green pixels. Again, for example, M is descriptively near A, since M and A contain subsets with red pixels. There is also an isometry between the descriptions of points in X and the descriptions of the points in Y. From these observation, we obtain the descriptive motif pattern $\mathfrak{P}_\Phi = \{A, B1, B2\}$. ■

5.1. Visual patterns in descriptive T1 spaces

To find visual patterns in descriptive T_1 spaces, do the following:

(1) Choose Φ, a set of probe functions representing features of points in a T_1^Φ space X.
(2) Select a pair of descriptively distinct points $x, y \in X$. By definition, $x \underline{\delta}_\Phi y$. Hence, the T_1^Φ space property is satisfied.
(3) Let M_1, M_2 denote point sets $\{x\}, \{y\}$, respectively.
(4) Determine all subsets of X containing points that descriptively match M_1 and then determine all subsets of points that descriptively match M_2.

As a result of the above steps, we can identify a pair of descriptive motif patterns $\mathfrak{P}_\Phi(M_1), \mathfrak{P}_\Phi(M_2)$ in a T_1^Φ space X. In addition, each such a motif pattern is a member of a descriptive Herrlich topology ξ_Φ defined on X.

Let X be endowed with a proximity δ_Φ such that X is a T_1^Φ space and let $M = \{x\}$ be a motif containing a single point $x \in X$, which defines a descriptive motif pattern $\mathfrak{P}_\Phi(M)$. If $A, B \in \mathfrak{P}_\Phi(M)$, then $A \underset{\Phi}{\cap} B \neq \emptyset$. From this, we obtain the following result.

Theorem 5.1. *Let (X, δ_Φ) be a T_1^Φ space with nearness structure ξ_Φ on X and let $\mathfrak{P}_\Phi(M)$ be a descriptive motif pattern determined by a motif M containing a single point x in X. Then $\mathfrak{P}_\Phi(M) \in \xi_\Phi$.*

5.2. Visual patterns in descriptive T2 spaces

To find visual patterns in descriptive T_2 spaces, do the following:

(1) Choose Φ, a set of probe functions representing features of points in a T_2^{Φ} space X.
(2) Select a pair of descriptively distinct points $x, y \in X$. By definition, $N_{\Phi(x)} \underline{\delta}_{\Phi} N_{\Phi(y)}$, since the description of each point in a descriptive neighbourhood matches the description of the point at the centre of the neighbourhood and $x \underline{\delta}_{\Phi} y$). That is, neighbourhoods $N_{\Phi(x)} \underline{\delta}_{\Phi} N_{\Phi(y)}$ are descriptively disjoint. Hence, the T_2^{Φ} space property is satisfied.
(3) Let M_1, M_2 denote neighbourhoods $N_{\Phi(x)} \underline{\delta}_{\Phi} N_{\Phi(y)}$, respectively.
(4) Determine all subsets of X that are descriptively near M_1 and then determine all subsets of X such that descriptively near M_2.

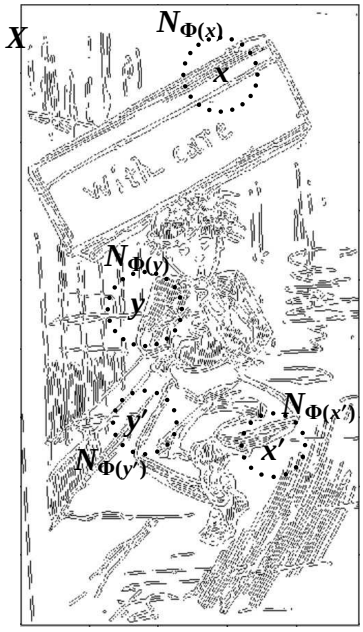

Figure 13. Sample T_2^{Φ} visual edge patterns.

As a result of the above steps, we can identify a pair of descriptive motif patterns $\mathfrak{P}_{\Phi}(M_1)$, $\mathfrak{P}_{\Phi}(M_2)$ in a T_2^{Φ} space X. In general, each such a motif pattern is not a member of the same descriptive Herrlich nearness structure ξ_{Φ} defined on X. To see this, consider a pair of neighbourhoods $N_{\Phi(x')}, N_{\Phi(x'')}$ that are descriptively near $N_{\Phi(x)}$. We know that $N_{\Phi(x)} \delta_{\Phi} N_{\Phi(x')}$ but it is possible that $N_{\Phi(x')} \underline{\delta}_{\Phi} N_{\Phi(x'')}$, if, for example, we compare pixel colours. $N_{\Phi(x)}$ may have a mixture of red and green colours, where $N_{\Phi(x')}$ has pixels with red colours but no green colours and $N_{\Phi(x'')}$ has pixels with green colours but no red colours. In other words, many different Herrlich nearness structures can be found in the same digital image.

Example 5.2. Edge motif pattern in T_2^{Φ} space.
Let X be the set of edge points in Figure 13, extracted from the 1870 Punch image in Figure 11,

using the edge function with the Canny filter[6] available in Matlab. Choose Φ to be a set of probe functions representing the orientation (gradient direction) of edge pixels in X. Observe that if pixels x, y in X have different orientations (*i.e.*, x and y are descriptively distinct), then $x \underline{\delta}_\Phi y$. Then $N_{\Phi(x)}, N_{\Phi(y)}$ are descriptively disjoint neighbourhoods. Hence, X is an example of T_2^Φ space.

Then let M_1, M_2 denote motif neighbourhood edge point sets $N_{\Phi(x)}, N_{\Phi(y)}$ of points x, y, respectively. An indication of the descriptive motif patterns $\mathfrak{P}_\Phi(M_1), \mathfrak{P}_\Phi(M_2)$ determined by M_1, M_2 is suggested by the edge regions containing points x', y'. In the pattern representing $\mathfrak{P}_\Phi(M_1)$, for example, notice that x' is the centre of bounded descriptive neighbourhood $N_{\Phi(x')}$ containing points with matching orientations. And the M_1 edge point neighbourhood is descriptively near $N_\Phi(x')$, since the orientation of one or more edges in $N_{\Phi(x)}$ match the orientation of one or more edges in $N_{\Phi(x')}$, *i.e.*,

$$N_{\Phi(x)} \, \delta_\Phi \, N_{\Phi(x')} : M_1 \doteqdot N_{\Phi(x)}.$$

Similarly, there is a descriptive neighbourhood $N_{\Phi(y')}$ in the edge pattern $\mathfrak{P}_\Phi(M_2)$ so that

$$N_{\Phi(y)} \, \delta_\Phi \, N_{\Phi(y')} : M_2 \doteqdot N_{\Phi(y)}.$$

Continuing this process, one can observe many other edge motif patterns in this particular T_2^Φ space. ■

Theorem 5.2. *A descriptive T_2^Φ space contains distinct descriptive motive patterns.*

Proof. Immediate from Lemma 4.1 and the definition of descriptive motif patterns. □

6. Stability in pattern constructions

A meaningful theory of stable pattern selection requires models of pattern-forming mechanisms that are simple enough to be understood in detail (Dee & Langer, 1983). An approach to achieving pattern selection stability in propagating patterns in either T_1 or T_2 spaces is introduced in this section. Basically in this study of descriptive patterns in a pair of digital images A, B, it is necessary to propagate a pattern in image B with some assurance that the pattern generated in B will belong to the class of images containing the image A and each new set added to a pattern does not wander or drift away from the pattern generator. That is, given a pattern generator M, each new set A added to pattern $\mathfrak{P}_\Phi(M)$ must be sufficiently near M, *spatially*.

P.E. Forsseén and D. Lowe observe that shape descriptors are reliable in detecting maximally stable extremal regions in digital images (Forsseén & Lowe, 2007, 1-8). In this work, descriptive motif set pattern growth is stable, provided the shape-based description of each set added to the pattern matches the shape-based description of the pattern motif. This interpretation of pattern stability is comparable to U. Grenander's notion of configuration transformation stability (Grenander, 1993, §4.1.1). To arrive at a formal definition of pattern stability, we introduce the descriptive distance between collections in terms of the Čech distance between sets.

[6] The Matlab canny filter is based on J.F. Canny's approach to edge detection introduced in his M.Sc. thesis completed in 1983 at the MIT Artificial Intelligence Laboratory (Canny, 1983). For details about this considered in the context of a topology of digital images, see (Peters, 2013*d*, §6.2).

Let $A, B \in C$ be nonempty sets in a space C and let

$$D(A, B) = \inf \{|a - b| : a \in A, b \in B\}$$

be the Čech distance between A and B. That is, a configuration transformation T on a configuration space C is stable, if, for any $\varepsilon > 0$, there exists a δ such that

$$D(A, B) \leq \delta \Rightarrow D(T(A), T(B)) \leq \varepsilon.$$

Let (X, δ_Φ) be a descriptive proximity Hausdorff space and let $A, B \in \mathcal{P}, \mathcal{A}, \mathcal{B} \in \mathcal{P}^2(X)$. Next, consider a descriptive form of a Grenander configuration transformation, namely, T_Φ. That is, the transformation $T_\Phi \doteqdot \mathfrak{P}_\Phi : \mathcal{P}(X) \to \mathcal{P}^2(X)$ is defined by

$$\mathfrak{P}_\Phi(M) = \mathcal{A} : M \, \delta_\Phi \, B \text{ for } B \in \mathcal{A}, \text{and } D(M, B) \leq \varepsilon.$$

Definition 6.1. Pattern stability sufficiently near criterion.
Let $\mathfrak{P}_\Phi(M)$ be a descriptive motif pattern constructed on a nonempty set X, $\varepsilon > 0$ and let $A \in \mathfrak{P}_\Phi(M)$. The pattern $\mathfrak{P}_\Phi(M)$ is stable, provided the distance requirement $D(M, A) < \varepsilon$ is satisfied. That is, $\mathfrak{P}_\Phi(M)$ is stable, provided A is *sufficiently near* M for each A added to $\mathfrak{P}_\Phi(M)$. ■

Let $B \ll A$ denote the fact that B is a *proximal neighbourhood* of A, provided $A \subset B$. From Def. 6.1, we obtain the following result.

Lemma 6.1. *Let $M \subset X$, a T_2^Φ space and let $\mathfrak{P}_\Phi(M)$ be a descriptive motif pattern. Let $A, B \in \mathfrak{P}_\Phi(M)$. $\mathfrak{P}_\Phi(M)$ is stable, if and only if, $D(M, A) < \varepsilon$ and $B \ll A$ implies $D(M, B) < \varepsilon$.*

From Def. 6.1 and Lemma 6.1, we obtain the following result.

Theorem 6.1. Descriptive pattern stability.
Let $\mathfrak{P}_\Phi$ be a pattern configuration transformation used to construct collections of patterns on X, a T_2^Φ space endowed with a descriptive proximity δ_Φ such that Φ is a set of probe functions representing shape descriptors, let $M \in \mathcal{P}(X)$, $\varepsilon > 0$. Then the following are equivalent.
(1) $\mathfrak{P}_\Phi(M)$ is stable.
(2) $D(M, A) < \varepsilon$ for each $A \in \mathfrak{P}_\Phi(M)$.
(3) $D(M, A) < \varepsilon$ and $B \ll A$ implies $D(M, B) < \varepsilon$.

Proof.
(1) ⇔ (2): $\mathfrak{P}_\Phi(M)$ is stable, if and only if, from Def. 6.1, $D(M, A) < \varepsilon$ for each $A \in \mathfrak{P}_\Phi(M)$.
(1) ⇔ (3): $\mathfrak{P}_\Phi(M)$ is stable, if and only if, from Lemma 6.1, $D(M, A) < \varepsilon$ and $B \ll A$ implies $D(M, B) < \varepsilon$.
(2) ⇔ (3): $D(M, A) < \varepsilon$ for each $A \in \mathfrak{P}_\Phi(M)$, if and only if, $B \in \mathfrak{P}_\Phi(M)$, provided $B \ll A$. □

Remark 6.1. Pattern stability and clustering stability.
Observe that descriptive pattern generation is a form of clustering. Recall that data clustering is a *natural grouping* of a set of patterns or points or objects (Jain, 2010). Let X be a T_2^Φ space and let $M \in \mathcal{P}(X)$. Then the use of M to generate the pattern $\mathfrak{P}_\Phi(M)$ can be considered a natural grouping

of sets in the pattern relative to the pattern generator M. That is, $A \in \mathfrak{P}_\Phi(M)$, provided $A\ \delta_\Phi\ M$. Hence, an obvious research path in the study of descriptive pattern generation is to consider the parallel between clustering stability (*e.g.*, (Ben-Hur *et al.*, 2002; Wang, 2010; Reizer, 2011)) and descriptive pattern generation stability. For example, it has been found (Ben-Hur *et al.*, 2002) that pairwise similarity between clusterings of sub-samples in a dataset provides a basis for clustering stability. A partial guarantee that descriptive pattern generation is stable, stems from the fact that $A \in \mathfrak{P}_\Phi(M)$, if and only if, A is descriptively near M. But this is only a partial guarantee of pattern generation stability, since subset similarity in a descriptive pattern does not prevent subsets from drifting or wandering away *spatially* from the pattern generator M. To achieve full descriptive pattern generation stability, we consider distance-based pattern generation in keeping with recent work on the stability of distance-based clustering (see,*e.g.*, (Wang, 2010)). In the distance-based approach to descriptive pattern stability, we introduce the *sufficiently near* criterion in Def. 6.1. ■

6.1. Multiple pattern generation stability

Since we are interested in constructing multiple patterns across disjoint regions of digital images that resemble each other in a T_2^Φ space, we introduce a stability criterion for the generation of multiple patterns. Again, the goal is to arrive at a view of stability of multiple patterns in a T_2^Φ space such that patterns do not wander or drift away from each other. Let $\mathcal{A}, \mathcal{B} \in \mathcal{P}^2(X)$ be collections containing sets $A, B \in \mathcal{P}(X)$, respectively. To complete the definition of pattern stability, we introduce the descriptive distance D_Φ, which a descriptive form of the distance between sets introduced by E. Čech (Čech, 1966, §18.A.2). The distance D_Φ is used to define the descriptive distance $\mathbb{D}_\Phi$ between collections of sets. The descriptive distance $\mathbb{D}_\Phi : \mathcal{P}^2(X) \times \mathcal{P}^2(X) \to \mathbb{R}$ between collections $\mathcal{A}, \mathcal{B}$ is defined by

$$\mathbb{D}_\Phi(\mathcal{A}, \mathcal{B}) = \inf \{D_\Phi(A, B) : A \in \mathcal{A}, B \in \mathcal{B}\}, \text{ where,}$$
$$D_\Phi(A, B) = \inf \{d(\Phi(a), \Phi(b)) : a \in A, b \in B\}.$$

The descriptive distance $\mathbb{D}_\Phi$ can be used to measure the distance between descriptive motif set patterns, since such patterns are collections of nonempty sets that are descriptively near each other. Let $\{A\}, \{B\}$ denote collections, each containing one set. Then $\mathfrak{P}_\Phi$ is a *stable descriptive pattern*, if, for any $\varepsilon > 0$, there exists a $\delta > 0$ such that

$$\mathbb{D}_\Phi(\{A\}, \{B\}) \leq \delta \ \Rightarrow \mathbb{D}_\Phi(\mathfrak{P}_\Phi(A), \mathfrak{P}_\Phi(B)) < \varepsilon.$$

That is, whenever sets A and B are descriptively near, then the corresponding patterns $\mathfrak{P}_\Phi(A), \mathfrak{P}_\Phi(B)$ are descriptively near. This form of set pattern stability works well in comparing regions of pairs of digital images, where we need to guarantee that the transformation that produces the descriptive set patterns in separate image regions is stable.

Definition 6.2. Multiple pattern stability criterion.
Let $\mathfrak{P}_\Phi$ be a pattern configuration transformation used to construct collections of patterns on X, a T_2^Φ space endowed with a descriptive proximity δ_Φ and let $\varepsilon > 0, \delta > 0$. Let $x, y \in X$ be distinct

points and let M_1, M_2 be disjoint neighbourhoods of x, y, respectively. Further, let $\mathcal{A}, \mathcal{B} \in \mathcal{P}^2(X)$. Patterns $\mathfrak{P}_\Phi(M_1) \in \mathcal{A}, \mathfrak{P}_\Phi(M_2) \in \mathcal{B}$ are stable, provided

$$\mathbb{D}_\Phi(\mathcal{A}, \mathcal{B}) \leq \delta \Rightarrow \mathbb{D}_\Phi(\mathfrak{P}_\Phi(M_1), \mathfrak{P}_\Phi(M_2)) < \varepsilon. \quad \blacksquare$$

To achieve stability in comparing image regions in the same digital image regions in pairs of images, it is necessary to consider pixel features that can be reliably matched, regardless of the appearance of the surroundings of a region. In this article, the focus is on constructing motif set patterns containing neighbourhoods of points defined by connected point sets that are straight edges. Neighbourhood selection is determined by the gradient orientation of the focal point of a pattern motif neighbourhood. The construction of a pattern motif (a descriptive neighbourhood of point) reduces to finding a connected set of points along an edge such that the edge points have matching gradient orientation. Hence, a gradient orientation-based motif set pattern results from finding neighbourhoods of points containing straight edges with pixel gradient orientations that match the gradient orientation of the points in the motif neighbourhood of the pattern.

Keeping in mind the underlying descriptive uniform topology in a Hausdorff T_2^Φ space X endowed with a descriptive proximity δ_Φ, an image pixel y belongs to a neighbourhood of point x, provided the gradient orientation of y matches the gradient orientation of x. Let Φ be a set of shape descriptors that includes pixel gradient orientation. In addition, let the descriptive neighbourhood $N_{\Phi(x)}$ be a pattern motif M that is a connected set of points belonging to a straight edge, *i.e.*, $y \in N_{\Phi(x)}$, provided $\Phi(y) = \Phi(x)$. Then the pattern $\mathfrak{P}_\Phi(M)$ is a collection of straight edges defined by

$$\mathfrak{P}_\Phi(M) = \left\{ N_{\Phi(y)} \in \mathcal{P}(X) : N_{\Phi(y)} \; \delta_\Phi \; M \right\}.$$

Pattern stability is achieved by guaranteeing that only matching straight edges belong to the pattern $\mathfrak{P}_\Phi(M)$. In comparing regions across pairs of digital images, stability is achieved by comparing straight edge patterns. Let $x, y \in X, Y$ be a pixels in a pair of digital images X, Y, respectively. Further, let $\mathfrak{P}_\Phi(M_1), \mathfrak{P}_\Phi(M_2)$ be straight edge shape patterns in images X, Y, respectively, such that $M_1 = N_{\Phi(x)}, M_2 = N_{\Phi(y)}$. Pattern $\mathfrak{P}_\Phi(M_x)$ is close to pattern $\mathfrak{P}_\Phi(M_y)$, provided the straight edges represented by neighbourhoods in the patterns have matching edge-neighbourhood motifs, *i.e.*,

$$\begin{aligned} &\mathfrak{P}_\Phi(M_1) \; \delta_\Phi \; \mathfrak{P}_\Phi(M_2), \text{ if and only if,} \\ &N_{\Phi(x)} \; \delta_\Phi \; N_{\Phi(y)}, \text{ if and only if,} \\ &\Phi(x) = \Phi(y). \end{aligned} \quad \blacksquare$$

From Def. 6.2 and Theorem 6.1, we obtain the following result.

Theorem 6.2. Multiple pattern generation stability.
Let $\mathfrak{P}_\Phi$ be a pattern configuration transformation used to construct collections of patterns on X, a T_2^Φ space endowed with a descriptive proximity δ_Φ such that Φ is a set of probe functions representing shape descriptors, let $M_1, M_2 \in \mathcal{P}(X)$, and let $\varepsilon > 0$. Further, let $\mathcal{A}, \mathcal{B} \in \mathcal{P}^2(X)$. Then the following are equivalent.
(1) $\mathfrak{P}_\Phi(M_1) \in \mathcal{A}, \mathfrak{P}_\Phi(M_2) \in \mathcal{B}$ *are stable.*
(2) $D(M_1, A) < \varepsilon, D(M_2, B) < \varepsilon$ *for each* $A \in \mathfrak{P}_\Phi(M_1)$ *and for each* $B \in \mathfrak{P}_\Phi(M_2)$.

6.2. Comparison with existing clustering stability analysis

One of the most widely used clustering techniques is k-means clustering. This is a non-hierarchical clustering approach, which aims to partition n p-dimensional observations into k clusters ($k \leq n$) by minimizing a measure of dispersion within the clusters. In k-means clustering, the selection of the number of clusters affects the clustering stability significantly (Ben-Hur *et al.*, 2002). Let k be the true number of clusters in an image. If the number of clusters is greater than k, then some of the true clusters will be split into smaller clusters during clustering. On the other hand, if the number of clusters is less than k, then some of the true clusters will be merged into bigger clusters during clustering. Both cases will lead to unstable clusterings. Hence, clustering stability can be used as a quality measure of the clustering algorithm.

Ben-Hur, Elisseeff and Guyon propose distribution of pairwise similarity between clusterings of sub-samples of a dataset as a stability measure of a partition (Ben-Hur *et al.*, 2002). Another notion of stability as proposed in (Lange *et al.*, 2004) is based on the average dissimilarity of solutions computed on two different data sets. While the aforementioned approaches focus on maximizing the within-cluster similarity and within-cluster dissimilarity, Wang proposes a new measure of the quality of clusterings based on the clustering instability from sample to sample (Wang, 2010). On the other hand, Reizer proposes to measure the quality of clustering through stability from sample to sample (Reizer, 2011).

In contrast to the traditional clustering methods, the descriptive-based pattern generation method proposed in this article does not require the number of clusters to be pre-determined. The pattern $\mathfrak{P}_\Phi(M)$ may grow as long as it satisfies the condition that each new set A added to pattern $\mathfrak{P}_\Phi(M)$ is sufficiently near M, both spatially and descriptively. However, similar to clustering stability, we may say that the pattern generation is stable, provided it produces similar patterns on data originating from the same source. Based on this argument, a definition for pattern stability can be derived from the clustering stability model given in (Reizer, 2011).

Since we are interested in determining when a generated pattern in a sample digital image Y serves as an indicator that Y belongs to the class of digital images represented by a pattern generated in a query image X, we define pattern stability in terms of the expected descriptive distance between $\mathfrak{P}_\Phi(M, X)$ (pattern generated in X) and $\mathfrak{P}_\Phi(M, Y)$ (pattern generated in Y).

Definition 6.3. Pattern Stability.
Let $th > 0$ denote an expectation threshold and let $E[\cdot]$ denote the expected value of $\cdot$. Further, let $\mathfrak{P}_\Phi(M, X)$ be a pattern generated by M in X and $\mathfrak{P}_\Phi(M, Y)$, pattern generated by M in Y. The *stability of any description-based pattern* $\mathfrak{P}_\Phi(M)$ (denoted by $Stab(\mathfrak{P}_\Phi(M))$) is defined by

$$Stab(\mathfrak{P}_\Phi(M)) = \begin{cases} 1, & \text{if } E\left[\mathbb{D}_\Phi(\mathfrak{P}_\Phi(M, X), \mathfrak{P}_\Phi(M, Y))\right] \leq th, \\ 0, & \text{otherwise } \mathfrak{P}_\Phi(M) \text{ is unstable.} \end{cases}$$

where X and Y are two independent samples from some unknown distribution. Pattern $\mathfrak{P}_\Phi(M)$ is stable, provided $Stab(\mathfrak{P}_\Phi(M)) = 1$. ■

Furthermore, given two patterns $\mathfrak{P}_\Phi(M_1)$ and $\mathfrak{P}_\Phi(M_2)$, pattern generation will be stable, provided $M_1 \underline{\delta}_\phi M_2$ *and* $Stab(\mathfrak{P}_\Phi(M_1)) = Stab(\mathfrak{P}_\Phi(M_2)) = 1$. In addition, for any set A, $A \delta_\Phi M_1$ and $A \underline{\delta}_\phi M_2$ will ensure that set A will always be added to pattern $\mathfrak{P}_\Phi(M_1)$. This is advantageous in

achieving pattern stability for the method proposed in this article compared to the traditional clustering methods such as k-means clustering, since pattern stability, in our case, derives its strength from the fact that each set A added to a pattern has *descriptive proximity* to the pattern generator M in a descriptive proximity space.

Acknowledgments

Research supported by Natural Sciences and Engineering Research Council of Canada (NSERC) grant 185986.

References

Alexandroff, P. and H. Hopf (1935). *Topologie*. Springer-Verlag. Berlin. xiii + 636pp.

Beckman, F. S. and D. A. Quarles (1953). On isometries of Euclidean space. *Proc. Amer. Math. Soc.* **4**, 810–815.

Ben-Hur, A., A. Elisseeff and I. Guyon (2002). A stability based method for discovering structure in clustered data. *Pacific Symp. on Biocomputing* **7**, 6–17.

Canny, J. F. (1983). Finding edges and lines in images. Master's thesis. MIT Artificial Intelligence Laboratory, supervisor: J.M. Brady. ftp://publications.ai.mit.edu/ai-publications/pdf/AITR-720.pdf.

Čech, E. (1966). *Topological Spaces, revised Ed. by Z. Frolik and M. Katětov*. John Wiley & Sons. London. 893pp.

Dee, G. and J. S. Langer (1983). Propagating pattern selection. *Physical Review Letters* **50**(6), 383–386.

Düntsch, I. and D. Vakarelov (2007). Region-based theory of discrete spaces: A proximity approach. *Ann. Math. Artif. Intell.* **49**, 5–14. doi: 10.1007/s10472-007-9064-3.

Efremovič, V. A. (1951). The geometry of priximity, I. *Mat. Sb.* **31**, 189–200.

Forsseén, P. E. and D. Lowe (2007, 1-8). Shape descriptors for maximally stable external regions. In: *Proc. IEEE Conf. on Computer Vision*. IEEE.

Grenander, U. (1993). *General Pattern Theory. A Mathematical Study of Regular Structures*. Oxford Univ. Press. Oxford, UK. xxi + 883 pp.

Grenander, U. (1996). *Elements of Pattern Theory. A Mathematical Study of Regular Structures*. Johns Hopkins Univ. Press. Baltimore, USA. xiii + 222 pp.

Grünbaum, B. and G. C. Shepard (1987). *Tilings and Patterns*. W.H. Freeman and Co.. New York. ix + 700 pp.

Hausdorff, F. (1957*a*). *Set Theory*. AMS Chelsea Publishing. Providence, RI. Mengenlehre, 1937, trans. by J.R. Aumann, *et al.*

Hausdorff, F. (1957*b*). *Set Theory, trans. by J.R. Aumann*. AMS Chelsea Publishing. Providence, RI. 352 pp.

Henry, C.J. (2010). Near Sets: Theory and Applications. PhD thesis. Dept. Elec. Comp. Engg. supervisor: J.F. Peters.

Jain, A. K. (2010). Data clustering: 50 years beyond k-means. *Pattern Recognition* **31**, 651–666.

Klette, R. and A. Rosenfeld (2004). *Digital Geometry. Geometric Methods for Digital Picture Analysis*. Morgan-Kaufmann Pub.. Amsterdam, The Netherlands.

Lange, Tilman, Volker Roth, Mikio L. Braun and Joachim M. Buhmann (2004). Stability-based validation of clustering solutions. *Neural computation* **16**(6), 1299–1323.

Leader, S. (1959). On clusters in proximity spaces. *Fundamenta Mathematicae* **47**, 205–213.

Naimpally, S. A. and J. F. Peters (2013). *Topology with Applications. Topological Spaces via Near and Far*. World Scientific. Singapore.

Peters, J. F. (2012). How near are Zdzisław Pawlak's paintings? Study of merotopic distances between digital picture regions-of-interest. In: *Rough Sets and Intelligent Systems* (A. Skowron and Z. Suraj, Eds.). pp. 89–114. Springer.

Peters, J. F. (2013*a*). Local near sets: Pattern discovery in proximity spaces. *Math. in Comp. Sci.* **7**(1), 87–106. doi: 10.1007/s11786-013-0143-z.

Peters, J. F. (2013*b*). Near sets: An introduction. *Math. in Comp. Sci.* **7**(1), 3–9. doi: 10.1007/s11786-013-0149-6.

Peters, J. F. (2013*c*). Nearness of sets in local admissible covers. Theory and application in micropalaeontology. *Fund. Inform.* **126**, 433–444. doi:10.3233/FI-2013-890.

Peters, J. F. (2013*d*). *Topology of Digital Images. Visual Pattern Discovery in Proximity Spaces*. Springer Intelligent Systems Reference Library. Berlin. vii+355pp, *to appear*.

Peters, J. F. and S. A. Naimpally (2012). Applications of near sets. *Amer. Math. Soc. Notices* **59**(4), 536–542. doi: `http://dx.doi.org/10.1090/noti817`.

Peters, J. F., S. Tiwari and R. Singh (2013). Approach merotopies and associated near sets. *Theory and Appl. of Math. & Comp. Sci.*

Reizer, G. V. (2011). Stability selection of the number of classes. Master's thesis. Dept. of Math. and Stat., Georgia State University. supervisor: Y. Fang.

Rocchi, N. (1969). *Parliamo Di Insiemi*. Instituto Didattico Editoriale Felsineo. Bologna, Italy. 316 pp.

Smith, A. R. (1995). A pixel is not a little square (and a voxel is not a little cube). Technical report. No. 6, Microsoft.

Thomas, R. S. D. (2009). Isonemal prefabrics with only parallel axes of symmetry. *Discrete Math.* **309**, 2696–2711.

Thron, W. J. (1966). *Topological Structures*. Holt, Rinehart and Winston. New York, USA. x+231pp.

Wang, J. (2010). Consistent selection of the number of clusters via crossvalidation. *Biometrika* **97**(4), 893–904.

Theory and Applications of Mathematics & Computer Science

(ISSN 2067-2764, EISSN 2247-6202)
http://www.uav.ro/applications/se/journal/index.php/tamcs

Theory and Applications of Mathematics & Computer Science 3 (2) (2013) 59–74

Analyzing Trends for Maintenance Request Process Assessment: Empirical Investigation in a Very Small Software Company

Zeljko Stojanov[a,*], Dalibor Dobrilovic[a], Jelena Stojanov[a]

[a]*University of Novi Sad, Technical Faculty "Mihajlo Pupin", Djure Djakovica BB, 23000 Zrenjanin, Serbia*

Abstract

Assessment and improvement of software maintenance processes in small software companies is very important because of large costs of maintenance and constraints of small software companies. This study presents an approach to assessment of software maintenance requests' processing in a very small local software company. The approach is context dependent and uses trend analysis and feedback sessions for assessing the current state of maintenance request processing. The analysis is based on various sources of data such as: internal repository of maintenance requests, company documents, transcribed records of interviews with company employees, and transcribed records of feedback sessions. Monthly trends for maintenance requests, working hours and types of maintenance tasks, by considering clients and software products are presented in the article. Identified trends were discussed during feedback sessions in the company. Participants in feedback sessions were company employees and researchers. During discussions of trends, some directions for further improvement of maintenance requests' processing were proposed. The article concludes with implications for practitioners from industry and researchers, as well as further research directions.

Keywords: software maintenance, process assessment, trend analysis, feedback session, very small software company.
ACM CCS: D.2.7 Distribution, Maintenance, and Enhancement, D.2.9 Management—Life cycle, K.6.3 Software Management—Software maintenance.

1. Introduction

Software maintenance includes all activities related to the preservation of consistency and efficiency of complex software systems. Maintenance consumes most of the costs of software systems (between 40% and 90% of the total costs) in software life-cycle (Lientz *et al.*, 1978; Kajko-Mattsson *et al.*, 2001; Abran *et al.*, 2004). Maintenance costs for systems that are in use for a very long time usually greatly exceed the costs of development. Despite that fact, software maintenance attracts less attention in scientific literature comparing to software development.

*Corresponding author
Email addresses: zeljko.stojanov@tfzr.rs (Zeljko Stojanov), ddobrilo@tfzr.rs (Dalibor Dobrilovic), jelena@tfzr.uns.ac.rs (Jelena Stojanov)

Software Maintenance is in literature recognized as the last phase in software life-cycle, which does not attract enough attention when compared with software development. Developers and managers consider maintenance requests as short-term jobs that should be done as quickly as it is possible (Junio *et al.*, 2011). Research on the maintenance process conducted with people involved in the process indicates that only 2.7% thought that the maintenance process is effective, while 70.2% of them believe that the maintenance process is ineffective (Sousa, 1998).

Small companies are dominant in economies across the globe (Richardson & von Wangenheim, 2007). U.S. Census Bureaus "1995 County Business Patterns" pointed that the vast majority of software and data processing companies are small, and that those with more than 50 employees comprise only a few percent of the total number (Fayad *et al.*, 2000). Laporte *et al.* (2006) reported that in Europe, 85% of IT sector companies have between 1 and 10 employees.

Small software companies are typically characterized as economically vulnerable with low budget to perform corrective post delivery maintenance, as well as with limited resources and the lack of knowledge and capacities to implement software process assessment and improvement activities (Laporte *et al.*, 2008). According to Vasilev (2012), rationalization of processes indirectly affects company business and reduces managerial costs. Small software companies have not adopted assessment directives proposed by software process improvement (SPI) models (Capability Maturity Model (CMM) and more recently CMMI) or intenational process-related standards (ISO 15504 and ISO 9001) (Fayad & Laitinen, 1997). Because of limitations in scale and resources, small software companies find software process improvement a major challenge that should be supported with short, light and tailored assessment methods (Mc Caffery *et al.*, 2007). Qualitative empirical study about the maintenance practice in local small software companies (companies from Timisoara and Zrenjanin), with the focus on collecting and processing client requests, revealed that they face many problems, both technical and organizational (Stojanov, 2011; Stojanov *et al.*, 2011; Stojanov, 2012*b*). Therefore, software maintenance practice assessment and improvement in these companies require more attention.

This paper presents an approach to maintenance assessment in a very small software company based on analyzing trends in available maintenance data. Practice assessment is based on a tailored lightweight approach with frequent feedback, with the following phases: initialization, planning, execution, and final reporting on assessment. Since the aim of this paper is to present the use of trend analysis as a valuable tool in process assessment, assessment phases will not be discussed in more details.

The research was conducted in a very small software company with seven employees (classified as micro enterprise according to (Commission, 2005)). This study is a part of a large project (from 2011 to 2014) with the aim to assess and improve maintenance practice in the selected software company. Data collected in the company through practice observation, interviews with programmers, and analysis of company documents and maintenance repository provide the basis for assessment of the maintenance practice. The objective of the paper is to present a light assessment approach of software maintenance practice based on trend analysis.

The paper is organized as follows. Section 2 contains related work that presents the use of trend analysis in software engineering. After that are described the context of the research in section 3, and analysis of maintenance trends in section 4. Discussion of results follows in section 5, while discussion of treats to validity is in section 6. The last section of the paper contains concluding

remarks with implications for research community and practitioners from industry, and further research directions.

2. Related work

Software maintenance trend analysis requires systematic data collection over an appropriate period. This is very important since maintenance requests occur randomly, and cannot be planned neither technically nor in budget. It is also important to note that maintenance workload cannot be managed using project management techniques (April, 2010).

Trend analysis can help in analyzing and controlling the activities and processes, and in assessing the efficiency of observed processes. Trend analysis is based on real empirical data and provides information of prime importance for organization (Buglear, 2001). A trend can be seen as an underlying longer-term movement in the observed data series. In addition, trend analysis is also important for providing evidence on deviations from trends. Trends are generally related to long-term observation and data collection, although the term "*long term*" is based on the subjective assessment (Chatfield, 1996). Kanoun & Laprie (1996) argued that trend analyses are usually applied intuitively and empirically rather than in quantified and well-defined manner. Results of trend analyses provide valuable information for assessing maintenance activities and workload of maintenance personnel.

In the paper (Kenmei *et al.*, 2008) is proposed a trend analysis approach of change requests based on time series analysis of data extracted from version control and bug tracking systems. The empirical study is based on data from three large-scale open source software projects (Eclipse, Mozilla and JBoss). The study proved that time series are efficient tools for modeling change request density and further trends in receiving new change requests.

The study (Ahmed & Gokhale, 2009) presented an approach to modelling the behaviour of bugs inside Linux kernels. The study included the analysis of bug distribution, lifetime, and clustering inside the kernel modules, as well as a deeper analysis of the statistical trends in the bug data from an architectural perspective. The aim of the study was to gain insight into the factors that impact system reliability. The analysis was related to: trends across the three releases of the kernel, the manner in which bugs were resolved, and on understanding the impact of bug severities on the resolution time of the bugs. From the architectural perspective of the kernel, the results of the study based on the statistical trends suggested that the module dependencies and interactions have higher impact on the bugs than the individual modules themselves.

April (2010) presented trend analysis of software maintenance services. Analysis includes supply and demand of software maintenance services. The research was conducted as a part of a process improvement activity in Integratik, an ERP development firm in Canada. The improvement aim is the implementation of maintenance request tracking process and information system. This process should ensure that each request would be recorded, dispatched and tracked formally, as well as time recording of maintenance personnel effort. In addition, this improvement ensured that the maintenance demands would be properly measured and analyzed. The author investigated trends related to distribution of requests per months, maintenance personnel effort per months, distribution of requests and work effort for particular software applications.

Zhu *et al.* (2011) proposed an approach for quality evolution monitoring based on the analysis of deviation trends of different modularity views of software. The approach includes monitoring the following views: package view that prescribes how developers intentionally group related source files as modules (packages), structural cluster view that reflects the nature of inter-file dependencies and method invocation relations, and semantic cluster view that reflects the nature of vocabulary used and topics involved in different source files and their correlations. The approach is based on an assumption that the deviation between different modularity views can influence quality evolution. If the views are properly aligned, the developers will be able to easily locate concepts and implement modifications. Deviation between different trends was measured with SiMo (Similarity between the Modularity views) metrics. Deviations for individual versions were computed and analyzed, and after that deviation trends in a sequence of versions were analyzed. The main activities in the approach are: construction of modularity views, computation of similarity metrics and analysis of deviation trends. Deviation trend of different modularity views is a combination of three change trends (i.e. rise, drop, hold) of three SiMo metrics, which is totally 27 patterns of deviation trends. Empirical study was conducted on three open-source Java systems, JFreeChart, JHotDraw and Jedit, that are available at SourceForge.net Subversion (SVN) repositories. Presented empirical study confirms that continuous monitoring of deviation trends provides useful feedback.

3. Context

Proper understanding of the assessment approach requires more detailed insight into the organizational context where the study is conducted. The approach is tailored to a selected small software company and therefore it is necessary to outline basic facts about the company.

This research was realized in a very small software company with seven employees (six programmers and one technical secretary). Software development and maintenance activities are organized in the way that one or more programmers are assigned to each software application. When a maintenance request (MR) is received from a client, it is forwarded to a programmer from a set of assigned programmers. Programmers' assignments to software applications are documented and available to all employees.

The company maintains over 30 business software applications used by local clients in Serbia. Clients are classified in two groups: clients that have signed Maintenance Service Agreement (MSA) and pay for maintenance services on the monthly basis, and clients that do not have signed MSA and pay for each maintenance service after its completion.

3.1. Maintenance request processing

Analysis of trends for a long period of time requires the existence of systematically collected data, and the process that is implemented and followed by all stakeholders. All requests are recorded in the internal software application with the repository for issues tracking (requests, tasks, work orders). Although a process is usually tailored for the current request and a user, a general process is defined and implemented in the company. The process includes the following steps: receiving and recording a request in the internal repository, sending a notification email with the request info to an appropriate programmer, checking a client's status in order to define

the priority of the request, assigning a programmer to a request, collecting additional information that is necessary for understanding and solving a request (if necessary), preparing a bid for work that is supposed to be done for clients that do not have signed MSA, and solving the request.

The request processing is completed when a client confirms correctness of finished work. In the repository is recorded who confirms the correctness, the date and the way of confirming. After that a working order is printed and sent to a client, and a request is labeled as closed.

3.2. Internal repository

The repository provides the efficient platform for storing and tracking tasks and maintenance requests. Practically, maintenance requests include all types of requests for maintenance, not only requests related to modification of software applications. In order to provide support for complete set of activities related to tracking requests, in the repository are also stored data about clients, software applications and work orders that are associated to requests. The repository is managed through an internal Web based application.

Issue tracking system does not contain only records for clients maintenance requests, but also records for all other, non-maintenance, tasks. However, analysis of all records for the period from May 2010 to November 2011 provides the evidence that 1896 tasks of totally 2252 tasks are related to software maintenance (84%), while 356 tasks are related to other activities (16%). A period of 19 months that begins two years after introducing the issue tracking system in the company is selected for the analysis. Discussions with programmers in the company confirmed that they are accustomed in using the system, which ensures extraction of more reliable data from the repository.

3.3. Programmers' working hours

Working hours spent on solving clients' requests provide the real basis for charging maintenance services. These working hours are hours that a programmer spends on a specific task associated to a request. In addition, these working hours are a part of a programmer's daily activities. Repository of MRs contains recorded working hours for each request. Three types of working hours exist in the repository: working hours spent in the company, working hours spent on Internet (activities that require Internet access to clients' information system), working hours spent at client side (in client's company). The total number of working hours can be calculated as a sum of these three types of working hours.

4. Maintenance trends analysis

Two sources of data were used for the trend analysis: company documents containing description of organizational structure of the company, and data extracted from the internal repository by using SQL script. Data about programmers' assignments to software applications, and the list of clients with MSA were extracted from company documents. Internal repository contains data about users' requests and other entities that are necessary to track all activities associated to each request. Data was extracted from tables `UserRequest`, `Worker` (programmers), `SoftwareApplication`, `User` (clients) and `WorkOrder`. In table 1 is presented the monthly distribution of solved (completed) maintenance requests used for the analysis in this paper, for clients

Table 1. Monthly distribution of solved maintenance requests

Month	Clients with MSA	Clients without MSA
5.2010.	43	17
6.2010.	37	29
7.2010.	52	24
8.2010.	57	16
9.2010.	42	18
10.2010.	80	18
11.2010.	94	28
12.2010.	88	41
1.2011.	73	49
2.2011.	85	33
3.2011.	85	44
4.2011.	88	30
5.2011.	57	28
6.2011.	60	35
7.2011.	64	30
8.2011.	83	39
9.2011.	49	30
10.2011.	78	54
11.2011.	70	48
Total	**1285**	**611**

with MSA and clients without MSA. The following trends can be drawn: (1) Clients with MSA submit more requests, which is expected since the costs of their requests usually fit the contracted amount in MSA, and (2) The average number of requests per month is 99.79, which practically means that all clients submit approximately four request per working day.

These trends do not provide enough information on maintenance requests' processing. Trends are too general, and therefore not suitable for more detailed analysis. However, these trends prove the high demand for maintenance services. In addition, these trends show that clients with MSA require more maintenance services than clients without MSA. In order to get deeper insight into maintenance trends it is necessary to include details about particular software applications that are maintained, about clients, and about types of maintenance tasks. This analysis enables detection of trends in demands for maintenance by various clients, discovery of distribution of requests per applications, and detection of trends for types of maintenance tasks.

4.1. Monthly trends for maintenance requests per client

Previous analysis shows that clients with MSA submit two times more requests. Therefore, it would be beneficial to find out the distribution of requests per clients, to find out clients with the highest demand for maintenance and based on that to suggest improved versions of MSA that will be tailored to each client or a group of clients. Detailed monthly trends with the number of requests for clients that submit more than five requests per month in average is presented in figure 1. Names of clients' companies are coded with letters *A*,*B*,*C*,*D* and *E* in order to preserve their anonymity according to guidelines for ethical issues in empirical studies in software engineering (Singer &

Table 2. Total and average number of MRs for clients with MSA

	Client A	Client B	Client C	Client D	Client E
Total number	171	170	95	184	142
Average	9.00	8.95	5.00	10.82	9.47

Vinson, 2002). It should be noted that clients D and E have zero requests in the beginning of observed interval because client D started to use software applications in July 2010 and client E in September 2010.

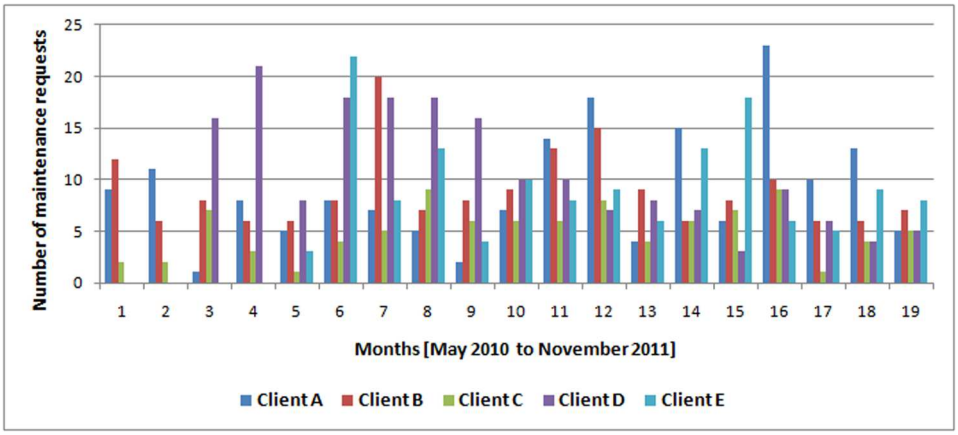

Figure 1. Monthly distribution of MRs for clients that submit more than five requests per month in average

Data presented in figure 1 are related to requests submitted by clients with MSA. Total number of requests, and the average number of requests per month for clients *A*,*B*,*C*,*D* and *E* are shown in table 2. Other clients with MSA submit smaller number of requests, but they submit them in each month.

Clients without MSA submit smaller number of requests than clients with MSA. In addition, they do not submit requests regularly. This means that there are longer periods of time without requests from them. Typical trends for requests submitted by clients (*K*,*M* and *N*) without MSA are presented in figure 2.

Trend analysis of the number of MRs for particular clients can be used for the proactive management of software maintenance activities. In addition, these data can be used also for improvement of policies in MSAs. Since trends for clients with MSA are regular, they could be also used as parameters for estimating future maintenance activities and workload. For clients without MSA it is very hard to draw any conclusion because of irregularity in trends.

Analysis of the number of working hours spent for each client shows the real state of the maintenance workload per client. Figure 3 shows the monthly distribution of working hours for selected clients with MSA.

The average number of working hours for clients *A*,*B*,*C*,*D* and *E* that have MSA per month, and the average number of working hours for clients *K*,*M* and *N* that do not have MSA are shown

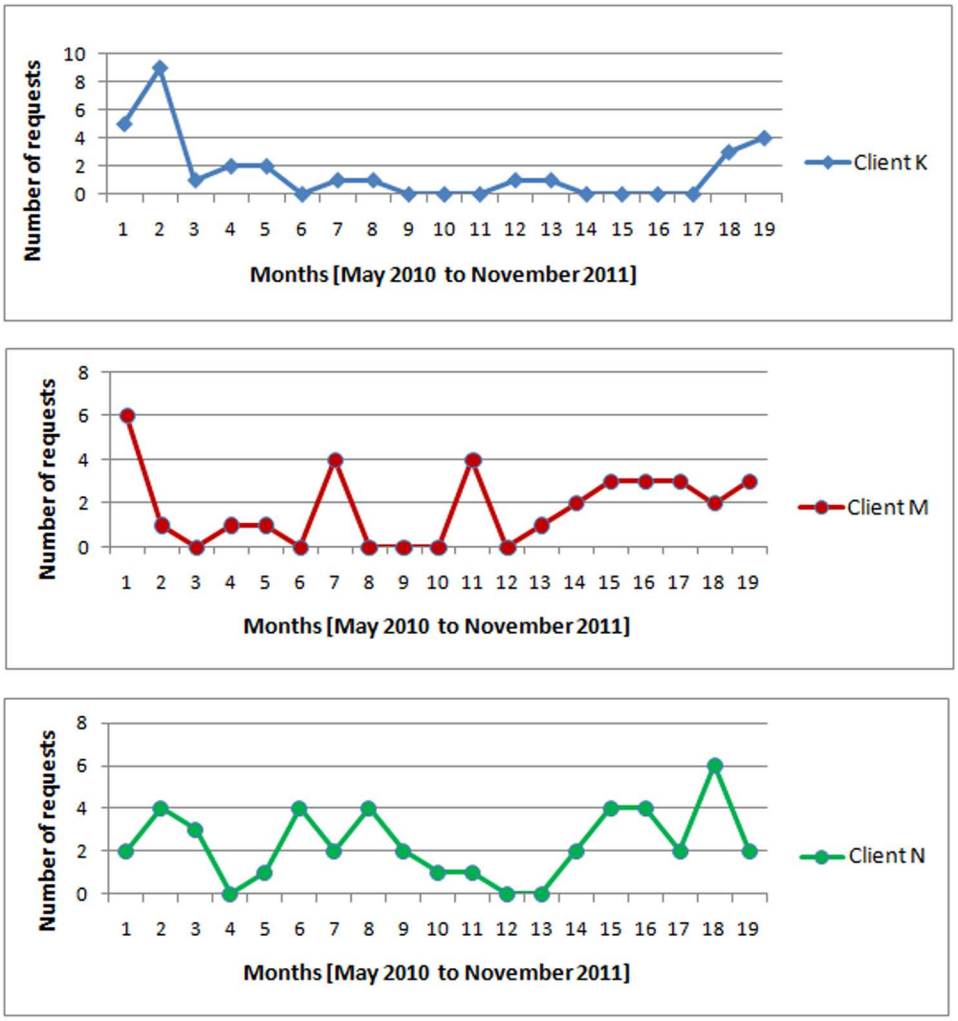

Figure 2. Typical MRs monthly trends for clients without MSA

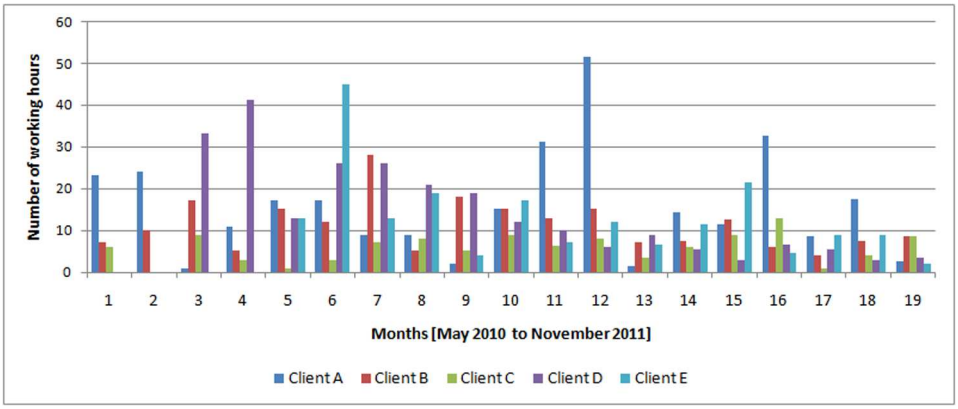

Figure 3. Monthly distribution of working hours for clients with MSA that submit more than five requests per month in average

Table 3. Average number of of working hours per month and per request for clients with MSA that submit more than five requests per month in average

	Client A	Client B	Client C	Client D	Client E
Average number of working hours per month	15.72	11.21	5.81	14.29	12.93
Average number of working hours per request	1.65	1.30	1.16	1¿,17	1.42

Table 4. Average number of of working hours per month and per request for clients without MSA

	Client K	Client M	Client N
Average number of working hours per month	1.13	2.61	1.76
Average number of working hours per request	0.44	0.92	0.64

in tables 3 and 4 respectively.

The first insight into the data related to clients and their requests suggests that clients with MSA consume more time and resources than clients without MSA. This is somehow expected, but directs the thinking towards tailoring appropriate service agreements for particular clients that have not signed agreements yet.

4.2. Monthly trends for maintenance requests per software application

Application portfolio consists of over 30 software applications used by local clients. Organization of maintenance activities is based on assignments of programmers to software applications, which is documented in the company. This means that when somebody receives a request, he/she knows who are potential programmers that should solve it. It is very important to know the distribution of MRs and working hours per software applications in order to improve the maintenance practice.

For that purpose was conducted trend analysis that shows the distribution of maintenance requests per applications, and the distribution of working hours per applications. Analysis disclosed that 75.84 percent of all requests are related to five software applications (named *app1*, *app2*, *app3*, *app4* and *app5*), while 87.39 percent of all requests are distributed to totally nine software applications (see figure 4).

Table 5 shows the average number of working hours per month for five most frequently used software applications, and the average number of working hours per request for these five applications.

4.3. Trends for types of maintenance tasks associated to requests

Classification of maintenance tasks, or maintenance types in the practice is subjected of several studies. From the first typology of software maintenance proposed by Swanson (1976), many authors have proposed different typologies. General agreement among the researchers and practitioners is that maintenance types are: corrective, perfective, adaptive and preventive. However, in practice, software organizations define their typologies according to their needs (Stojanov, 2012*a*).

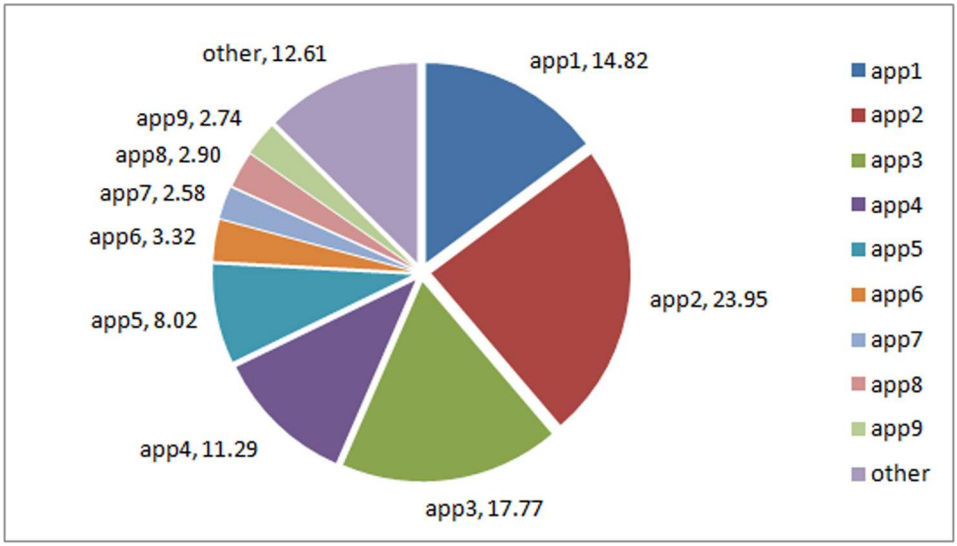

Figure 4. Monthly distribution of MRs per sotware applications

Table 5. Average number of working hours per month and per request for five most frequently used applications

	app1	**app2**	**app3**	**app4**	**app5**
Average number of working hours per month	19.05	33.07	20.91	19.99	9.51
Average number of working hours per request	1.20	1.41	1.18	1.78	1.10

Jones (2010) proposed the list of 23 types of maintenance tasks based on the best practice in industry.

In the selected small company, all maintenance tasks have been recorded in the internal repository. Despite of the large experience in industry, leading experts in the company have not proposed any classification of maintenance tasks based on proposals in available literature, but rather on their own experience and needs. In the repository are defined the following types of tasks: change (any type of change on software products), training, mandatory change (changes proposed by regulative and law), and all other tasks (updates, adaptations). However, more helpful analysis requires more detailed classification of maintenance tasks. For that purpose, general change tasks were manually classified by the company leading programmer in two groups: corrections tasks related to fixing detected faults, and enhancements tasks related to adding new features and other changes not related to faults. Classification was based on detailed description of tasks provided by clients and programmers.

The new classification schema for maintenance tasks is: corrections, enhancements, training, mandatory changes and other. Figure 5 presents trends for types of maintenance tasks in the company. The most of maintenance work is related to enhancing software product capabilities (60.18%), while corrections are related to 23.32% of all maintenance works. All other maintenance tasks contribute with about 10% .

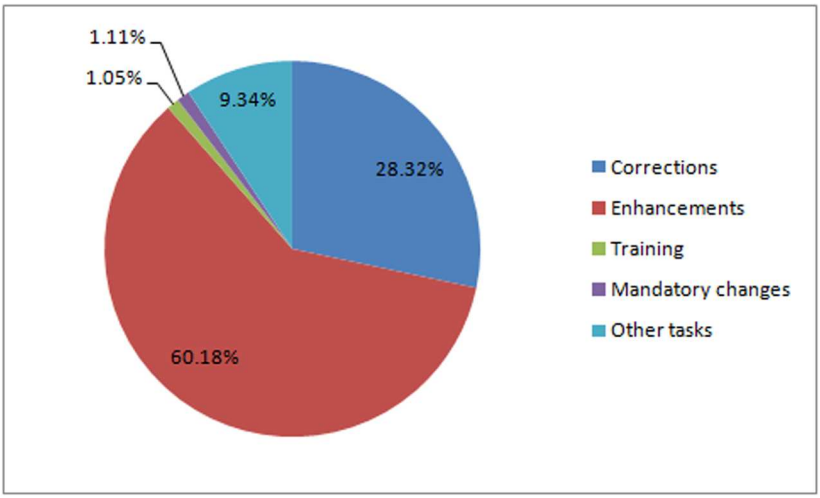

Figure 5. Trends for maintenance tasks

5. Discussion of results in the company

According to assessment plan, feedback meetings (sessions) were regularly organized in the company. Feedback meeting is an effective tool that helps in discussing the state of the assessment process, current findings, and further steps (Dyba *et al.*, 2004; Oktaba & Piattini, 2008). Hattie & Timperley (2007) argued that feedback provides directions for the current practice assessment, learning based on the experience, and further performance improvement.

Company manager and leading programmers participated in the feedback sessions. All sessions were prepared in advance in order to reflect the current state, discussions were type-recorded,

and records were later transcribed and analyzed. Session lasted between 30 and 60 minutes. Practically, sessions were semi-structured, which means that a session plan and initial discussion had been prepared in advance, but discussions during the sessions included many issues that had not been planed.

Discussions related to the analysis of the average number of working hours per clients revealed the following trends:

- Programmers spend approximately six times more time on average for the realization of requests submitted by clients with MSA. According to MSA, clients pay for contracted number of working hours on the monthly basis, and that makes them to feel more comfortable in submitting new requests.
- On the other hand, clients without MSA submits less requests. In addition, their requests require less time in average on the monthly basis.
- The next issues that is obvious is that MRs submitted by clients with MSA consume more time comparing to requests originated from clients without MSA. In addition, clients without MSA are less interested in the improvement of the software applications they use.

Discussions related to the analysis of the average number of working hours per software applications revealed the following trends:

- Software applications labeled with *app1* to *app5* are usually installed as comprehensive business solution for accounting and management of resources in organizations. This explains their dominance regarding the number of requests and consumed working hours. Other applications are not so frequently used and usually are sold as independent software solutions. This implies that the package of these applications should be considered as a candidate for tailoring a special type of MSA for clients that regularly use them, and to offer this option also to other clients.
- For software applications that consume less working hours, solutions that will increase their usability to clients should be identified, which will lead to increase of associated maintenance activities and, therefore, to increased profit to the company. There are few possible directions for further activities that will help in increasing the profit from software applications that are not regularly used: include them in integrated business software solutions, or retire some of them and introduce substitutions that are more attractive to clients.

Discussions related to the analysis of trends in maintenance tasks revealed that the most of the work is related to enhancements and corrections. However, data available in the repository are not suitable for detailed analysis of trends because maintenance tasks have not been properly differentiated.

5.1. Improvement directions

Software process assessment is usually considered in literature as the initial phase of a process improvement (Gray & Smith, 1998). Assessment leads to the identification of key process (practice) elements that need improvements, or towards identification of the strengths and weaknesses that should be considered during improvements' planning (von Wangenheim *et al.*, 2006). Based on the presented trend analysis, the following improvement directions are identified:

- Development of effort estimation models that will be useful in planning programmers' workload. These models will consider monthly distributions of maintenance requests per software applications and per clients and distribution of responsibilities in the company.
- Improvement of planning activities in the company related to distribution of workloads among programmers in order to achieve more efficient and faster processing of maintenance requests.
- Improvements of service agreements for clients. This direction includes proposing different types of MSA that will include various types of software applications. This will lead to portfolio of MSAs that are tailored for special clients' needs.
- Improvements of software applications portfolio management that will consider software applications that are irregularly used, and have very small number of maintenance requests.This direction includes planning the retirement of unsuccessful software and introduction of appropriate substitutions.
- Development of more detailed typology of maintenance tasks that will enable derivation of trends that will cross data about software applications, clients, programmers workload, and maintenance tasks.

6. Limitations and threats to validity

Discussion about internal end external validity, and any other possible limitation is mandatory for empirical studies (Kitchenham *et al.*, 2002).

Internal validity relates to the design of the research, consistency of analysis, and the influence of unexpected sources of bias. Analysis is based on trend analysis techniques that are easy to implement, but requires deeper understanding of the context and full engagement of both researchers (assessors) and company employees that perform the process. This is accomplished by joint work on proposing general improvement and assessment goals, selection of appropriate techniques and methods, and joint analysis of all findings during feedback meetings in the company. The problem with the bias is not addressed since the general goal of the study is practice assessment and improvement and we assume that company employees will provide the full assistance in order to achieve the best results for them. In addition, using rigorous data analysis methods based on traceable data minimized researchers' bias in the research.

The threat to the external validity primarily is related to applicability of this approach in other industrial settings. The approach assumes deeper understanding of the context and involvement

of all company employees in all phases of the research from planning, through collecting and analysing data, to discussing and presenting research findings. Since very small software companies have the similar problems in their business, the approach could be adapted to other small software companies, by considering specificity of their internal organization. The analysis process presented in this study could be also adapted to other, preferably small software companies or small teams. Subsequent applications of this approach would provide evidence about its validity and usefulness.

7. Conclusions

In this paper is presented an approach to software maintenance assessment based on trend analysis and feedback sessions. The study was conducted in a very small software company in Serbia, which is oriented towards local clients. Trend analysis includes analysis of maintenance requests' processing trends with the focus on the number of requests and working hours spent per clients and software applications, as well as simple analysis of maintenence tasks' trends.

The observations and conclusions from trend analysis will be used as directions for process improvement activities in the company. Both technical and organizational issues in the company are subject of improvement based on the results of trend analysis. For example, improvement of client service agreements is the obvious directions for practice improvement related to organizational issues. Improvement of the practice can be achieved also by proposing effort estimation models based on the current trends, such as the model presented by Stojanov *et al.* (2013). The next direction for practice improvement is related to development of more detailed typology of maintenance tasks that will enable analysis of trends for various types of tasks regarding software applications and clients.

The main contribution of the presented approach is related to implementation of assessment method based on trend analysis tailored to a very small software company. The method is based on collecting field data from company maintenance repository, analyzing data by using trend analysis, and identification of relevant conclusions and directions for further improvements of the maintenance practice. The next contribution is detailed presentation of trend analysis as a part of assessment method tailored to specific context, which will be helpful for other small software companies.

The approach is designed for small software companies or teams, and can be tailored to other similar settings. Findings of this research contain lessons that can be used by software practitioners in small software companies in order to assess and improve their decision-making and maintenance requests' processing. On the other hand, researchers could find some useful guidelines how to conduct *light* maintenance assessment based on trend analysis by considering given context.

Further work includes developing a formal model of light assessment approach for software maintenance in very small software companies, and adaptation and implementation of the approach in other similar settings. This will provide the opportunity to replicate the research in order to validate usability of presented approach. The next promising research direction is related to adapting this assessment approach to other processes in small software companies, or to companies that are mostly oriented towards outsourcing of products and services.

Acknowledgement

Ministry of Education and Science, Republic of Serbia, supports this research under the project "*The development of software tools for business process analysis and improvement*", project number TR32044, 2011-2014.

References

Abran, Alain, Bourque, Pierre, Dupuis, Robert, Moore, James W. and Tripp, Leonard L., Eds. (2004). *Guide to the Software Engineering Body of Knowledge (SWEBOK)*. 2004 version ed.. IEEE Press. Piscataway, NJ, USA.

Ahmed, Mohamed F. and Swapna S. Gokhale (2009). Linux bugs: Life cycle, resolution and architectural analysis. *Information and Software Technology* **51**(11), 1618–1627.

April, Alain (2010). Studying supply and demand of software maintenance and evolution services. In: *Proceedings of the 2010 Seventh International Conference on the Quality of Information and Communications Technology*. QUATIC '10. pp. 352–357.

Buglear, John (2001). *Stats means business: a guide to business statistics*. Buttworth-Heinemann. Oxford, UK.

Chatfield, Christopher (1996). *The analysis of time series: an introduction*. Texts in statistical science. fifth edition ed.. Chapman & Hall. London, UK.

Commission, European (2005). *The new SME definition: user guide and model declaration*. Enterprise and industry publications. Office for Official Publications of the European Communities. url: http://ec.europa.eu/enterprise/policies/sme/files/sme_definition/sme_user_guide_en.pdf [accessed 17.2.2013.].

Dyba, Tore, Torgeir Dingsoyr and Nils Brede Moe (2004). *Process Improvement in Practice - A Handbook for IT Companies*. Vol. 9 of *International Series in Software Engineering*. Kluwer Academic Publishers. Norwell, MA, USA.

Fayad, Mohamed E. and Mauri Laitinen (1997). Process assessment considered wasteful. *Communications of the ACM* **40**(11), 125–128.

Fayad, Mohamed E., Mauri Laitinen and Robert P. Ward (2000). Thinking objectively: software engineering in the small. *Communications of the ACM* **43**(3), 115–118.

Gray, E. M. and W. L. Smith (1998). On the limitations of software process assessment and the recognition of a required re-orientation for global process improvement. *Software Quality Control* **7**(1), 21–34.

Hattie, John and Helen Timperley (2007). The power of feedback. *Review of Educational Research* **77**(1), 81–112.

Jones, Capers (2010). *Software Engineering Best Practices*. McGraw-Hill, Inc.. New York, NY, USA.

Junio, Gladston Aparecido, Marcelo Nassau Malta, Humberto de Almeida Mossri, Humberto T. Marques-Neto and Marco Tulio Valente (2011). On the benefits of planning and grouping software maintenance requests. In: *15th European Conference on Software Maintenance and Reengineering*. pp. 55–64.

Kajko-Mattsson, Mira, Ulf Westblom, Stefan Forssander, Gunnar Andersson, Mats Medin, Sari Ebarasi, Tord Fahlgren, Sven-Erik Johansson, Stefan Törnquist and Margareta Holmgren (2001). Taxonomy of problem management activities. In: *Proceedings of the Fifth European Conference on Software Maintenance and Reengineering (CSMR '01)*. Lisbon, Portugal. pp. 1–10.

Kanoun, Karama and Jean-Claude Laprie (1996). Trend analysis. In: *Handbook of Software Reliability Engineering* (Michael R. Lyu, Ed.). Chap. 10, pp. 401–437. IEEE Computer Society Press and McGraw-Hill. New York, USA.

Kenmei, Benedicte, Giuliano Antoniol and Massimiliano di Penta (2008). Trend analysis and issue prediction in large-scale open source systems. In: *Proceedings of the 2008 12th European Conference on Software Maintenance and Reengineering*. CSMR '08. Athens, Greece. pp. 73–82.

Kitchenham, Barbara A., Shari Lawrence Pfleeger, Lesley M. Pickard, Peter W. Jones, David C. Hoaglin, Khaled El

Emam and Jarrett Rosenberg (2002). Preliminary guidelines for empirical research in software engineering. *IEEE Transactions on Software Engineering* **28**(8), 721–734.

Laporte, Claude Y., Alain Renault, Simon Alexandre and Tanin Uthayanaka (2006). The application of iso/iec jtc 1/sc7 software engineering standards in very small enterprises. *ISO Focus* (September), 36–38.

Laporte, Claude Y., Simon Alexandre and Rory V. OConnor (2008). A software engineering lifecycle standard for very small enterprises. In: *Software Process Improvement* (Rory V. OConnor, Nathan Baddoo, Kari Smolander and Richard Messnarz, Eds.). Vol. 16 of *Communications in Computer and Information Science*. pp. 129–141. Springer Berlin Heidelberg.

Lientz, B. P., E. B. Swanson and G. E. Tompkins (1978). Characteristics of application software maintenance. *Communications of the ACM* **21**(6), 466–471.

Mc Caffery, Fergal, Philip S. Taylor and Gerry Coleman (2007). Adept: A unified assessment method for small software companies. *IEEE Software* **24**(1), 24–31.

Oktaba, Hanna and Piattini, Mario, Eds. (2008). *Software Process Improvement for Small and Medium Enterprises: Techniques and Case Studies*. 1st ed.. Information Science Reference - Imprint of: IGI Publishing. Hershey, PA, USA.

Richardson, Ita and Christiane Gresse von Wangenheim (2007). Guest editors' introduction: Why are small software organizations different?. *IEEE Software* **24**(1), 18–22.

Singer, Janice and Norman G. Vinson (2002). Ethical issues in empirical studies of software engineering. *IEEE Transactions on Software Engineering* **28**(12), 1171–1180.

Sousa, Maria Joao (1998). A survey on the software maintenance process. In: *Proceedings of the International Conference on Software Maintenance*. ICSM '98. Bethesda, MD, USA. pp. 265–274.

Stojanov, Zeljko (2011). Discovering automation level of software change request process from qualitative empirical data. In: *Proceedings of the 6th IEEE International Symposium on Applied Computational Intelligence and Informatics, SACI 2011*. Timisoara, Romania. pp. 51–56.

Stojanov, Zeljko (2012*a*). *Software change management methods improvement: Integration of service for specifying change requests in software product model*. Lambert Academic Publishing. Saarbrcken, Germany.

Stojanov, Zeljko (2012*b*). Using qualitative research to explore automation level of software change request process: A study on very small software companies. *Scientific Bulletin of The Politehnica University of Timisoara, Transactions on Automatic Control and Computer Science* **57 (71)**(1), 31–40.

Stojanov, Zeljko, Dalibor Dobrilovic and Vesna Jevtic (2011). Identifying properties of software change request process: Qualitative investigation in very small software companies. In: *Proceedings of the 9th IEEE International Symposium on Intelligent Systems and Informatics, SiSY 2011*. Subotica, Serbia. pp. 47–52.

Stojanov, Zeljko, Dalibor Dobrilovic, Jelena Stojanov and Vesna Jevtic (2013). Context dependent maintenance effort estimation: Case study in a small software company. In: *IEEE 8th International Symposium on Applied Computational Intelligence and Informatics (SACI 2013)*. Timisoara, Romania. pp. 461–466.

Swanson, E. Burton (1976). The dimensions of maintenance. In: *Proceedings of the 2nd international conference on Software engineering (ICSE '76)*. pp. 492–497.

Vasilev, Julian (2012). Guidelines for improvement information processes in commerce by implementing the link between a web application and cash registers. *Theory and Applications of Mathematics & Computer Science* **2**(2), 55–66.

von Wangenheim, Christiane Gresse, Alessandra Anacleto and Clenio F. Salviano (2006). Helping small companies assess software processes. *IEEE Software* **23**(1), 91–98.

Zhu, Tianmei, Yijian Wu, Xin Peng, Zhenchang Xing and Wenyun Zhao (2011). Monitoring software quality evolution by analyzing deviation trends of modularity views. In: *Proceedings of the 2011 18th Working Conference on Reverse Engineering*. WCRE '11. Limerick, Ireland. pp. 229–238.

Theory and Applications of Mathematics & Computer Science

(ISSN 2067-2764, EISSN 2247-6202)
http://www.uav.ro/applications/se/journal/index.php/tamcs

Theory and Applications of Mathematics & Computer Science 3 (2) (2013) 75–92

Steady Non Isothermal Two-Dimensional Flow of Newtonian Fluid in a Stenosed Channel

A. M. Siddiqui[a], T. Haroon[b], A. A. Mirza[b,*], A. R. Ansari[c]

[a]*Department of Mathematics, York Campus, Pennsylvania State University, York, PA 17403, United States*
[b]*COMSATS Institute of Information Technology, Park Road,Chak Shahzad, Islamabad, Pakistan*
[c]*Department of Mathematics & Natural Sciences, Gulf University for Science & Technology, P.O. Box 7207, Hawally 32093, Kuwait*

Abstract

In this paper, the steady two-dimensional motion of an incompressible Newtonian fluid between two parallel plates with heat transfer in the presence of a cosine shaped stenosis is studied. The governing equations are transformed into a compatibility and energy equations, which is solved analytically with the help of the regular perturbation technique. The solutions obtained from the present analysis are given in terms of streamlines, wall shear stress, separation and reattachment points, pressure and temperature distributions through the stenosed channel. The accuracy of the results are verified from available literature. It is found that the wall shear stress, pressure gradient and temperature increase with the development of the stenosis, causing separation and reattachment points in the region. It is also observed that even at low velocity, separation occurs if the thickness of the stenosis is increased. We present the results in graphical form.

Keywords: Newtonian fluid, stenosis, heat transfer.
2010 MSC: 76-XX.

1. Introduction

The motivation of this study comes from the investigation of abnormal blood flow in a stenosed artery, which may be due to atherosclerotic plaques developed at various locations in the artery. Its effect on the flow of blood is discussed by many authors theoretically, experimentally as well as numerically. Forrester and Young (Forrester & Young, 1970) presented the theoretical as well as experimental results of an axisymmetric, steady flow through a converging and diverging tube with mild stenosis. It is observed that there is an abundant amount of evidence to support the conclusion that the abnormal flow conditions developed in a stenotic obstruction can be an important

*Corresponding author
Email address: azharali_mirza1@yahoo.com (A. A. Mirza)

factor in the development and progression of arterial disease. Further indicate that even a mild collarlike stenosis in a small artery can create significant abnormalities in the flow. Morgan and Young (Morgan & Young, 1974) provided the approximate analytical solution of axisymmetric, steady flow of incompressible Newtonian fluid both for mild and severe stenosis by using an integral method; basically they presented the extension of Forrester (Forrester & Young, 1970). It is observed that even a mild stenosis can cause a radical alteration in flow characteristics and that the effect in general becomes more drastic as the stenosis becomes more severe and the Reynolds number increases and also wall shearing stress is especially affected. Analysis of blood flow using an incompressible Newtonian fluid through an axisymmetric stenosed artery of cosine shape has been done by K. Haldar (Haldar, 1991). It is shown that for any given Reynolds number or tube constriction the separation point moves towards the throat of the tube and the reattachment point moves downstream with the enlargement of the region of separation which is physiologically unfavorable. Layek and Midya (Layek & Midya, 2007) presented the numerical solution of a time dependent incompressible Newtonian fluid for symmetric stenosis in a two dimensional channel. It is noticed that the maximum stress and the length of the recirculating region associated with two shear layers of the constriction increase with the increase of the area reduction of the constriction. It is observed that the critical values for three constriction heights $h = 0.25, 0.3, 0, 35$ are $600, 300, 210$ respectively. Chow et al. (Chow *et al.*, 1971) analyzed the steady laminar flow of an incompressible Newtonian fluid for different physical parameters by considering a sinusoidal boundary. It is observed that by increasing either Re or ϵ, the separation point would move down towards the throat in the divergent part of the channel with subsequent enlargement of the region of separation. Lee and Fung (Lee & Fung, 1970) solved the flow model of the Newtonian fluid numerically through locally constricted tube for the low Reynolds number. The constraints in their numerical procedure restricted the shape of the tube to be fixed and the Reynolds number to be moderate. Haldar (Haldar, 1985) discussed the effect of the shape of constriction on the resistance of blood flow through an artery with mild local narrowing. It is shown that the resistance to flow decreases as the shape of the stenosis changes and maximum resistance is attained for symmetric stenosis. S. Chakravarty and A. Ghosh Chakravarty (Chakravarty & Chakravarty, 1988) presented analytical solutions by considering an anisotropically elastic cylindrical tube filled with viscous incompressible fluid representing blood having stenosis. The analysis is carried out for an artery with mild local narrowing in its lumen forming a stenosis. K. Haldar (Kruszewski *et al.*, 2008) studied the oscillatory flow of blood which behaves as a Newtonian fluid having surface roughness of cosine shape. It is observed that the resistive impedance and wall shear stress increases as the phase lag increases for a particular value of stenosis height. It is also observed that impedance and wall shear stress increases with the increase in the stenosis height. Newman et al. (Newman *et al.*, 1979) investigated the oscillatory flow numerically in a rigid tube with stenosis. The predictions of the numerical results agreed well with the experimental works. This paper deals with the problem of oscillatory blood flow through a rigid tube with a mild constriction under a simple-harmonic pressure gradient examines the effect of stenosis on the flow field by considering blood as a Newtonian fluid. Mehrotra et al. (Mehrotra *et al.*, 1985) presented analysis by considering the flow in a stenotic tube where the cross-section is elliptic. It is observed that the theoretical study of pulsatile flow in a stenotic tube confirms the view that the fluid dynamics characteristics of the flow are affected by the percentage of stenosis as well as the geometry of the stenosis. The

frequency of oscillation also influences the shearing stress. Srivastava and Rastogi (Srivastava & Rastogi, 2010) investigated the blood flow through narrow catheterized artery with an axially nonsymmetrical stenosis. It is found that the flow resistance increases with the catheter size, the hematocrit and the stenosis size but decreases with the shape parameter. A significant increase in the magnitude of the impedance and the wall shear stress occurs even for a small increase in the catheter size. The shear stress at the stenosis throat decreases with the increasing catheter size. The abnormal flow conditions developed due to stenosis can be an important factor in the development and progression of arterial diseases. Some of the further major complications developed through these stenosis are the growth of tissues into arteries, development of an intravascular clot and post-stenotic dilatation. This type of flow also has applications in various fields like physiological flows and polymer science.

In the present paper, the effect of stenosis height and Reynolds number on flow characteristics, wall shear stress, pressure gradient, separation and reattachment points and heat transfer are analyzed. The study of the Peclet number and Brinkman number on the temperature distribution is also presented. It is observed that the general pattern of flow is similar to the results given in (Haldar, 1991) - (Chow *et al.*, 1971). The results of the present investigation indicate that even a mild collar like stenosis in a small artery can create significant abnormalities in the flow including the phenomenon of separation. This study presents the steady, two-dimensional motion of an incompressible Newtonian fluid in a cosine shaped stenosed channel with heat transfer. In this analysis blood is assumed as Newtonian fluid and the geometry of the artery is approximated by a channel. The layout of the paper is as follows: The basic equations governing the flow, in the Cartesian coordinate, are given in section 2. Problem formulation is presented in Section 3. In Section 4 the method is discussed and section 5 is dedicated the solution for different parameters. Section 6 provides a graphical discussion. A summary is given in section 7.

2. Governing equations

The basic governing equations for steady two dimensional flow of a non-isothermal, incompressible linearly viscous fluid in the absence of body forces are

$$\widetilde{\nabla} \cdot \widetilde{\mathbf{V}} = 0, \tag{2.1}$$

$$\rho \frac{d\widetilde{\mathbf{V}}}{dt} = -\widetilde{\nabla}\widetilde{p} + \widetilde{\nabla}\widetilde{\tau}, \tag{2.2}$$

$$\rho c_p \frac{d\widetilde{T}}{dt} = \kappa \widetilde{\nabla}^2 \widetilde{T} + \phi, \tag{2.3}$$

where $\widetilde{\mathbf{V}}$, $\widetilde{T}$ and ρ are the velocity vector, temperature and constant density of the fluid respectively, $\widetilde{p}$ is the dynamic pressure, c_p and κ are the specific heat and thermal conductivity parameters respectively, $\widetilde{\nabla}^2$ is the Laplacian, ϕ the viscous dissipation function defined as $\phi = \widetilde{\tau} \cdot \widetilde{\nabla}\widetilde{\mathbf{V}}$ and d/dt the material time derivative defined as

$$\frac{d}{dt} = \frac{\partial}{\partial t} + \widetilde{u}\frac{\partial}{\partial \widetilde{x}} + \widetilde{v}\frac{\partial}{\partial \widetilde{y}}, \tag{2.4}$$

where $\widetilde{u}$ and $\widetilde{v}$ are the velocity components in $\widetilde{x}$ and $\widetilde{y}$ directions, respectively and $\widetilde{\tau}$ is the extra stress tensor defined as follows

$$\widetilde{\tau} = \mu \widetilde{\mathbf{A}}_1, \tag{2.5}$$

where μ is the dynamic viscosity and $\mathbf{A}_1$ the first Rivlin-Ericksen tensor defined as

$$\widetilde{\mathbf{A}}_1 = \widetilde{\nabla}\widetilde{\mathbf{V}} + (\widetilde{\nabla}\widetilde{\mathbf{V}})^{\top}, \tag{2.6}$$

here $\top$ indicates the transpose.

3. Problem formulation

Consider the non-isothermal Newtonian flow through the channel of infinite length with heat transfer having stenosis of length $l_o/2$. The coordinate system is chosen in such a way that the arterial system lies in the $\widetilde{xy}-plane$, such that $\widetilde{x}-axis$ coincide with the center line in the direction of flow and $\widetilde{y}-axis$ perpendicular to $\widetilde{x}-axis$.

Consider the boundary of the stenosed region of the form (Haldar, 1991)

$$\begin{aligned} h(\widetilde{x}) &= h_o - \frac{\lambda}{2}\left(1 + \cos\left(\frac{4\pi\widetilde{x}}{l_o}\right)\right) \quad -\frac{l_o}{4} < \widetilde{x} < \frac{l_o}{4}, \\ &= h_o \quad \text{otherwise}, \end{aligned} \tag{3.1}$$

where $h(\widetilde{x})$ is variable gap between the stenosis, $2h_o$ the width of unobstructed channel and λ the maximum height of stenosis.

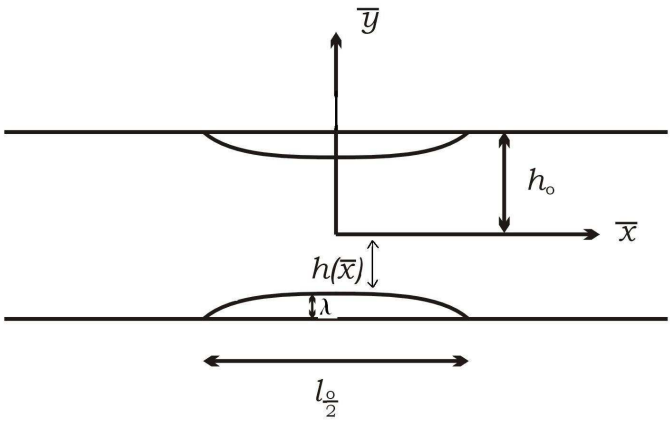

Figure 1. Geometry of the problem.

Boundary conditions for the present problem are

$$\begin{aligned} &\widetilde{u} = \widetilde{v} = 0, \quad \widetilde{T} = T_1 \quad at \quad \widetilde{y} = h(\widetilde{x}), \\ &\frac{\partial \widetilde{u}}{\partial \widetilde{y}} = 0, \quad \frac{\partial \widetilde{T}}{\partial \widetilde{y}} = 0 \quad at \quad \widetilde{y} = 0, \\ &\widetilde{Q} = 2\int_0^{h(\widetilde{x})} \widetilde{u} d\widetilde{y} = -u_o h_o, \end{aligned} \tag{3.2}$$

where u_o is the average velocity and $\widetilde{Q}$ the volume flow rate. Assume that the blood behaves like Newtonian fluid and for steady, homogeneous, incompressible two dimensional flow of blood velocity field is assumed as

$$\widetilde{\mathbf{V}} = \left(\widetilde{u}\left(\widetilde{x},\widetilde{y}\right), \widetilde{v}\left(\widetilde{x},\widetilde{y}\right), 0\right). \tag{3.3}$$

Introducing the dimensionless parameters as follows

$$u = \frac{\widetilde{u}}{u_o}, \quad v = \frac{\widetilde{v}}{u_o}, \quad x = \frac{\widetilde{x}}{l_o}, \quad y = \frac{\widetilde{y}}{h_o}, \quad p = \frac{h_o^2}{\mu u_o l_o}\widetilde{p}, \quad \theta = \frac{\widetilde{T} - T_o}{T_1 - T_o}, \tag{3.4}$$

where T_1 and T_o are temperatures on the boundary of stenosis and fluid respectively.

Substituting equations (2.4)-(2.6) in equations (2.1) - (2.3) and making use of (3.3) and (3.4), nondimensional form of equations becomes

$$\delta\frac{\partial u}{\partial x} + \frac{\partial v}{\partial y} = 0, \tag{3.5}$$

$$Re\left(\delta u\frac{\partial u}{\partial x} + v\frac{\partial u}{\partial y}\right) = -\frac{\partial p}{\partial x} + \nabla^2 u, \tag{3.6}$$

$$Re\delta\left(\delta u\frac{\partial v}{\partial x} + v\frac{\partial v}{\partial y}\right) = -\frac{\partial p}{\partial y} + \delta\nabla^2 v, \tag{3.7}$$

$$Pe\left(\delta u\frac{\partial}{\partial x} + v\frac{\partial}{\partial y}\right)\theta = \nabla^2\theta + Br\left(4\delta^2\left(\frac{\partial u}{\partial x}\right)^2 + \left(\frac{\partial u}{\partial y} + \delta\frac{\partial v}{\partial x}\right)^2\right), \tag{3.8}$$

where

$$\delta = \frac{h_o}{l_o}, \quad Re = \frac{u_o h_o}{\nu}, \quad Br = \frac{\mu u_o^2}{\kappa(T_1 - T_o)}, \quad Pe = \frac{\rho c_p h_o u_o}{\kappa}, \tag{3.9}$$

in which Re is the Reynolds number, Br the Brinkman number, Pe the Peclet number.

Now to convert these equations in single variable, introducing the stream function defined as

$$u = \frac{\partial\psi}{\partial y}, \quad v = -\delta\frac{\partial\psi}{\partial x}, \tag{3.10}$$

which satisfy the continuity equation (3.5) identically. After eliminating pressure gradient term from momentum equations (3.6)-(3.7) and making use of (3.10), compatibility equation is obtained of the form

$$Re\delta\frac{\partial\left(\psi, \nabla^2\psi\right)}{\partial\left(y, x\right)} = \nabla^4\psi, \tag{3.11}$$

where $\nabla^2 = \delta^2\frac{\partial^2}{\partial x^2} + \frac{\partial^2}{\partial y^2}$, is the dimensionless form of the Laplacian. Energy equation (3.8) in terms of stream function becomes

$$Pe\delta\frac{\partial(\psi,\theta)}{\partial(y,x)} = \nabla^2\theta + Br\left(4\delta^2\left(\frac{\partial^2\psi}{\partial x\partial y}\right)^2 + \left(\frac{\partial^2\psi}{\partial y^2} - \delta^2\frac{\partial^2\psi}{\partial x^2}\right)^2\right). \tag{3.12}$$

The dimensionless stenosis profile (3.1) takes the form

$$\begin{aligned} f(x) &= 1 - \frac{\epsilon}{2}(1 + \cos 4\pi x) \quad -\frac{1}{4} < x < \frac{1}{4}, \\ &= 1 \quad \text{otherwise}, \end{aligned} \tag{3.13}$$

where $f = \frac{h(\overline{x})}{h_o}$ and $\epsilon = \frac{\lambda}{h_o}$.
Boundary conditions in terms of stream function becomes

$$\begin{aligned} &\frac{\partial \psi}{\partial y} = 0, \quad \psi = -\frac{1}{2}, \quad \theta = 1 \quad at \quad y = f, \\ &\frac{\partial^2 \psi}{\partial y^2} = 0, \quad \psi = 0, \quad \frac{\partial \theta}{\partial y} = 0 \quad at \quad y = 0. \end{aligned} \tag{3.14}$$

Due to non-linearity of (3.11) and (3.12), the regular perturbation technique is applied to find the analytical solution along with the boundary conditions defined in (3.14).

4. Perturbation method

In this section we shall discuss the perturbation method by considering a linear or nonlinear differential equation

$$L(\psi, \delta) = 0, \tag{4.1}$$

that depends on the small positive parameter δ. The boundary or initial conditions may depend on δ. The reduced or unperturbed problem associated with the problem is obtained by setting $\delta = 0$ along with its boundary or initial conditions. We expand the solution ψ in the perturbation series

$$\psi = \sum_{n=0}^{\infty} \psi_n \delta^n, \tag{4.2}$$

the difference between ψ and ψ_o is refereed to as a perturbation on the solution ψ_o of the reduced problem. Inserting this equation into (4.1) gives

$$L(\psi, \delta) = L(\sum_{n=0}^{\infty} \psi_n \delta^n, \delta) = 0. \tag{4.3}$$

We assume that $L(\psi, \delta)$ can be expanded in a power series in ψ and δ. As a result above equation (4.3) can be expanded in the form of the series

$$L(\psi, \delta) = \sum_{n=0}^{\infty} L_n(\psi_n, \psi_{n-1}, ...\psi_1, \psi_o)\delta^n = 0, \tag{4.4}$$

where L_n represents differential operator, which may be linear or nonlinear. The series (4.2) is also inserted into the given initial and boundary conditions for the problem.

To solve the given problem by means of the perturbation method, we put the coefficient of δ^n in (4.4) equal to zero and obtain

$$L_n(\psi_n, \psi_{n-1}, \cdots \psi_1, \psi_o) = 0, n = 0, 1, 2, \cdots. \tag{4.5}$$

Similarly we equate coefficient of like powers of δ in the initial or boundary conditions. This yields the system of equations (4.5) with appropriate boundary conditions that we solve recursively. We first solve the reduced equation

$$L_o(\psi_o) = 0, \tag{4.6}$$

with relevant boundary conditions. Once ψ_o is found, then equation for ψ_1 with boundary conditions is

$$L_1(\psi_1, \psi_o) = 0, \tag{4.7}$$

is solved and then the equations for $\psi_2, \psi_3, \cdots$ with relevant boundary or initial conditions are solved successively.

5. Solution

To solve the compatibility equation and energy equation along with boundary conditions (3.14), the flow variables ψ and θ are perturbed as

$$\begin{aligned} \psi &= \psi_o + \delta\psi_1 + \delta^2\psi_2 + \cdots, \\ \theta &= \theta_o + \delta\theta_1 + \delta^2\theta_2 + \cdots. \end{aligned} \tag{5.1}$$

where δ is a small parameter.

5.1. Zeroth order problem and its solution

Zeroth order system of equations is obtained by substituting (5.1) in equations (3.11)-(3.12), (3.14) and equating the coefficients of δ^0 as

$$\frac{\partial^4\psi_o}{\partial y^4} = 0, \tag{5.2}$$

$$\frac{\partial^2\theta_o}{\partial y^2} = -Br\left(\frac{\partial^2\psi_o}{\partial y^2}\right)^2, \tag{5.3}$$

and corresponding boundary conditions

$$\begin{aligned} &\frac{\partial\psi_o}{\partial y} = 0, \quad \psi_o = -\frac{1}{2}, \quad \theta_o = 1 \quad at \quad y = f, \\ &\frac{\partial^2\psi_o}{\partial y^2} = 0, \quad \psi_o = 0, \quad \frac{\partial\theta_o}{\partial y} = 0 \quad at \quad y = 0. \end{aligned} \tag{5.4}$$

The solution of equation (5.2) along with boundary conditions (5.4) is given of the form

$$\psi_o = \frac{\eta}{4}\left(\eta^2 - 3\right), \qquad where \quad \eta = \frac{y}{f}. \tag{5.5}$$

After substitution of (5.5) in (5.3) subject to (5.4), zeroth order temperature is obtained as

$$\theta_o = 1 - \frac{3Br}{16f^2}\left(\eta^4 - 1\right), \tag{5.6}$$

which indicates that the temperature depends upon the ratio of heat production by viscous dissipation to heat transport by conduction.

5.2. First order problem and its solution

For the first order system comparing the coefficients of δ, we get

$$\frac{\partial^4\psi_1}{\partial y^4} = Re\frac{\partial\left(\psi_o, \frac{\partial^2\psi_o}{\partial y^2}\right)}{\partial(y,x)}, \tag{5.7}$$

$$\frac{\partial^2\theta_1}{\partial y^2} = Pe\frac{\partial(\psi_o,\theta_o)}{\partial(y,x)} - 2Br\left(\frac{\partial^2\psi_o}{\partial y^2}\frac{\partial^2\psi_1}{\partial y^2}\right), \tag{5.8}$$

and boundary conditions

$$\begin{aligned} &\frac{\partial\psi_1}{\partial y} = 0, \quad \psi_1 = 0 \quad \theta_1 = 0 \quad at \quad y = f, \\ &\frac{\partial^2\psi_1}{\partial y^2} = 0, \quad \psi_1 = 0, \quad \frac{\partial\theta_1}{\partial y} = 0 \quad at \quad y = 0. \end{aligned} \tag{5.9}$$

The solution of equation (5.7) by making use (5.5) and (5.9) becomes

$$\psi_1 = -\frac{3Ref'\eta}{1120}\left(\eta^6 - 7\eta^4 + 11\eta^2 - 5\right). \tag{5.10}$$

By substitution of (5.5) and (5.10) in equation (5.8) and making use of (5.9), the first order temperature profile is obtained of the form

$$\theta_1 = \frac{3Brf'\left(\eta^2-1\right)}{8960f^2}\left\{2Re\left(9\eta^6 - 47\eta^4 + 19\eta^2 + 19\right) + Pe\left(15\eta^6 - 13\eta^4 - 83\eta^2 + 337\right)\right\}. \tag{5.11}$$

It is observed that the first order temperature depends upon the ratio of heat production by viscous dissipation and heat transport by convection to heat transport by conduction.

5.3. Second order problem and its solution

Comparing the coefficients of δ^2 to get the second order system as

$$\frac{\partial^4\psi_2}{\partial y^4} = Re\left[\frac{\partial\left(\psi_o, \frac{\partial^2\psi_1}{\partial y^2}\right)}{\partial(y,x)} + \frac{\partial\left(\psi_1, \frac{\partial^2\psi_o}{\partial y^2}\right)}{\partial(y,x)}\right] - 2\frac{\partial^4\psi_o}{\partial x^2\partial y^2}, \tag{5.12}$$

$$\frac{\partial^2\theta_2}{\partial y^2} = Pe\left[\frac{\partial(\psi_o,\theta_1)}{\partial(y,x)} + \frac{\partial(\psi_1,\theta_o)}{\partial(y,x)}\right] - \frac{\partial^2\theta_o}{\partial x^2} - Br\left[4\left(\frac{\partial^2\psi_o}{\partial x\partial y}\right)^2 + \left(\frac{\partial^2\psi_1}{\partial y^2}\right)^2 + 2\frac{\partial^2\psi_o}{\partial y^2}\frac{\partial^2\psi_2}{\partial y^2} - 2\frac{\partial^2\psi_o}{\partial y^2}\frac{\partial^2\psi_o}{\partial x^2}\right], \tag{5.13}$$

boundary conditions for second order system are

$$\begin{aligned} &\frac{\partial\psi_2}{\partial y} = 0, \quad \psi_2 = 0, \quad \theta_2 = 0 \quad at \quad y = f, \\ &\frac{\partial^2\psi_2}{\partial y^2} = 0, \quad \psi_2 = 0, \quad \frac{\partial\theta_2}{\partial y} = 0 \quad at \quad y = 0. \end{aligned} \tag{5.14}$$

Using (5.5) and (5.10) in equation (5.12), the solution is obtained by successive integration along with the boundary conditions defined in (5.14) as follows

$$\begin{aligned} \psi_2 = {} & CRe^2\eta\left[f'^2\left(98\eta^{10} - 1155\eta^8 + 4488\eta^6 - 8778\eta^4 + 8222\eta^2 - 2875\right)\right. \\ & \left. - f f''\left(35\eta^{10} - 385\eta^8 + 1518\eta^6 - 3234\eta^4 + 3279\eta^2 - 1213\right)\right] - \frac{3\eta(4f'^2 - f f'')}{40}(\eta^4 - 2\eta^2 = 1), \end{aligned} \tag{5.15}$$

which is second order solution for stream lines. To find the second order temperature, using (5.5), (5.10) and (5.15) in equation (5.13), with the help of MATHEMATICA, we get

$$\begin{aligned} \theta_2 = {} & \frac{C_1(\eta^2-1)}{f^2}\left[-4f'^2\left\{7Pe^2\left(225\eta^{10} - 721\eta^8 - 220\eta^6 + 30134\eta^4 - 94771\eta^2 + 238859\right)\right.\right. \\ & + 2PeRe\left(840\eta^{10} - 6860\eta^8 + 11455\eta^6 + 3139\eta^4 - 26891\eta^2 + 56269\right) + Re^2\left(2303\eta^{10}\right. \\ & \left. - 21721\eta^8 + 63122\eta^6 - 68086\eta^4 + 17183\eta^2 + 17183\right) - 517440(13\eta^4 + 9\eta^2 - 36)\Big\} \\ & + f f''\left\{3Br\left(7Pe^2\left(225\eta^{10} - 721\eta^8 - 2206\eta^6 + 30134\eta^4 - 94771\eta^2 + 238859\right)\right)\right. \\ & + 2PeRe\left(525\eta^{10} - 5173\eta^8 + 14132\eta^6 - 7120\eta^4 - 29065\eta^2 + 102605\right) + 8Re^2\left(175\eta^{10}\right. \\ & \left.\left.\left. - 1673\eta^8 + 5158\eta^6 - 7778\eta^4 + 2059\eta^2 + 2059\right) - 2069760\left(7\eta^4 - 4\eta^2 - 9\right)\right)\right\}\Big]. \end{aligned} \tag{5.16}$$

5.4. *Velocity and temperature fields*

The dimensionless velocity components in x and y directions are obtained from (3.10), we arrive at the axial component of velocity as

$$\begin{aligned} u = {} & \frac{\left(\eta^2-1\right)}{f}\left[\frac{3}{4} - \frac{3Re\delta f'}{1120}\left(7\eta^4 - 28\eta^2 + 5\right) + \delta^2\left\{\frac{3}{40}\left(f f'' - 4f'^2\right)\left(5\eta^2 - 1\right)\right.\right. \\ & + CRe^2\left\{f'^2\left(1078\eta^8 - 9317\eta^6 + 22099\eta^4 - 21791\eta^2 + 2875\right)\right. \\ & \left.\left. - C f f''\left(385\eta^8 - 3080\eta^6 + 7546\eta^4 - 8624\eta^2 + 1213\right)\right\}\right], \end{aligned} \tag{5.17}$$

and the normal component of velocity is

$$\begin{aligned} v =& \frac{\delta\eta\left(\eta^2-1\right)}{f}\left[\frac{3}{4}f' + \frac{3Re\delta}{20}\left(f f''\left(\eta^2-1\right)\left(\eta^2-5\right) - f'^2\left(7\eta^4-28\eta^2+5\right)\right)\right. \\ &+\delta^2\left\{\frac{3f f' f''}{10}\left(3\eta^2-1\right) - \frac{3f^2 f''}{40}\left(\eta^2-1\right) - \frac{3f'^3}{10}\left(5\eta^2-1\right) + Re^2\left\{C f'^3\left(1078\eta^8\right.\right.\right. \\ &-93172\eta^6 + 22099\eta^4 - 21791\eta^2 + 28875\big) - C_2 f f' f''\left(273\eta^8 - 2422\eta^6 + 6620\eta^4\right. \\ &\left.\left.\left.\left.-8626\eta^2 + 2875\right) + C f^2 f''\left(\eta^2-1\right)\left(35\eta^6 - 315\eta^4 + 853\eta^2 - 1213\right)\right\}\right\}\Big]. \end{aligned} \tag{5.18}$$

The temperature distribution up to second order is obtained from (5.1), we arrive

$$\begin{aligned} \theta =& 1 - \frac{Br}{f^2}\left[\frac{3}{16}(\eta^4-1) - \delta\left\{\frac{3f'(\eta^2-1)}{8960}\left(2Re\left(9\eta^6 - 47\eta^4 + 19\eta^2 + 19\right) + Pe\left(15\eta^6 - 13\eta^4\right.\right.\right. \\ &\left.\left.-83\eta^2 + 337\right)\right)\Big\} - \delta^2\Big[C_1(\eta^2-1)\left\{-2f'^2\left\{7Pe^2\left(225\eta^{10} - 721\eta^8 - 2206\eta^6 + 30134\eta^4\right.\right.\right. \\ &\left.\left.-94771\eta^2 + 238859\right) + 4PeRe\left(840\eta^{10} - 6860\eta^8 + 11455\eta^6 + 3139\eta^4 - 26891\eta^2 + 56269\right) \\ &+2Re^2\left(2303\eta^{10} - 21721\eta^8 + 63122\eta^6 - 68086\eta^4 + 17183\eta^2 + 17183\right) - 1034880\left(13\eta^4\right. \\ &\left.\left.+9\eta^2 - 36\right)\right\} + f f''\left\{3Br\left\{7Pe^2\left(225\eta^{10} - 721\eta^8 - 2206\eta^6 + 30134\eta^4 - 94771\eta^2 + 238859\right)\right.\right. \\ &+2PeRe\left(525\eta^{10} - 5173\eta^8 + 14132\eta^6 - 7120\eta^4 - 29065\eta^2 + 102605\right) + 8Re^2\left(175\eta^{10} - 1673\eta^8\right. \\ &\left.\left.\left.+5158\eta^6 - 7778\eta^4 + 2059\eta^2 + 2059\right) - 2069760\left(7\eta^4 - 4\eta^2 - 9\right)\right\}\right\}\Big]\Big], \end{aligned} \tag{5.19}$$

where $C = \frac{1}{3449600}$, $C_1 = \frac{1}{55193600}$, $C_2 = \frac{1}{1724800}$. Dimensionless wall shear stress for viscous fluid up to second order is given by

$$\begin{aligned} \tau_\omega &= \left(\frac{\partial u}{\partial y} + \delta\frac{\partial v}{\partial x}\right)_{y=f} \\ &= \frac{3}{f^2}\left[\frac{1}{2} + \frac{Re f'}{35}\delta + \frac{\delta^2}{10}\left\{\frac{Re^2}{8085}\left(40 f f'' - 79 f'^2\right) + \left(2 f f'' - 13 f'^2\right)\right\}\right]. \end{aligned} \tag{5.20}$$

The points of separation and reattachment are defined as the back flow at wall, where the wall shear stress is zero, i.e.$\tau_\omega = 0$, then above equation reduces as

$$40425 + 2310Re f'\delta + \delta^2\left\{10 f f''\left(40Re^2 + 16170\right) - f'^2\left(79Re^2 + 105105\right)\right\} = 0. \tag{5.21}$$

The solution of (5.21) in terms of Reynolds number Re is

$$Re = \frac{7}{\delta\left(40 f f'' - 79 f'^2\right)}\left\{-165 f' \pm \sqrt{165\left\{165 f'^2 - \left(40 f f'' - 79 f'^2\right)\left(5 - 13\delta^2 f'^2 + 2\delta^2 f f''\right)\right\}}\right\}. \tag{5.22}$$

By using equation (5.22), our aim is to find graphically the critical Reynolds number at which the back flow occur.

5.5. Pressure distribution

To find the pressure distribution along x-axis within the channel, the equations (3.6) and (3.7) are converted in terms of stream function and then perturb these equation by using (5.1) and

$$p = p_o + \delta p_1 + \delta^2 p_2 + \cdots, \tag{5.23}$$

system of equations is obtained as follows.

5.5.1. Zeroth order pressure and solution

Comparing the coefficients of δ^0 , we get

$$\frac{\partial p_o}{\partial x} = \frac{\partial^3 \psi_o}{\partial y^3}, \tag{5.24}$$

$$\frac{\partial p_o}{\partial y} = 0. \tag{5.25}$$

By integrating the above two equations and making use of (5.5), the zeroth order pressure is obtained of the form

$$\begin{aligned} p_o = &\frac{3}{32\pi(\epsilon-1)^2}\left[\frac{1}{\sqrt{1-\epsilon}}\left(3\epsilon^2-8\epsilon+8\right)\tan^{-}1\left(\frac{\tan 2\pi x}{\sqrt{1-\epsilon}}\right)-\frac{f'}{8\pi f^2}\left\{16(\epsilon-1)-3\epsilon^2\right.\right. \\ &\left.\left.-3\epsilon(\epsilon-2)\cos(4\pi x)\right\}\right], \end{aligned} \tag{5.26}$$

which involves the trigonometric and inverse trigonometric function.

5.5.2. First order pressure and solution

Equating the coefficients of δ , we obtain

$$\frac{\partial p_1}{\partial x} = \frac{\partial^3 \psi_1}{\partial y^3} - Re\frac{\partial\left(\psi_o, \frac{\partial \psi_o}{\partial y}\right)}{\partial(y,x)}, \tag{5.27}$$

$$\frac{\partial p_1}{\partial y} = 0, \tag{5.28}$$

by making use of equations (5.5), (5.10) and solving (5.27)-(5.28), the first order solution for pressure is obtained by applying

$$p_1 = \int_0^x \frac{\partial p_1}{\partial x}dx + \int_0^y \frac{\partial p_1}{\partial y}dy, \tag{5.29}$$

of the form

$$p_1 = \frac{27Re}{140 f^2}\left(\frac{1}{(1-\epsilon)^2} - \frac{1}{f^2}\right). \tag{5.30}$$

5.5.3. Second order pressure and solution

Comparing the coefficients of δ^2 , we arrive at

$$\frac{\partial p_2}{\partial x} = \frac{\partial^3 \psi_2}{\partial y^3} - Re\left[\frac{\partial\left(\psi_o, \frac{\partial \psi_1}{\partial y}\right)}{\partial (y, x)} + \frac{\partial\left(\psi_1, \frac{\partial \psi_o}{\partial y}\right)}{\partial (y, x)}\right], \tag{5.31}$$

$$\frac{\partial p_2}{\partial y} = -\frac{\partial^3 \psi_o}{\partial x \partial y^2}, \tag{5.32}$$

by integrating the equations (5.31)-(5.32) and making use of (5.5), (5.10) and (5.15) ,we arrive at the second order pressure as follows

$$\begin{aligned} p_2 =& \frac{3}{13475}\left[\frac{\pi\epsilon^2}{(1-\epsilon)^{\frac{3}{2}}}\left(13Re^2 + 8085\right)\tan^{-}1\left(\frac{\tan 2\pi x}{\sqrt{1-\epsilon}}\right)\right. \\ &\left. + f'\left\{\frac{40425\eta^2}{2f^2} + \frac{52Re^2 - 18865}{4f^2} + \frac{(\epsilon-2)(13Re^2+8085)}{4f(\epsilon-1)}\right\}\right]. \end{aligned} \tag{5.33}$$

Now one can easily find the pressure up to second order by using equations (5.26), (5.30) and (5.33).

6. Graphical discussion

In this section the effect of different pertinent parameters on stream lines, wall shear stress, pressure distribution, separation and reattachment points and analysis for heat transfer are presented graphically. The geometry of the proposed model for the study of the stenosed artery is depicted in Figure 1. The radii of obstructed and unobstructed regions are $h(x)$ and h_o. The point of separation lies near the throat of the stenosed region in the converging section. Separation point means the point where reverse flow occurs. Figure 2,3 presents the behavior of stream lines for zeroth order in 2(a), first order in 2(b), second order in 3(a) and up to second order in 3(b) respectively, for the fixed values of $Re = 12, \epsilon = 0.2, \delta = 0.1, \alpha = 0.04$. In these figures $x - axis$ lies in the horizontal direction and $y - axis$ perpendicular to it. The zeroth order solution corresponds to the flow with vanishing wall slopes and reduces to the flow between parallel plates for $\epsilon = 0$. The stream lines are relatively straight in the center of the channel. The first order solution induces the clockwise and counterclockwise rotational motion in the converging and diverging regions, which indicates the separation point in the converging region and reattachment point in the diverging region. Figure 3(a) shows the stream lines for second order solution reinforce the first order solution and observe the rotational motion which predicts the separation and reattachment points. Figure 3(b) presents the stream lines up to second order. It is observed that the stream lines becomes relatively straight in the center of the channel as compares to the walls of the channel and similar to (Chow *et al.*, 1971).

The distribution of wall shear stress across the stenosis has been described for the variation of *Re* in figure 4(a) for fixed $\epsilon = 0.2, \delta = 0.1$. An increase in *Re*, wall shear stress increases near the throat of stenosed region and becomes negative in the converging and diverging section of channel

due to back flow. The adverse shearing in converging and diverging sections of channel indicates that there is point of separation in the upstream region and reattachment point in the downstream region of channel. It is observed that wall shear stress holds for both small and large *Re*.

In figure 4(b) effect of ϵ on wall shear stress is presented. The straight line indicates that there is no stenosis and the flow is Poiseuille flow. By the increase in ϵ wall shear stress increases over the stenosed region and becomes negative in the converging section of channel due to adverse flow, which is prediction for the point of separation. The separation point was considered to be the point nearest the throat where reversed flow along the wall of channel could be observed. The point farthest down stream from the throat where back flow occur is defined as reattachment point. It is expected that the wall shear stress plays an important role in the formation of the stenosis and its further growth. Because the deposit of cholesterol and proliferation of connective tissue may be responsible for the abnormal growth in lumen of artery. Its actual cause may not be known exactly but its effect on the cardiovascular system can easily be understood by studying the blood flow in its vicinity. One of the practical applications of blood flow through a membrane oxygenator is the flow with an irregular wall surface.

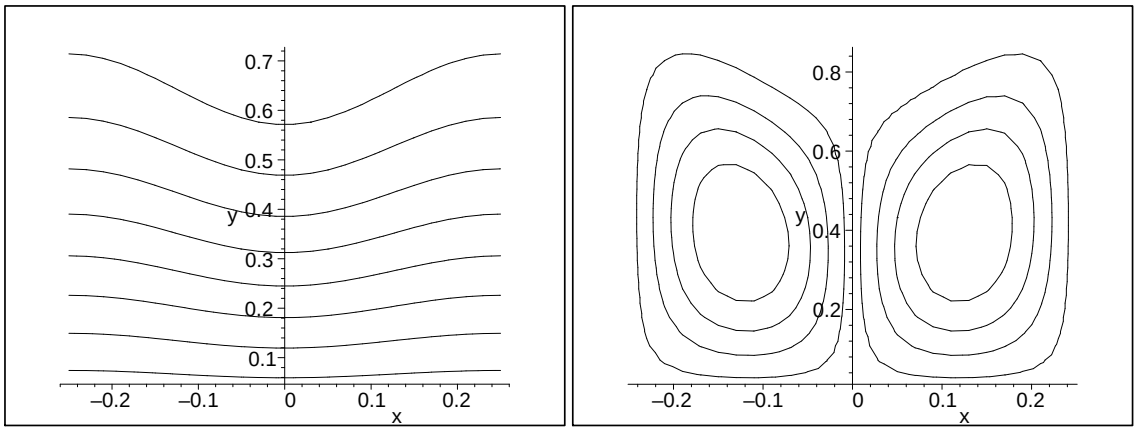

Figure 2. The zeroth order stream lines for $\epsilon = 0.20, Re = 12, \delta = 0.1$ are shown in (a) and the first order stream lines are shown in (b).

Figure 5(a) depict the distribution for the point of separation in converging section of channel for different ϵ along with fixed δ. The separation point lie to the right of minimum point, actually the purpose for zero wall shear stress is to find the critical Reynolds number where separation occur. The critical value of *Re* in the converging region for $\epsilon = 0.6$ is 70. The theory that the critical *Re* decreases with the increase in ϵ is verified. In figure 5(b) zero wall shear stress is plotted for ϵ having fixed value of δ in diverging section of channel. The aim of investigation is to determine the critical value of *Re* at which reattachment occurred in the diverging region of the channel. As the critical *Re* reached the reattachment occur in the diverging region of channel and separation point occur in the upstream region of channel. It is observed that the critical value of *Re* for $\epsilon = 0.6$ is 380. It is also observed form figure 6 that as ϵ increases critical value of *Re* decreases.

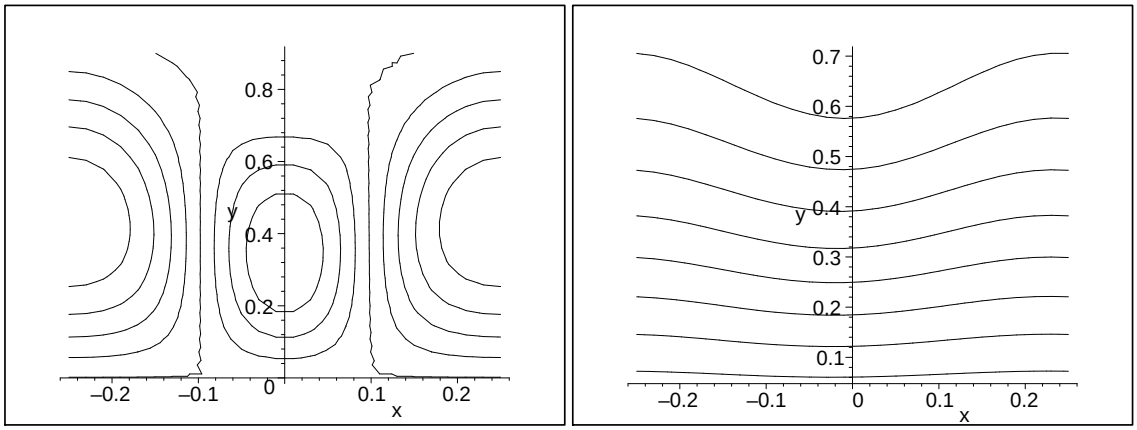

(a) (b)

Figure 3. The second order stream lines are shown in (a) and the streamlines correct up to the second order in δ are shown in (b).

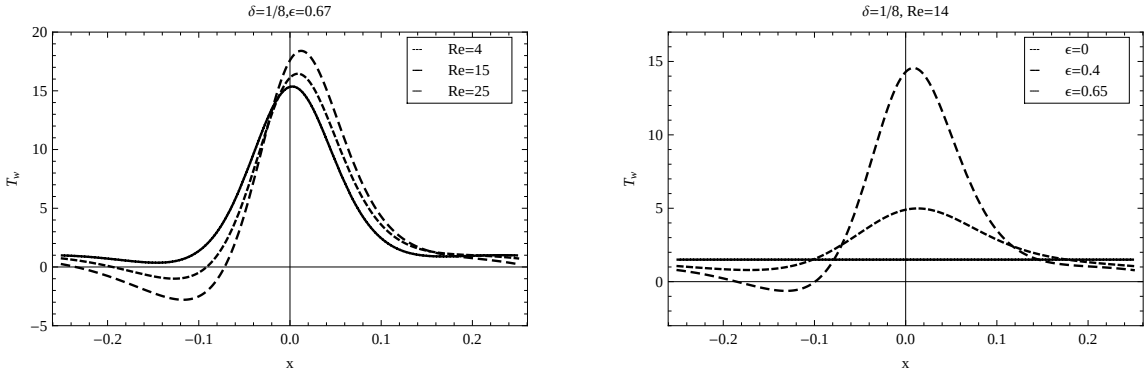

(a) (b)

Figure 4. The effect of *Re* on wall shear stress is shown in (a) and the effect of ϵ on wall shear stress is shown in (b).

Figure 6(a) presents the effect for the various values of *Re* on pressure distribution. It may be noted that with the increase in *Re* leads to increase the pressure gradient over the stenosed region and becomes negative in the converging and diverging regions, due to the dependence of *Re* on average velocity. The adverse pressure gradient in these regions causes back flows as observed earlier. These back flows predicts the separation point in converging region and reattachment point in diverging region of the channel. It is observed that the magnitude of adverse pressure gradient in the diverging region is smaller as compared to that in the converging region.

Effect of ϵ on pressure gradient is studied in figure 6(b). It is observed that with the increase in ϵ, pressure gradient increases over the region having stenosis and becomes negative in the upstream and downstream regions of channel due to back flow. The adverse pressure gradient in the converging part of stenosis describing the flow separation and reattachment in the diverging

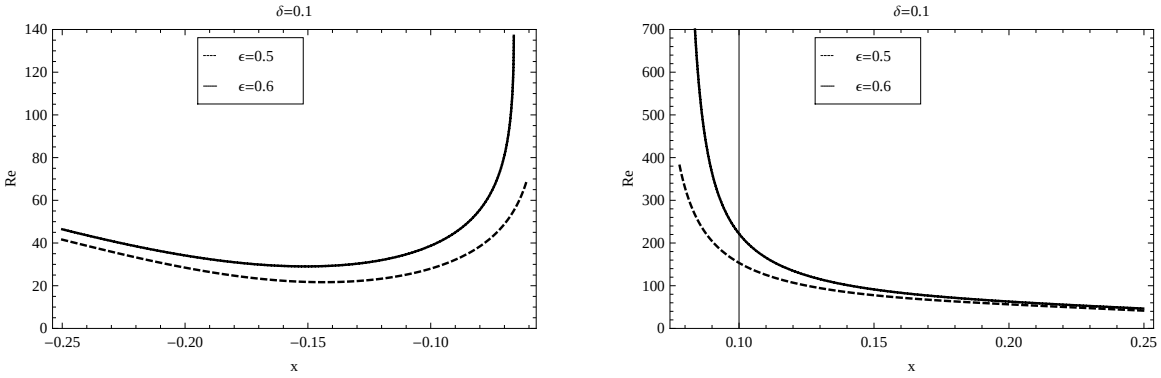

(a) (b)

Figure 5. The separation point in converging region are shown in (a) and the reattachment point in diverging region are shown in (b).

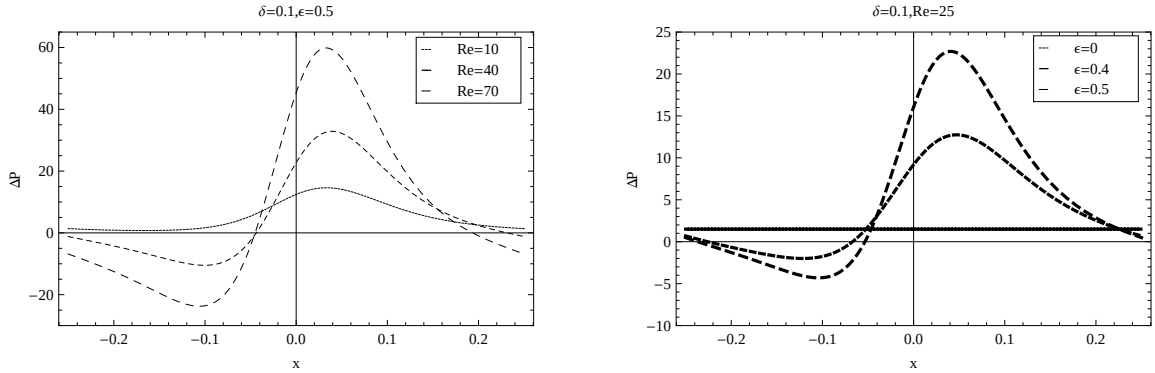

(a) (b)

Figure 6. The pressure distribution for *Re* is shown in (a) and the pressure distribution for ϵ is shown in (b).

part. The straight line preserve Poiseuille flow as there is no stenosis.

Figure 7(a) depict for various values of *Re* on axial component of velocity. It is observed that with the increase in *Re* the axial velocity is maximum over the obstructive region and becomes negative causing back flow in the converging and diverging sections of the channel. Figure 7(b) shows the effect of ϵ on velocity distribution. It is observed that as the ϵ increases the velocity increases over the stenosed region and decreases sharply in the converging section and then recover it in the diverging section of channel. Negative velocity indicates the back flow, due to separation and reattachment points in the channel.

Figure 8(a) shows the effect of *Pe* on temperature distribution. It is observed that with the increase in *Pe*, temperature increases over the stenosed region and becomes negative in the converging and diverging regions. The adverse temperature in the upstream and downstream sections

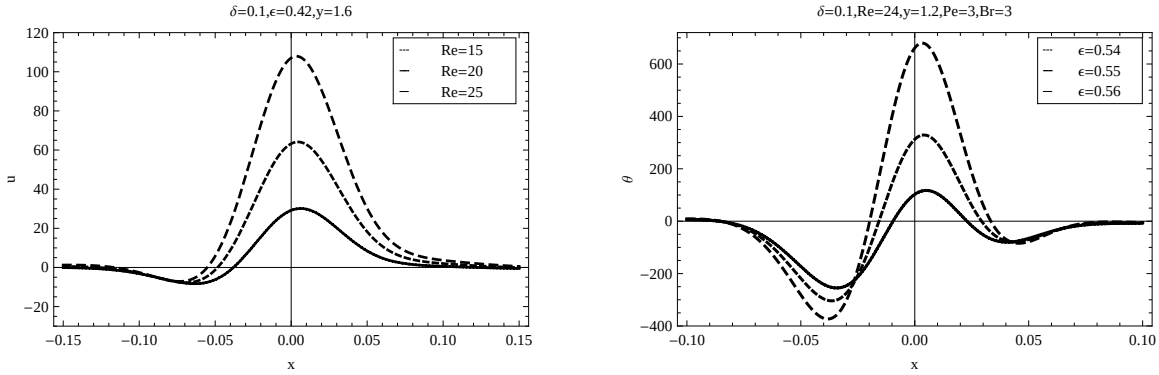

(a) (b)

Figure 7. The axial velocity distribution for *Re* is shown in (a) and the axial velocity distribution for ϵ is shown in (b).

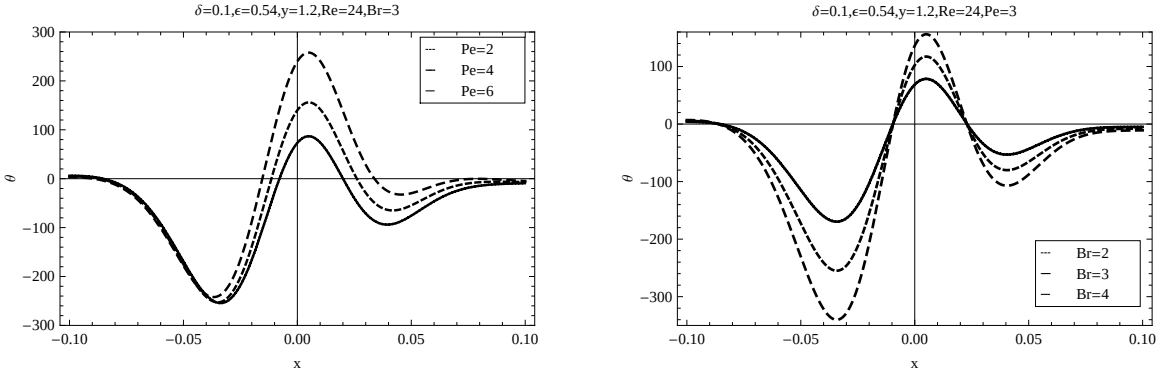

(a) (b)

Figure 8. The effect of *Pe* on temperature distribution is shown in (a) and the effect of *Br* on temperature distribution is shown in (b).

describing flow separation and reattachment from the wall also confirm the results for velocity and wall shear stress. Temperature distribution across the stenosis has been described in figure 8(b) for different values of *Br*. Temperature increases steeply from its axial axis in the converging section of the stenosis to the peak value at the throat, then drop to a minimum value downstream behind the stenosis and again approaches to the axial axis in the region away from stenosis. The magnitude of adverse temperature in the diverging region of stenosis is smaller as compared to that in the converging section of the stenosis. The adverse temperature in these regions cause back flow as observed earlier in velocity and pressure fields.

7. Summary

In the present study, steady two-dimensional flow of incompressible Newtonian fluid with heat transfer between two parallel plates in the presence of a cosine shaped stenosis is presented. The underlying problem is solved with the help of the regular perturbation method. The results thus obtained are discussed graphically in terms of stream lines, pressure gradient, wall shear stress, separation and reattachment points and temperature distribution. It is observed that the general pattern of streamlines is similar as discussed in (Layek & Midya, 2007) - (Chow *et al.*, 1971), wall shear stress is same as given by (Morgan & Young, 1974) - (Haldar, 1991) and separation and reattachment points are in agreement with (Haldar, 1991). It is observed that:

- Stream lines for zeroth order and up to second order are similar due to small δ and first and second order shows rotational motion.
- Increase in Reynolds number increases the wall shear stress, velocity and pressure gradient.
- Increase in thickness of stenosis increases pressure gradient, temperature and wall shear stress causing separation and reattachment in the channel.
- Increase in the thickness of stenosis decreases the critical Reynolds number for separation and reattachment points, means even at low velocity separation occurs.
- By the increase in Peclet and Brinkman number increases the temperature between the channel.
- For $\epsilon = 0$ Poiseuille flow is recovered.

References

Chakravarty, S. and A. G. Chakravarty (1988). Response of blood flow through an artery under stenotic conditions. *Rheologica Acta*.

Chow, J. C. F., K. Soda and C. Dean (1971). On laminar flow in wavy channel. In: *Developments in Mechanics, Vol. 8, Proceedings of the* 12^{th}. *Midwestern Mechanics Conference, University of Notre Dame Press, Notre Dame, Indiana*. pp. 247–260.

Forrester, J. H. and D. F. Young (1970). Flow through a converging-diverging tube and its implications in occlusive vascular disease. *Journal of Biomechanics* **3**, 297–316.

Haldar, K. (1985). Effect of the shape of stenosis on the resistance to blood flow through an artery. *Bulletin of Mathematical Biology* **47**, 545–550.

Haldar, K. (1991). Analysis of separation of blood flow in constricted arteries. *Archives of Mechanics* **43**(1), 107–113.

Kruszewski, A., R. Wang and T.M. Guerra (2008). Nonquadratic stabilization conditions for a class of uncertain nonlinear discrete time ts fuzzy models: A new approach. *IEEE Transactions on Automatic Control* **53**(2), 606–611.

Layek, G. C and C. Midya (2007). Effect of constriction height on flow seperation in a two-dimensional channel. *Communications in Nonlinear Science and Numerical Simulation* **12**, 745–759.

Lee, J. S. and Y. C. Fung (1970). Flow in locally constricted tubes at low Reynolds number. *Journal of Applied Mechanics* **37**, 9–16.

Mehrotra, R., G. Jayaraman and N. Padmanabhan (1985). Pulsatile blood flow in a stenosed artery - a theoretical model. *Medical Biological Engineering and Computing* **23**, 55–62.

Morgan, B. E. and D. F. Young (1974). An integral method for the analysis of flow in arterial stenoses. *Bulletin of Mathematical Biology* **36**, 39–53.

Newman, D. L., N. Westerhof and P. Sipkema (1979). Modelling of aertic stenosis. *Journal of Biomechanics* **12**, 229–235.

Srivastava, V. P. and R. Rastogi (2010). Blood flow through a stenosed catheterized artery: Effects of hematocrit and stenosis shape. *Computers and Mathematics with Applications* **59**(4), 1377–1385.

Appendix 1

List of Mathematical Symbols

$\mathbf{V}$	Velocity vector (m/s)
∇	del operator
p	scalar pressure(Pa)
d/dt	material time derivative
c_p	specific heat(J/kgK)
T	temperature(C^o)
u, v	velocity components(m/s)
x, y	coordinate axis(m)
$\mathbf{A}_1$	first Rivlin-Ericksen tensor
$l_o/2$	length of stenosis(m)
$h(x)$	variable width between the stenosis(m)
h_o	radius of unobstructed channel(m)
u_o	average velocity(m/s)
Q	volume flow rate(m^3/s)
T_1, T_o	temperatures on boundary of stenosis and fluid(C^o)
Re	Reynolds number
Br	Brinkman number
Pe	Peclet number
$f(x)$	boundary profile
τ	extra stress tensor
ρ	density
κ	thermal conductivity
ϕ	viscous dissipation function
μ	dynamic viscosity(Pa/s)
$\top$	transpose
λ, ϵ	maximum height of stenosis
θ	dimensionless temperature
ν	kinematic viscosity(m^2/s)
ψ	stream function
δ	constant
η	ratio of y and f
τ_ω	wall shear stress

Theory and Applications of Mathematics & Computer Science

(ISSN 2067-2764, EISSN 2247-6202)
http://www.uav.ro/applications/se/journal/index.php/tamcs

Theory and Applications of Mathematics & Computer Science 3 (2) (2013) 93–102

Starlikeness and Convexity of Certain Classes of Meromorphically Multivalent Functions

H. M. Srivastava[a,*], A. Y. Lashin[b], B. A. Frasin[c]

[a]*Department of Mathematics and Statistics, University of Victoria, Victoria, British Columbia V8W 3R4, Canada*
[b]*Department of Mathematics, Faculty of Science, Mansoura University, Mansoura 35516, Egypt*
[c]*Department of Mathematics, Al al-Bayt University, P. O. Box 130095, Mafraq, Jordan*

Abstract

The purpose of this paper is to investigate the problems of finding the order of starlikeness and the order of convexity of the products of certain meromorphically p-valent functions belonging to some interesting classes of β-uniformly p-valent starlike functions and β-uniformly p-valent convex functions in the open unit disk $\mathbb{U}$. The main results presented in the paper are capable of being specialized suitably in order to deduce the solutions of the corresponding problems for relatively more familiar subclasses of meromorphically p-valent functions in $\mathbb{U}$.

Keywords: Analytic functions, Meromorphically p-valent starlike functions, Meromorphically p-valent convex functions, Products of meromorphic functions, Uniformly starlike functions, Uniformly convex functions.
2010 MSC: Primary 30C45.

1. Introduction and definitions

Let $\mathcal{A}$ denote the class of all functions $f(z)$ which are analytic in the open unit disk

$$\mathbb{U} = \{z : z \in \mathbb{C} \quad \text{and} \quad |z| < 1\}$$

and normalized by

$$f(0) = 0 \qquad \text{and} \qquad f'(0) = 1.$$

A function $f(z) \in \mathcal{A}$ is said to be *uniformly convex* (or *uniformly starlike*) in $\mathbb{U}$ if, for every circular arc Γ contained in $\mathbb{U}$, with center at ω_0 also in $\mathbb{U}$, the arc $f(\Gamma)$ is convex (or starlike) with respect to the point $f(\omega_0)$. The classes of all uniformly convex function in $\mathbb{U}$ and all uniformly starlike

*Corresponding author
Email addresses: harimsri@math.uvic.ca (H. M. Srivastava), aylashin@mans.edu.eg (A. Y. Lashin), bafrasin@yahoo.com (B. A. Frasin)

functions in $\mathbb{U}$ are denoted by UCV and UST, respectively. These analytic function classes UCV and UST were introduced and studied by Goodman (Goodman, 1991*a*,*b*) who showed, among other things, that

$$f \in UCV \Longleftrightarrow \Re\left(1 + (z-\zeta)\,\frac{f''(z)}{f'(z)}\right) \geqq 0 \qquad (z, \zeta \in \mathbb{U})$$

and

$$f \in UST \Longleftrightarrow \Re\left(\frac{(z-\zeta)\,f'(z)}{f(z)-f(\zeta)}\right) \geqq 0 \qquad (z, \zeta \in \mathbb{U}).$$

Rønning (Rønning, 1993, 1994) and Ma and Minda (Ma & Minda, 1992) gave the following one-variable characterization of the class UCV of uniformly convex functions in $\mathbb{U}$.

Theorem A. *A function $f(z) \in \mathcal{A}$ is said to be in the class UCV of uniformly convex functions in $\mathbb{U}$ if it satisfies the following condition*:

$$\Re\left(1 + \frac{zf''(z)}{f'(z)}\right) \geqq \left|\frac{zf''(z)}{f'(z)}\right| \qquad (z \in \mathbb{U}).$$

Since the Alexander type result that

$$f \in UCV \Longleftrightarrow zf'(z) \in UST$$

does not hold true (Rønning, 1994), the class $\mathcal{S}_{\mathfrak{p}}$ defined by

$$\mathcal{S}_{\mathfrak{p}} := \{f : zf'(z) \in UCV\}$$

was introduced by Rønning (Rønning, 1993). On the other hand, Shams *et al.* (Shams *et al.*, 2004) initiated a study of the class $SD(\alpha,\beta)$ of β-uniformly starlike functions of order α $(0 \leqq \alpha < 1)$ in $\mathbb{U}$ consisting of functions $f(z) \in \mathcal{A}$ which satisfy the following inequality:

$$\Re\left(\frac{zf'(z)}{f(z)} - \alpha\right) > \beta\left|\frac{zf'(z)}{f(z)} - 1\right| \qquad (\beta \geqq 0;\ 0 \leqq \alpha < 1;\ z \in \mathbb{U}).$$

The class $KD(\alpha,\beta)$ of β-uniformly convex of order α $(0 \leqq \alpha < 1)$ in $\mathbb{U}$ is defined as follows:

$$f \in KD(\alpha,\beta) \Longleftrightarrow zf'(z) \in SD(\alpha,\beta).$$

Motivated by the above-defined function classes $SD(\alpha,\beta)$ and $KD(\alpha,\beta)$, Nishiwaki and Owa (Nishiwaki & Owa, 2007) introduced the class $MD(\alpha,\beta)$ consisting of all functions $f(z) \in \mathcal{A}$ which satisfy the following inequality:

$$\Re\left(\frac{zf'(z)}{f(z)} - \alpha\right) < \beta\left|\frac{zf'(z)}{f(z)} - 1\right| \qquad (\beta \leqq 0;\ \alpha > 1;\ z \in \mathbb{U}).$$

The function class $ND(\alpha,\beta)$ may also be considered as a subclass of $\mathcal{A}$ consisting of all functions $f(z)$ such that $zf'(z) \in MD(\alpha,\beta)$.

The class of uniformly convex functions and various other related function classes have been studied by several authors (see, for example, (Ali & Ravichandran, 2010; Frasin, 2011; Kanas & Srivastava, 2000; Kanas & Wisniowska, 1999, 2000; Murugusundaramoorthy & Magesh, 2004; Rønning, 1991); see also (Srivastava & Owa (Editors), 1992)).

Let Σ_p denote the class of functions of the form:

$$f(z) = z^{-p} + \sum_{k=1}^{\infty} a_{k-p} z^{k-p} \qquad (p \in \mathbb{N} := \{1, 2, 3, \cdots\}), \tag{1.1}$$

which are analytic and p-valent in the *punctured* unit disk

$$\mathbb{U}^* = \{z : z \in \mathbb{C} \quad \text{and} \quad 0 < |z| < 1\} = \mathbb{U} \setminus \{0\}.$$

A function $f \in \Sigma_p$ is said to be in the class $\Sigma S_p^*(\alpha)$ of meromorphically p-valent starlike functions of order α in $\mathbb{U}$ if and only if

$$\Re\left[\frac{1}{p}\left(\frac{zf'(z)}{f(z)}\right)\right] < -\alpha \qquad (z \in \mathbb{U};\ 0 \leqq \alpha < 1). \tag{1.2}$$

Also a function $f \in \Sigma_p$ is said to be in the class $\Sigma C_p(\alpha)$ of meromorphically p-valent convex functions of order α in $\mathbb{U}$ if and only if

$$\Re\left[\frac{1}{p}\left(1 + \frac{zf''(z)}{f'(z)}\right)\right] < -\alpha \qquad (z \in \mathbb{U};\ 0 \leqq \alpha < 1). \tag{1.3}$$

It is easy to observe from (1.2) and (1.3) that

$$f(z) \in \Sigma C_p(\alpha) \Longleftrightarrow -\frac{zf'(z)}{p} \in \Sigma S_p^*(\alpha). \tag{1.4}$$

We note that the meromorphically p-valent function classes $\Sigma S_p^*(\alpha)$ and $\Sigma C_p(\alpha)$ were introduced by Kumar and Shukla (Kumar & Shukla, 1982).

We next denote by $\Sigma M_p(\alpha)$ and $\Sigma N_p(\alpha)$ the subclasses of the meromorphically p-valent function class Σ_p which satisfy the following inequalities:

$$\Sigma M_p(\alpha) := \left\{f : f \in \Sigma_p \quad \text{and} \quad \Re\left[-\frac{1}{p}\left(\frac{zf'(z)}{f(z)}\right)\right] < \alpha \quad (z \in \mathbb{U};\ \alpha > 1)\right\}$$

and

$$\Sigma N_p(\alpha) := \left\{f : f \in \Sigma_p \quad \text{and} \quad \Re\left[-\frac{1}{p}\left(1 + \frac{zf''(z)}{f'(z)}\right)\right] < \alpha \quad (z \in \mathbb{U};\ \alpha > 1)\right\},$$

respectively. The meromorphically p-valent function classes $\Sigma M_p(\alpha)$ and $\Sigma N_p(\alpha)$ are analogous, respectively, to the subclasses $M(\alpha)$ and $N(\alpha)$ of the analytic function class $\mathcal{A}$ which were introduced by Owa and Nishiwaki (Owa & Nishiwaki, 2002).

Recently, Kumar *et al.* (Kumar *et al.*, 2005) introduced the following subclass $\Sigma\mathcal{S}_p^*(\alpha,\beta)$ of meromorphically p-valent starlike functions $f \in \Sigma_p$ in $\mathbb{U}$, which is similar to the class $SD(\alpha,\beta)$, by means of the following inequality:

$$\Re\left[-\frac{1}{p}\left(\frac{zf'(z)}{f(z)}\right)\right] > \alpha\left|\frac{1}{p}\left(\frac{zf'(z)}{f(z)}\right)+1\right|+\beta \tag{1.5}$$

$$(z \in \mathbb{U};\ \alpha \geqq 0;\ 0 \leqq \beta < 1).$$

Analogously, we define here the subclass $\Sigma C_p(\alpha,\beta)$ of meromorphically p-valent convex functions in $\mathbb{U}$, which is similar to the class $KD(\alpha,\beta)$, consisting of all functions $f \in \Sigma_p$ which satisfy the following inequality:

$$\Re\left[-\frac{1}{p}\left(1+\frac{zf''(z)}{f'(z)}\right)\right] > \alpha\left|\frac{1}{p}\left(1+\frac{zf''(z)}{f'(z)}\right)+1\right|+\beta \tag{1.6}$$

$$(z \in \mathbb{U};\ \alpha \geqq 0;\ 0 \leqq \beta < 1).$$

Similarly, for $-1 < \alpha \leqq 0$ and $\beta > 1$, we let $\Sigma\mathcal{M}_p(\alpha,\beta)$ be the subclass consisting of all functions $f \in \Sigma_p$ which satisfy the following inequality:

$$\Re\left[-\frac{1}{p}\left(\frac{zf'(z)}{f(z)}\right)\right] < \alpha\left|\frac{1}{p}\left(\frac{zf'(z)}{f(z)}\right)+1\right|+\beta \tag{1.7}$$

$$(z \in \mathbb{U};\ -1 < \alpha \leqq 0;\ \beta > 1).$$

We also let $\Sigma\mathcal{N}_p(\alpha,\beta)$ be the subclass consisting of all functions $f \in \Sigma_p$ which satisfy the following inequality:

$$\Re\left[-\frac{1}{p}\left(1+\frac{zf''(z)}{f'(z)}\right)\right] < \alpha\left|\frac{1}{p}\left(1+\frac{zf''(z)}{f'(z)}\right)+1\right|+\beta \tag{1.8}$$

$$(z \in \mathbb{U};\ -1 < \alpha \leqq 0;\ \beta > 1).$$

The main purpose of this paper is to investigate the problems of finding the order of starlikeness and the order of convexity of certain products of meromorphically p-valent functions belonging to some of the above-defined classes of β-uniformly p-valent starlike functions in $\mathbb{U}$ and β-uniformaly p-valent convex functions in $\mathbb{U}$. Our main results in Section 2 (stated as Theorems 1 to 4 *and* Corollaries 1 to 5) can indeed be specialized suitably in order to deduce the solutions of the corresponding problems for relatively more familiar subclasses of meromorphically p-valent functions in $\mathbb{U}$.

2. The main results and their consequences

Our first main result is asserted by Theorem 1 below.

Theorem 1. *Let* $f_j \in \Sigma S_p^*(\gamma_j) \quad (j = 1,\cdots,n)$, *where*

$$\gamma_j := 1-\alpha_j \geqq 0 \qquad \textit{and} \qquad \alpha_j \geqq 0 \qquad (j = 1,\cdots,n).$$

Also let

$$\kappa := 1 - \sum_{j=1}^{n} \alpha_j \geqq 0.$$

Then the product $F_p(z)$ *defined by*

$$F_p(z) := z^{-p} \prod_{j=1}^{n} \left\{ z^p f_j(z) \right\} \tag{2.1}$$

is in the class $\Sigma S_p^*(\kappa)$ *of meromorphically p-valent starlike functions of order* κ *in* $\mathbb{U}$.

Proof. Clearly, $F_p(z) \in \Sigma_p$. By differentiating (2.1) logarithmically with respect to z, we obtain

$$\frac{1}{p}\left(\frac{zF_p'(z)}{F_p}\right) = -1 + \sum_{j=1}^{n} \left[\frac{1}{p}\left(\frac{zf_j'(z)}{f_j(z)}\right) + 1 \right], \tag{2.2}$$

which readily yields

$$\frac{1}{p}\left(\frac{zF_p'(z)}{F_p}\right) = -1 + \left(1 - \gamma_j\right) + \sum_{j=1}^{n} \left[\frac{1}{p}\left(\frac{zf_j'(z)}{f_j(z)}\right) + \gamma_j \right]. \tag{2.3}$$

We thus find that

$$\Re\left[\frac{1}{p}\left(\frac{zF_p'(z)}{F_p}\right)\right] = -1 + \sum_{j=1}^{n} \alpha_j + \sum_{j=1}^{n} \Re\left[\frac{1}{p}\left(\frac{zf_j'(z)}{f_j(z)}\right) + \gamma_j \right]. \tag{2.4}$$

Since, by hypothesis, $f_j \in \Sigma S_p^*(\gamma_j) \quad (j = 1, \cdots, n)$, we have

$$\Re\left[\frac{1}{p}\left(\frac{zF_p'(z)}{F_p}\right)\right] < -\left(1 - \sum_{j=1}^{n} \alpha_j\right) =: \kappa, \tag{2.5}$$

which evidently completes the proof of Theorem 1. □

Upon setting

$$f_j(z) = f(z), \quad \gamma_j = \gamma \quad \text{and} \quad \alpha_j = \alpha \qquad (j = 1, \cdots, n)$$

in Theorem 1, we have the following corollary.

Corollary 1. *Let* $f \in \Sigma S_p^*(\gamma) \quad (\gamma := 1 - \alpha \geqq 0)$, *where* $\alpha \geqq 0$. *Also let* $1 - n\alpha \geqq 0$. *Then the product* $\Theta_p(z)$ *defined by*

$$\Theta_p(z) := z^{-p} \left[z^p f(z) \right]^n$$

is in the class $\Sigma S_p^*(1 - n\alpha)$ *of meromorphically p-valent starlike functions of order* $1 - n\alpha$ *in* $\mathbb{U}$.

Corollary 2. *Let* $f_j \in \Sigma S_p^*(\gamma_j) \quad (j = 1, \cdots, n)$, *where*

$$\gamma_j := 1 - \alpha_j \geqq 0 \qquad \text{and} \qquad \alpha_j \geqq 0 \qquad (j = 1, \cdots, n).$$

Also let

$$\kappa := 1 - \sum_{j=1}^{n} \alpha_j \geqq 0.$$

Then the function $\Phi_p(z)$ *defined by*

$$\Phi_p(z) := -p \int_0^z t^{-p-1} \prod_{j=1}^{n} \left\{ t^p f_j(t) \right\} \mathrm{d}t \tag{2.6}$$

is in the class $\Sigma C_p(\kappa)$ *of meromorphically p-valent convex functions of order* κ *in* $\mathbb{U}$.

Proof. The result asserted by Corollary 2 follows immediately from Theorem 1, since

$$\Phi_p(z) \in \Sigma C_p(\kappa) \Longleftrightarrow -\frac{z\Phi'(z)}{p} =: F_p(z) \in \Sigma S_p^*(\kappa).$$

□

Corollary 3. *Let* $f_j \in \Sigma C_p(\gamma_j) \quad (j = 1, \cdots, n)$, *where*

$$\gamma_j := 1 - \alpha_j \geqq 0 \qquad \text{and} \qquad \alpha_j \geqq 0 \qquad (j = 1, \cdots, n).$$

Also let

$$\kappa := 1 - \sum_{j=1}^{n} \alpha_j \geqq 0.$$

Then the product $G_p(z)$ *defined by*

$$G_p(z) = z^{-p} \prod_{j=1}^{n} \left\{ -\left(\frac{z^{p+1} f_j'(z)}{p} \right) \right\} \tag{2.7}$$

is in the class $\Sigma S_p^*(\kappa)$ *of meromorphically p-valent starlike functions of order* κ *in* $\mathbb{U}$.

Proof. From the fact that

$$f_j(z) \in \Sigma C_p(\gamma_j) \Longleftrightarrow -\frac{z f_j'(z)}{p} \in \Sigma S_p^*(\gamma_j) \qquad (j = 1, \cdots, n),$$

by replacing $f_j(z)$ by $-\frac{z f_j'(z)}{p}$ in Theorem 1, we are led easily to Corollary 3. □

Corollary 4. *Let* $f_j \in \Sigma C_p(\gamma_j) \quad (j = 1, \cdots, n)$, *where*

$$\gamma_j := 1 - \alpha_j \geqq 0 \qquad \text{and} \qquad \alpha_j \geqq 0 \qquad (j = 1, \cdots, n).$$

Also let

$$\kappa := 1 - \sum_{j=1}^{n} \alpha_j \geqq 0.$$

Then the function $\Psi_p(z)$ *defined by*

$$\Psi_p(z) = -p \int_0^z t^{-p-1} \prod_{j=1}^{n} \left\{ -\left(\frac{t^{p+1} f_j'(t)}{p} \right) \right\} \mathrm{d}t \tag{2.8}$$

is in the class $\Sigma C_p(\kappa)$ *of meromorphically p-valent convex functions of order* κ.

Proof. The result asserted by Corollary 4 follows immediately from Corollary 3, since

$$\Psi_p(z) \in \Sigma C_p(\kappa) \Longleftrightarrow -\frac{z\Psi_p'(z)}{p} =: G_p(z) \in \Sigma S_p^*(\kappa).$$

□

By applying the same method and technique as in our proofs of Theorem 1 as well as of Corollaries 2, 3 and 4, we can establish Theorem 2 below.

Theorem 2. *Let* $f_j \in \Sigma_p \quad (j = 1, \cdots, n)$. *Suppose that*

$$\gamma_j := 1 + \alpha_j \geqq 0 \qquad \text{and} \qquad \alpha_j \geqq 0 \qquad (j = 1, \cdots, n).$$

Also let

$$\sigma := 1 + \sum_{j=1}^{n} \alpha_j \geqq 0.$$

Then each of the following assertions holds true:

(i) *If* $f_j \in \Sigma M_p(\gamma_j) \quad (j = 1, \cdots, n)$, *then the product* $F_p(z)$ *defined by* (2.1) *is in the class* $\Sigma M_p(\sigma)$.

(ii) *If* $f_j \in \Sigma M_p(\gamma_j) \quad (j = 1, \cdots, n)$, *then the integral operator* Φ_p *defined by* (2.6) *is in the class* $\Sigma N_p(\sigma)$.

(iii) *If* $f_j \in \Sigma N_p(\gamma_j) \quad (j = 1, \cdots, n)$, *then the product* $G_p(z)$ *defined by* (2.7) *is in the class* $\Sigma M_p(\sigma)$.

(iv) *If* $f_j \in \Sigma N_p(\gamma_j) \quad (j = 1, \cdots, n)$, *then the integral operator* Ψ_p *defined by* (2.8) *is in the class* $\Sigma N_p(\sigma)$.

Theorem 3. *Let*

$$\alpha_j \geqq 0 \qquad \text{and} \qquad 0 \leqq \beta_j < 1 \qquad (j = 1, \cdots, n)$$

and suppose that

$$\delta := 1 - \sum_{j=1}^{n} \left(\frac{1 - \beta_j}{1 + \alpha_j} \right).$$

Also let the products $F_p(z)$ and $G_p(z)$ be defined by (2.1) *and* (2.7), *respectively. Then each of the following assertions holds true*:

(i) *If* $f_j \in \Sigma\mathcal{S}_p^*(\alpha_j,\beta_j) \quad (j = 1,\cdots,n)$, *then* $F_p(z) \in \Sigma S_p^*(\delta)$.

(ii) *If* $f_i \in \Sigma\mathcal{C}_p(\alpha_j,\beta_j) \quad (j = 1,\cdots,n)$, *then* $G_p(z) \in \Sigma S_p^*(\delta)$.

Proof. By following the lines as in (Kumar *et al.*, 2005), we first prove that

$$\Sigma\mathcal{S}_p^*(\lambda,\mu) \subset \Sigma S_p^*\left(\frac{\lambda+\mu}{1+\lambda}\right).$$

Indeed, if we let $f \in \Sigma\mathcal{S}_p^*(\lambda,\mu)$, then the quantity w defined by

$$w := \frac{1}{p}\left(\frac{zf'(z)}{f(z)}\right)$$

satisfies the following inequality:

$$-\Re(w) - \mu \geqq \lambda\,|w+1| \geqq \lambda\Re\,(w+1)\,,$$

which immediately yields

$$-\Re(w) \geqq \frac{\lambda+\mu}{1+\lambda}.$$

We thus have

$$f \in \Sigma\mathcal{S}_p^*(\lambda,\mu) \Longrightarrow f \in \Sigma S_p^*\left(\frac{\lambda+\mu}{1+\lambda}\right).$$

Next, since

$$f_j \in \Sigma\mathcal{S}_p^*(\alpha_j,\beta_j) \quad (j = 1,\cdots,n),$$

we have

$$f_j \in \Sigma S_p^*\left(\frac{\alpha_j+\beta_j}{1+\alpha_j}\right) \quad (j = 1,\cdots,n),$$

The assertion (i) of Theorem 3 now follows readily from an application of Theorem 1.

The proof of the assertion (ii) of Theorem 3 follows similarly by using Corollary 3. □

Corollary 5. *Let*

$$\alpha_j \geqq 0 \qquad \text{and} \qquad 0 \leqq \beta_j < 1 \qquad (j = 1,\cdots,n)$$

and suppose that

$$\delta := 1 - \sum_{j=1}^{n}\left(\frac{1-\beta_j}{1+\alpha_j}\right).$$

Also let the functions $\Phi_p(z)$ and $\Psi_p(z)$ be defined by (2.6) *and* (2.8), *respectively. Then each of the following assertions holds true*:

(i) *If* $f_j \in \Sigma\mathcal{S}_p^*(\alpha_j,\beta_j) \quad (j = 1,\cdots,n)$, *then* $\Phi_p(z) \in \Sigma\mathcal{C}_p(\delta)$.

(ii) *If* $f_j \in \Sigma\mathcal{C}_p(\alpha_j,\beta_j) \quad (j = 1,\cdots,n)$, *then* $\Psi_p(z) \in \Sigma\mathcal{C}_p(\delta)$.

Proof. The results asserted by Corollary 5 would follow immediately from Theorem 3, since

$$\Phi_p(z) \in \Sigma C_p(\delta) \Longleftrightarrow -\frac{z\Phi_p'(z)}{p} =: F_p(z) \in \Sigma S_p^*(\delta)$$

and

$$\Psi_p(z) \in \Sigma C_p(\delta) \Longleftrightarrow -\frac{z\Psi'(z)}{p} =: G_p(z) \in \Sigma S_p^*(\delta).$$

□

Finally, if we make use of the same method and technique as in our proofs of Theorem 3 and Corollary 5, we are led easily to Theorem 4 below.

Theorem 4. *Let*

$$-1 < \alpha_j \leqq 0 \qquad \text{and} \qquad \beta_j > 1 \qquad (j = 1, \cdots, n)$$

and suppose that

$$\nu := 1 + \sum_{j=1}^{n} \left(\frac{\beta_j - 1}{1 + \alpha_j} \right).$$

Also let the products $F_p(z)$ and $G_p(z)$ be defined by (2.1) *and* (2.7)*, respectively, and the functions $\Phi_p(z)$ and $\Psi_p(z)$ be defined by* (2.6) *and* (2.8)*, respectively. Then each of the following assertions holds true*:

(i) *If* $f_j \in \Sigma\mathcal{M}_p(\alpha_j, \beta_j)$ $(j = 1, \cdots, n)$, *then* $F_p(z) \in \Sigma M_p(\nu)$.

(ii) *If* $f_j \in \Sigma\mathcal{N}_p(\alpha_j, \beta_j)$ $(j = 1, \cdots, n)$, *then* $G_p(z) \in \Sigma M_p(\nu)$.

(iii) *If* $f_j \in \Sigma\mathcal{M}_p(\alpha_j, \beta_j)$ $(j = 1, \cdots, n)$, *then* $\Phi_p(z) \in \Sigma N_p(\nu)$.

(iv) *If* $f_j \in \Sigma\mathcal{N}_p(\alpha_j, \beta_j)$ $(j = 1, \cdots, n)$, *then* $\Psi_p(z) \in \Sigma N_p(\nu)$.

3. Concluding remarks and observations

In our present investigation, we have considered several interesting subclasses of the familiar class of meromorphically p-valent functions in the open unit disk $\mathbb{U}$. Our main purpose has been to successfully address the problems of finding the order of starlikeness and the order of convexity of the products of functions belonging to each of the various classes of β-uniformly p-valent starlike functions and β-uniformly p-valent convex functions in $\mathbb{U}$, which we have introduced here. The main results (stated as Theorems 1 to 4 *and* Corollaries 1 to 5) can indeed be specialized suitably in order to deduce the solutions of the corresponding problems for relatively more familiar subclasses of meromorphically p-valent functions in $\mathbb{U}$.

References

Ali, R. M. and V. Ravichandran (2010). Integral operators on Ma-Minda type starlike and convex functions. *Math. Comput. Modelling* **51**, 601–605.

Frasin, B. A. (2011). Convexity of integral operators of p-valent functions. *Math. Comput. Modelling* **53**, 581–586.

Goodman, A. W. (1991*a*). On uniformly convex functions. *Ann. Polon. Math.* **56**, 87–92.

Goodman, A. W. (1991*b*). On uniformly starlike functions. *J. Math. Anal. Appl.* **155**, 364–370.

Kanas, S. and A. Wisniowska (1999). Conic regions and k-uniformly convexity. *J. Comput. Appl. Math.* **105**, 327–336.

Kanas, S. and A. Wisniowska (2000). Conic regions and starlike functions. *Rev. Roumaine Math. Pures Appl.* **45**, 647–657.

Kanas, S. and H. M. Srivastava (2000). Linear operators associated with k-uniformly convex functions. *Integral Transforms Spec. Funct.* **9**, 121–132.

Kumar, S. S., V. Ravichandran and G. Murugusundaramoorthy (2005). Classes of meromorphic p-valent parabolic functions with positive coefficients. *Austral. J. Math. Anal. Appl.* **2**(2), 1–9. Article 3.

Kumar, V. and S. L. Shukla (1982). Certain integrals for classes of p-valent meromorphic functions. *Bull. Austral. Math. Soc.* **25**, 85–97.

Ma, W. and D. Minda (1992). Uniformly convex functions. *Ann. Polon. Math.* **57**, 165–175.

Murugusundaramoorthy, G. and N. Magesh (2004). A new subclass of uniformly convex functions and a corresponding subclass of starlike functions with fixed second coefficient. *J. Inequal. Pure Appl. Math.* **5**(4), 1–10. Article 85 (electronic).

Nishiwaki, J. and S. Owa (2007). Certain classes of analytic functions concerned with uniformly starlike and convex functions. *Appl. Math. Comput.* **187**, 350–355.

Owa, S. and J. Nishiwaki (2002). Coefficient estimates for certain classes of analytic functions. *J. Inequal. Pure Appl. Math.* **3**(5), 1–5. Article 72 (electronic).

Rønning, F. (1991). On starlike functions associated with the parabolic regions. *Ann. Univ. Mariae Curie-Skłodowska Sect. A* **45**, 117–122.

Rønning, F. (1993). Uniformly convex functions and a corresponding class of starlike functions. *Proc. Amer. Math. Soc.* **118**, 189–196.

Rønning, F. (1994). On uniform starlikeness and related properties of univalent functions. *Complex Variables Theory Appl.* **24**, 233–239.

Shams, S., S. R. Kulkarni and J. M. Jahangiri (2004). Classes of uniformly starlike and convex functions. *Internat. J. Math. Math. Sci.* **55**, 2959–2961.

Srivastava, H. M. and S. Owa (Editors) (1992). *Current Topics in Analytic Function Theory*. World Scientific Publishing Company. Singapore, New Jersey, London and Hong Kong.

Theory and Applications of Mathematics & Computer Science

(ISSN 2067-2764, EISSN 2247-6202)
http://www.uav.ro/applications/se/journal/index.php/tamcs

Theory and Applications of Mathematics & Computer Science 3 (2) (2013) 103–113

Satellite Formation Control Using the Approximating Sequence Riccati Equations

Ashraf H. Owis[a,*], Morsi A. Amer[b]

[a]*Department of Astronomy, Space and Meteorology*
Cairo University, Giza, Egypt
[b]*Astonomy Department King Abdulaziz University, Jeddah, Saudi Arabia and Department of Astronomy, Space and Meteorology Cairo University, Giza, Egypt*

Abstract

In this study we develop a reliable algorithm to control the satellite formation using the Approximating Sequence of Riccati Equations(ASRE) minimizing the fuel consumption and the deviation of the orbit from the nominal orbit. The nonlinear Clohessy -Wiltshire(CW) equations of motions are used to describe the motion of the satellite formation about a virtual reference position maintained at the formation center. The nonlinear dynamics of the system will be factorized in such a way that the new factorized system is accessible. The problem is tackled using the Approximating Sequence Riccati Equations(ASRE) method. The technique is based on Linear Quadratic Regulator(LQR) with fixed terminal state, which guarantees closed loop solution.

Keywords: Nonlinear Feedback, Linear Quadratic Regulator, Approximation Sequence Riccati Equation, Satellite Formation.

1. Introduction

Satellite formation flying is one of the space dynamics branches which gained much consideration in recent years. Despite the topic evolved two decades ago, the implementation of formation flying is not yet mature.

A satellite formation consists of two or more satellite flying together in close proximity, cooperating together to achieve some space mission such as terrestrial or deep space one. This system of distributed satellites has several advantages over the single satellite system such as, larger capability, reliability, flexibility, and more importantly less cost. *Satellite formation in contrast to satellite constellation in which the satellites are moving independently, the satellites affecting each other in co orbital motion about a virtual reference position maintained at the formation center.* The

*Corresponding author
Email addresses: aowis@eun.eg (Ashraf H. Owis), morsi.amer@gmail.com (Morsi A. Amer)

nonlinear Clohessy -Wiltshire equations of motions are used to describe the motion of the satellite formation. CW equations are developed for rendezvous(Clohessy & Wiltshire, 1960). Later on the linear inhomogeneous CW are studied(Meirovitch, 1970). CW equations have been solved by simplifying the nonlinear equations of motion via coordinate transformation of the central gravity field dynamics in presence of quadratic drag force(Thomas Carter, 2002).

The nonlinear dynamics of the system will be factorized in such a way that the new factorized system is accessible. The problem is tackled using the Approximating Sequence Riccati Equations method. The most common way of solving the orbit rendezvous of a satellite is the low thrust orbit rendezvous approach, which is a nonlinear optimal control problem. In the open loop context the problem can be solved via indirect and then direct method. The indirect method was developed through Pontryagin Maximum Principle(PMP) (A. J. Bryson, 1975),(L. Pontryagin & Mishchenko, 1952) . The direct method was developed using the Karush-Kuhn-Tucker(KKT) algebric equation(Enright & Conway, 1992).

one of the most common methods for solving the nonlinear feedback optimal control problem in the is the State Dependent Riccati Equations(SDRE) (Cimen, 2006). The Approximating Sequence of Riccati Equations (Cimen, 2004) technique is an iterative approach to solve the nonlinear optimal control problem. The ASRE is developed(Topputo & Bernelli-Zazzera, 2012) using the state transition matrix. By the virtue of the closed-loop nature of this control law, a trajectory designed in this way has the property to respond to perturbations acting during the transfer that continuously alter the state of the spacecraft. The optimal feedback control for linear systems with quadratic objective functions is addressed through the matrix Riccati equation: this is a matrix differential equation that can be integrated backward in time to yield the initial value of the Lagrange multipliers (A. J. Bryson, 1975). Recently, the nonlinear feedback control of circular coplanar low-thrust orbital transfers has been faced using continuous orbital elements feedback and Lyapunov functions(Chang & Marsden, 2002) and proved optimal by(Alizadah & Villac, 2011). Later on the problem has been solved using the primer vector approximation method(Haung, 2012). The problem is tackled using the Approximating Sequence Riccati Equation(ASRE) method based on Linear Quadratic Regulator(LQR) with fixed terminal state and the method is applied to GNSS circular constellation (Owis, 2013). In this work the control of the satellite formation described in the Earth Centered Earth Fixed Frame Fig. 1 is developed.

Linear Quadratic Regulator(LQR) with Fixed Terminal State

Consider the following system with linear dynamics and quadratic performance index as follows:

$$\dot{X} = AX + BU, \qquad X(t_0) = X_0 \in \mathbb{R}^n, \tag{1.1}$$

the following performance index

$$J = X_f^T Q_f X_f + \frac{1}{2}\int_{t_0}^{t_f} [X^T QX + U^T RU]dt, \tag{1.2}$$

Where A , B , Q , and R are constant coefficients matrices of the suitable dimen-

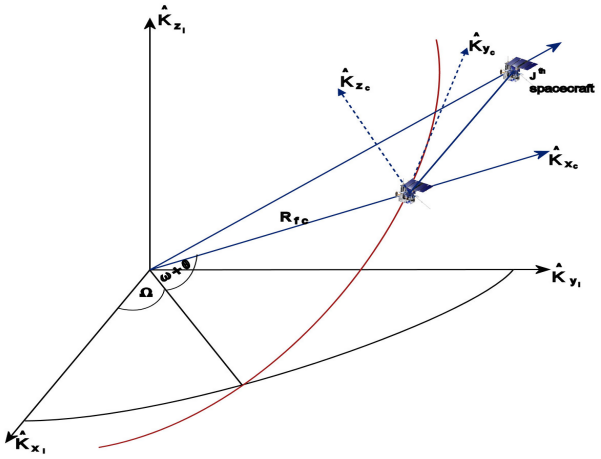

Figure 1. Satellite Formation Flying in the Earth Centered Earth Fixed Frame

sions. we have to find the m-dimensional control functions $U(t)$, $t \in [t_0\ t_f]$ which minimizes the J, which is an open loop (with t_0 fixed) optimal control. We optimize the performance index J, by adjoining the dynamics and the performance index (integrand) to form the Hamiltonian:

$$H(X, \lambda, U, t) = \frac{1}{2}(X^T QX + U^T RU) + \lambda^T (A(t)X + B(t)U),$$

where the Lagrange multiplier λ is called the adjoint variable or the costate. The necessary conditions for optimality are:

1. $\dot{X} = H_\lambda = A(t)X + B(t)U, \qquad X(t_0) = X_0,$
2. $\dot{\lambda} = -H_x = -QX - A^T\lambda, \qquad \lambda(t_f) = Q_f X_f,$
3. $H_u = 0 \Longrightarrow RU + B^T\lambda = 0 \Longrightarrow U^\star = -R^{-1}B^T\lambda.$

To find the minimum solution we have to check for $H_{uu} = \dfrac{\partial^2 H}{\partial \lambda^2} > 0$ or equivalently $R > 0$. Now we have that

$$\dot{X} = AX + BU^\star = AX - BR^{-1}B^T\lambda,$$

which can be combined to the the equation of the costate as follows

$$\begin{bmatrix} \dot{X} \\ \dot{\lambda} \end{bmatrix} = \begin{bmatrix} A & -BR^{-1}B^T \\ -Q & -A^T \end{bmatrix} \begin{bmatrix} X \\ \lambda \end{bmatrix}, \tag{1.3}$$

which is called the Hamiltonian matrix, it represents a $2n$ boundary value problem with $X(t_0) = X_0$ and, $\lambda(t_f) = Q_f X_f$.

We can solve this $2n$ boundary value problem using the transition matrix method as follows. Let's define a transition matrix

$$\phi_(t_1, t_0) = \begin{bmatrix} \phi_{11}(t_1, t_0) & \phi_{12}(t_1, t_0) \\ \phi_{21}(t_1, t_0) & \phi_{22}(t_1, t_0) \end{bmatrix},$$

we use this matrix to relate the current values of X and λ to the final values X_f and λ_f as follows

$$\begin{bmatrix} X \\ \lambda \end{bmatrix} = \begin{bmatrix} \phi_{11}(t, t_f) & \phi_{12}(t, t_f) \\ \phi_{21}(t, t_f) & \phi_{22}(t, t_f) \end{bmatrix} \begin{bmatrix} X(t_f) \\ \lambda(t_f) \end{bmatrix},$$

so we have

$$\begin{aligned} X &= \phi_{11}(t, t_f)X(t_f) + \phi_{12}(t, t_f)\lambda(t_f) \\ &= [\phi_{11}(t, t_f) + \phi_{12}(t, t_f)Q_f]X(t_f), \end{aligned}$$

we can eliminate $X(t_f)$ to get

$$\begin{aligned} X &= [\phi_{11}(t, t_f) + \phi_{12}(t, t_f)Q_f][\phi_{11}(t_0, t_f) + \phi_{12}(t_0, t_f)Q_f]^{-1}X(t_0) \\ &= X(t, X_0, t_0), \end{aligned}$$

now we can find $\lambda(t)$ in terms of $X(t_f)$ as

$$\lambda(t) = [\phi_{21}(t, t_f) + \phi_{22}(t, t_f)Q_f]X(t_f),$$

then we can eliminate $X(t_f)$ to get

$$\begin{aligned} \lambda(t) &= [\phi_{21}(t, t_f) + \phi_{22}(t, t_f)Q_f][\phi_{11}(t, t_f) + \phi_{12}(t, t_f)Q_f]^{-1}X(t), \\ &= \phi_{\lambda x}X(t). \end{aligned}$$

Now we search a solution for $\phi_{\lambda x}$. By differentiating $\lambda(t)$ we get

$$\dot{\lambda}(t) = \dot{\phi}_{\lambda x}X(t) + \phi_{\lambda x}\dot{X}(t).$$

Comparing the last equation with the Hamiltonian matrix we get

$$-QX(t) - A^T\lambda(t) = \dot{\phi}_{\lambda x}X(t) + \phi_{\lambda x}\dot{X}(t),$$

then we have

$$\begin{aligned} -\dot{\phi_{\lambda x}}(t)X(t) &= QX(t) + A^T\lambda(t) + \phi_{\lambda x}\dot{X}(t) \\ &= QX(t) + A^T\lambda(t) + \phi_{\lambda x}(AX - BR^{-1}B^T\lambda(t)) \\ &= (Q + \phi_{\lambda x}A)X(t) + (A^T - \phi_{\lambda x}BR^{-1}B^T)\lambda(t) \\ &= (Q + \phi_{\lambda x}A)X(t) + (A^T - \phi_{\lambda x}BR^{-1}B^T)\phi_{\lambda x}X(t) \\ &= [Q + \phi_{\lambda x}A + A^T\phi_{\lambda x} - \phi_{\lambda x}BR^{-1}B^T\phi_{\lambda x}]X(t). \end{aligned}$$

Since this is true for arbitrary $X(t)$, $\phi_{\lambda x}$ must satisfy

$$-\dot{\phi}_{\lambda x}(t) = Q + \phi_{\lambda x}A + A^T\phi_{\lambda x} - \phi_{\lambda x}BR^{-1}B^T\phi_{\lambda x}, \tag{1.4}$$

which is the matrix differential Riccati Equation . We can solve for $\phi_{\lambda x}$ by solving Riccati Equation backwards in time from t_f with $\phi_{\lambda x}(t_f) = Q_f$. The optimal control is then given by

$$U^\star = -R^{-1}B^T\lambda(t) = -R^{-1}B^T\phi_{\lambda x}X = -K(t)X(t, X_0, t_0). \tag{1.5}$$

From 1.5 we notice that the optimal control is a linear full-state feedback control, therefore the linear quadratic terminal controller is feedback by default.

2. The Approximating Sequence of Riccati Equations(ASRE)

Assume that we have the following nonlinear system

$$\dot{X} = f(X, U, t) \tag{2.1}$$

$$X(t_0) = X_0, \quad X(t_f) = X_f \in R^n \tag{2.2}$$

with performance index

$$J = \phi(X_f, t_f) + \int_{t_0}^{t_f} L(X, U, t)dt \tag{2.3}$$

This system can be rewritten in the state dependent quasi-linear system as follows

$$\dot{X}^i = A(X^{i-1})X^i + B(X^{i-1})U^i \tag{2.4}$$

$$X(t_0) = X_0^0, \quad X(t_f) = X_f^n \in R^n \tag{2.5}$$

$$J = {X_f^i}^T Q(X_f^{i-1}) X_f^i + \frac{1}{2}\int_{t_0}^{t_f} [{X^i}^T Q(X^{i-1}) X^i + {U^i}^T R(X^{i-1}) U^i] dt, \tag{2.6}$$

where i represents the iteration step over the time interval $[t_i - 1, t_i]$ Fig. the technique is based of the previously introduced Linear Quadratic Regulator with fixed terminal state, which is a full state feedback and therefore the obtained solution will be a closed loop one, I.e. able to respond to the unexpected change in the inputs. The technique works as follows: the initial state is used to compute A_0, and B_0 and we solve for the first LQR iteration and compute X^1 and then used to compute new value of A_1, and B_1 for the second iteration until the final state error reaches a value below a set threshold.

3. Satellite formation control

Consider a satellite in the central gravity field. The eqaution of motion can be written in the cartesian frame as follows

$$\ddot{\mathbf{r}}) = -\frac{\mu}{r^3}\mathbf{r} + \frac{\mathbf{f}}{m} \tag{3.1}$$

Where μ is the gravitational constant of the Earth($3.986005 \times 10^{14} m^3/s^2$). In the rotating coordinate frame along a circular orbit at a constant angular velocity, the position, velocity, and the acceleration become

$$\begin{aligned} \mathbf{r} = &\quad \mathbf{R} + \delta\mathbf{r} = (R + x)i + yj + zk \\ \dot{\mathbf{r}} = &\quad (\dot{x} - \omega y)i + [(\dot{y} + \omega(R + x)]j + \dot{z}k \\ \ddot{\mathbf{r}} = &\quad [\ddot{x} - 2\omega\dot{y} - \omega^2(R + x)]i + [(\ddot{y} + 2\omega\dot{x}) - \omega^2 y]j + \ddot{z}k \end{aligned} \tag{3.2}$$

Plugging third equation of (3.2) into equ. (3.1) and substituting $r = \sqrt{[(R + x)^2 + y^2 + z^2]}$ we get

$$\begin{aligned} \ddot{x} - 2\omega\dot{y} - \omega^2(R + x) &= -\frac{\mu}{r^3}(R + x) + U_x \\ \ddot{y} + 2\omega\dot{x} - \omega^2 y &= -\frac{\mu}{r^3} y + U_y \\ \ddot{z} &= -\frac{\mu}{r^3} z + U_z \end{aligned} \tag{3.3}$$

If we nondimensionalize the problem by setting the radius of the reference orbit $R = 1$ and reference time $\frac{1}{\omega}$ and in this system of units the gravitational constant μ is unity the nondimensionalized equation of motion can be written as

$$\begin{aligned} \ddot{x} - 2\dot{y} - (1+x)(\frac{1}{r^3} - 1) &= U_x \\ \ddot{y} + 2\dot{x} + y(\frac{1}{r^3} - 1) &= U_y \\ \ddot{z} + \frac{1}{r^3} z &= U_z \end{aligned} \tag{3.4}$$

where $r = \sqrt{[(1+x)^2 + y^2 + z^2]}$, for simplicity we consider the in plan motion. We define the state vector of the system

$$\mathbf{x} = \begin{bmatrix} x_1 \\ x_2 \\ x_3 \\ x_4 \end{bmatrix} = \begin{bmatrix} x \\ y \\ \dot{x} \\ \dot{y} \end{bmatrix} \tag{3.5}$$

$$\mathbf{u} = \begin{bmatrix} u_1 \\ u_2 \end{bmatrix} = \begin{bmatrix} T_x \\ T_y \end{bmatrix} \tag{3.6}$$

Then Equation (3.4) can be written in the form :

$$\dot{\mathbf{x}} = \mathbf{f}(\mathbf{x}) + \mathbf{B}(\mathbf{x})\mathbf{u} \tag{3.7}$$

Choosing a suitable factorization equation (3.7) is rewritten in the factored state variable form :

$$\dot{\mathbf{x}} = \mathbf{A}(\mathbf{x})\mathbf{x} + \mathbf{B}(\mathbf{x})\mathbf{u} \tag{3.8}$$

where :

$$\mathbf{A}(\mathbf{x}) = \begin{bmatrix} 0 & 0 & 1 & 0 \\ 0 & 0 & 0 & 1 \\ \Gamma + \frac{\Gamma}{x_1} & 0 & 0 & 2 \\ 0 & \Gamma & 2 & 0 \end{bmatrix} \tag{3.9}$$

$$\mathbf{B}(\mathbf{x}) = \begin{bmatrix} 0 & 0 \\ 0 & 0 \\ 1 & 0 \\ 0 & 1 \end{bmatrix} \tag{3.10}$$

where $\Gamma = \frac{1}{r^3} - 1$

4. Factored Controllability

For the factored system (3.8) the controllability is established by verifying that the controllability matrix

$$\mathbf{M}_{cl} = [\mathbf{B}\ \mathbf{AB}\ \mathbf{A}^2\mathbf{B}\ \mathbf{A}^3\mathbf{B}]$$

has a rank equals to $n = 4\ \forall x$ in the domain.
Since **A** and **B** have nonvanishing rows the controllability matrix $\mathbf{M}_{cl}$ for the System (3.8) is of rank 4.

Nondimensionalization of the problem In order to simplify the calculation we dimensionalize the system by removing the units from the equations of motion via multiplying or dividing some constants. The two constant we divid by are the radial distance of the initial orbit and the gravitational constant μ in this case the radius of the initial orbit is unity and velocity is divided by the circular velocity of the initial orbit $\sqrt{\frac{\mu}{r_0^2}}$ and the time is multiplied by $\sqrt{\frac{\mu}{r_0^3}}$ In application we would like to make an optimal orbit transfer(i.e. from $(r = 1)$ to $(r = 1.2)$ in time $t_f = 4.469, 5.2231$ (time unit) Fig. 2 with optimal velocity Fig. 3 and optimal control function of both radial and tangential components Figs. 4, 5. The initial angle is $(\theta_0 = \frac{\pi}{2})$ and the final angle is $(\theta_f = \frac{3\pi}{2})$. $\dot{r}_0 = 0$ and $\dot{r}_f = 0$ for the initial and final orbits. $\dot{\theta}_0 = \sqrt{\frac{1}{r_0^3}} = 1$ and $\dot{\theta}_f = \sqrt{\frac{1}{r_f^3}} = 0.54433105395$. In the second $\theta_f = \frac{5\pi}{2}$ with $t_f = 6.866$.
in example the matrices **Q** and **R** are the identity matrices.

$$\mathbf{Q} = \begin{bmatrix} 1 & 0 & 0 & 0 \\ 0 & 1 & 0 & 0 \\ 0 & 0 & 1 & 0 \\ 0 & 0 & 0 & 1 \end{bmatrix}$$

$$\mathbf{R} = \begin{bmatrix} 1 & 0 \\ 0 & 1 \end{bmatrix}$$

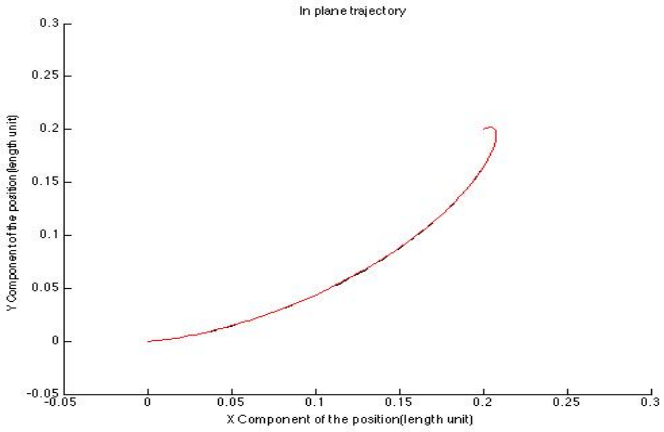

Figure 2. Trajectory of orbit rendezvous manoeuvre in the non dimensional coordinates

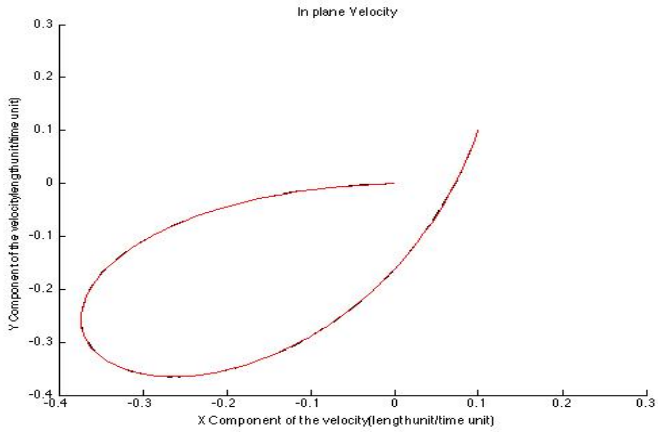

Figure 3. Velocity in the non dimensional coordinates

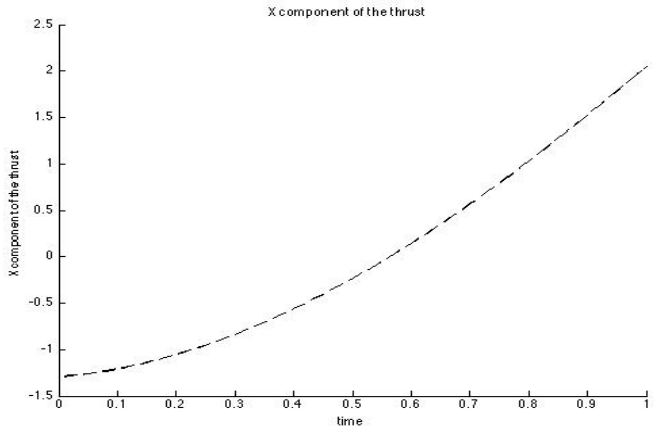

Figure 4. Control X component in the non dimensional coordinates

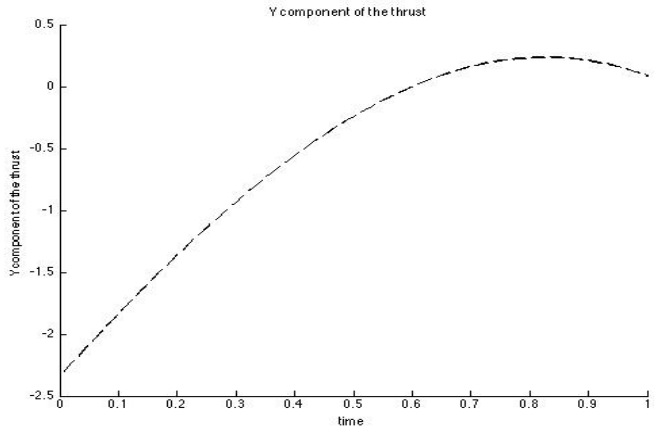

Figure 5. Control Y component in the non dimensional coordinates

5. Conclusion

The nonlinear orbital dynamics of the satellite formation with respect to the Earth Center Earth Fixed Coordinates are developed. The feedback optimal control of the satellite formation can be solved by factorizing the original nonlinear dynamics into accessible (weakly controllable) linear dynamics of state dependent factors. The factorized problem has been solved using the the Approximating Sequence Riccati Equations(ASRE) method. The technique is based on Linear Quadratic Regulator(LQR) with fixed terminal state, which guarantees closed loop solution. A computer simulation verified that the adopted technique is relaible.

6. Acknowledgments

This project was supported financially by the Science and Technology Development Fund (STDF), Egypt, Grant No 1834

References

A. J. Bryson, and Y. C. Ho (1975). *Applied Optimal Control :Optimization, Estimation, and Control*. Taylor and Francis Group. NY.

Alizadah, I. and B. F. Villac (2011). Static solutions of the hamilton-jacobi-bellman equation for circular orbit transfer. *Jounal of Guidance, Control and Dynamics* **34**(5), 1584–1588.

Chang, D. E. and D. F. Marsden (2002). Lyapunov based transfer between elliptic keplerian orbits. *Descrete and Continuos Dynamical Systems. Series B* **2**, 57–67.

Cimen, T. (2004). Global optimal feedback control for general nonlinear systems with nonquadratic performance criteria. *& Control Letters* **53**(5), 327–346.

Cimen, T. (2006). Recent advances in nonlinear optimal feedback control design. In: *9th WSEAS International Conference on Applied Mathematics, Anonymous ROKETSAN Missiles IndustriesInc*.

Clohessy, W. H. and R. S. Wiltshire (1960). Terminal guidance system for satellite rendezvous. *Journal of the Aerospace Sciences* **27**, 653–638.

Enright, P. and B. Conway (1992). Discrete approximations to optimal trajectories using direct transcription and nonlinear programming. *Journal of Guidance, Control, and Dynamic* **15**, 994–1002.

Haung, W. (2012). Solving coplanar power-limited orbit transfer probelm by primer vector approximation method. *Internation Journal of Aerospace Engineering*.

L. Pontryagin, V.Boltyanskii, R. Gamkrelidze and E. Mishchenko (1952). *The Mathematical Theory of Optimal Processes*. 2nd ed.. John Wiley & Sons, New York. New York.

Meirovitch, Leonard (1970). *Methods of Analytical Dynamics*. Dover Publications, Inc.. New York.

Owis, A. (2013). Satellite constellation reconfiguration using the approximating sequence riccati equations. *Theory and Applications of Mathematics & Computer Science* **3**(1), 99–106.

Thomas Carter, Mayer Humi. (2002). Clohessy-wiltshire equations modified to include quadratic drag. *Journal of Guidance, Control, and Dynamics* **25**(6), 1058–1063.

Topputo, F. and F. Bernelli-Zazzera (2012). A methofd to solve the nonlinear optimal control problem in astrodynamics. In: *The 1St IAA Conference on Dynamics and Control of Space Systems*. Porto, Portugal.

Theory and Applications of Mathematics & Computer Science

(ISSN 2067-2764, EISSN 2247-6202)
http://www.uav.ro/applications/se/journal/index.php/tamcs

Theory and Applications of Mathematics & Computer Science 3 (2) (2013) 114–119

New Fractional Integral Results Using Euler Functions

Zoubir Dahmani[a,*]

[a] *Laboratory LPAM, Faculty SEI, UMAB University of Mostaganem, Algeria.*

Abstract

In this paper, we use the the Riemann-Liouville fractional integral to develop some new results related to the Hermite-Hadamard inequality. Our results have some relationships with the paper of M.Z. Sarikaya et al. published in [Int. J. Open Problems Comput. Math., Vol. 5, No. 3, September, 2012]. Some interested inequalities of this paper can be deduced as some special cases.

Keywords: Integral inequalities, fractional integral, log convexity, Euler functions.
2010 MSC: 26D10, 26A33.

1. Introduction

Let us consider the famous Hermite-Hadamard inequality (Hadamard, 1893; Hermite, 1883) :

$$\frac{f(a+b)}{2} \leq \frac{2}{b-a}\int_a^b f(x)dx \leq \frac{f(a)+f(b)}{2}, \tag{1.1}$$

where f is a convex function on $[a, b]$.
Many researchers have given considerable attention to (1.1) and a number of extensions and generalizations have appeared in the literature, see (Belaidi *et al.*, 2009; Dahmani, 2010; Dragomir & Pearse, 2000; Florea & Niculescu, 2007; Set *et al.*, 2010; Sarikaya *et al.*, 2012).
The aim of this paper is to present new extensions for a Hermite-Hadamard type inequality involving log-convex functions and using Euler Functions. Our results have some relationships with the work of M.Z. Sarikaya et al. (Sarikaya *et al.*, 2012). Some interested results of this reference can be deduced as particular cases.

*Corresponding author
Email address: zzdahmani@yahoo.fr (Zoubir Dahmani)

2. Preliminaries

We shall introduce the following definitions and properties which are used throughout this paper.

Definition 2.1. The Riemann-Liouville fractional integral operator of order $\alpha > 0$, for a continuous function on $[a, b]$ is defined by:

$$J^{\alpha} f(t) = \frac{1}{\Gamma(\alpha)} \int_a^t (t-\tau)^{\alpha-1} f(\tau) d\tau; \quad \alpha > 0, a \leq t \leq b, \tag{2.1}$$

where $\Gamma(\alpha) := \int_0^{\infty} e^{-u} u^{\alpha-1} du$.

We give the semigroup property:

$$J^{\alpha} J^{\beta} f(t) = J^{\alpha+\beta} f(t), \alpha > 0, \beta > 0. \tag{2.2}$$

For more details, one can consult (Gorenflo & Mainardi, 1997).

3. Main Results

Theorem 3.1. *Let f and g be two differentiable positive log-convex functions on I^0 (the interior of the interval I and $a, b \in I^0$.) Then, for $\alpha > 0$, the following inequalities hold.*

$$\begin{aligned} &2\Gamma^{-2}(\alpha)\Gamma(2\alpha-1)(b-a)J^{2\alpha-1} fg(b) \\ &\geq J^{\alpha}\Big[g(t)exp\Big(bA_b\Big)\Big]exp\Big[\tfrac{-J^{\alpha-1}bf(b)+J^{\alpha}bf'(b)}{J^{\alpha}f(b)}\Big]J^{\alpha} f(b) \\ &+J^{\alpha}\Big[f(b)exp\Big(bD_b\Big)\Big]exp\Big[\tfrac{-J^{\alpha-1}g(b)+J^{\alpha}bg'(b)}{J^{\alpha}g(b)}\Big]J^{\alpha} g(b), \end{aligned} \tag{3.1}$$

where $A_b := \frac{-J^{\alpha-1}f(b)+J^{\alpha}f'(b)}{J^{\alpha}f(b)}, D_b := \frac{-J^{\alpha-1}g(b)+J^{\alpha}g'(b)}{J^{\alpha}g(b)}$.

Proof. Let us consider:
$K(x) := \frac{(t-x)^{\alpha-1}}{\Gamma(\alpha)} f(x), x \in [a, t], a < t \leq b, \alpha > 0.$
We remark immediately that, if $\alpha = 1$, then $K(x) = f(x)$ and hence, we can obtain the first main result of (Sarikaya *et al.*, 2012).
Now, let us take $\alpha \neq 1$. We can write

$$logK(x) - logK(y) \geq \frac{d}{dy}(logK(y))(x-y), x, y \in [a, t]. \tag{3.2}$$

Therefore,

$$log\frac{K(x)}{K(y)} \geq \frac{K'(y)}{K(y)}(x-y). \tag{3.3}$$

Hence,

$$\frac{K(x)}{K(y)} \geq exp\Big(\frac{(1-\alpha)(t-y)^{\alpha-2}f(y) + (t-y)^{\alpha-1}f'(y)}{(t-y)^{\alpha-1}f(y)}(x-y)\Big). \tag{3.4}$$

Consequently,

$$\frac{(t-x)^{\alpha-1}f(x)g(x)}{\Gamma(\alpha)} \geq \frac{(t-y)^{\alpha-1}f(y)g(x)}{\Gamma(\alpha)} exp\Big(\frac{(1-\alpha)(t-y)^{\alpha-2}f(y)+(t-y)^{\alpha-1}f'(y)}{(t-y)^{\alpha-1}f(y)}(x-y)\Big). \quad (3.5)$$

Integrating the above inequality with respect to y over $[a,t], a < t \leq b$, yields

$$\begin{aligned} &\frac{(t-a)(t-x)^{\alpha-1}f(x)g(x)}{\Gamma(\alpha)} \\ &\geq g(x)\int_a^t \frac{(t-y)^{\alpha-1}f(y)}{\Gamma(\alpha)} exp\Big[\frac{(1-\alpha)(t-y)^{\alpha-2}f(y)+(t-y)^{\alpha-1}f'(y)}{(t-y)^{\alpha-1}f(y)}(x-y)\Big]dy. \end{aligned} \quad (3.6)$$

For the right hand side of (3.6) we use Jensen inequality. We obtain

$$\begin{aligned} &\int_a^t \frac{(t-y)^{\alpha-1}f(y)}{\Gamma(\alpha)} exp\Big(\frac{(1-\alpha)(t-y)^{\alpha-2}f(y)+(t-y)^{\alpha-1}f'(y)}{(t-y)^{\alpha-1}f(y)}(x-y)\Big)dy \\ &\geq \Big(\int_a^t \frac{(t-y)^{\alpha-1}f(y)}{\Gamma(\alpha)}dy\Big) exp\Big[\frac{\int_a^t \frac{(1-\alpha)(t-y)^{\alpha-2}f(y)+(t-y)^{\alpha-1}f'(y)}{\Gamma(\alpha)}(x-y)dy}{\Big(\int_a^t \frac{(t-y)^{\alpha-1}f(y)}{\Gamma(\alpha)}dy\Big)}\Big]. \end{aligned} \quad (3.7)$$

Consequently,

$$\begin{aligned} &\int_a^t \frac{(t-y)^{\alpha-1}f(y)}{\Gamma(\alpha)} exp\Big(\frac{(1-\alpha)(t-y)^{\alpha-2}f(y)+(t-y)^{\alpha-1}f'(y)}{(t-y)^{\alpha-1}f(y)}(x-y)\Big)dy \\ &\geq exp\Big[\frac{-J^{\alpha-1}(x-t)f(t)+J^{\alpha}(x-t)f'(t)}{J^{\alpha}f(t)}\Big]J^{\alpha}f(t). \end{aligned} \quad (3.8)$$

That is

$$\begin{aligned} &\int_a^t \frac{(t-y)^{\alpha-1}f(y)}{\Gamma(\alpha)} exp\Big(\frac{(1-\alpha)(t-y)^{\alpha-2}f(y)+(t-y)^{\alpha-1}f'(y)}{(t-y)^{\alpha-1}f(y)}(x-y)\Big)dy \\ &\geq exp\Big[\frac{J^{\alpha-1}tf(t)-J^{\alpha}tf'(t)}{J^{\alpha}f(t)}\Big]exp\Big[\frac{-J^{\alpha-1}f(t)+J^{\alpha}f'(t)}{J^{\alpha}f(t)}x\Big]J^{\alpha}f(t). \end{aligned} \quad (3.9)$$

Thanks to (3.6) and (3.9), we obtain

$$\frac{(t-a)(t-x)^{\alpha-1}f(x)g(x)}{\Gamma(\alpha)} \geq g(x)exp\Big[\frac{J^{\alpha-1}tf(t)-J^{\alpha}tf'(t)}{J^{\alpha}f(t)}\Big]exp\Big[\frac{-J^{\alpha-1}f(t)+J^{\alpha}f'(t)}{J^{\alpha}f(t)}x\Big]J^{\alpha}f(t). \quad (3.10)$$

Then,

$$\Gamma^{-2}(\alpha)\Gamma(2\alpha-1)(t-a)J^{2\alpha-1}fg(t) \geq J^{\alpha}\Big[g(t)exp\Big(tA_t\Big)\Big]exp\Big[\frac{-J^{\alpha-1}tf(t)+J^{\alpha}tf'(t)}{J^{\alpha}f(t)}\Big]J^{\alpha}f(t), \quad (3.11)$$

where

$$A_t := \frac{-J^{\alpha-1}f(t) + J^{\alpha}f'(t)}{J^{\alpha}f(t)}.$$

With the same arguments, we obtain:

$$\Gamma^{-2}(\alpha)\Gamma(2\alpha-1)(t-a)J^{2\alpha-1}fg(t) \geq J^{\alpha}\Big[f(t)exp\Big(tB_t\Big)\Big]exp\Big[\frac{-J^{\alpha-1}tg(t) + J^{\alpha}tg'(t)}{J^{\alpha}g(t)}\Big]J^{\alpha}g(t), \quad (3.12)$$

where

$$D_t := \frac{-J^{\alpha-1}g(t) + J^{\alpha}g'(t)}{J^{\alpha}g(t)}.$$

Adding (3.11) and (3.12), yields

$$\begin{aligned} 2\Gamma^{-2}(\alpha)\Gamma(2\alpha-1)(t-a)J^{2\alpha-1}fg(t) &\geq J^{\alpha}\Big[g(t)exp\Big(tA_t\Big)\Big]exp\Big[\frac{-J^{\alpha-1}tf(t) + J^{\alpha}tf'(t)}{J^{\alpha}f(t)}\Big]J^{\alpha}f(t) \\ &+J^{\alpha}\Big[f(t)exp\Big(tD_t\Big)\Big]exp\Big[\frac{-J^{\alpha-1}tg(t)+J^{\alpha}tg'(t)}{J^{\alpha}g(t)}\Big]J^{\alpha}g(t). \end{aligned} \quad (3.13)$$

Taking $t = b$, we obtain the desired inequality (3.1). □

Theorem 3.2. *Let f and g be two differentiable positive log-convex functions on I^0 and $a, b \in I^0$. Then, for $\alpha > 0, \beta > 0, \alpha + \beta \neq 1$, we have:*

$$\begin{aligned} &2\Gamma(2\alpha+2\beta-3)(b-a)\frac{J^{2\alpha+2\beta-3}fg(b)}{\Gamma^2(\alpha)\Gamma^2(\beta)} \\ &\geq exp[\frac{-J^{\alpha+\beta-2}bf(b) + J^{\alpha+\beta}bf'(b)}{J^{\alpha+\beta-1}f(b)}]\frac{J^{\alpha+\beta-1}(g(b)exp[bE_b])}{(\alpha+\beta-1)B(\alpha,\beta)}\frac{J^{\alpha+\beta-1}f(b)}{(\alpha+\beta-1)B(\alpha,\beta)} \\ &+exp[\frac{-J^{\alpha+\beta-2}bg(b) + J^{\alpha+\beta}bg'(b)}{J^{\alpha+\beta-1}g(b)}]\frac{J^{\alpha+\beta-1}(f(b)exp[bL_b])}{(\alpha+\beta-1)B(\alpha,\beta)}\frac{J^{\alpha+\beta-1}g(b)}{(\alpha+\beta-1)B(\alpha,\beta)}, \end{aligned} \quad (3.14)$$

where

$$E_b := \frac{-J^{\alpha+\beta-2}f(b) + J^{\alpha+\beta-1}f'(b)}{J^{\alpha+\beta-1}f(b)}, L_b := \frac{-J^{\alpha+\beta-2}g(b) + J^{\alpha+\beta-1}g'(b)}{J^{\alpha+\beta-1}g(b)}.$$

Proof. We consider: $K(x) := \frac{(t-x)^{\alpha-1}(t-x)^{\beta-1}}{\Gamma(\alpha)\Gamma(\beta)}f(x), x \in [a,t], a < t \leq b, \alpha > 0, \beta > 0.$

We remark immediately that if $\alpha = 1, \beta = 1$, then we obtain the first main result in (Sarikaya *et al.*, 2012).

To prove Theorem 3.2, we need to take $\alpha + \beta \neq 1$. We have

$$\frac{K(x)}{K(y)} \geq exp\Big(\frac{(2-\alpha-\beta)(t-y)^{\alpha+\beta-3}f(y) + (t-y)^{\alpha+\beta-2}f'(y)}{(t-y)^{\alpha+\beta-2}f(y)}(x-y)\Big). \quad (3.15)$$

Then,

$$\begin{aligned} &\frac{(t-x)^{\alpha-1}(t-x)^{\beta-1}f(x)g(x)}{\Gamma(\alpha)\Gamma(\beta)} \\ &\geq \frac{(t-y)^{\alpha+\beta-2}f(y)g(x)}{\Gamma(\alpha)\Gamma(\beta)}exp\Big(\frac{(2-\alpha-\beta)(t-y)^{\alpha+\beta-3}f(y) + (t-y)^{\alpha+\beta-2}f'(y)}{(t-y)^{\alpha+\beta-2}f(y)}(x-y)\Big). \end{aligned} \quad (3.16)$$

Integrating the above inequality with respect to y over $[a,t], a < t \leq b$, yields

$$\frac{(t-a)(t-x)^{\alpha+\beta-2}f(x)g(x)}{\Gamma(\alpha)\Gamma(\beta)}$$

$$\geq g(x)\int_a^t \frac{(t-y)^{\alpha+\beta-2}f(y)}{\Gamma(\alpha)\Gamma(\beta)} exp\Big[\frac{(2-\alpha-\beta)(t-y)^{\alpha+\beta-3}f(y)+(t-y)^{\alpha+\beta-2}f'(y)}{(t-y)^{\alpha+\beta-2}f(y)}(x-y)\Big]dy. \quad (3.17)$$

Thanks to Jensen inequality, we can write

$$\int_a^t \frac{(t-y)^{\alpha+\beta-2}f(y)}{\Gamma(\alpha)\Gamma(\beta)} exp\Big(\frac{(2-\alpha+\beta)(t-y)^{\alpha+\beta-3}f(y)+(t-y)^{\alpha+\beta-2}f'(y)}{(t-y)^{\alpha+\beta-2}f(y)}(x-y)\Big)dy$$

$$\geq \Big(\int_a^t \frac{(t-y)^{\alpha+\beta-2}f(y)}{\Gamma(\alpha)\Gamma(\beta)}dy\Big) exp\Big[\frac{\int_a^t \frac{(2-\alpha-\beta)(t-y)^{\alpha+\beta-3}f(y)+(t-y)^{\alpha+\beta-2}f'(y)}{\Gamma(\alpha)\Gamma(\beta)}(x-y)dy}{\Big(\int_a^t \frac{(t-y)^{\alpha+\beta-2}f(y)}{\Gamma(\alpha)\Gamma(\beta)}dy\Big)}\Big]. \quad (3.18)$$

By simple calculation, we can state that

$$\int_a^t \frac{(t-y)^{\alpha+\beta-2}f(y)}{\Gamma(\alpha)\Gamma(\beta)} exp\Big(\frac{(2-\alpha-\beta)(t-y)^{\alpha+\beta-3}f(y)+(t-y)^{\alpha+\beta-2}f'(y)}{(t-y)^{\alpha+\beta-2}f(y)}(x-y)\Big)dy$$

$$\geq exp\Big[\frac{-J^{\alpha+\beta-2}tf(t)+J^{\alpha+\beta-1}tf'(t)}{J^{\alpha+\beta-1}f(t)}\Big] exp\Big[\frac{-J^{\alpha+\beta-2}f(t)+J^{\alpha+\beta-1}f'(t)}{J^{\alpha+\beta-1}f(t)}x\Big]\frac{J^{\alpha+\beta-1}f(t)}{(\alpha+\beta-1)B(\alpha,\beta)}, \quad (3.19)$$

where $B(\alpha,\beta)=\frac{\Gamma(\alpha)\Gamma(\beta)}{\Gamma(\alpha+\beta)}$.

Thanks to (3.17) and (3.19), we obtain

$$\frac{(t-a)(t-x)^{\alpha+\beta-2}f(x)g(x)}{\Gamma(\alpha)\Gamma(\beta)}$$

$$\geq exp\Big[\frac{-J^{\alpha+\beta-2}tf(t)+J^{\alpha+\beta-1}tf'(t)}{J^{\alpha+\beta-1}f(t)}\Big] exp\Big[\frac{-J^{\alpha+\beta-2}f(t)+J^{\alpha+\beta-1}f'(t)}{J^{\alpha+\beta-1}f(t)}x\Big]g(x)\frac{J^{\alpha+\beta-1}f(t)}{(\alpha+\beta-1)B(\alpha,\beta)}. \quad (3.20)$$

Then,

$$\Gamma(2\alpha+2\beta-3)(t-a)\frac{J^{2\alpha+2\beta-3}fg(t)}{\Gamma^2(\alpha)\Gamma^2(\beta)}$$

$$\geq exp\Big[\frac{-J^{\alpha+\beta-2}tf(t)+J^{\alpha+\beta}tf'(t)}{J^{\alpha+\beta-1}f(t)}\Big]\frac{J^{\alpha+\beta-1}\Big(g(t)exp\Big[\frac{-J^{\alpha+\beta-2}f(t)+J^{\alpha+\beta-1}f'(t)}{J^{\alpha+\beta-1}f(t)}t\Big]\Big)}{(\alpha+\beta-1)B(\alpha,\beta)}\frac{J^{\alpha+\beta-1}f(t)}{(\alpha+\beta-1)B(\alpha,\beta)}. \quad (3.21)$$

With the same arguments, we obtain

$$\Gamma(2\alpha+2\beta-3)(t-a)\frac{J^{2\alpha+2\beta-3}fg(t)}{\Gamma^2(\alpha)\Gamma^2(\beta)}$$
$$\geq exp\Big[\frac{-J^{\alpha+\beta-2}tg(t)+J^{\alpha+\beta}tg'(t)}{J^{\alpha+\beta-1}g(t)}\Big]\frac{J^{\alpha+\beta-1}\Big(f(t)exp\Big[\frac{-J^{\alpha+\beta-2}g(t)+J^{\alpha+\beta-1}g'(t)}{J^{\alpha+\beta-1}g(t)}t\Big]\Big)}{(\alpha+\beta-1)B(\alpha,\beta)}\frac{J^{\alpha+\beta-1}g(t)}{(\alpha+\beta-1)B(\alpha,\beta)}. \tag{3.22}$$

Adding (3.21) and (3.22), yields

$$2\Gamma(2\alpha+2\beta-3)(t-a)\frac{J^{2\alpha+2\beta-3}fg(t)}{\Gamma^2(\alpha)\Gamma^2(\beta)}$$
$$\geq exp\Big[\frac{-J^{\alpha+\beta-2}tf(t)+J^{\alpha+\beta}tf'(t)}{J^{\alpha+\beta-1}f(t)}\Big]\frac{J^{\alpha+\beta-1}\Big(g(t)exp\Big[\frac{-J^{\alpha+\beta-2}f(t)+J^{\alpha+\beta-1}f'(t)}{J^{\alpha+\beta-1}f(t)}t\Big]\Big)}{(\alpha+\beta-1)B(\alpha,\beta)}\frac{J^{\alpha+\beta-1}f(t)}{(\alpha+\beta-1)B(\alpha,\beta)}$$
$$+exp\Big[\frac{-J^{\alpha+\beta-2}tg(t)+J^{\alpha+\beta}tg'(t)}{J^{\alpha+\beta-1}g(t)}\Big]\frac{J^{\alpha+\beta-1}\Big(f(t)exp\Big[\frac{-J^{\alpha+\beta-2}g(t)+J^{\alpha+\beta-1}g'(t)}{J^{\alpha+\beta-1}g(t)}t\Big]\Big)}{(\alpha+\beta-1)B(\alpha,\beta)}\frac{J^{\alpha+\beta-1}g(t)}{(\alpha+\beta-1)B(\alpha,\beta)}. \tag{3.23}$$

Taking $t=b$, we obtain (3.14). Theorem 3.2 is thus proved. □

Remark. Applying Theorem 3.2 for $\alpha=1,\beta\neq 1$ or $\beta=1,\alpha\neq 1$, we obtain Theorem 3.1.

References

Belaidi, B., A. El Farissi and Z. Latreuch (2009). Hadamard-type inequalities for twice differentiable functions. *RGMIA Monographs:http://rgmia.vu.edu.au/monographs/hermite hadamard.html, Victoria University* **12**(1), 15–22.

Dahmani, Z. (2010). On minkowsky and hermite-hadamard integral inequality via fractional integration. *Annal of Functional Analysis* **1**(1), 51–58.

Dragomir, S.S. and C.E.M. Pearse (2000). Selected topic in hermite-hadamard inequalities. *RGMIA Monographs:http://rgmia.vu.edu.au/monographs/hermite hadamard.html, Victoria University* **5**(12), 1–10.

Florea, A. and C.P. Niculescu (2007). A hermite hadamard convex-concave symetric functions. *Bul. Soc. Sci. Math. Roum.* **50**(98), 149–156.

Gorenflo, R. and F. Mainardi (1997). *Fractional calculus: integral and differential equations of fractional order*. Springer Verlag, Wien.

Hadamard, J. (1893). Etude sur les proprietes des fonctions entieres et en particulier d'une fonction considree par riemann. *J. Math. Pures et Appl.* **58**, 171–215.

Hermite, Ch. (1883). *Sur deux limites d'une integrale definie*. Mathesis 3.

Sarikaya, M.Z., H. Yaldiz and H. Bozkurt (2012). On the hermite-hadamard type integral inequalities involving several log-convex functions. *Int. J. Open Problems Comput. Math.* **5**(3), 1–9.

Set, E., M.E. Ozdemir and S.S. Dragomir (2010). On the hermite-hadamard inequality and other integral inequalities involving two functions. *Journal of Inequalities and Applications*.

Theory and Applications of Mathematics & Computer Science

(ISSN 2067-2764, EISSN 2247-6202)
http://www.uav.ro/applications/se/journal/index.php/tamcs

Theory and Applications of Mathematics & Computer Science 3 (2) (2013) 120–128

Possibility of Hypercomputation from the Standpoint of Superluminal Particles

Takaaki Musha[a,*]

[a]*Advanced Science-Technology Research Organization, 3-11-7-601, Namiki, Kanazwa-ku, Yokohama 236-0005 Japan.*

Abstract

In mathematics and computer science, an accelerated Turing machine is a hypothetical computational model related to Turing machines, which can perform the countable infinite number of computational steps within a finite time. But this machine cannot be physically realized from the standpoint of the Heisenberg uncertainty principle, because the energy required to perform the computation will be exponentially increased when the computational step is accelerated and it is considered that it is mere a mathematical concept and there is no possibility for its realization in a physical world. However, by using superluminal particles instead of subluminal particles including photons, it can be shown that the hypercomputation system which can perform infinite steps of computation within a finite time length and energy can be realized.

Keywords: Turing machine, Zeno machine, hypercomputation, superluminal particle, tachyon, halting problem.
2010 MSC: 68Q05, 81P68, 83A05.

1. Introduction

In mathematics and computer science, an accelerated Turing machine is a hypothetical computational model related to Turing machines which can perform the countable infinite number of computational steps within a finite time. It is also called a Zeno machine which concept was proposed by B. Russel, R. Blake and H. Weyl independently, which performs its first computational step in one unit of time and each subsequent step in half the time of the step before, that allows an infinite number of steps can be completed within a finite interval of time (Ord, 2006), (Hamkins & Lewis, 2000). However this machine cannot be physically realized from the standpoint of the Heisenberg uncertainty principle $\Delta E \cdot \Delta t \approx \hbar$, because the energy to perform the computation will be exponentially increased when the computational step is accelerated. Thus it is considered that the Zeno machine is mere a mathematical concept and there is no possibility to realize it in

*Corresponding author
Email address: takaaki.mushya@gmail.com (Takaaki Musha)

a physical world. Contrary to this conclusion, the author studied the possibility to realize it by utilizing superluminal particles instead of subliminal particles including photons.

2. Computational time required to perform infinite steps of computation by using ordinary particles

Feynman defined the reversible computer model as shown in Fig.1, which requires energy per step given by (Feynman, 2000):

$$\text{energy per step} = k_{\mathrm{B}}T\frac{f-b}{(f+b)/2} \quad , \tag{2.1}$$

where k_{B} is Boltzmann's constant, T is a temperature, f is a forward rate of computation and b is backward rate.

Supposing that there in no energy supply and parameters f and b are fixed during the computation, we can consider the infinite computational steps given by:

$$E_1 = kE_0,\ E_2 = kE_1,\ \cdots,\ E_n = kE_{n-1}, \cdots, \tag{2.2}$$

where we let the initial energy of computation be $E_0 = k_{\mathrm{B}}T$, $k = 2(f-b)/(f+b)$ and E_n is the energy for the n-th step computation.

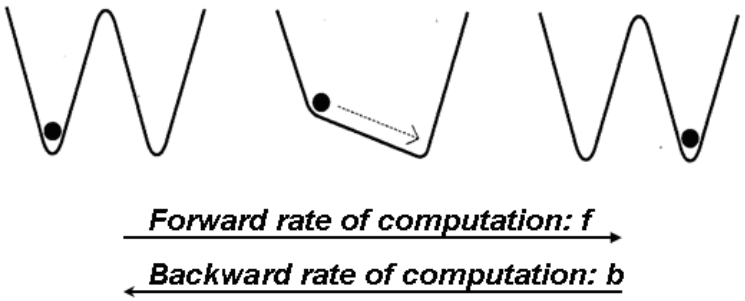

Figure 1. Computational steps for the reversible computation (Feynman, 2000).

From which, we have $E_n = k^n E_0$, then the energy loss for each computational step becomes:

$$\begin{aligned} \Delta E_1 &= E_0 - E_1 &&= (1-k)E_0 \\ \Delta E_2 &= E_1 - E_2 &&= (1-k)kE_0 \\ &\vdots \\ \Delta E_n &= E_{n-1} - E_n &&= (1-k)k^{n-1}E_0. \end{aligned} \tag{2.3}$$

According to the paper by (Lloyd, 2000), it is required for the quantum system with average energy ΔE to take time at least Δt to evolve to an orthogonal state given by:

$$\Delta t = \frac{\pi\hbar}{2\Delta E}, \tag{2.4}$$

From which, the total energy for the infinite steps yields E_0 if setting $E = \Delta E_i$ in equation (2.4), then the total time for the computation with infinite steps becomes:

$$T_n = \sum_{j=1}^{n} \Delta t_n = \frac{\pi\hbar}{2E_0} \sum_{j=1}^{n} \frac{1}{(1-k)k^{j-1}}. \tag{2.5}$$

As the infinite sum of equation (2.5) diverges to infinity as shown in Fig. 2, the Feynman model of computation requires infinite time to complete the calculation when satisfying $0 < k < 1$.

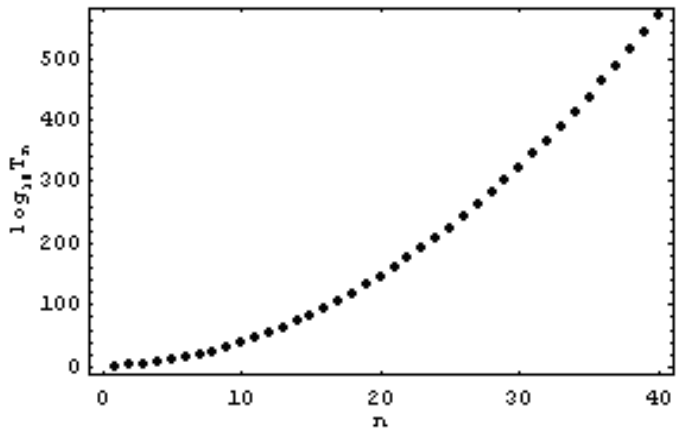

Figure 2. Computational time to complete the n-th step of computation by using subluminal particles (for the case, $k = 1/2\,, \gamma = 1.0$).

Hence it can be seen that a computer system utilizing subluminal particles including photons requires infinite time to complete infinite steps of computation.

3. Computational time by using superluminal elementary particles

3.1. Uncertainty Principle for superluminal particles

E. Recami claimed in his paper (Recami, 2001) that tunneling photons which travel in evanescent mode can move with superluminal group speed inside the barrier. Chu and S. Wong at AT&T Bell Labs measured superluminal velocities for light traveling through the absorbing material (Brown, 1995). Furthermore Steinberg, Kwait and Chiao measured the tunneling time for visible light through the optical filter consisting of the multilayer coating about 10^{-6} m thick. Measurement results by Steinberg and co-workers have shown that the photons seemed to have traveled at 1.7 times the speed of light (Steinberg *et al.*, 1993). Recent optical experiments at Princeton NEC have verified that superluminal pulse propagation can occur in transparent media (Wang *et al.*, 2000). These results indicate that the process of tunneling in quantum physics is superluminal as claimed by E. Recami. From relativistic equations of energy and momentum of the moving particle, shown as:

$$E = \frac{m_0 c^2}{\sqrt{1 - v^2/c^2}}\,, \tag{3.1}$$

and

$$p = \frac{m_0 v}{\sqrt{1 - v^2/c^2}}, \tag{3.2}$$

the relation between energy and momentum can be shown as $p/v = E/c^2$.

From which, we have (Musha, 2012):

$$\frac{v\Delta p - p\Delta v}{v^2} = \frac{\Delta E}{c^2}, \tag{3.3}$$

Supposing that $\Delta v/v^2 \approx 0$, equation (3.3) can be simplified as:

$$\Delta p \approx \frac{v}{c^2}\Delta E\,. \tag{3.4}$$

This relation is also valid for the superluminal particle called a tachyon which has an imaginary mass im_* (Musha, 2012), the energy and the momentum of which are given by following equations, respectively.

$$E = \frac{m_* c^2}{\sqrt{v^2/c^2 - 1}}, \tag{3.5}$$

$$p = \frac{m_* v}{\sqrt{v^2/c^2 - 1}}. \tag{3.6}$$

According to the paper by M. Park and Y. Park (Park & Park, 1996), the uncertainty relation for the superluminal particle can be given by:

$$\Delta p \cdot \Delta t \approx \frac{\hbar}{v - v'}, \tag{3.7}$$

where v and v' are the velocities of a superluminal particle after and before the measurement. By substituting equation (3.4) into (3.7), we obtain the uncertainty relation for superluminal particles given by:

$$\Delta E \cdot \Delta t \approx \frac{\hbar}{\beta(\beta - 1)}, \tag{3.8}$$

when we let $v' = c$ and $\beta = v/c$.

3.2. Computational time required for the superluminal particle

Instead of subluminal particles including photons, the time required for the quantum system utilizing superluminal particles becomes

$$T_n = \sum_{j=1}^{n} \Delta t_j = \frac{\pi\hbar}{2E_0} \sum_{j=1}^{n} \frac{1}{\beta_j(\beta_j - 1)(1-k)k^{j-1}}, \tag{3.9}$$

from the uncertainty principle for superluminal particles given by equation (3.8), where β_j can be given by:

$$\beta_j = \sqrt{1 + \frac{{m_*}^2 c^4}{{E_j}^2}} = \sqrt{1 + \frac{\gamma^2}{k^{2j}}}\ , \tag{3.10}$$

which is derived from equation (3.6), where $\gamma = m_* c^2 / E_0$.

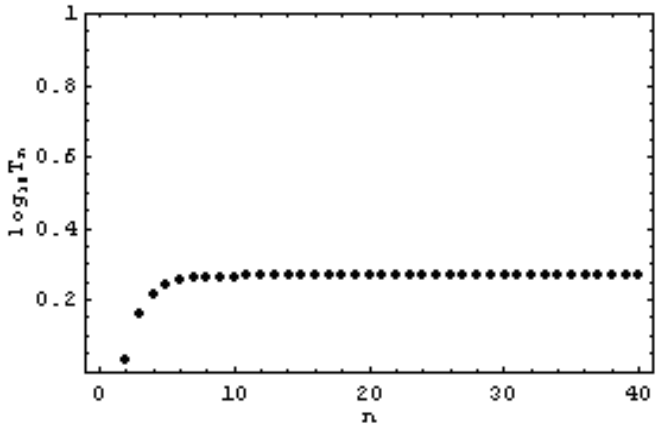

Figure 3. Computational time to complete the n-th step of computation by using superluminal particles (for the case, $k = 1/2$, $\gamma = 1.0$).

Hence it is seen that the computation time can be accelerated according to equation (3.10).

By the numerical calculation, it can be shown that the infinite sum of equation (3.9) converges to a certain value satisfying $0 < k < 1$ as shown in Fig.4.

In this figure, the horizontal line is for the parameter $\gamma = m_* c^2 / E_0$ and the vertical line is for the time to complete infinite step calculations. From these calculation results, an accelerated Turing machine can be realized by utilizing superluminal particles instead of subliminal particles for the Feynman's model of computation.

Thus, contrary to the conclusion for the Feynman's model of computation by using ordinary particles, it can be seen that superluminal particles permits the realization of an accelerated Turing machine.

It is known that an accelerate Turing machines allow us to be computed some functions which are not Turing-computable such as the halting problem (Kieu, 2004), described as "given a description of an arbitrary computer program, decide whether the program finishes running or continues to run forever".

This is equivalent to the problem of deciding, given a program and an input, whether the program will eventually halt when run with that input, or will run forever.

Halting problem for Turing machines can easily solved by an accelerated Turing machine using the following pseudocode algorithm (as shown in Fig.5). As an accelerated Turing machines are more powerful than ordinary Turing machines, they can perform computation beyond the Turing limit which is called hypercomputation, such as to decide any arithmetic statement that is infinite

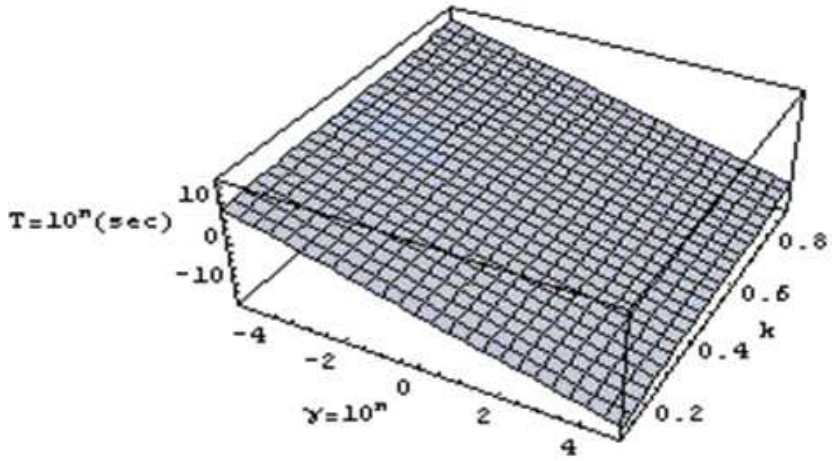

Figure 4. Computational time by using superluminal particles.

```
begin program
  write 0 on the first position of the output tape;
  begin loop
    simulate 1 successive step of the given Turing
    machine on the given input;
    if the Turing machine has halted, then write 1 on
    the first position of the output tape and break out
    of loop;
  end loop
end program
```

Figure 5. Psedocode algorithm to solve the halting problem (Wikipedia, 2009).

time decidable. From this result, we can construct an oracle machine (van Melkebeek, 2000) by using a superluminal particle, which is an abstract machine used to study decision problems. It can be conceived as a Turing machine with a black box, called an oracle, which is able to decide certain decision problems in a single operation.

4. Human mind from the standpoint of superluminal hyper computation

There are some papers on the hypothesis that the human mind is consisted of evanescent tunneling photons which has a property of superluminal particles called tachyons (Georgiev, 2003), (Musha, 2005, 2009).

Professor Dutheil proposed his hypothesis in his book titled, ”L’homme superlumineux” (Dutheil

& Dutheil, 2006), that consciousness is a field of superluminal matter belonging to the true fundamental universe shown in Fig.6, and our world is merely a subluminal holographic projection of it.

He proposed the hypothesis based on superluminal consciousness shown as follows;

- The brain is nothing more than a simple computer that transmit information.
- Consciousness, or the mind is composed of a field of tachyons or superluminal matter, located on the other side of the light barrier in superluminal space-time.

If the human consciousness is consisted of superluminal particles as claimed by Prof. Dutheil, the superiority of the human brain to conventional silicon processors may be explained because it can perform infinite steps of computation within a finite time.

To further interpret this result, we consider S.Berkovich suggestion of a ”cloud computing paradigm”, in which is given an elegant constructive solution to the problem of the organization of mind. Within his article, he defines a situation where individual brains are not stand-alone computers but collective users whom have shared access to portions of a holographic memory of the Universe (Berkovich, 2010). He proposed that the cosmic background radiation (CMB) has nothing at all to do with the residual radiation leftover from the Big Bang.

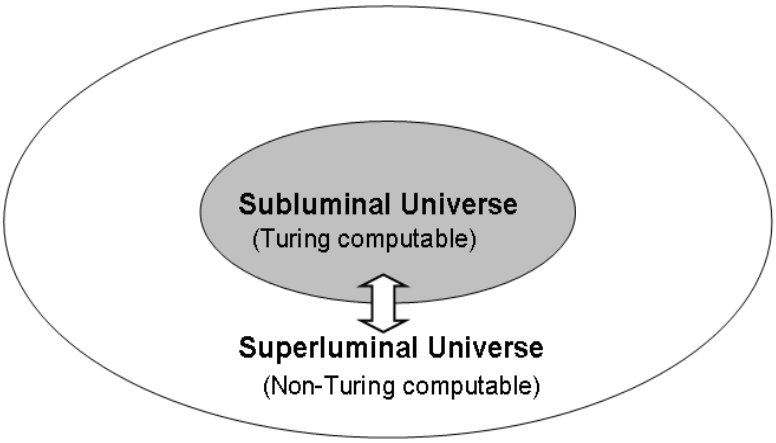

Figure 6. Superluminal Universe model proposed by Prof. Dutheil.

Instead, he claimed that CMB is nothing but noise from writing operations in the holographic memory of the Universe. Such holographic write operations would require some type of universal clocking rate for these operations. Since the virtual superluminal particle pairs are created and annihilated in the vacuum within a short, finite period of time according to the uncertainty principle, we could logically consider this duration as the clock rate for these operations (Fig.7).

From this standpoint, the extraordinary capability of a human brain such as the enigma of Srinivasa Ramanujan (Kanigel, 1991), who invented numerous remarkable and mysterious mathematical formulas from his inspiration without proofs, can be explained from the capability of superluminal consciousness which is superior to that of conventional Turing type computer systems.

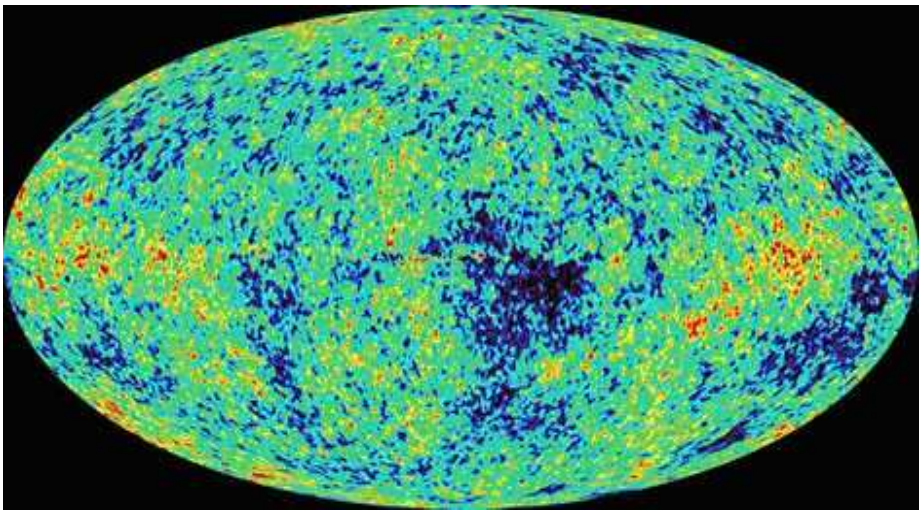

Figure 7. Is CBR an activity of zero-point energy fluctuations of vacuum which relates to the writing operations in the holographic memory of the Universe? (www.computus.org).

5. Conclusion

From the theoretical analysis, it is seen that a hypercomputational system which can complete infinite steps of computation within a finite time and energy can be realized by using superluminal particles from the standpoint of quantum mechanics. Thus an extraordinary capability of human consciousness such as intuition compared with the ordinary silicon processors might be explained if they are composed of superluminal particles, because they have a capability to function beyond the ordinary Turing machines.

References

Berkovich, S. (2010). Obtaining inexhaustible clean energy by parametric resonance under nonlocality clocking. Technical report. Institute for Time Nature Explorations - Russian Interdisciplinary Temporology Seminar, M. V. Lomonosov's Moscow State University.

Brown, J. (1995). Faster than the speed of light. *New Scientist* **01 April 1995**, 26–30.

Dutheil, R. and B. Dutheil (2006). *L'homme superlumineux*. Recherches (Paris. 1985). Sand.

Feynman, R. P. (2000). *Feynman Lectures on Computation*. Westview Press.

Georgiev, D. (2003). On the dynamic timescale of mind-brain interaction. In: *Proceedings Quantum Mind 2003 Conference: Consciousness, Quantum Physics and the Brain , Tucson, Arizona, Usa*.

Hamkins, J. D. and A. Lewis (2000). Infinite time Turing machines. *J. Symbolic Logic* **65**(2), 567–604.

Kanigel, R. (1991). *The man who knew infinity : a life of the genius Ramanujan*. Washington square press biography. Pocket books. New York, London, Toronto.

Kieu, Tien D. (2004). Hypercomputation with quantum adiabatic processes. *Theoretical Computer Science* **317**(13), 93 – 104.

Lloyd, S. (2000). Ultimate physical limits to computation. *Nature* **406**, 1047–1054.

Musha, T. (2005). Superluminal effect for quantum computation that utilizes tunneling photons. *Physics Essays* **18**(4), 525–529.

Musha, T. (2009). Possibility of high performance quantum computation by superluminal evanescent photons in living systems. *Biosystems* **96**(3), 242 – 245.

Musha, T. (2012). Possibility of hypercomputation by using superluminal elementary particles. *Advances in Computer Science and Engineering* **8**(1), 57–67.

Ord, T. (2006). The many forms of hypercomputation. *Applied Mathematics and Computation* **178**(1), 143 – 153.

Park, M. and Y. Park (1996). On the foundation of the relativistic dynamics with the tachyon. *Il Nuovo Cimento B* **111**(11), 1333–1368.

Recami, E. (2001). Superluminal motions ? a bird's-eye view of the experimental situation. *Foundations of Physics* **31**(7), 1119–1135.

Steinberg, A. M., P. G. Kwiat and R. Y. Chiao (1993). Measurement of the single-photon tunneling time. *Phys. Rev. Lett.* **71**, 708–711.

van Melkebeek, D. (2000). *Randomness and Completeness in Computational Complexity*. Vol. 1950 of *Lecture Notes in Computer Science*. Springer.

Wang, L. J., A. Kuzmich and A. Dogariu (2000). Gain-assisted superluminal light propagation. *Nature* (6793), 277–279.

Wikipedia (2009). Zeno machine. http://en.wikipedia.org/wiki/Zeno_machine.